

51559 / 1059  
ACTA UNIVERSITATIS SZEGEDIENSIS



# ACTA MINERALOGICA-PETROGRAPHICA

TOMUS XXIV, Fasc. 2.

1980 APR 26

SZEGED, HUNGARIA  
1980

ACTA UNIVERSITATIS SZEGEDIENSIS

**ACTA  
MINERALOGICA-PETROGRAPHICA**

**TOMUS XXIV, Fasc. 2.**

**SZEGED, HUNGARIA  
1980**

HU ISSN 0365—8066

Adjuvantibus  
BÉLA MOLNÁR et TIBOR SZEDERKÉNYI

Redigit  
GYULA GRASSELLY

Edit  
Institutum Mineralogicum, Geochimicum et Petrographicum  
Universitatis Szegediensis de Attila József nominatae  
Egyetem u. 2—6, H-6722 Szeged, Hungary

Nota  
Acta Miner. Petr., Szeged

Szerkeszti  
GRASSELLY GYULA

a szerkesztőbizottság tagjai  
MOLNÁR BÉLA és SZEDERKÉNYI TIBOR

Kiadja  
a József Attila Tudományegyetem Ásványtani, Geokémiai és Kőzettani Tanszéke,  
H-6722 Szeged, Egyetem u. 2—6

Kiadványunk címének rövidítése  
Acta Miner. Petr., Szeged

## SULPHUR-, GYPSUM- AND ALGINITE-BEARING STRATA IN THE ZSÁMBÉK BASIN

Cs. RAVASZ and G. SOLTÍ

### INTRODUCTION

The Zsámbék Basin is the easternmost member of a series of smaller-larger Tertiary subsidences in the NE part of Transdanubia parallel to the NE-SW range of the Gerecse Mts. The basin is bordered by Triassic, Oligocene and Miocene sediments, and filled by Tertiary sediments. Its deepest point probably lies south of Budajenő (Fig. 1).

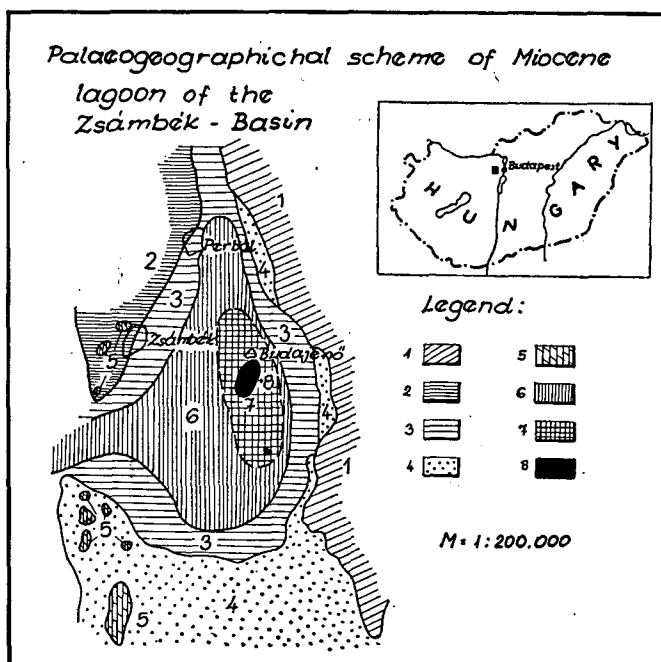


Fig. 1. Legend: 1. Area of Mesozoic limestone and dolomite of Buda Mt.; 2. Oligocene rocks; 3. Sarmatian littoral oolitic limestone overlaid by Lower Pannonian rocks; 4. Oolitic limestone overlaid by Pleistocene formation; 5. Triassic dolomite outcrops of Gőböljárás-puszta and Strázsa-hill; 6. Supposed area of the alginite bearing formations; 7. Supposed area of the deep-sitting evaporitic and alginitic formations; 8. Area of the native sulphur and gypsum bearing Miocene formations limited by boreholes No. Bő-2, 3, 4, 5, and 6.



In 1974 a borehole, Bő-2, was drilled near Budajenő to provide data about the structural conditions, hydrology and stratigraphy of the basin. This borehole intersected native sulphur- and gypsum-bearing evaporites, of Miocene age, as well as alginites in the Lower Pannonian [A. JÁMBOR, 1976, 1977, A. JÁMBOR *et al.*, 1976, Cs. RAVASZ, 1978].

In 1977 four more diamond boreholes, 400 m deep each, were drilled around the Bő-2 to collect detailed informations about the reserves and geology of the potential economic raw materials. Two of them (Bő-3, Bő-5) were sited in the supposed NNE-SSW strike of the evaporites in 2 km distance from each other. The other two boreholes were drilled in perpendicular direction, at 1 km distances (Bő-4, Bő-6).

The thorough investigation of the cores of these five holes, along with the re-interpretation of the previous geological explorations [S. JASKÓ, 1943; A. JÁMBOR, 1969, 1971] has given the opportunity to summarize the geological and mineralogical data about these notable mineral indications.

## THE GEOLOGY OF THE BASIN

The basement of the basin is consisted of Upper Ladinian dolomites [J. ORAVECZ, 1976], with 15–20° dip. The Bő-2 has reached this formation at 766.2 m depth, and has not cut through until the 1200.5 m depth bottom of the hole. The dolomite is covered by about 40 m thick dolomite breccia, dolomite-debris (Nagyegyháza Dolomite-breccia) of possibly Eocene age based on lithological analogy. The younger Paleogene is represented by alternating marine argillaceous and arenaceous sediments of Oligocene age with a dip of 12 to 5° in about 230 m thickness (Mány Formation). Paleontological evidences [T. BÁLDI, M. BÁLDI—BEKE and L. RÁKOSI, 1976] have placed its age in the Upper Oligocene (Egerian), however, its litho-stratigraphic character suggests that it might span through the whole Oligocene period [A. JÁMBOR, L. KÖRPÁS, 1976].

The Oligocene is unconformably overlain by the lowermost part of the Neogene complex, the Middle Rhyolitic Tuff Member of Lower Badenian age. The unconformity is obvious not only from the different bedding directions (0–5° angular unconformity), but also from the different colouring, oxidation, of the uppermost 40 m of the Oligocene as a result of pre-Miocene terrestrial weathering.

The formation begins with a pebbly argillaceous siltstone. It is unsorted, the pebbles are of different grade of rounding and of different materials like rhyolitic tuff, calcareous concretions, Oligocene siltstone, quartzite. It can be considered as terrestrial stream-sediment. The representative rock-type of the formation is a light grey-grey vitroclastic plagioclase rhyolitic tuff. It consists of 20 per cent of crystal fragments, andesine, quartz, less K-feldspar and biotite and 80 per cent of altered, devitrified glass-shards and pumice. At its base it is introduced by sandy tuffites, while its top shows a transition towards a calcareous argillaceous tuffite. The scarce fossil content of these volcanogenic sediments (Echinodermata spines, Mollusca fragments) indicate subaquatic deposition. The widely differing coloring of the strata as well as the modular parting of the rocks, however, suggest a dry, oxidizing environment for diagenesis.

The uppermost part of the Lower Badenian is represented by the Zsámbék Member. This is composed of alternating strata of two rock types. The first one is a greyish-yellow to yellow argillaceous silty sand and sandstone. The other variety is a pale green, yellow and grey clayey siltstone. In the series there are several thin pebble-

$\begin{array}{c} W/W \\ | \\ \hline 300^\circ \end{array}$  ,  $\begin{array}{c} 120^\circ \\ | \\ \hline 300^\circ \end{array}$  ,  $\begin{array}{c} ESE \\ | \\ \hline 120^\circ \end{array}$   
 $B_0^\circ - 6$  ,  $B_0^\circ - 2$  ,  $B_0^\circ - 4$   
 $\begin{array}{c} 0.0 \\ 4.0 \end{array} \begin{array}{c} m \\ m \end{array} \begin{array}{c} (216, 7 m \text{ a.s.l.}) \\ (212, 4 m \text{ a.s.l.}) \end{array}$

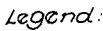




Fig. 2. and 3. Legend: 1. Soil; 2. Loess; 3. Gravel, pebble and conglomerate; 4. Sand; 5. Sandstone; 6. Silt, siltstone; 7. Clay; 8. Carbonaceous clay; 9. Variegated clay; 10. Alginite; 11. Diatomite, diatomaceous shale; 12. Clayey marl; 13. Marl; 14. Argillaceous limestone; 15. Limestone; 16. Tuff (acidic), tuffite; 17. Native sulphur (layer, seam etc.); 18. Gypsum (bed, layer etc.).

SSW




Bd-3



Bd-2

NNE



Bd-5

Fig. 2. and 3. Legend: 1. Soil; 2. Loess; 3. Gravel, pebble and conglomerate; 4. Sand; 5. Sandstone; 6. Silt, siltstone; 7. Clay; 8. Carbonaceous clay; 9. Variegated clay; 10. Alginite; 11. Diatomite, diatomaceous shale; 12. Clayey marl; 13. Marl; 14. Argillaceous limestone; 15. Limestone; 16. Tuff (acidic), tuffite; 17. Native sulphur (layer, seam etc.); 18. Gypsum (bed, layer etc.).

rich intercalations and beds rich in fossilized carbonaceous plant-fragments. Variegated clay has been developed on the top of the formation. Bő-2 has intersected the uppermost horizons of the Middle Rhyolitic Tuff at 409.0 m depth (Figs 2 and 3). Due to lack of molluscs; paleontological investigations have been restricted to Foraminifera. The genera *Rotalia*, *Borelis* and *Peneroplis*, and *Rotalia*, *Elphidium*, *Gyroidina*, *Spiroplectammina* and *Eponides* were identified from the Bő-2 and Bő-3 holes, respectively. These fossils indicate a shallow-marine, hyperhaline environment of deposition [I. KORECZ-LAKY, 1978]. On the whole the basin can be considered a near-shore belt, with repeated uplifting on its edges, associated by short-duration terrestrial stream sedimentation which resulted in the accumulation of coarse grained detritus.

The Alsóörspusztá Member represents the Upper Badenian. Clay with sand and silt forms the base in the central parts, which gradually gives place to clayey-sandy siltstone. In the other parts a more abrupt facies change is recorded with argillaceous conglomerate, pebbly sandstone, and pebbly clay-marl. Upwards these are overlain by light grey, finely laminated, rather homogeneous clay-marl. The monotony of these strata, however, is interrupted by occasional intraformation brecciation, slumping, and intercalations of beds enriched in carbonaceous plant fragments, or tuffites and lumachelles.

It was the Alsóörspusztá Member, where the environmental conditions necessary for the formation of evaporites, like gypsum and native sulphur, became predominant. The number of gypsum- or sulphur-rich intersections in the boreholes varies between 17 and 2. The structure of these deposits is also variable, from the randomly disseminated "porphyric" form to chaotic folded laminae. Native sulphur frequently forms fine-grained crystal aggregates, or the crystals are evenly disseminated, always in a gypsum matrix. Dolomite, dolomitic marl, marl and calcareous marl are found interbedded with the evaporites.

The types, number of species and individuals of Foraminifera and molluscs have clearly indicated both the Upper Badenian age, and the evolutionary facies changes, of the Member. Sedimentation took place in waters of normal salinity along the shorelines of a lagoon. The decrease of the amount of fauna and its disappearance are bi-directional and due mainly to two factors: shallowing, which is indicated by the presence of *Pirenella* and *Hydrobia* and enrichment of carbonaceous fossilized plant fragments, and the increasing degree of salinity, evidenced by evaporation. A continuity of sedimentation, though abrupt changes in lithology, called the Szomor Member, marks the beginning of the Sarmatian stage. The rocks are light grey poorly bedded, occasionally laminated brittle marls, less clay-marls, calcareous marls. This horizon is easily traceable in every borehole. A rather thin (0.2—1.0 m) intercalation of crystalloclastic glassy rhyolitic tuff with low sulphur content is found in the upper levels of the Member. Radiometric age determination was made in a sample from Bő-3 (313.8—314.0 m), with a result of  $13.2 \pm 1$  m. y. This age corresponds to the Lower Sarmatian "upper rhyolitic tuff" horizon according both to the recommendations of the RCMNS Congress [1975] and the Paratethys standard proposed by BAGDASARIAN, VASS and SLAVIK [1975]. It is also well fit into the local stratigraphic pattern.

According to the rich Foraminifera fauna, and the bivalves, which are represented by few genera, but in high amounts (*Cardium transcarpaticum* GRISK., *Abra reflexa* [EICHW.]), and a number of external moulds of gastropods, the sediments belong to the Kozárdi substage. The depositional environment was still the same, not agitated, lagoonal. Beds essentially free of marine fauna, i. e. of molluscs, indicate hyper-salinity during sedimentation.

The Máty Member (with alginites and evaporites) is predominant one in the Sarmatian stage. This gives the bulk of the sulphur and gypsum mineralization in the area. The Member is slightly thickening towards the centre of the Budajenő Basin. The individual evaporite strata have greater thickness, the rocks have lower Ca-content in this Member than either in the underlying or the overlying ones. It is also characterized by the predominance of silty clay-marls. The proportion of pelites — especially in the higher parts of the Member — is also increased by the high amount of oil-shales and diatomites.

20—30 native sulphur and gypsum deposits have been recorded in the Member, which can be arranged in three groups. The lowermost one has developed in the lower first quarter of the Member, and seems to thin out SE-wards. It consists mainly of gypsum.

The middle group contains the highest enrichments of native sulphur in the basin. This occupies the lower (No. Bő-2) or the upper middle parts of the Member.

A small number of gypsum- and sulphur-rich strata comprise the upper group, near the top of the formation. The individual beds are generally discontinuous, but the groups can well be correlated by the help of characteristic intercalations (like rhyolitic tuffite, carbonaceous clay). Concerning the evaporites, the native sulphur forms either separate beds or occurs in disseminated, patchy form, thin laminae. The bulk of gypsum is finely crystalline, laminar, but at the beginning of the evaporation it tended to be arranged in "porphyric" disseminations. The decrease in the amount of gangue minerals is coupled with a decrease in grain-size and crystallinity of evaporite minerals.

Mineralogical analysis of evaporites revealed the existence of celestite and trace amounts of barite in several samples.

Laminated limestone, dolomite, dolmitic marl and calcareous marl are the most frequent barren intercalations. Clay, clay-marl and clay-marl with felsic volcanogenic material are also present in lesser amounts. In general the Member is characterized by a low carbonate content. This is in apparent contradiction with the frequency of barren limestone-dolomite intercalations in the evaporites. The contradiction can probably be solved by assuming the epigenetic alteration of evaporites to produce carbonates.

Based on the mollusc fauna, the lower one-third of the Member belongs to the Kozárd substage, while the upper two-thirds occupies the lower *Cardium latisulcum* zone of the Tinnye substage.

Sedimentation began in a shallow water not agitated marine environment. The landlocking of the lagoon, the shallowing associated with it and, as a consequence, the interruption of evaporation are marked by the development of *Hydrobia*-containing lumachelles and carbonaceous clay beds. Following these processes, the lagoon gradually subsided, as proved by the reappearance of rich fauna, Diatomas, Foraminiferas. Finally, the increasing rate of evaporation and salinity as well as contemporaneous precipitation of evaporites resulted in the development of unfavourable conditions for marine life. Thus rocks, almost free of fauna were formed.

The youngest Miocene sequence in the area is the Strázsahegy Member. This was continuously formed on the overlying rocks, separated from those only by a 0.5 m thick marl-bed. Slump structures, allotigenic brecciation and the lack of evaporite minerals are the main characteristics for this intercalation. The main lithology of the series is a clay-marl, which frequently contains alginitic clay marl and diatomites (diatomite-earth, microbedded diatomite, laminated diatomite, Fig. 4). The rocks are predominantly pelitic, with varying Ca-content.

Compared to the Máty Member (alginites and evaporites) these strata are characterized by more abundant diatom flora and a mollusc fauna, but a poorer foraminiferal assemblage. Among the frequent bivalvae remnants *Cardium vindobonense* PARTSCH is predominant indicating the upper level of the Tinnye substage as well

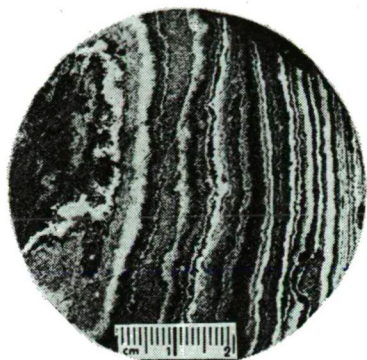


Fig. 4. Microlaminated oil shale built up of alternating diatomite and alginite lamellae. — Borehole No. Bő-5, 252 m.

as the completeness of Sarmatian stratigraphy. The boundary with Pannonian has been drawn on a paleontological basis with a view to the decrease in size of *C. vindobonense* individuals, the flattening of its ribs, the extinction of most other Sarmatian species, and the appearance of larger ostracods and sparsely fish remnants (Fig. 5).

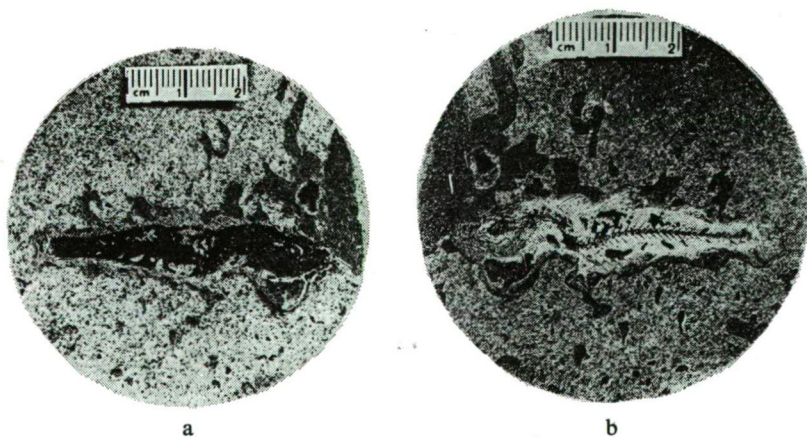


Fig. 5. Positive (a) and negative (b) print of *Gadus* sp. (?) in Sarmatian oil shale. — Borehole No. Bő-5, 252 m.

The Strázsahegy Member shows a gradual transition towards the Laminated Marl Member of the Lower Pannonian Formation. These latter differ from the Miocene lithologies mainly by their well-formed laminated structure. Lamination is due to alternation of laminae with different materials and colours in 2—20 mm thicknesses. The different stain is reflected by different tones of grey, material differences are

manifested in the variation of the silt and  $\text{CaCO}_3$  content. The rocks of this formation show a quite uniform grain-size distribution, no arenaceous members have been encountered in this series. The argillaceous fraction makes 47.0 to 48.9 per cent of weight, which largely differs from that of Strázsahegy Member (max. 29.7% weight per cent) and of Csákvár Member (36.0%).

In the Laminated Marl Member alginitic clay-marl intercalations were recorded in the Budajenő B6-4 and B6-6 holes. This proves the transition of alginites to the Lower Pannonian. The oil-shale, which was found in 10–20 cm thicknesses, exhibits interlamination of light-green and greyish green diatomite and alginite in 0.1 mm laminae. Cleavage is well-developed along bedding. Characteristic "oil-shale" odour is felt on the fresh cores immediately after their being pulled out of the hole.

Upwards in the sequence the alginites gradually disappear. A possible explanation of this phenomenon could be the intense subsidence of the basin and its environment during this period.

Although deposition continued on the Sarmatian-Pannonian boundary, it is marked by the decrease of relief energy of the neighbouring terrestrial areas as well as the diminution of salinity of the depositional media. This fact brought about an abrupt change in fauna, however, the Pannonian still contains several intercalations with a marine fauna.

In the lower horizons of the Lower Pannonian Formation the *Limnocardium praeponticum* and the *Planorbis praeponticus* Horizons have been recognized. Except for undeterminable fragments no *Congerina* has been found.

The mollusc fauna is represented by only a few species. The fossils are brownish-yellow coloured, well-preserved, lying always conformably with the depositional bedding. Complete individuals or shell-pairs are very rare.

Their biostratigraphical separation from the Sarmatian is indicated by the extinction of *Cardium vindobonense*, *Irus gregarius*, *Acteocina lajonkairina*.

The rich Sarmatian foraminiferal assemblage gradually disappears at the top of the Sarmatian, though 5 m above the boundary a *Milliammina* sp. was found, which otherwise was limited to the Sarmatian. Like in Tököl-1 and Tp-63 at Perbál the extension of Foraminiferas beyond the boundary of the Sarmatian and Lower Pannonian was suggested by I. KORECZ-LAKY.

Ostracods are locally abundant in several strata of the Laminated Marl Member, as double or single shells, parallel with bedding. They mostly belong to the form-species *Pectinaria Ostracopannonicus* JÁMBOR—RADÓCZ.

The microfloral assemblage also allows to trace the Sarmatian-Pannonian boundary. All Sarmatian species disappear at this boundary, and three other species appear: *Colonias placentula* EHR. var. *enghyptia* (EHR.) Cl. *Melisia praeislandica* JOUSÉ, and *Chrisostomum sphaericum* HAJÓS.

In the diatom assemblage of the alginitic clay marls (oil-shales) the *Penneatae* forms are predominant. These mostly epiphytic species often comprise continuous colonies. The diatoms existed and were subsequently deposited in such shallow lakes (up to several meters deep) which were substantially lower in salinity than the Sarmatian sea.

Local enrichment of fossilized plant fragments of 2–10 mm width and 1–8 cm length, partly replaced by spherical bacterio-pyrite are abundant in the rocks of this formation, so are the Y-shaped fossil traces.

The thin rhyolitic tuff intercalations characteristic as they are of the Lower Pannonian Formation elsewhere [A. JÁMBOR, M. KÖRPÁS-HÓDI, 1971] could not be identified in the Budajenő drill-holes in spite of careful logging.

Slow, continuous subsidence caused an increase of water-depth, and diminished the effects of swelling. Dessication cracks, which are quite abundant elsewhere in the series, are absent here. The whole sequence becomes more monotonous. Further dilution of water is probably due to the higher humidity of climate.

Middle part of the Lower Pannonian of the Zsámbék Basin is the Csákvár Member. This shows a more marked monotony and greater thickness than either the underlying Laminated Marl or the overlying Csór Member. Its lithology differs from the adjacent older formation by the lack of laminated clay-marls and marls. The results of geophysical logging of the drill-holes is in good accordance with this fact. Its thickness considerably varies throughout the basin, due to the uneven subsidence of the latter.

The gradual changes of lime-content and stain allows only poor subdivision of the monotonous, pale-grey to greyish-green coloured pelitic, mostly clayey-siltstone sedimentary sequence. Besides this main lithology, clay, carbonaceous clay, diatomaceous clay-marls, limestones, and bentonites also occur occasionally.

Upwards in the formation the ratio of the silt fraction increases from 30 to 60—70 per cent at the expense of the argillaceous fraction. At the top of the sequence the finer-grained fraction is increasing marking a gradual transition towards the Csór Beds. The carbonate content of the rocks drops to 20—30%, with the appearance of dolomite. A peculiar rock type of the Member is a silty clay, of dark-grey or greenish-grey colour, intense lamination, low lime content, and pelitic huminite stain. According to its fossil content, it represents the typical facies of the Pannonian inland sea, though its huminite content indicates greater depth of deposition.

The trace element enrichment of the Pannonian sediments is only one half of the respective Miocene average values. This is probably due to the initial low trace element content of the terrestrial source areas, or the lack of that enrichment process, which is usually linked with the evaporation of sea-water [Á. JÁMBOR, 1976].

Constant variation of water depth and salinity (0.5—1.0%) can be suggested for the Lower Pannonian Formation according to the analyses of its rich diatom flora. The species-poor assemblage shows the predominance of mesohaline-oligohaline species. Marine forms, if any, are considered to be allochthonous.

Considering Mollusca, it is the disappearance of *Limnocardium praeponticum* and the introduction and gradually larger abundance of *Didacna subdeserta*, *Limnocardium triangulocostatum*, *Monodacna viennensis*, *Orygoceras* that marks the Csákvár Member.

The *Melanopsis* gain their virulence at the base of the upper part of the Csákvár Member, and so the *Paradacna*, which may also become locally abundant. Besides the *Paradacna*, the larger forms of *Limnocardium*, *Congeria partschi* and *Pisidium* sp. are also common fossils. The accessory species of this bio-stratigraphical horizon are *Limnocardium huminocostatum*, *L. conjugens*, *L. schedelianum*, *Monodacna viennensis*. The top of this formation is marked by *Parvidacna laevicostata*, *Pontalmyra tinnyeana*, *Limnocardium carnuntium*, *L. schedelianum*, *L. winkleri* and *Congeria czjzeki* assemblage delineates the *Congeria banatica* Horizon of the Lower Pannonian Formation.

It is worth to notice that while the whole series is lithologically unseparable, the mollusc fauna allows a subdivision of the series into four identifiable horizons, separated by fossil-free sections.

The youngest member of the Lower Pannonian is the Csór Member. In spite of its great thickness the series is uncomplete. The erosion at the beginning of the Pleistocene has removed a part of these beds and all the overlying later Pannonian strata.

The NE part of the basin was affected most intensely by this erosion.

In lithology the lower boundary of this formation is drawn with a marked increase of the silt and fine-sand fraction. The lithology is broadly similar to that of Csákvár Member, except for this change in grain-size distribution. The most abundant rock type is a clayey, marly siltstone. The carbonate content is again decreasing by 50 per cent compared to the former formation.

Pectinaria tubes are common and abundant in siltstones [A. JÁMBOR, M. KORPÁS-HÓDI, 1971].

In the Csór Member the *Congerina* sp. dff. *czjzeki* Horizon contains remnants of *Congerina czjzeki*, a non-typical variety of *C. czjzeki*, in great numbers. *Micromelania* sp., *Planorbis* cf. *tenuistriatus*, *P.* cf. *okrugici*, *Monodacna* cf. *viennensis*, *Pisidium krembergi*, *Limnocardium rogenhoferi*, *L.* cf. *secans*, *L.* cf. *off. triangulocostatum*, *L. hoffmani*, *L.* cf. *winkleri*, *L. riegeli* are also characteristic species.

A pebble bed has deposited unconformably on the eroded surface of the Lower Pannonian Formation rocks. It consists of poorly sorted, weakly rounded pebbles with 0.2—5.0 cm size, of Triassic dolomite, limestone, less quartzite and lydite. This is overlain by sandy silts, silty clays and Würmian loess under the Holocene soil cover.

Looking at the Miocene paleogeography of the area, a gradual infilling of a periodically isolated lagoon can be assumed as environment of deposition. A barrier on the SW side of this lagoon controlled the rate of water inflow. According to dynamic balance between the rate of inflow and evaporation, the shore zone seems to have shallowed the basin, to have split up into several subbasins or even to have reached the stage necessary for the development of evaporites. The oscillation of the water level was probably due to an alternating local uplifting and subsidence of the bottom as well as larger, regional processes like transgression and regression. The shifting of the shore-line — especially in the Sarmatian — is well shown not only by lithology (carbonate-content, grain-size variation) but in the change of the faunal and floral assemblage, like appearance, alteration and mass-extinction of different species. The extreme increase of salinity is demonstrated by the precipitation and accumulation of evaporites: calcite, dolomite, gypsum, native sulphur, barite, celestite.

The age determination of the sequence could be satisfactorily carried out both by lithostratigraphy and biostratigraphy. The difference between the two methods is in most places negligible, and even where it is larger, like in the case of the Sarmatian-Pannonian boundary, it is unessential for exploration.

Taking the lithology into consideration, the formation of gypsum already began sporadically in the Lower Badenian Middle Rhyolitic Tuff and continued through the Zsámbék Member. Its first appearance in individual beds occurs in the Upper Badenian Alsóörpuszta Member, in association with the first alginites and native sulphur bed. Above the Upper Rhyolitic Tuff, in the Sarmatian native sulphur and gypsum with alginites were formed, thus the Mátyás Member represents the most favourable paleogeographic and geological conditions for the formation of evaporites.

Most of the gypsum deposits and associated minerals are considered to be of sedimentary origin. The bulk of native sulphur was formed epigenetically after gypsum, the proportion of syngenetic precipitations is subordinate.



Several test results and analyses give evidences for the process of reduction of sulphates as well as the existence of hydrocarbons. There is also evidence for the subsequent oxidation process of the sulphur deposits: secondary formation of gypsum and carbonatization. The results of petrological investigations, the geology and geochemistry of evaporites and alginites have already been published previously [A. JÁMBOR, G. SOLTÍ, 1975; Cs. RAVASZ, 1976, 1978], so are not discussed here in detail.

If the age of the sulphur- and gypsum deposits of the Zsámbék Basin and those of the Carpathian Foreland are correlated by biostratigraphy, the Zsámbék Member and the Middle Rhyolitic Tuff correspond with the Moravian, the Alsóörspuszta Member with the Wielician, the upper one with the Cosovian, respectively. The Sarmatian deposits comprise a special type, as no similar deposits of similar age have been found in the Carpathian area. As a consequence, it can be said that the other, less-explored intramontane basins in the Transdanubian Central Mountains are promising for sulphur, gypsum and alginite explorations.

Sedimentation was not interrupted on the Sarmatian-Pannonian boundary, though there was marked decrease of the environmental relief energy and of the salinity of sea-water. As a consequence of this latter effect, the faunal assemblage showed a quite abrupt change, however, marine element still persist locally. By the help of its relatively rich Mollusca fauna, the clay-marl, marl, sandy siltstone sequence of the Lower Pannonian Formation can well be subdivided into distinct stages. The Marl Member corresponds with the *Limnocardium praeponiticum* Horizon. The Csákvár Member consists of four biostratigraphical horizons — as it was previously discussed. Its lower part is characterized by *Monodacna viennensis* and *Orygoceras* species. The upper part consists of three different horizons with the predominance of *Melanopsis*, *Limnocardium* and *Pervidacna*.

As one proceeds upwards in the sequence, the Ca-content decreases. The reduction of  $\text{CaCO}_3$  content is coupled with a slight dolomitization. According to the microfloral assemblage no geographical or ecological change of considerable value could take place during the Lower Pannonian sedimentation. Shallow water, gradual subsidence of the basin and constant oscillation of water-level seem to be characteristic features of these sediments, coupled with a decrease of salinity. The freshening of the water indicates a more humid climate, together with the huminitic clays, which are indicative of nearby swampy areas. The monotony of the Lower Pannonian sedimentation indicates the low relief values the environment must have had and a pelitic transport by lake-currents from NE towards SW.

The Upper Pannonian, which has been preserved in other places, like in the Buda Mts., might also reach considerable thickness in this area, but along with the upper part of the Lower Pannonian, it has been eroded away in the early Pleistocene. This deflation, and/or erosion might have been a very significant process, as the pebble beds deposited on Lower Pannonian surface.

100—200 m of the sequence was removed and the base level further dropped by 35—25 m: an anomalously high value for Transdanubian Central Mts. With these facts in mind a conclusion arises that following the Early Styrian movements an intense uplift must have taken place.

## Evaporites

In the Budajenő area these deposits are of sedimentary stratified type. With strike parallel with the N-S trending longer axis of the basin they dip to ENE at 2—5° angle.

The pattern becomes more complex in the case of identification of individual evaporite strata. The number of these varies between 47 and 24 in the drill-holes. Several horizons tend to diversify or be merging, or pinch out in the area. This brings about large variations in thickness, structure and composition even of the otherwise correlable deposits.

The immediate footwall and hanging wall of the evaporites, as well as the intercalations, except for tuffs, are high-carbonate, low-porosity rocks, marl, calcareous marl, limestone and dolomite. These are essentially primary evaporites or secondary alteration products with the oxidation of sulphur. The host rock in a general sense is a silty clay-marl, which is the most abundant rock type of the basin.

The precipitation of evaporites decreased or even ceased with decreasing water depth as indicated by the appearance of sandy clays with carbonaceous plant fossils, tuffites and diatoms, alginites. This proves that an increase of grain-size due to the shifting of shore-line and the decrease of pH and Eh created unfavourable environmental conditions for the formation of evaporites. On the other hand, the accumulation of organic materials was a necessary factor for the process of reduction of sulphates. The deposits themselves and pelitic rocks of the immediate footwall and hanging wall have in fact a relatively high bitumoid-content (*Fig. 11*). Deeper in the underlying sequence the high organic content is due to the enrichment of carbonaceous plant fossil fragments in the clays and siltstones. These observations are in accordance with the analysis of cores of the Bő-2, 3, and 4 boreholes by the Fischer-extraction method for alginites, by the tar and bitumoid determination of chloroformic and fluorescent bitumoid solutions or  $C_{org}$ -analysis of other rock types, which have given reliable quantitative results.

Concerning the most indicative component, the organic C-content, the following results have been obtained:

alginites	3.5 — 7.6 wt%
diatoms	2.0 — 3.3 wt%
carbonaceous clay and clay-marl	1.7 — 2.4 wt%
gypsum-containing marl	0.25—0.45 wt%
sulphur and gypsum-containing marl	1.8 — 3.8 wt%

The pH seems to be the major controlling factor for the precipitation of gypsum, while for sulphur the Eh values were more important. Thus gypsum still contains carbonaceous clay, but in tuff hosts only sulphur occurs. This indicates a sublittoral lagoonal facies of high salinity (20%), high pH (8—9) and Eh (between 0.0 and +0.01) values for the formation of gypsum. The native sulphur precipitated from poorly aerated waters of lower pH and Eh near to the bottom of the basin.

Structural deformation is well-developed in several parts of the deposit groups, mostly on their middle and top levels. This is exhibited in the intense fracturing and shearing of the originally flat and subparallel gypsum and sulphur beds as well as the development of chaotic folding (*Figs 6, 7*) subsequent fracturing and displacement of strata, and the formation of convolute structures (*Figs 8, 9*).

These structures have resulted from primary diagenetic processes, like sub-aquatic slumping in a still plastic state, and the contractive stresses affecting the sub-consolidated incompetent gypsum rocks. Anhydrite-gypsum alteration is excluded from the causes of deformation for mineralogical reasons.

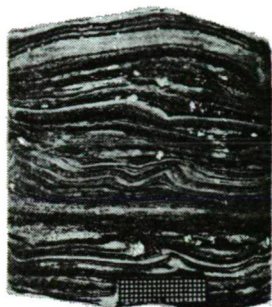


Fig. 6



Fig. 7

Fig. 6. Folded gypsum (grey, black) and dolomitic marl lamella-fascicles (white, light grey), and native sulphur (white lentils, spots). — Borehole No. B6-3, 255.0—255.2 m.

Fig. 7. Flow folding of lamellar gypsum. Contorted, fragmented gypsum laminae (white, dirty white), and intercalating argillaceous marl (grey). — Bore hole No. B6-3, 354.8—352.9 m.

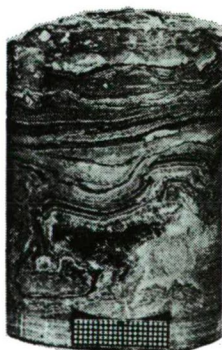


Fig. 8. Composite bedding and micro-faulting. Paralell-lamellar and convolute structure of a gypsum seam. Gypsum (black), argillaceous marl (middle- and light grey), and magnesian limestone (white). — Borehole No. B6-4, 378.6—378.8 m.

The two main economic minerals, native sulphur and gypsum, may occur separately or form assemblages. The pure sulphur deposits are generally thinner than the gypsum deposits. The average thickness of the deposits is 0.5 m, their sulphur content is 12.5 wt%, the gypsum content is about 30 wt%. The sulphur-rich deposits have 30—38 wt% S content, while the gypsum deposits contain 75—83% of the economic mineral. The thickest known deposit is 3.3 m.

Preliminary results of the mineralogical-petrological analysis of evaporites in the B6-2 intersections have already been published [RAVASZ, 1978]. The mineralogy of

the evaporites from other holes, B6-3, 4, 5 and 6 are in correspondence with these previous data. Therefore only generalized conclusions are given here in detail, complemented with a few interesting data.

Evaporites are more or less well-crystallized. Native sulphur is usually fine-grained, subhedral. Gypsum exhibits variable crystallinity from fine-grained to porphyric (up to 2.5 cm). The largest crystals of sulphur are found in sulphur-rich strata. Euhedral porphyric gypsum has developed usually in a large amount of barren matrix.

Sulphur occurs in thin laminae or beds, associated with gypsum and carbonates, and forms nodules or patches several mm in size (*Fig. 10*). Crystal aggregates of sulphur have occasionally precipitated in clays and rhyolitic tuffs.



Fig. 9



Fig. 10

*Fig. 9.* Bent-lamellar and flat-lenticular gypsum lamellae and layers (black, dark grey) with marl intercalations. — Borehole No. B6-4, 379.3—379.5 m.

*Fig. 10.* Native sulphur and gypsum seams of different crystallinity and bedding. Native sulphur layer and lamellae (at the bottom and the middle of the uppermost member of the core), lenses, spots (tiny, white area in the same part). Porphyric gypsum crystals (at the top and the lower thirds part of the core), gypsum layers and lenses composed of middle- and fine grained crystals and interbedded argillaceous marl. — Borehole No. B6-3, 252.0—252.4 m.

Both the habits of crystals and their combination, and their accumulation-types show greater variation in the case of gypsum than in that of sulphur. Several drill-holes have intersected — within the evaporite complexes — thin beds of fibrous gypsum and hemihydrate (identified by XRD). The matrix of the Upper Badenian basal conglomerate in the Bő-4 is a gypsum-bearing sandstone. Here the gypsum is fibrous, mostly altered to hemihydrate, porphyric grains are rare.

Accessory minerals are celestite, barite, thenardite, and the "gangue" minerals: nalcite, dolomite, aragonite, ankerite, rodochrosite, pyrite and other opaque minerals.

Celestite and barite, usually embedded in gypsum, form small patches, semi-continuous stringers, less frequently disseminations of separate crystals. From the 85 samples analysed so far (Bő-2, 3, 4, 6 holes) fifteen samples contain celestite in higher amounts (up to 17%), 31 samples have an average celestite content characteristic of evaporites, and 39 samples have celestite in amounts less than the average. 23 samples contained some barite up to the evaporite average, while 62 samples had a barite content equal to more than the sedimentary average (max. 0.75%).

Siderite, ankerite, rodochrosite have been identified from the Upper Badenian sequence of Bő-3 and the Sarmatian from the Bő-4 boreholes. These minerals are of only genetic importance. So does the thenardite, which appears to be formed on the core surfaces after several weeks of exposure. Though this is clearly secondary, it may give information about the salinity of the original media of sedimentation.

### Oil-shales

Oil-shales were discovered at Pula (Balaton Highlands) and Gérce (Vas county) in 1973 [Á. JÁMBOR, G. SOLTÍ, 1975]. The careful investigations of their genetics have opened up ways for the perspectives of oil-shale explorations in Hungary. Two alternatives have been provided for us to determine the future exploration targets. The first was the prospecting and exploration of maar-like tuff-rings like those of Pula and Gérce. The other one was to find sediments which have developed in the same facies as oil-shales discovered. Certain specific paleogeographical and sedimentological conditions are known to be indicative of the formation of oil-shales, as shown by several examples, like Green River (USA), Estonia etc. The proportion of these factors, their predominant or exclusive appearance controls whether a pelite may be altered to oil-shale or not.

Field evidences have been obtained for the important controlling nature of the association of volcanic tuff material, which independently of its acidity (silica-content), provided a suitable environment, biotop, for the growth of oil-producing algae.

The shallow depth of the basin, as well as the lack of detritus coarser than silt-grade are other characteristic features. Lamination is mainly due to the seasonal changes (precipitation, temperature) causing rhythmic sedimentation. The greenish colours and low density of alginites can be attributed to the high organic content. Finally, the so-called oil-shale odour, is a unique feature of these rocks in a freshly exposed, still wet state. According to our investigations only the slightly diagenised Neogene or younger alginites may have represent an economic potential for oil-shale explorations in Hungary. This consideration has drawn our attention to the Neogene basins in the forelands of the Transdanubian Central Mountains. The first of these occurrences was discovered in the Öcs — Kapolcs Basin, and therefore it is being



referred to as Kapolcs-type. The alginites of the Zsámbék Basin are of similar type. Based on these two occurrences, paleogeographic and lithological features were analyzed in detail for determining the future perspectives of oil-shale explorations in Transdanubia [Cs. RAVASZ, 1977].

The existence of alginites in the sequence of the Zsámbék Basin has been convincingly proven by exploratory drilling.

The lack of enclosement and the varying subsidence of the basement brought about variations in the relief-energy and water depth during the Badenian. These factors prevented a continuous undisturbed sedimentation.

Close to the Sarmatian-Badenian boundary, the Parathetys Basin was isolated, the water of the newly formed inner sea was gradually diluted, and changes in sedimentation took place. The early members of the Sarmatian were still affected by synorogenic movements. This period was followed by a relatively undisturbed sedimentation during the middle and upper stages of the Sarmatian in what is now the Zsámbék basin.

Sedimentation is characterized not only by evaporites but the abundance of diatoms and algae as well. At the time of the sedimentation of the Mátyás Member and the Strázsahegy Member the Zsámbék Basin had limited communications in SW direction only with the Mátyás basin. This environment has created suitable conditions for the specific sedimentation, with the accumulation of evaporites, planktonogenic, organic-rich pelites. The products of the distant felsic volcanic activity have reached the basin and provided favourable conditions for the rapid growth of planktonic organisms.

In dry seasons dead planktonic organisms fell onto the dull bottom of the basin, accumulating under anaerobic condition. Subsequent wet seasons brought about the formation of organic-poor pelites in thin beds.

The landlocked lagoon was recharged with water from the south-west, where a morphological barrier may also have existed, preventing the more saline dull bottom waters to recycle into the open sea.

It should be noted that two rock types may contain alginites. These are the clay-marl-siltstones and the aleuritic clay-marls. Both are exclusively laminated or finely bedded, grey or greenish-grey coloured. This intimate bedding is reflecting the alternations in the proportion of clay to silt grain size fractions, and also in the alginite and lime content, producing 1 to 100 mm thick individual beds.

The laminated sediments are nearly always free of macrofossils, and greyish-green coloured. The poorly bedded types generally enclose a rich mollusc fauna, and show light-grey or grey colours. The alginites are preferentially abundant in the first type.

The disappearance of mollusc fossils is in connection with the formation of highly organic — therefore oil-shale like — sediments.

Alginites are common throughout the Zsámbék Basin. This has been proven not only by the five Budajenő drillholes, but the geological log of the water-exploratory well drilled in 1975 between Zsámbék and Bő-2, too (Fig. 1).

It can be established that while the most favourable conditions for oil-shale sedimentation existed in the Mátyás and Strázsahegy Members during the Sarmatian, the richly algal rock-types in the lower part of the Lower Pannonian Formation, in the Laminated Marls indicate only a less favourable environment.

Detailed investigations were carried out on the alginitic clay-marl samples of Bő-2 borehole to determine the qualitative features and nature of oil-shales.

*Fischer - analysis data of Sarmatian boundary of the bore hole No. Bő-2 (Budajenő)*

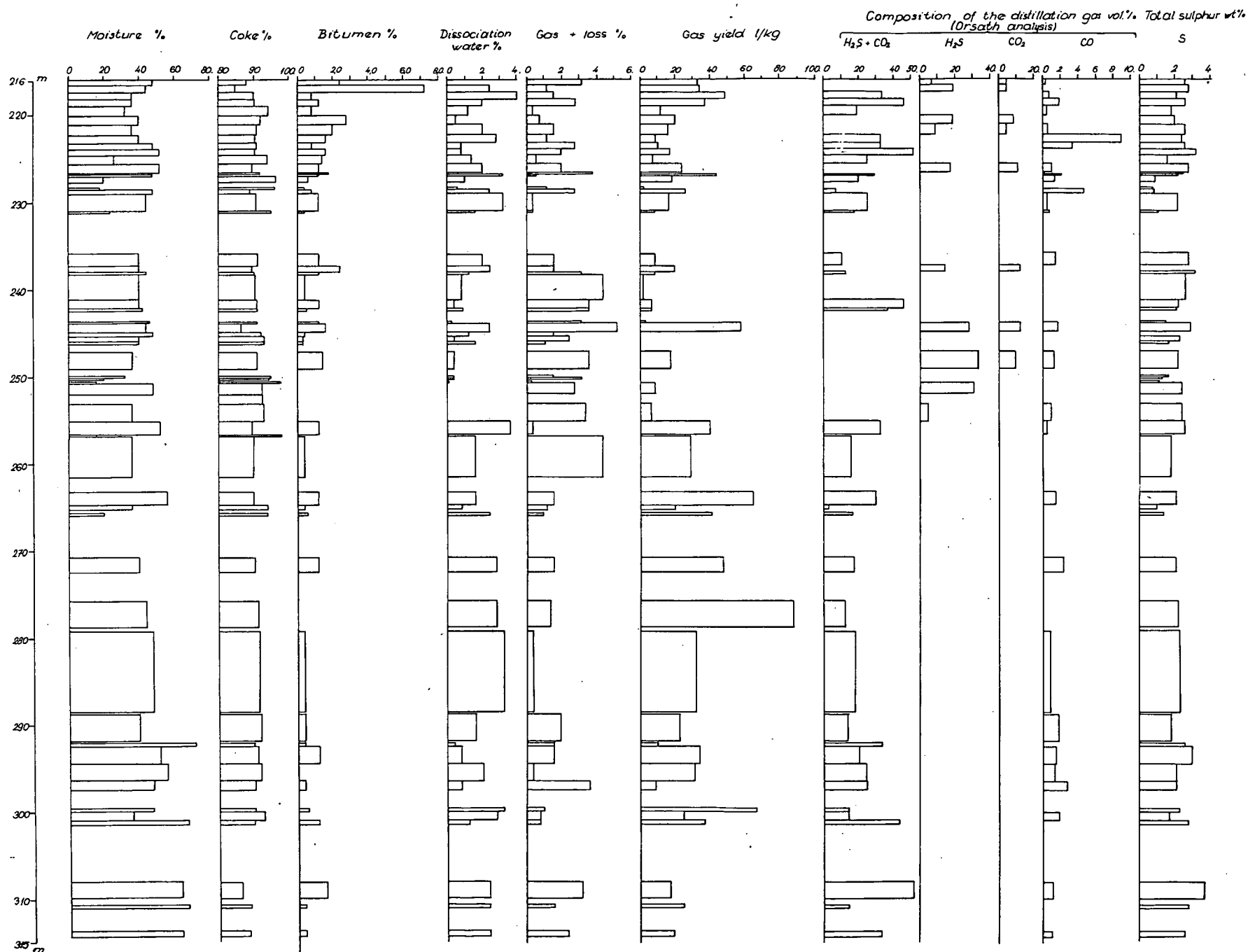


Fig. 11

Analytical results are given in *Fig. 11*.

According to our previous practice, the organic content of alginitic rocks has been determined by differential thermal analysis (DTA).

The lower clay-marl beds of the Laminated Marls in the Lower Pannonian Formation contain 8—9 wt% of organic material. This value abruptly rises to more than 20 wt% in the Sarmatian Strázsahegy Member.

This average value persists in the 216.0—228.5 m section of the hole, with a range between 17—22%. An exception is the clay-marl siltstone in the 221.1—222.3 m interval with more than 32 wt% organic content. Upwards in the sequence only one test gave more than 24 wt% value, the average was 15—17 wt%, ranging from 12 to 24%.

A further decrease of organic content is observed in the Csákvár Member, with few anomalous values over 27—28 wt% (261.7—261.85 m). The decrease in the average value is mainly attributed to the increasing abundance of evaporites in the middle part of the sequence.

At the base of Mátyás Member the organic content is 7—8 wt% — like on the Sarmatian-Pannonian boundary — i. e. abruptly reduced from 14—15 wt% of the silty clay-marl of Szomor Member.

Only sparse control analyses were made on the materials of Bő-2 to 6 boreholes. The results provided evidences of the existence of organic-rich alginites. An important find was the high organic content (5—29%) of the alginitic clay-marls of the Laminated Marls in the Lower Pannonian.

The tar content by the Fischer-method gives the best image about the distillable oil content of the alginites. Similarly to the previously detailed results of the DTA, this method showed the upper horizons of the Strázsahegy Member to have a higher tar content. 7.2 wt% maximum values were analyzed in the 216.6—217.4 m interval. Down to 237.9 m depth, 4 intersections with 3.5 m overall thickness have reached the lower limit of the oil-shale economic cut-off grade by API-standards (more than 2%) [K. E. STANFIELD *et al.*, 1951]. Between 216.0 and 244.8 m only 9 beds from the 27 contained less than 0.4 wt% of tar. This nearly 30 m thick interval has an average of 1.5 wt% tar content.

The tar content of the lower parts of the Strázsahegy Member as well as the Csákvár Member is lower than 1.0 wt%, though 1.4—1.6 wt% maxima were also recorded.

The distillation refinery gas yield of alginites, oil-shales, in Bő-2 borehole have also been investigated. The rocks of higher than 2 wt% tar content produced 14.5—34.0 l/kg values, with calorific values ranging between 316.6—890.6 kcal/m<sup>3</sup>. The high H<sub>2</sub>S content of gas (6.75—19.2 vol%) is rather due to the high pyrite concentration. The 2.0—3.0 vol% total sulphur content of the gas is unfavourably high.

Summarizing the analytical test results of the Budajenő oil-shales the following conclusions can be drawn. The organic content of the rocks is very high, though intensely varying between 3 and 32%. The ash-content is averaged at 90.9%, with 88.0 and 98.0 wt% minimum and maximum values, respectively. Their oil and gas yield is low. The tar content by Fischer's method is ranging between 7.2 wt% and zero, with 0.85% average value. Gas yield provided values from 0 up to 88.0 m<sup>3</sup>/t. The high sulphur content (2.26% average, 0.8—3.7 wt% range) is also unfavourable.

The DTA and Fischer analysis of samples from Budajenő has supported the earlier observations about the broad correlation of the tar content and the thermically analysed organic content (as determined by DTA) of the oil-shales. This correlation, however, should be treated with great caution, with consideration of all other factors.



In the oil-shale at Pula 30% organic content was accompanied by 4—8% tar content, 35—75% organics were coupled with 13—25% tar. At Gércse the oil-shales with 25% organics yielded only 1.2—5.5% tar. At Budajenő 20% average organic content produced 0.4—7.2% tar (average is 0.85%) in dry samples.

The alginites and diatomites of the Strázsahegy and Csákvár Members in Bő-3 showed fluorescent bitumoid content in 0.01—0.015 wt%. This value is twice as much as the bitumoid content of the Badenian rock types deeper in the section. An anomalously high value of 0.14 wt% was recorded in the diatomite-silty clay marl in the 307.0—307.2 m interval of the Bő-4 borehole as resin-asphalthene type bitumoid.

## CONCLUSIONS

In the Zsámbék Basin such paleogeographical environment and specific sedimentation processes prevailed from the beginning of the Miocene to the Early Pannonian, which were sufficient for the fast and extensive growth of "oil-producing" algae. These algae, accumulated in the sediments and diagenized produced oil-shales. However, taking their low tar content into consideration, only few samples reach economically important grades, and only one sample can be classified as low-grade oil-shale.

Their poor quality does not allow economic evaluation. One considerable depth is also an unfavorable factor.

Despite these discouraging economic value, this exploration has largely contributed to our knowledge of the genesis of oil-shales in the Carpathian basin. The detailed evaluation of the genesis of basin facies as oil-shales has provided further possibilities for future explorations.

## ACKNOWLEDGEMENT

The authors wish to express their thanks to all of colleagues and co-workers, who did richer in success this work by their special study of technical activity, namely to: DR. J. BODA, DR. M. BOHN-HAVAS, DR. M. KÖRÖS-HÓDI (Mollusca determination), DR. I. KÖRÖS-LÁNYI (Foraminifera det.), MISS M. SZÉLES (Ostracoda det.), DR. M. ÖRSZ-HAJÓS (Diatoma det.), MRS. GY. BAKÓ, MR. A. BARTHA, DR. M. EMSZT, MRS. K. GUZY, MRS. L. NEMES, MRS. I. SOHA, DR. T. SZABADOS, MISS T. SZÜCS, DR. V. TOLNAY (chemical analyses) DR. L. RAVASZ-BARANYAI (micromineralogy), DR. M. FÖLDVÁRI, MRS. L. RIMANÓCZI (DTA), DR. I. CORNIDES, MISS A. SZEMETHY (X-ray analysis), MRS. É. ÁRVA-SÓS, DR. K. BALOGH (radiometric age det.), MRS. F. HÓZER, MISS K. KISS, MRS. I. PETRÓCZY (sedimentary petrographical analyses), and finally to DR. Á. JÁMBOR for his valuable, intensive, and complex help.

## REFERENCES

- BATEMAN, A. E. [1950]: Economic mineral deposits. — New York.  
BATEMAN, A. E. [1951]: The formation of mineral deposits. — New York.  
BODA, J. [1959]: A magyarországi szarmata emelet gerinctelen faunája. — Földt. Int. Évk., 47, 569—862.  
CZERMINSKI, J. [1968]: Epigenetic Processes within Tortonian Sulphur-Bearing Series. — XXIII. International Geol. Cong., Vol. 8, 121—127.  
HAJÓS, M. [1977]: A budajenői Bő-2 sz. fúrás neogén képződményeinek Diatoma flórája. — Földt. Int. Évi Jel. 1975-ről, 383—400.  
HÁMOR, G., JÁMBOR, Á. [1971]: A magyarországi középsőmiocén. — Földt. Közlöny, 101, 91—102.

- JASKÓ, S. [1943]: A Bicskei öböl fejlődéstörténete, hegységszerkezete és fúrásai. — Beszámoló a Földt. Int. Vitaüléseiről, 5, 254—302.
- JÁMBOR, Á. [1967]: Adatok a Zsámbéki- és a Mányi medence neogénjének ismeretéhez. — Manuscript.
- JÁMBOR, Á. [1969]: A Budapest környéki neogén képződmények ösföldrajzi vizsgálata. — Földt. Int. Évi Jel. 1967-ről, 135—142.
- JÁMBOR, Á. [1971]: A magyarországi szarmata. — Földt. Közlöny, 101, 103—106.
- JÁMBOR, Á. [1976]: Üledékes kéntelep a Zsámbéki medence szarmata sorozatából. — Földt. Int. Évi Jel. 1974-ről, 301—306.
- JÁMBOR, Á. [1977]: Jelentés a mányi medencerész neogén képződményei szervesanyagtartalmának, olajpala és kén előfordulási lehetőségeinek vizsgálatáról. — Manuscript.
- JÁMBOR, Á., KORPÁS-HÓDI, M. [1971]: A pannóniai képződmények szintezési lehetőségei a Dunántúli-középhegység DK-i előterében. — Földt. Int. Évi Jel. 1969-ről, 155—192.
- JÁMBOR, Á., KORPÁS-HÓDI, M., KRETZOI, M. PÁLFALVY, I., RÁKOSI, L. [1971]: A dunántúli oligocén képződmények rétegtani problémái. — Földt. Int. Évi Jel. 1969-ről, 141—154.
- JÁMBOR, Á., KORPÁS, L., ORAVECZ, J., RAVASZ, Cs. [1976]: A budajenői Bő-2 sz. fúrás földtani eredményei. — Manuscript.
- JÁMBOR, Á., RADÓCZ, Gy. [1970]: Pectinariák Magyarország felsőneogénjéből. — Földt. Közlöny, 100, 360—371.
- JÁMBOR, Á., Solti, G. [1975]: Geological conditions of the pannonian oil-shale deposit recovered in the Balaton Highland and the Kemeneshát. — Acta Miner. Petr. Szeged, 22, 9—28.
- LJJUNGREN, P. [1960]: A sulfur mud formed through bacterial transformation of fumarolic hydrogen sulfide. — Econ. Geol., 55, no. 3.
- RAVASZ, Cs. [1975]: A kéntelepek keletkezése. — Manuscript.
- RAVASZ, Cs. [1977]: Prospekciós olajpala kutatás a Dunántúli középhegységben. — Manuscript.
- RAVASZ, Cs. [1978]: A budajenői kéntartalmú evaporitok ásvány-kőzettani vizsgálata. — Földt. Int. Évi Jel. 1976-ról, 177—188.
- STANFIELD, K. E. *et al.* [1951]: Properties of Colorado oil shale. — U. S. Bur. Mines Rept., Inv. 4825.
- SCHHELLMANN, G. A. [1959]: Formation of sulfur by reduction of anhydrite of Ras Gemsa, Egypt. — Econ. Geol., 54, no. 5.

*Manuscript received, November 8, 1979*

DR. CSABA RAVASZ  
DR. GÁBOR Solti  
Hungarian Geological Survey  
Népstadion út 14  
H-1442 Budapest, Hungary



## **PRELIMINARY STUDIES OF FLUORITE MINERALIZATION IN KALAT REGION, BALUCHISTAN PROVINCE, PAKISTAN**

**SYED IQBAL MOHSIN and GHULAM SARWAR**

### **ABSTRACT**

Fluorite-barite-massive sulphide mineralization has been noted in the Jurassic carbonate rocks at various localities in the collisional belt of Pakistan. Fluorite deposits are in the central part of the belt mainly in Kalat region while barite mineralization characterizes southern part of the belt. Sulphide minerals, of which only galena is notable, are associated with barite deposits. The characteristics and behaviour of fluorite deposits of Kalat region alongwith those of barite-massive sulphide deposits of the belt suggest a sedimentary origin of Mississippi-valley type.

### **INTRODUCTION**

Fluorite occurrences have been reported from several localities in the Cenozoic-Mesozoic folded belt of Pakistan. The host rock for each of the described deposit is Jurassic limestone. The mineral association varies from fluorite-calcite, barite-fluorite to barite-galena. Most of these occurrences are mere mineral showings except those of Kalat which are of some economic significance. Thin fluorite veins and stringers in Kalat were first located by the Geological Survey of Pakistan at Koh-i-Maran [BAKR, 1962]. Later a viable economic deposit was discovered by a mining company at Koh-i-Dilband [MOHSIN and SARWAR, 1974].

### **REGIONAL GEOLOGICAL SETTING**

The most dominant feature of the geology of the country is a folded belt running meridionally from Karachi in the south to Waziristan in the north separating Indian platform from Makran flysch zone (*Fig. 1*). The folded belt is a part of Alpine-Himalayan Cenozoic orogenic belt and consists of well known Kirthar and Sulaiman Ranges beside several parallel, less known but distinct ranges. The folded belt has variously been named as Axial belt (Hunting Survey Corporation, 1960), Baluchistan borderland [ZUBERI and DUBOIS, 1962], West Pakistan folded arch [SOKOLOV and SHAH, 66], Collisional mountain belt [SILLITOE, 1975], QUETTA line [GANSSE, 1966] and Southern axial ophiolite belt [STOCKLIN, 1977]. The oldest rocks exposed in the axial part of the belt are of Jurassic though some are considered to be older. Many prominent ranges and high peaks which are formed by this massive and resistant Jurassic limestone, generally represent the cores of the individual anticlines. The overlying Cretaceous and lower Tertiary formations are present on the flanks constituting the intervening syncline and are expressed as valleys. Most of the barite-fluorite mineralization is found in such anticlinal ridges including Mor range east of Bela, Shekran and Monar Talar hills near Khuzdar, Koh-i-Maran and Koh-i-Dilband in Kalat and Kakar ranges in Fort Sandeman.

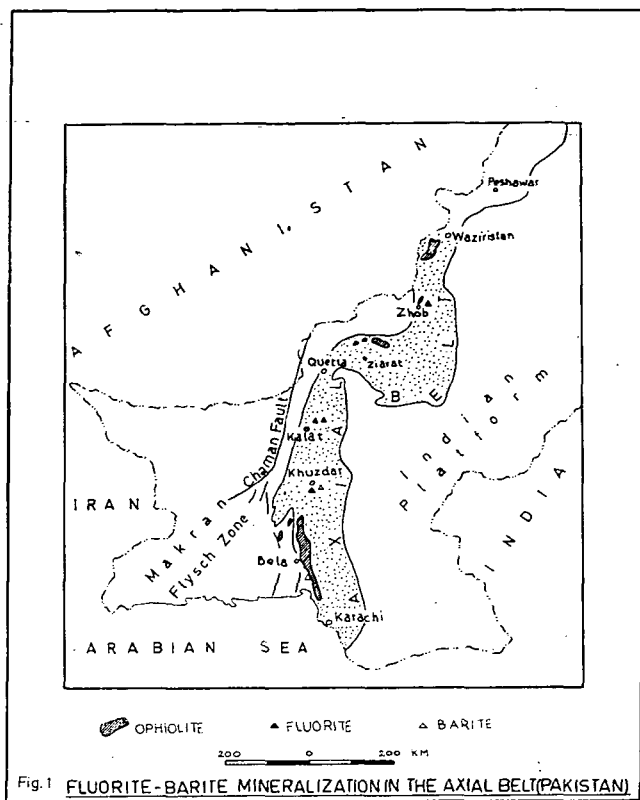


Fig. 1. Fluorite-barite mineralization in the Axial belt of Pakistan

Mesozoic rocks of several thousand meter thickness are exposed in the Axial belt. The western part of the Indian platform remained as land since the close of Vindhyan [SASTRI and DATTA, 1969] until the initial transgression in Triassic. By middle Jurassic marine conditions were well established and mainly carbonate rocks were deposited. The close of middle Jurassic is marked by a regressive phase and marine sedimentation again continues in the Cretaceous [FATMI, 1977].

#### STRATIGRAPHY OF THE REGION

Koh-i-Maran, Koh-i-Siah, Koh-i-Negrani and Koh-i-Dilband are parallel ranges wholly made up of Chiltan limestone of Jurassic age (Fig. 2). Each of these ridges represent the core of plunging or doubly plunging anticline. The fold axes are oriented NE-SW and generally plunge towards SW. Cretaceous shales and limestone formations such as those of Parh group and Moro formation occupy the intervening synclines. The flanks of each of the anticline are affected by strike faults of reverse movement running parallel to the anticlinal axes. The rocks of Parh group are more severely affected by strike faulting and are repeated several times. Koh-i-Maran and Koh-i-Siah are symmetrical open folds while Koh-i-Dilband is a broad undulating gentle folded structure. The fluorite deposits are located in an area where Chiltan li-

mestone is exposed as a very gently dipping plunging syncline flanked by similar gentle anticlines (Fig. 3). The rock units encountered in the mineralized area are shown in Table 1.

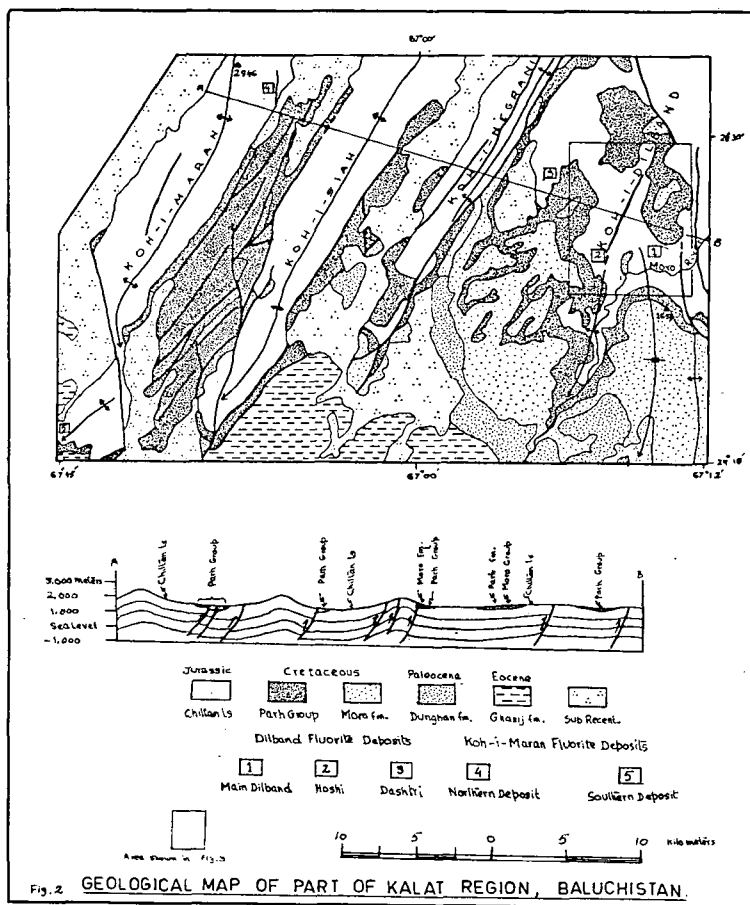


Fig. 2. Geological map of part of Kalat Region, Baluchistan.

The Chiltan limestone is well exposed in Koh-i-Maran while at Dilband about 1000 meters of limestone can be seen in the gorge of Moro river. The unit is generally microfossiliferous. However, few shell fragments were found on the top beds. Irregular patches of yellow, reddish, highly oolitic and pisolitic concretionary bed of ferruginous and clayey matter is found to mark the unconformity between Chiltan limestone and shales of Parh group. Such a bed is not a general feature of the Axial belt but is conspicuously present in the mineralized area. SHAH [1975] has also noted a ferruginous bed at the base of Cretaceous formation in Ziarat laterite area. The Parh group has been divided into three formations namely Sember formation, Goru formation and Parh limestone. In the Dilband fluorite area olive green shales of Sember formation with abundant belemnites, are poorly developed. Towards the top, the shales inter-

calate with clayey limestone and without any appreciable development of Goru formation, grade into Parh limestone. The upper contact of Parh limestone with Moro formation is disconformable, sharp and well exposed. Several small ridges in Dilband area are capped by Moro formation making steep excarps due to their superior resistance to weathering. Dunghan formation is not exposed in fluorite area either at Diltand or at Koh-i-Maran. However, the formation is present above Parh limestone in the synclinal structures.

#### FORMS OF THE ORE BODIES

Fluorite mineralization, associated with calcite, has taken place at Koh-i-Maran in the forms of veins in the upper part of Chiltan limestone. Although calcite veins are frequent in most of the rock units, fluorite has been found only in those that are

TABLE 1

##### *Stratigraphic Sequence in Kalat Region*

Age	Formation	Description	Thickness
Paleocene	Dunghan Formation	Dominantly massive, nodular, dark, gray, brown or creamy white limestone with subordinate olive coloured shale; coarse grained brownish green sandstone and minor pebbly conglomerate.	80 m
Upper Cretaceous	Moro Formation	Gray, medium-thick bedded argillaceous limestone with dark greenish gray calcareous shale; minor conglomerate and marl at the base.	100 m
Upper Cretaceous	Parh Group	Dominantly limestone of white cream, olive green or yellow colour; cherty, thin bedded, porcellaneous and argillaceous; with subordinate green shales and red marls in the lower part; ferruginous bed upto 5 m thick at the base.	
<hr/>			
	Unconformity		
Middle Jurassic	Chiltan Limestone	Thick bedded, massive, brownish gray to bluish gray limestone.	1000 m base not exposed

in the Jurassic limestone. These veins are found in fractures and joints in limestone, widening out to lenticular bodies or branching into multiple veins [PAKR, 1962]. Some of the veins are wedge-shaped and are aligned with the fold axis [MUŠLIM, 1972]. A few pockets of violet coloured fluorite crystals occur in Koh-i-Neghrani but no workable veins have so far been located.

The ore bodies, as observed in a number of pits and trenches at Diltand, are parallel to the bedding of the host rock and are flat lying tabular or lenticular masses [MOHSIN and SARWAR, 1974]. The flat nature of the bodies is obscured by the irregular contact with the limestone beds, by local bulging and by fracture filling which are inclined at steep angles to the general trend of bedding. The shallow depths of pits and trenches at present, do not reveal more than one layer in any single excavation. However, by comparison, they seem to occur at more than one level. The length and

breadth of individual ore bodies may vary from few meters to a hundred meters, while the thickness of any single, tabular body ranges from a few centimeters to two meters. The ore boundary is mostly gradational though only for a short distance and wall rock consists of disseminated fluorite grains in limestone.

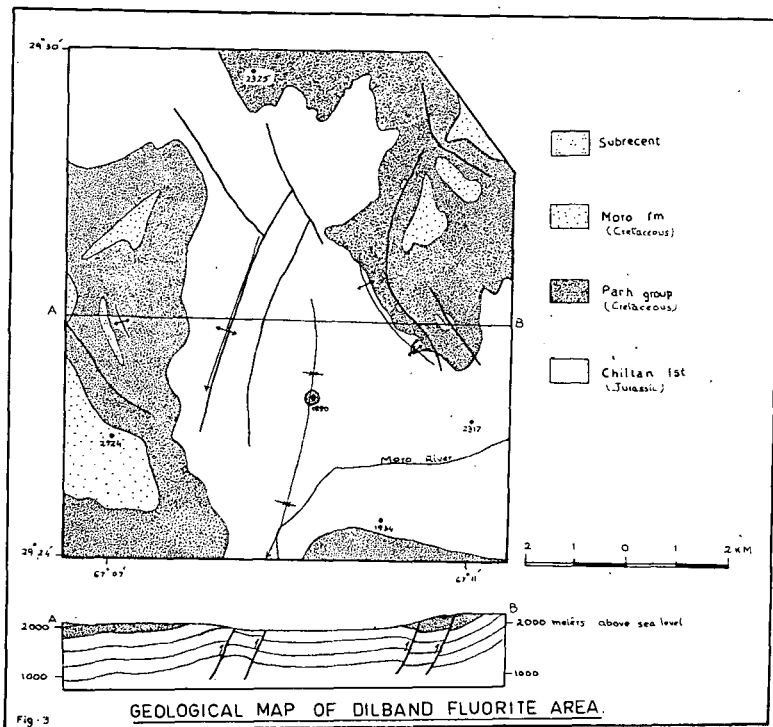


Fig. 3. Geological map of Dilband fluorite area

A number of solutional cavities filled by fluorite and calcite are found in several places in the Dilband area. One of the larger exposed ore body is oval shaped about 2 m wide and 4 m high, and appears to fill a solution cave in limestone. At few places crustified veins comprising of calcite and fluorite bands as well as fluorite bands of different hues and purity are seen. Vugs of a few centimeters to ten centimeter diameter are present in most of the thick ore bodies whether flat lying or cutting across the beddings. The vugs are lined with pink to violet coloured aggregate of cubic crystals of fluorite. The individual cubes range in size from 2 millimeter to 2 centimeter. Several layers of fluorite packed up in a comb fashion often make a thick tabular ore body parallel to the bedding.

#### MINERALOGY, GRADE AND RESERVES

The mineralogy of the ore is simple being composed of fluorite and calcite. Tabular crystals of barite associated with fluorite have been noted only in the veins at the southern faulted end of Koh-i-Maran anticline. Occasionally a pyrite grain can be seen in the fluorspar lumps. The lumps mined at Koh-i-Maran are milky white or



buff coloured. Fluorite at Dilband varies in colour from white to yellow, pink, red, violet, colourless and brown, in transparency from opaque to transparent and in crystallinity from massive to perfect crystals. The transparent variety displays an octahedral cleavage. Calcite is either mixed with fluorite as grains or forms aggregate of rhombohedral crystals which are transparent to milky white. The ore mined at Dilband can be divided in three grades:

1. Transparent; colourless, pink or violet; crystalline variety.
2. Translucent; white, yellow, red; crystalline aggregate.
3. Opaque; brown coloured; massive variety.

The first variety is of high purity containing more than 97% of  $\text{CaF}_2$  and is of acid grade. It does not contain more than 1.0% silica and sulphur is present only in traces. The second variety consists of varied coloured fluorspar and range in calcium fluorite content from 90 to 96%. The third variety is not very different in chemical composition from the second variety and both can be grouped in ceramic grade. Fluorite mixed with calcite or from the boundaries where it is disseminated in limestone may have as low as 40 to 50%  $\text{CaF}_2$ . The second variety is the prevalent type in Dilband area. Chemical analyses of one acid grade and three ceramic grade ores are shown in the Table 2.

TABLE 2

*Chemical Analysis of Fluorspar*

	1	2	3	4
$\text{CaF}_2$	97.89	95.47	93.22	91.77
$\text{CaCO}_3$	0.40	1.70	2.50	3.84
$\text{Fe}_2\text{O}_3$	0.20	0.25	2.01	0.95
$\text{SiO}_2$	0.26	1.48	1.88	1.49
$\text{Al}_2\text{O}_3$	0.94	1.51	1.03	1.00

BAKR [1962] has measured a number of lean veins and stringers of fluorite at the northern part of Koh-i-Maran and estimates about 100 tons to be present in the veins. AHMAD [1969] in the Mineral Directory has indicated 1400 tons of fluorite at Koh-i-Maran.

Fluorite deposits of Dilband were opened in 1971 when a number of pits and trenches were made and about 2000 tons were produced in that year. No further work was undertaken until the lease disputes were settled in 1978 and plans are now under-way for systematic work. No exploratory holes have been drilled to ascertain the shape and size of the bodies at depths. However, to gain some insight about the quantity of the ore, the area is divided into blocks where clusters of pits and trenches are present. The blocks are about 300 m long, 100 to 125 m wide and about one meter thick. The ore body in each block is assumed to be tabular in shape. Thus as a preliminary statement of reserve 93,350 tons of fluorite is estimated in three blocks namely Main Dilaband, Hoshi and Dashtari lease holdings.

#### FORMATION AND LOCALIZATION OF ORE

Fluorite alongwith barite and some sulphide minerals appears to be stratabound in the Axial belt, localized within the Jurassic carbonate sediments of Indo-Pakistan platform. The host rocks are invariably brown to gray, medium-thick bedded limestone which may be massive, oolitic, nodular or reefoid at places. Dolomitization is

appreciable [AHMAD, 1974]. Shales are associated as minor to subordinate constituents. Within the host rocks the ore bodies occur both as veins e. g. at Koh-i-Maran and tabular or lenticular concordant bodies e. g. at Dilband. The ore may be restricted to top beds of the Jurassic limestone and fills such distinct solutional features as have been described by CALLAHAN [1967] from the Mississippi valley. The solutional features at Dilband developed during the hiatus that preceded the deposition of the overlying Cretaceous shales. MUSLIM [1972] has also noted that mineralization at Koh-i-Maran is confined to the top beds of Chiltan limestone which are above the intercalated shale horizon; the limestone beds below the shale are barren. But in southern areas of Khuzdar and Lasbela, the ore being generally concordant and lenticular does not appear to be restricted only to the top horizons of the Jurassic limestone [MOHSIN and SARWAR, in prep.]. The mineralization, therefore, probably follows several levels within Jurassic sequence. At Dilband, Chiltan limestone is overlain by shales of Parh group with a distinct unconformity marked by a ferruginous bed which varies from one to three meters in thickness. The ore appears to be localized below the unconformity on a mild karst topography. The ore is observed to be stratiform, though small cross cutting veins do occur; lining of cavities, filling of collapse breccia and pipe-like bodies are also common features.

The ores at various places in the belt have invariably a simple mineralogy and wall rock alteration is only slightly discernible. SHCHEGLOV [1969] mentions the presence of bitumen inclusions in fluorite from Koh-i-Maran. B. L. HEDGE [personal com.] has collected samples with inclusions as big as 1 mm with air bubble in the center. This indicates a low temperature of formation, generally in the range of 100—150 °C. Both cavity-filling and replacement processes appear to have been active. The distribution of minerals in somewhat zoned veins and relationship between calcite, fluorite and unreplaced limestone in filled solutional caves, indicate the stages of mineralization. A first essentially carbonate stage when the cavities in limestone were filled by calcite and a second fluorite-calcite stage when the brines deposited fluorite or replaced host rocks, can be identified. A final calcite stage probably completes the ore formation process.

Lateral zoning of the constituent minerals in a N-S direction parallel to the axis of the belt is quite distinct. At present it is defined by two major minerals of the belt namely fluorite and barite; the former more important in northern areas of Fort Sandeman-Quetta-Kalat while the later is prominent towards the south in Khuzdar-Lasbela region. Sulphide minerals are known to occur only in traces in the northern areas and although their proportion seems to increase southward, no economic concentrations are known as yet. Among sulphides, galena seems to be a more common minor associate to barite while sphalerite, chalcopyrite, pyrite and tetrahedrite are so far seen only in traces.

Although igneous rocks are present within the limits of the Axial belt, they do not appear to be related with the mineralization in question. Most of these igneous occurrences are of ultramafic rocks, pillow lavas and dolerite sills and dykes known as Muslimbagh and Lasbela ophiolite complexes. These are interpreted as oceanic crust and according to ALLEMAN [1979] the obduction took place in Paleocene. If the ores are of Jurassic age, as has been argued below, then the igneous activity in the region is younger than the mineralization.

Stratabound deposits confined to particular stratigraphic horizons and concordant on large scale but discordant on a small scale, have been discussed by a large number of workers. The various possibilities of origin proposed can be grouped into two: *viz.* those related to sedimentation and those related to igneous solutions. Stratabound ores have recently been recognized in Pakistan and only preliminary studies have been undertaken. However, both possibilities of origin have already been proposed.

SHCHEGLOV [1969] has considered the fluorite deposits of Fort Sandeman and Koh-i-Maran region and barite-massive sulphide deposits of Khuzdar-Lasbela region as two distinctly different types. He argues that the former are epithermal veins of post-major folding (post-Oligocene) ages as they occupy the fracture zones cutting fold structures. According to him the fluorite deposits are endogenous being formed during the change of geosynclinal regime to the platformic one is the Neogene times. This very closely compares with the placement of fluorite by BILIBIN [1968] in his scheme of endogenetic mineralization in mobile belt where fluorite along with lead and zinc sulphides is considered to form telethermal deposits at the terminal stage of evolution of a mobile belt. For the barite-massive sulphide deposits at Khuzdar-Lasbela region SHCHEGLOV [1969] favours formation during an early stage of development of Baluchistan geosyncline and assigns a late Cretaceous-late Paleogene age.

In view of the characteristics of the deposits described above, SHCHEGLOV's views do not appear to be well justified. There is no convincing evidence for considering the fluorite and barite-massive sulphide deposits as of different stages of geosynclinal evolution at widely separated time intervals. The fluorite filled fractures cutting the folded structure could indicate remobilization of a much older mineralization. Similarly evidence for fluorite-barite-sulphide mineralization being of endogenic igneous derivation is also lacking.

A number of possibilities have been envisaged regarding the deposition of stratabound ores by sedimentary processes which include direct precipitation from sea water or precipitation from submarine exhalations. Another mechanism is the transport of metals by the pore-space fluids expelled during compaction of sediments with subsequent redeposition at suitable sites [JACKSON and BEALES, 1967]. DUNHAM [1964] has gone so far as to evolve neptunist concept in deposition of stratiform Keupferschiefermarl slate at Mansfeld, Germany.

The known characteristics of fluorite deposits of Kalat region along with those of barite-massive sulphide deposits of the Axial belt in general suggest a sedimentary origin of late-diagenetic-epigenetic type. MUSLIM [1972] has proposed that generation of the gaseous phase containing halides within Jurassic sediments could have altered the limestones. SILLITOE [1975] designates these deposits as Mississippi-valley type and suggests that these could have been precipitated by connate brine within the continental shelf bordering north of Gondwanaland prior to the separation of Indian Plate. The incipient rifting of Gondwanaland may have induced a rise in geothermal gradient which promoted the movement of brine. Although this appears to be a probable mode of origin, no related tectonomagmatic features such as grabens and alkali magmatic rocks have so far been noted in the Axial belt.

## ACKNOWLEDGEMENTS

We are thankful to PROF. M. VALIULLAH, MR. AQIL FAROOQI and MR. NASIM AHMAD for reading the manuscript critically. Thanks are also due to MR. M. U. QAUDRI for helping us in drawing figures.

## REFERENCES

- AHMAD, Z. [1969]: Directory of mineral deposits of Pakistan, Pakistan Geol. Surv. Recs. v. **15**, pt. 3, 220 p.
- AHMAD, H. [1974]: Interim report on dolomite deposits of Chiltan Range, Baluchistan, Pakistan: Pakistan Geol. Surv. Pre-Pub. Issue No. **85**, 8 p.
- ALLEMAN, F. [1974]: Time of emplacement of the Zhob Valley Ophiolites and Bela Ophiolites, in: FARAH and DE JONG (eds.), Geodynamics of Pakistan, Pak. Geol. Surv.
- BAKR, M. A. [1962]: Fluorspar deposits in the northern part of Koh-i-Maran Range, Kalat division, West Pakistan, Pakistan Geol. Surv. Recs. v. **9**, pt. 2, 7 p.
- BILIBIK, Y. A. [1968]: Metallogenic provinces and metallogenic epochs, Geol. Bull. Dept. Geology, Queens College Press, Y. Y.
- CALLAHAK, W. H. [1967]: Some spatial and temporal aspects of the localization of Mississippi-Valley-Appalachian type ore deposits, Econ. Geol. Monograph No. **3**, p. 14—19.
- DUNHAM, K. C. [1964]: Neptunist concepts in ore genesis, Econ. Geol. v. **59**, p. 2—21.
- FATMI, A. N. [1977]: Mesozoic, in S. M. I. SHAH (ed.) Stratigraphy of Pakistan, Pakistan Geol. Surv., Mems. v. **12**, 132 p.
- GANSSER, A. [1966]: The Indian ocean and Himalayas, Eclogae Geol. Helvetiae, v. **59**, p. 831—848.
- HUNTING SURVEY CORP. [1961]: Reconnaissance geology of part of West Pakistan, (Colombo Plan Cooperative Project), Canada Govt. Toronto, 550 p.
- JACKSON, S. A. and BEALES, P. W. [1967]: An aspect of sedimentary basin evolution: the concentration of Mississippi Valley-type ores during late stages of diagenesis, Bull. Can. Petrol. Geol., v. **15**, p. 383—433.
- MOHSIN, S. I. and SARWAR, G. [1974]: Geology of Dilband Fluorite Deposit, Pakistan Geol. Surv., Geonews, v. **4**, p. 24—30. An occurrence of barite at Gacheri Dhora, Pakistan. In press.
- MUSLIM, M. [1972]: Geology and geochemistry of fluorspar deposits Koh-i-Maram, Pakistan Geol. Surv., Geonews, v. **2**, p. 29—31.
- SASTRI, V. V. and DATTA, A. K. [1969]: Tectonic setting and Meso-Cenozoic palaeogeography of western part of the Indian subcontinent. ECAFE Symposium on the development of Petroleum Resources of Asia and Far East. p. 1—14.
- SHAH, S. H. A. [1975]: The laterite band of Ziarat, Baluchistan, Pakistan, Pakistan Geol. Surv. Recs. v. **37**, p. 17—26.
- SHCHEGLOV, A. D. [1969]: Main features of endogeneous metallogeny of the southern part of West Pakistan, Pakistan Geol. Surv. Mems. v. **7**, 12 p.
- SILLITOE, R. H. [1975]: Metallogenic evolution of a collisional mountain belt in Pakistan, Pakistan Geol. Surv. Recs. v. **34**, 16 p.
- SOKOLOV, B. A. and S. H. A. SHAH [1966]: Major tectonic features of Pakistan, Science and Industry v. **4**, No. 3, p. 175—199.
- STOCKLIN, J. [1977]: Structural correlation of the Alpine ranges between Iran and Central Asia, Mem. h. ser. Sock. Geol. France, no. **8**, p. 333—353.
- ZUBERI, W. A. and DUBOIS, E. P. [1962]: Basin architecture, West Pakistan, ECAFE Symposium on Development of Petroleum Resources of Asia and Far East, p. 272—275.

*Manuscript received, July 30, 1979*

DR. SYED IQBAL MOHSIN  
Department of Geology  
University of Karachi  
Karachi, Pakistan  
DR. GHULAM SARWAR  
Department of Geology  
University of Cincinnati  
Cincinnati, Ohio, 45221, USA



## PHOSPHORITES IN SINJAR FORMATION OF SULAIMANIAH AREA, IRAQ

I. AL-FADHLI and KHALIL AHMED MALLICK

### ABSTRACT

Phosphorites in Sinjar Limestone Formation of Paleocene age have been discovered and investigated for their petrographic and geochemical characters. The study of the rocks associated with the phosphorites was also made to determine the sources of the phosphorites and the degree of correspondence with the associated limestone beds.

The two horizons of phosphorites in the same stratigraphic succession are separated by 43 feet thick limestone beds which are completely non-phosphatic. The maximum content of  $P_2O_5$  in lower phosphorite horizon is 4.061% and the minimum is 1.460%. The upper horizon of the phosphorite has a maximum of 5.947% and the minimum of 1.360%  $P_2O_5$  at the top of this horizon.

It is concluded that the layered phosphorite beds are recycled sedimentary deposits from the near by source. No effects of phosphatization could be observed on the associated rocks.

Five phases of sedimentation representing different physico-chemical controls have been established on the bases of physical properties, chemical composition, petrographic characteristics and the fossils present in the beds. This discovery of phosphorites appeared very helpful in establishing the yet not reported linkage in the regional distribution of phosphorites of Paleocene age in Zagros Mountains of Iran in the east and Syria and Turkey on the west of Iraq.

### INTRODUCTION

Informations regarding the phosphate deposits of Iraq are found in many of the records of the Geological Survey of Iraq. J. A. SMITH an English geologist is considered pioneer in discovering the phosphate deposit of Paleocene age in Rutba area. His discovery was followed by a group of geologists in collaboration with Soviet specialists in 1960—62, to prospect over a larger area and to make a detail geological exploration and exploitation of Rutba phosphate deposit.

Later on, in 1964—65 investigation for phosphate deposits in Akashat area was made and ultimately suggestions were made for the exploitation of the reserve.

In spite of the fact that numerous occurrences of phosphorites in the Cretaceous, Paleocene and Eocene rocks of the Zagros folded belt have been found in Iran, Syria and Turkey but no attention was paid to prospect the continuation of the same rock units exposed in north eastern part of Iraq. Moreover, the available reports regarding the phosphate deposits of Akashat and Rutba do not provide any informations regarding the genesis of the phosphorites. Keeping in view the above facts, the present authors became more inquisitive to investigate Sinjar Limestone Formation of Paleocene age from Zagros Mountains of Sulaimaniah area in north eastern Iraq, with the possibilities of finding phosphorites in this formation. Although the phosphorites discovered during the present work are not of high grade but are useful enough to trace the continuation of phosphorites deposited in the Zagros trough

extending from Iran in the south east to Syria and Turkey in the north west of Iraq during Paleocene period.

The present paper is to report the discovery of phosphorite beds in Sinjar Limestone Formation of Paleocene age exposed in Sulaimaniah area of Iraq. Effort has also been made to discuss the genesis of the phosphorite in the light of chemical analysis data, petrographic investigations and the content of acid insoluble residues in addition to field evidences. This attempt is first of its kind for the study of Sinjar Formation.

## GEOLOGICAL DESCRIPTION OF THE AREA

The areas under present investigation are Kani Jinnah, Bazyan and Dukan of Sulaimaniah county in north eastern Iraq (*Fig. 1*). These areas are on the western flank of a major anticline in this region, trending northwest southeast in the Zagros Mountain belt of Iraq. The rocks exposed in the areas are of Sheranish and Tanjero Formations, Sinjar and Kolosh Formations, and Gercus Formation of upper Cretaceous, Paleocene and Miocene ages, respectively.

The rocks of Sheranish Formation are thinly bedded limestone and blue marl of transgressive cycle which tongue into the reef and fore reef deposits of Campanian age. Tanjero Formation is of clastics such as siltstones, shales and marls of various shades of colours, compactness and hardness. It is contemporaneous of Sheranish Formation.

Sinjar Formation is composed of a varieties of limestones which differ in colours, compactness, argillaceous matter contents and hardness. The total thickness of the formation in the areas of study is 530 feet. The content of microfossils in the beds increases in the upper part. Kolosh Formation of clastics is contemporaneous of Sinjar Limestone Formation and the main rocks of this formation are silstones, marls and shales of dark brown, grey and black colours. The shale is gypsiferous to some extent. A-aliji Formation is another contemporaneous formation of Sinjar and Kolosh Formations but it is not exposed in the areas under present investigation. It is well exposed in Sinjar Mountains which represents the type area for Sinjar Forma-

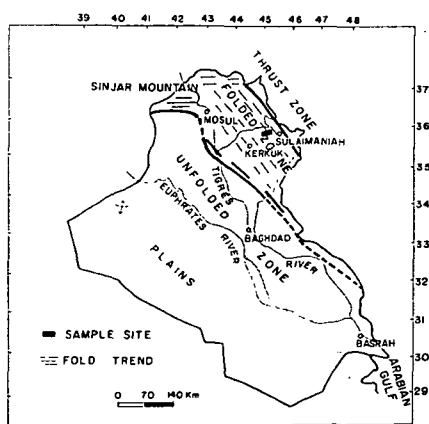


*Fig. 1.* Tectonic map of Iraq showing location of sample site

tion of Paleocene age in Iraq. It is mainly composed of shale, argillaceous marls and marly limestones. A-ali Formation is considered to be off shore deposit of Paleocene age on the basis of fossil contents and intertonguing with Sinjar Formation.

Gercus Formation overlies Sinjar and Kolosh Formations unconformably. The rocks are reddish brown and maroon coloured shales, siltstones and sandstones of different grades.

#### DESCRIPTION OF PHOSPHATIC BEDS

The phosphatic beds of Sinjar Limestone Formation are attributed to Paleocene in age on the basis of fossil evidences. The phosphatic beds of Sinjar Formation are contemporaneous to the phosphatic sediments of Akashat and Rutba areas which are in analogy with geological section of the adjacent regions in Jordan and Syria (open file report No. 1 and 2, 1961 & 1963, Geol. Surv. of Iraq).

Sinjar Formation has eight phosphatic beds which differ from each other in  $P_2O_5$  contents ranging from 1.615% to 5.930% and the petrographic characteristics. The percentage of acid insoluble residues is also not similar. Kolosh Formation which is mainly composed of siltstones, shales and marls intertongues with Sinjar Limestone Formation.

The descriptions of the phosphatic beds of Sinjar Limestone Formation are given according to stratigraphic succession and represent the beds from the lower part to the upper part of the section sampled for the present investigation. The number shows to the phosphatic bed exposed and the number in bracket is the actual number of the same bed in the section.



Fig. 2. Phosphatic limestone bed in Sinjar Formation of Kinn Jinnah area showing weathering effects similar to argillaceous limestone.

#### Phosphatic bed No. 1 (SK—3)

The first phosphatic bed encountered in the section measured for the present work, overlies light grey and brown banded limestone of variable hardness. Megascopically the phosphatic bed is buff coloured, dense and hard limestone. Calcite grains segregation appearing colourless to light grey under higher magnification of



hand lense can be seen. The bed is 6 feet thick and the texture of the limestone is clastic. The content of  $P_2O_5$  in the sample of this bed was 1.766%.

In thin section of the rock, cluster of sparry calcite grains with random orientation are quite prominent. Some of the fossil fragments which are partly or completely micritized can be seen. Partial micritization is in the inner parts of the fossil fragments. Peloids and argillaceous intraclasts of cylindrical to triangular shape are also present.

#### Phosphatic bed No. 2 (SK—4)

This immediately overlies phosphatic bed No. 1 and is marked by pronounced bedding. The colour of the rock is light grey with brown patches of ferruginous and argillaceous matters. The sample of this bed exhibits clastic texture due to the presence of calcite and aragonite seggregations and brown specks of ferro-argillaceous matters. The clastic texture is very easily visible with the aid of a magnifying lense and in thin section. The thickness of the bed is about 6 feet and  $P_2O_5$  content is 3.601%.

In thin section of the rock an aggregation of collichane and dahllite in pellets and lithic grains of variable sizes and shapes, embedded in calcareous matrix are observable. The corners and edges of the argillaceous grains are sharp and indicate very little effects of transport. Few lumps containing argillaceous fragments and microfossils exhibit micritization effects quite prominently. Development of sparry calcite and micrites due to recrystallization and diagenetic effects can easily be seen in calcareous matrix. It appears that the rock was porous in the beginning as a result of which intergranular spaces became the centre for the development of sparry calcite and micrites. Micritization is also visible in the argillaceous pellets, the clastics and microfossils (*Fig. 3-A*).

#### Phosphatic bed No. 3 (SK—5)

This bed overlies phosphatic bed No. 2 with well marked bedding plane and the characters like colour, hardness and to some extent the texture of the rock. The bed is mottled by light and dark brown shades and exhibits medium grained clastic texture. The light brown patches appeared to be clusters of calcite grains and darker parts in the rock specimen were found to be argillaceous matter when examined with the help of magnifying lense. The thickness of the bed is 21 feet and the  $P_2O_5$  content is 4.061%. In thin section it appears as lithic pelleted limestone which is highly micritized. Small clusters of calcite grains with random orientation are also present in argillaceous parts. Microfossils are not common but algal characters are visible.

#### Phosphatic bed No. 4 (SK—7)

It is not immediately above phosphatic bed No. 3 but a bed of light grey limestone of 10 feet thickness and free from phosphatic content is present between the two phosphatic beds.

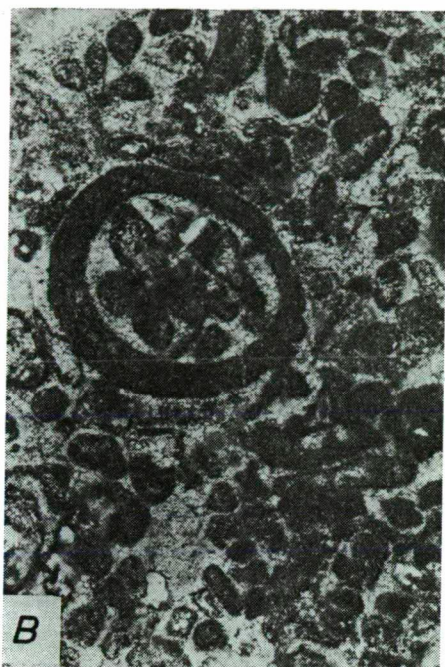
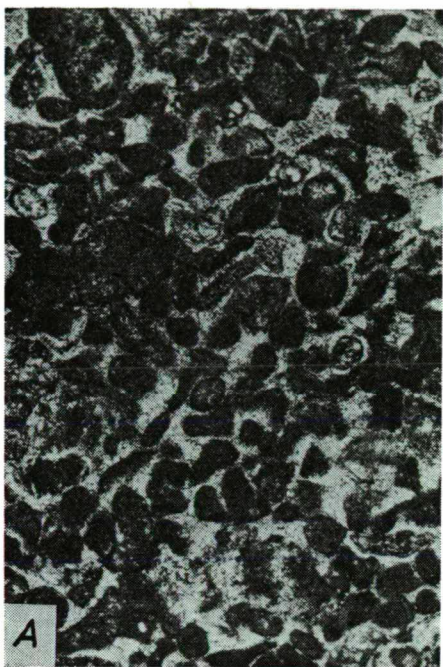
*Fig. 3.* Photomicrographs from phosphorite deposits, Sulaimaniah area, North Eastern Iraq

A) An aggregate of argillaceous intraclasts, pellets and some microfossils embedded in calcareous matrix. Micritization specially in the central parts of the microfossils. Pressure solution effects are also visible. Polarized light,  $\times 50.4$

B) Ooid showing concentric layers containing micrites, sparry calcite, collichane and dahllite are visible. Sparry calcite developed due to pressure solution effects is also observable. Polarized light,  $\times 50.4$

C) Lump, intraclast and peloids embedded in calcareous matrix. Micritization prominent. Collichane and dahllite and pressure solution effects can be seen. Polarized light,  $\times 50.4$

D) Phosphatic pisolite containing collichane and dahllite is embedded in algal and calcareous matrix. Micrites prominent. Polarized light,  $\times 50.4$



This phosphatic bed is reddish brown hard and compact. It appears like a lithic limestone but under higher magnification of hand lens, recrystallization effects are observable. This bed is 5 feet thick and the  $P_2O_5$  content is 1.46C%.

The thin section of the rock exhibits an aggregate of intraclasts, peloids and microfossils embedded in calcareous matrix and is recrystallized to a great extent into sparry calcite and micrites. Lumps encircling intraclasts were also found. Micritization is also well pronounced in the peloids, intraclasts and microfossils (*Fig. 3-B*).

#### Phosphatic bed No. 5 (SK—12)

Phosphatic bed No. 5 is separated from No. 4 by 43 feet thick limestone beds which are completely devoid of phosphatic contents. The limestone beds between the phosphatic beds are of different colours and textures and are marked by bedding planes. The phosphatic bed is mottled with light yellow and brown shades of colours. The texture of the rock is fine-grained. Under higher magnification of the hand lense, the light yellow patches show cluster of aragonite grains and the brown shades are dominated by argillaceous material. The bed is 19 feet thick and the  $P_2O_5$  content is 2.291%.

In thin section ooids with concentric structure marked by micritized stringes and darker rings of argillaceous and organic matters are quite pronounced. Sparry calcite and micrites can also be seen around the ooids (*Fig. 3-C*).

#### Phosphatic bed No. 6 (SK—13)

The colour of the rock is reddish brown and overlies phosphatic bed No. 5. It is very hard, compact and fine grained. However, under higher magnification of the hand lense reddish brown calcite grains and pink patches of argillaceous matter are easily observable. The thickness of the bed is 18 feet and  $P_2O_5$  content is 3.166%.

In thin sections, peloids, lumps and microfossils in calcareous matrix can easily be seen. It appears similar in characters to bed No. 4. Micrites and sparry calcite are well pronounced in the matrix. Some of the fossil fragments are completely micritized. The effects of micritization in the peloids and lumps can also be seen.

#### Phosphatic bed No. 7 (SK—14)

It is light brown, hard and massive calcareous bed and overlies bed No. 6. Clusters of calcite grains are visible with the help of magnifying lense. The thickness of the bed is 20 feet and  $P_2O_5$  content is 5.947% which is the highest content in all the phosphatic beds of this area (Table 1).

*Fig. 4.* Photomicrographs from the non-phosphatic beds associated with the phosphorite deposits of Sulaimaniah area, North Eastern Iraq.

A) Mud supported micritized shell fragments with argillaceous peloids and intraclasts embedded in argillo-calcareous matrix. Pressure solution effects not very prominent. Polarized light,  $\times 50.4$ ;

B) Skeletal limestone with argillaceous intraclasts. Effects of micritization and pressure solution prominent and sparry calcite present. Matrix argillo-calcareous. Polarized light,  $\times 50.4$ ;

C) Banded algal structure with ooids and fine shell fragments. Micritization and pressure solution effects prominent. Matrix calcaro-carbonaceous. Polarized light,  $\times 50.4$

D) Argillaceous pellets, intraclasts and shell fragments within tubicular part of a mud feeding organism and around it, micritization and pressure. solution effects prominent. Sparry calcite and dolomite can be seen. Crossed Nicols,  $\times 50.4$



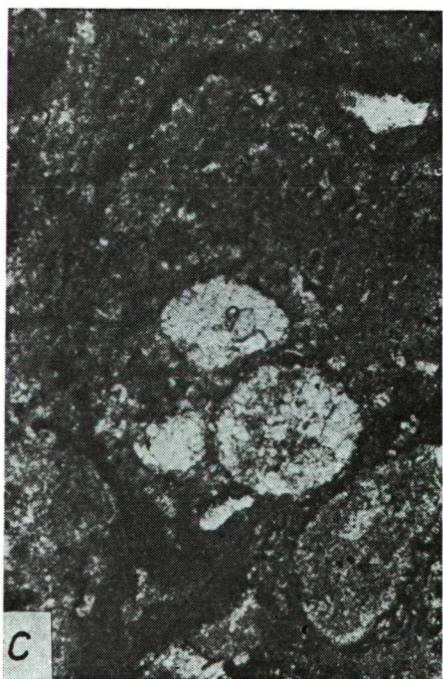
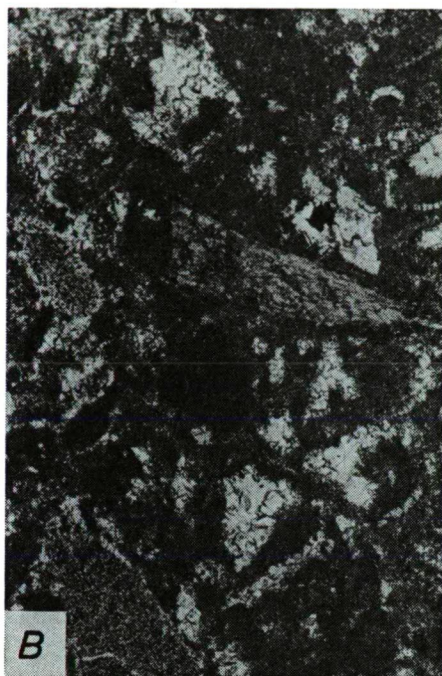


TABLE 1

*Chemical analysis data of the phosphorites and the associated rocks of Sinjar Formation*

Bed No.	Thickness in feet	CaO %	MgO %	P <sub>2</sub> O <sub>5</sub> %	AIR %	SiO <sub>2</sub> %
SK-2	10	49.532	6.341	ND	4.00	3.800
SK-3	6	51.301	4.634	1.766	5.40	2.373
SK-4	6	51.700	3.627	3.601	5.61	1.216
SK-5	21	54.008	3.573	4.061	7.79	2.929
SK-6	10	52.259	7.054	ND	3.82	0.328
SK-7	5	59.371	2.016	1.460	2.95	0.490
SK-8	2	48.290	8.920	ND	1.73	0.688
SK-9	16	46.111	5.524	ND	4.98	1.644
SK-10	17	47.566	7.039	ND	15.30	5.389
SK-11	8	48.686	4.735	ND	3.04	0.271
SK-12	19	54.935	3.526	2.291	4.59	0.980
SK-13	18	52.554	3.526	3.166	4.82	0.850
SK-14	20	53.275	9.120	5.947	6.38	0.329
SK-15	17	47.882	7.482	1.360	7.30	3.564
SK-16	51	53.701	6.517	ND	1.35	0.199

NB: AIR stands for acid insoluble residues and ND for not detectable.

In thin sections, argillaceous pellets of variable sizes are present in addition to argillaceous intraclasts which are angular and subangular in shapes. Other characteristics visible in thin sections are the same as in beds 5 and 6, except that sparry calcite appears to be more in percentage in this rock.

#### Phosphatic bed No. 8 (SK-15)

It immediately overlies the phosphatic bed No. 7. It is brown lithic limestone which is hard and massive in appearance. Dark brown specks can be seen in the rock samples. The thickness of the bed is 17 feet and P<sub>2</sub>O<sub>5</sub> content is 1.360%. In thin section recrystallized fossil fragments in argillaceous matrix can be seen. Algal bands and micritization of matrix are prominent. (*Fig. 3-D*).

The associated limestone beds which are completely devoid of phosphatic contents were found to be prominently dissimilar in their petrographic characteristics also. The 43 feet thick beds of limestones present between the lower and upper phosphatic horizons are of variable petrographic characters. The colours of the rocks are light and dark brown, pink and mottled of various tint. Generally the rocks are dense, hard and break with sub-conchoidal fractures. Clastic texture is not well pronounced in hand specimens. Action with dilute hydrochloric acid is strong. Recrystallization effects are observable with the help of magnifying lense.

The study of the thin sections of these rocks show the presence of micritized fossil fragments and some lithic peloids embedded in calcareo-argillaceous matrix (*Fig. 4-A-B*). Algal limestones containing calcareous peloids, fossil fragments and exhibiting prominent banded algal structures were observed. The peloids and fossil fragments show variable degree of recrystallization and replacements (*Fig. 4-C*). Tubular structures containing lithic intraclasts and fossil fragments in calcareous matrix were also seen (*Fig. 4-D*). The tubular structure is, perhaps, of some mud feeding organism. The development of sparry calcite and dolomite were also observable in thin sections. Micritization effects in the components of the rocks are well pronounced.

## MAJOR CHEMICAL CONSTITUENTS OF THE PHOSPHORITE AND THE ASSOCIATED ROCKS

The concentration of Ca and Mg oxides in the phosphatic beds and the associated beds of limestones of Sinjar Formation have been plotted with the assumption that Mg concentration in the near shore water is more as compared to the off shore deep sea water and reverse is true for Ca. Any change or abnormal concentration of either of the elements would be the indication of varying physico-chemical conditions giving rise to enrichment or depletion of the elements through replacement of diagenesis. Thus the causes of an overall change in the chemical composition of the mother rock, diagenetic changes and solution actions are expected to be explained on the basis of enrichment and depletion of these elements.

Likewise the graphs plotted for the concentration of  $P_2O_5$ ,  $SiO_2$  and acid insoluble residues are expected to help in describing the degree of correspondence, if any, between  $P_2O_5$  and the major constituent of the rocks like Ca,  $SiO_2$ , Mg and acid insoluble residues. The graphs plotted represent a cross section of the chemical constituents of the rocks of the area.

In the graph plotted for the concentration of CaO and MgO in the phosphatic beds and the associated rocks versus sample number, the sample No. 2 represents the non-phosphatic bed exposed at the bottom and lies immediately below the lower phosphatic horizon represented by sample Nos 3 to 7. Samples No. 8 to 11 having a total thickness of 43 feet are non-phosphatic limestone beds and separate the upper phosphatic horizon represented by samples Nos. 12 to 15. Sample No. 16 is from the non-phosphatic bed at the top of the uppermost phosphatic horizon exposed in the section.

The concentration of calcium and magnesium appear to show antipathic relationships with each other except in samples No. 9, 14 and 15 (Fig. 5). Bed No. 9 is non-phosphatic and bed Nos. 14 and 15 contain 5.947 and 1.360%  $P_2O_5$  respectively.

The highest concentration of calcium (59.37%) was found in bed No. 7 which shows the presence of phosphorous (1.460%  $P_2O_5$ ). The lowest content of calcium (46.11%) was present in bed No. 9 which is non-phosphatic. Bed No. 14 shows the

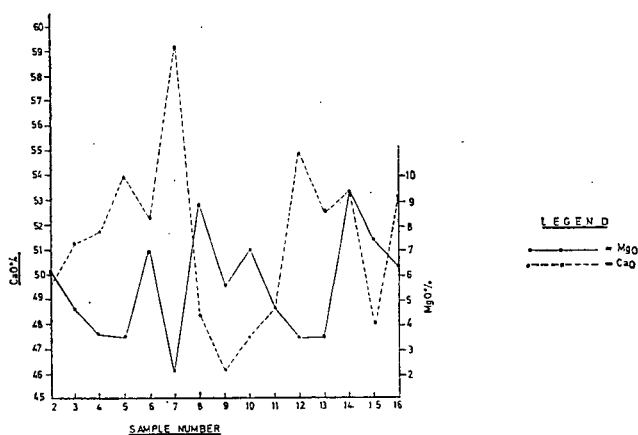


Fig. 5. Concentration of calcium and magnesium in phosphorites and associated rocks

maximum concentration of MgO (9.12%) and the lowest concentration of MgO was detected in bed No. 7, when both the beds are phosphatic.

The plot of Ca/Mg ratio versus Mg concentration for the samples under investigation show a fairly good inverse relationship in general (Fig. 6) but the beds from

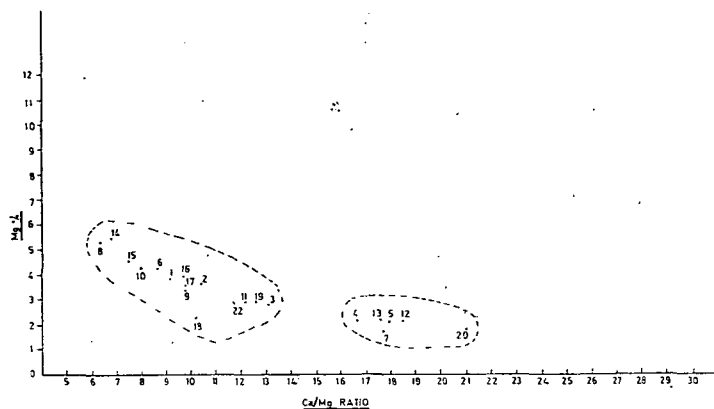


Fig. 6. Variation of Mg with Ca/Mg ratio in phosphorites and associated rocks

the bottom to the top of the section can not be separated as deep water of shallow water deposits. Since the concentration of Ca and Mg in the beds of the formation are variable, the symmetry in concentration of these elements can not be established. The variable and heterogeneous concentrations of Ca and Mg perhaps do not reflect to epigenetic percentages but are most probably caused by diagenetic factors and chemical conditions in the basin of deposition and afterwards.

Apparently cluster of points in two groups with a boundary of Ca/Mg ratio gap from 13.5 to 16.5 separates the beds of shallow and relatively deep marine water deposits or at least the formation has faced fluctuating basin conditions. The numbers with the points show to the beds in the sections studied. Petrographically, the phosphatic beds which contain angular to sub-angular argillaceous fragments, pellets, concretions, lumps etc and the non-phosphatic beds with ooids, algal bands and pronounced recrystallization effects can not be differentiated. In the light of such evidences it appears more probable that differential post-depositional changes

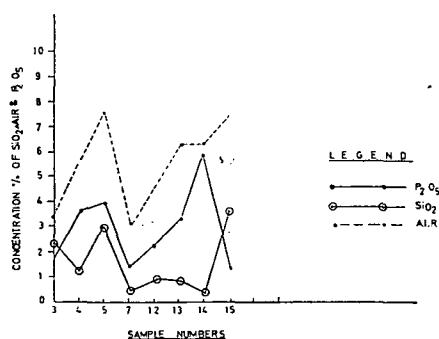


Fig. 7. Enrichment and depletion of  $P_2O_5$ ,  $SiO_2$  and A. I. R. in phosphorite beds

caused variable concentration of magnesium in the rocks under shallow sea condition.

The graphs plotted for the concentration  $\text{SiO}_2$ ,  $\text{P}_2\text{O}_5$  and acid insoluble residues are only for the phosphatic beds found in Sinjar Formation. These graphs give a fairly good pictorial view of the relationships of  $\text{P}_2\text{O}_5$  with respect to acid insoluble residues (Fig. 7). Similar enrichment and depletion of  $\text{P}_2\text{O}_5$  with respect to acid insoluble residues suggest that the concentration of phosphate is with the argillaceous contents of the rocks. The present observation is in accordance with the petrographic studies. The graph for the concentration of  $\text{SiO}_2$  does not show any conclusive positive or negative correspondence with the  $\text{P}_2\text{O}_5$  contents in the phosphatic beds. The positive correspondence between  $\text{P}_2\text{O}_5$  and acid insoluble residues can also be used as an important factor in making economic considerations and discussing the source of the layered phosphorites which appear to be of recycled sediments from near by source.

The variable concentrations of CaO and MgO in the beds of the formation are probably due to the fluctuation in conditions of the depth of the basin of deposition and influx of water from the open sea into the relatively restricted shallow part of the sea. The antipathic correspondence of Ca with Mg is probably an indication of period of calmness and turbulence in the sea. It appears probable that when the sea was oversaturated with Ca the precipitation of Ca took place in relatively agitating water condition but Mg remained in solution due to higher electronegative character. Chemical replacement of aragonite precipitate by Mg-iron in solution also appears as a reasonable cause of variable concentration of Mg in the rocks. Diagenesis may be considered as an important agent to cause variation in Mg contents.

As suggested by DEGENS [1965] that the variable concentration of Ca are a reflection of changing conditions such as temperature, agitation or aeration in the surrounding system by inorganic or organic means which cause removal of  $\text{CO}_2$  and increases the pH and thus favours the precipitation of lime, seems partly compatible with the present observation but it is difficult to explain the antipathic relationship between Ca and Mg which is more pronounced in the samples under present investigation. The wide scattering of points along an inverse relationship line is a reflection of fluctuation in the content of calcium composition of the sea water, perhaps, due to influx of water from the open sea into the restricted shallow basin of deposition.

The plot showing the concentration of Mg *versus* Ca/Mg ratio indicates scattering of points probably due to variable contents of Ca because of the presence of organisms which consume Ca and the turbidity of the water at the time of deposition.

The graph of  $\text{P}_2\text{O}_5$  content shows remarkably positive correspondence with the MgO content in the samples which are dominated by angular to subangular argillaceous fragments and pellets embedded in calcareous matrix (Table 1). The content of  $\text{P}_2\text{O}_5$  and also the Mg concentration show a fairly positive correspondence with the acid insoluble residues with the exception of sample No. 15 which is the topmost bed of the phosphatic horizon and contains very little  $\text{P}_2\text{O}_5$  (1.365%). It appears that the phosphate concentration is related to acid insoluble residues than to the fossils.

## DISCUSSIONS

The alternate occurrence of limestones and the phosphorite beds, the variation in the physical and petrographic characters, the fossil types and their relative abundance in Sinjar Formation suggest that there were at least five phases of sedimentation. The possible phases of sedimentation under varying physico-chemical conditions



were *i*) deposition of limestone with sugary texture and little percentage of fossils, *ii*) deposition of phosphorites, *iii*) deposition of clastic limestones with fossils, *iv*) deposition of phosphorites, *v*) deposition of fossiliferous limestones.

KAZAKOV [1937, 1950] concluded from the studies of phosphorite facies and the genesis of Permian phosphorite deposits of U. S. S. R. in addition to his investigation on fluor-apatite system of equilibria under conditions of formation of sedimentary rocks that phosphorites are formed as chemical precipitate from supersaturated sea waters. MCKELVEY [1953] also came to the same conclusion as KAZAKOV from his studies of Permian phosphorites of Western United States.

The petrographic studies and the results of chemical analysis data of the phosphatic beds and the associated limestones under present investigations show no compatibility with the findings of those of KAZAKOV and MCKELVEY. Had there been chemical precipitation of phosphate, then the minerals of apatite group would have been found in thin sections. Moreover, the limestone beds lying below the phosphorite beds would have been phosphatized at least up to the detectable limits, but such evidences were not found.

CAYOUX [1936] supported biochemical origin of phosphorites and considered bacteria as the main factor in the formation of sedimentary phosphates.

The significant role played by micro-organisms or bacteria does not seem to be plausible in case of the phosphorites of Sinjar Formation because the fossiliferous beds were not found as a more phosphatic than the non-fossiliferous beds but reverse was true to a greater extent. Likewise, the limestone beds containing algal material which could be considered rich in bacteria and bacterial actions did not show any enrichment with respect to phosphate contents.

BUSHINSKY concluded from the studies of structure and origin of the phosphorites of U. S. S. R. in 1935 and the shallow water phosphorite sediments of the same country in 1964, that the origin of phosphorite sediments is a result of simple replacement caused by the introduction of  $\text{PO}_4$  units into pre-existing calcareous materials. AMES [1959] observations from the study of the genesis of carbonate apatite were also in accordance with those of BUSHINSKY's conclusions.

Phosphatization due to replacement caused by the introduction of  $\text{PO}_4$  units into the pre-existing calcareous material means that fossils and fossil fragments, fish bones or teeth, Mg-calcite and aragonite would be the centres of replacement and enrichment of phosphorites. The present observation shows no relationships between the phosphate contents and the fossils or fossil fragments. On the contrary, more fossiliferous beds appeared to be devoid of phosphates. Similarly no correspondence could be found between the samples containing higher calcareous material and phosphate enrichment (Table 1). Under present observation the beds containing argillaceous pellets and fragments in calcareous matrix were found to be phosphatic.

DIETZ, EMERY and SHEPARD [1942] are of the opinion that nodules found abundantly in shallow areas of the sea were largely deposited inorganically from a colloidal suspensions. Further they suggested that stagnant waters, deficient in oxygen may allow the concentration of phosphorus in the absence of organisms which consume phosphorus and thus phosphate nodules or continuous bed or beds containing collophane and microcrystalline carbonate fluorapatite as main constituents are deposited.

The observations of DIETZ, EMERY and SHEPARD for the formation of nodules or beds of phosphate containing collophane and microcrystalline carbonate-fluorapatite appear in accordance with the results of the present investigation. Collophane and dahllite were observed as the common phosphatic minerals in the phosphatic

samples. The lumps encircling argillaceous fragments which are angular to subangular in shape were found to be promising for phosphate concretions. Pisolites and concretions showing concentric layering, micritization and the presence of collophane were found in the phosphatic beds. The absence of  $P_2O_5$  in the fossiliferous and algal limestone beds which are in association with the phosphatic beds reveals that either the phosphorites are recycled sediments from the nearby source or the physico-chemical conditions were not favourable to keep the  $PO_4$  in ionic state for a long time. However, the possibilities of recycling of phosphatic sediments appear more strong because of the fact that  $P_2O_5$  could be found only in the argillaceous pellets and fragments embedded in calcareous matrix. The limestone beds present between the two phosphatic horizons are more calcareous but without any phosphate contents. Diagenetic changes like pressure solution effects, micritization and development of sparry calcite are observable both in the phosphorite and the associated limestone beds. The source of the recycled phosphatic sediments seems to be some older sedimentary phosphatic rock from the nearby area but the rock is not exposed. The phosphorites from the Devonian rocks in the neighbouring countries like Iran in the east and Turkey and Syria in the north west are well known, and therefore, there are great possibilities for the occurrence of phosphorites of Devonian age in Iraq. However, it requires more work to come to the final conclusion.

GOLDBERG and PARKER [1960] who studied phosphatized wood from the Pacific Sea floor; ADAMS *et al.* [1961] from the investigation of phosphatic pebbles of the Bright Seat Formation of Maryland and ARRHENIUS [1963] on the basis of his studies of pelagic sediments concluded that phosphatization of all kinds of organic residues such as shell materials, wood, fecal pellets, teeth etc is a common feature in marine environment.

No compatibility could be found between the present work and the observations of GOLDBERG and PARKER, ADAMS *et al.* and ARRHENIUS regarding the phosphatization of organic remains like shell materials, wood, fecal pellets etc because the phosphate deposit of the area under present study is not from ionic solution but it is considered an accumulation of recycled sediments from the near by source.

According to DEGENS [1965] phosphorite facies is restricted to marine environment when the areas are neither too shallow nor too deep with access to the open sea at one side. The author further suggests that the content of phosphorus increases upto a certain point in the off shore direction and then falls off, because the dead photosynthesizing marine organisms are carried to ocean floor via organic matters (tripton) and the phosphorus is released due to decay of the animals. The released phosphorus becomes active in deposition of phosphorites due to metasomatic replacement of calcite. The conditions required are *i)* alkaline geochemical condition with pH greater than 7; *ii)* presence of calcareous materials and a system that is Ca saturated with respect to  $HCO_3$  content; *iii)*  $PO_4$  concentration exceeding 0.1 ppm; *iv)* non-depositional environment.

The contemporaneous formations of Sinjar Formation in Iraq are the Kolosh clastics intertonguing with the Sinjar Limestones and the off shore equivalent known as A-aliji Formation which is mainly composed of argillaceous marls, marly limestones and shales with scattered glauconite grains in them. Since no informations are available regarding the occurrence of phosphorites in the contemporaneous formations, therefore, it requires more work to discuss the possibilities of phosphatization due to photosynthesizing organisms. Apparently there are no possibilities of such processes to be active because the newly discovered phosphorites are simply recycled sediments.

The changes in facies and thickness of Paleocene formations are probably the results of epirogenic movements in pre-orogenic times which caused gentle large scale undulations of the sea floor aligned partly parallel to the Arabian Shield. This belt can be considered as a marginal mobile sedimentary Zagros Trough superimposed on the platform. Later phases of movements caused gradual shift of the axis of the Zagros Trough in Iranian part to its present position in the Arabian Gulf and close relationship of the folded belt of Zagros was established with the Arabian Platform (Shield) in territories of Iraq, Syria and Turkey.

#### ACKNOWLEDGEMENTS

The authors express their gratitude to the President of the University of Sulaimaniah and the Dean of the College of Science, for providing transport to carry out field work and laboratory facilities to complete the present research.

The assistance of MISS NIGAR ABDUL AZIZ of the Department of Soil Science during the determination of phosphorous is acknowledged with thanks.

We are also thankful to the Chairman of the Department of Geology University of Baghdad for extending facilities to prepare thin sections of the rock sampels.

#### REFERENCES

- AL-KUFAISHI, F. A. M. [1977]: A geochemical study on Sinjar Limestone in a subsurface section (K—16). *Jour. Geol. Soc. Iraq*, Vol. X, pp. 47—51.
- AL-SAIGH, A. Y. and AL-OMARI, F. S. [1977]: General Geology. p. 377, University Mosul Press, Mosul, Iraq.
- AL-SIDDIQI, A. A. M. [1968]: Stratigraphy and Microfacies of Sinjar Formation. Unpub. M. Sc. Thesis, Baghdad, University, Baghdad, Iraq.
- AMES, L. L. JR. [1959]: The genesis of carbonate-apatites. *Econ. Geol.* Vol. 54, pp. 829—841.
- ARRHENIUS, G. [1963]: "Pelagic sediments". In the Sea and observations on progress on the study of the sea. Edited by M. N. HILL, N. Y. Interscience Publishers, Inc. pp. 655—727.
- BATHURST, R. G. C. [1976]: Carbonate sediments and their diagenesis. Elsevier Scientific Publishing Company, N. Y. p. 77—90.
- BROMLEY, R. G. (1967): Marine phosphorites as depth indicators. *Marine Geol.* Vol. 7, 1. 503—509.
- BUSHINSKY, G. I. [1935]: Structure and origin of the phosphorites of the USSR. *Jour. Sed. Petrol.* Vol. 5, p. 81—92.
- BUSHINSKY, G. I. [1964]: On shallow water origin of phosphorite sediments. *Development in Sedimentology* Vol. 1, Edited by L. M. J. U. VAN STRAATEN, Elsevier Publishing Co. N. Y.
- CAYEUX, L. [1939]: Phosphate sedimentaires et bacteries. *Compt. Rend.* Vol. 203, pp. 1198—1200.
- CONSULTANTS OF USSR and IRAQI GEOLOGISTS [1965]: Report on geological prospecting and investigation into phosphate deposits of Rutba and Akashat areas. Open file report, Geol. Min. Surv. Div. Baghdad, Iraq.
- DEGENS, E. T. [1965]: Geochemistry of sediments. pp. 144—146, Prentice Hall, Inc. N. Y.
- DIETZ, R. S., EMERY, K. O. and SHEPARD, F. P. [1942]: Phosphorite deposits on the sea floor of southern California. *Bull. Geol. Soc. Am.* Vol. 53, pp. 815—810.
- GOLDBERG, E. D. and PARKER, R. H. [1960]: Phosphatized wood from the Pacific sea floor. *Bull. Geol. Soc. Am.* Vol. 71, pp. 631—633.
- GULBRANDSEN, R. A. [1966]: Chemical composition of phosphorites of the Phosphoria Formation. *Geochem. Cosmochim. Acta*, Vol. 30, No. 8, pp. 769—778.
- KAZAKOV, A. V. [1937]: The phosphorite facies and the genesis of phosphorites. *Trans. Sc. Inst. of Fertilizers and Insect Fungicides*. Moscow, Vol. 142, pp. 95—113.
- KAZAKOV, A. V. [1950]: Fluorapatite system equilibria under conditions of formation of sedimentary rocks. *Akad. Nauk. Vyp.* 114, *Geol. Ser.* No. 40, pp. 1—21.
- McKELVEY, V. E., SWANSON, R. W. and SHELDON, R. P. [1953]: The Permian phosphorite deposits of western United States. 19th Int. Geol. Congr. Algiers, *Compt. Rend.* X1, pp. 45—64.
- NOTHOLT, A. J. G. [1965]: Discussion on exploration for phosphorite in Turkey. *Econ. Geol.* Vol. 60, No. 4, pp. 822—823.

- NOTHOLT, A. J. G. (editor): [1977]: Phosphate rock in CENTO Region, CENTO Press, Ankara, Turkey.
- SAMIMI, M. and GHASEMIPOUR, R. [1977]: Phosphate deposits in Iran. Phosphate Rock in CENTO Region. Edited by NOTHOLT, A. J. G., pp. 1—40, Ankara, Turkey.
- SHAPIRO, L. [1952]: Simple field method for the determination of phosphate rocks. Am. Miner. Vol. 27, Mo. 3, pp. 341—343.
- SHELDON, R. P. [1964a]: Exploration for phosphorite in Turkey. Econ. Geol. Vol. 59, No. 6, pp. 1159—1175.
- SHELDON, R. P. [1964b]: Paleolatitudinal and paleogeographical distribution of phosphorite. Prof. Pap. No. 501—C, USGS Bull. pp. 106—113.
- SMITH, J. S. [1954]: Radioactive anomalies in the western part of the Republic of Iraq on the Syrian Desert. Open file report. Geol. and Mineral Surv. Division. Baghdad, Iraq.
- VAN BELLEN, R. C. [1956]: Lexique Stratigraphique International, Vol. 111, ASIE, Fascicule 100, pp. 108—112, 155—157, 274—285.
- YOUSEF, M. I. [1965]: Genesis of bedded phosphates. Econ. Geol. Vol. 60, No. 3, pp. 590—600.

*Manuscript received, October 21, 1979.*

DR. I. AL-FADHLI and  
DR KHALIL AHMED MALLICK  
Department of Geology,  
College of Science  
University of Sulaimaniah  
Sulaimaniah, Iraq.



## **PETROLOGICAL AND GEOCHEMICAL CHARACTER OF THE BÁR BASALT, BARANYA COUNTY, SOUTH HUNGARY**

**T. SZEDERKÉNYI**

### **SUMMARY**

Based on exploration carried out by deep-drillings near Bár village a small maar-like volcano covering by Quaternary loess and characterized by a sole eruption is proved. Producing a fairly well determinable thin volcanic sequence this eruption is represented by a very thin tuffaceous sheet on the base of the volcanic succession and a scoria member and a porous, sometimes churned rarely compact basaltic lava mass. The basalt is classified as a leucite basanite turning into analcitebearing basanite at the margins and at some places of the porous inner sections of the volcanic body. Being a conspicuous petrologic difference between Pannonian basalts of Hungary and Bár alkaline rocks, the latter is regarded as an independent volcanic event of the great Pannonian volcanism of Hungary.

### **INTRODUCTION**

On the flood-area of the Danube River near Bár village (*Fig. 1*) a few cubic meters of boulders of a basaltic rock were mapped and ranged into Lower Cretaceous alkaline diabase association of the Mecsek Mountains by T. SZEDERKÉNYI [1962, 1964]. A. KASZAP [1963] presumed a certain connection between volcanism of Bár and Popovác Hill (Yugoslav side of Baranya County) which latter is represented by andesite-basalt and penetrated the Late Miocene (Sarmatian) deposits according to L. LÓCZY JR. [1914]. Based on a petrographic description by I. VICZIÁN [1965] these volcanic rocks located near Bár may be considered as analcite basalts which are in a close genetic connection with Hungarian Pannonian basalts.

After detailed geophysical measuring (geoelectrical sounding and geomagnetic measurements) three deep-drillings were deepened to prove the existence of the basaltic mass below Quaternary loess sheet and to determine its geological setting.

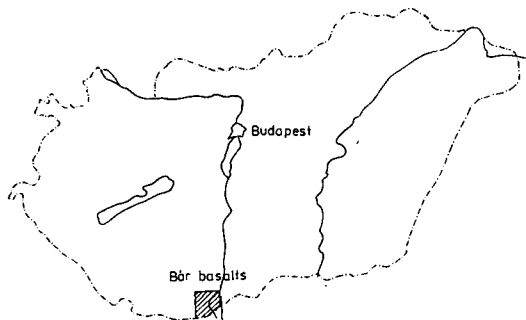


*Fig. 1.* Location map of Bár basalt.

As it was mentioned previously, our geological knowledge related to Bár basalt was confined to the boulders exclusively. After realization of the geophysical and deep-drilling research plan made T. SZEDERKÉNYI [1970] the reality of a basalt body was proved. Having about 0,5 km<sup>2</sup> extension it forms and elongated magnetic field arranged to NW — SE directions.

Based on the data of the deep-drillings their stratigraphic columns differ from each other. One of them (Bár No. 4) had penetrated not only the volcanic body and underlying fauna-free, probably Quaternary deposits, but deeply invaded to the Lower Pannonian fauna-bearing layers; another bore-hole (Bár No. 5) did to the volcanic body and stopped in the underlying red clay; and finally the third one (Bár No. 6.) crossing 54 m thick basalt section stopped within it.

Prior to the lava-flow a weak eruption had taken place which produced a small amount of agglomerates and tuffs having less than 20 cm thickness. A very characteristic contact zone represented by a 1,0 m thick "natural brick" material originating from a mixture of tuffs and clays and loose basaltic debris, formed by thermal effect of the lava-flow is also recorded. Belonging to the so-called *scoria* formation this rock-type has not been detected in Hungary so far.

The Pre-Tertiary bedrocks lying below the basalt body have not been explored yet and may be ranged into Middle Jurassic or Triassic. Finally a notice is taken about the age of the red clay member underlying the volcanic mass, and is ranged into Lower Quaternary by GY. HÖNIG [1971]: this classification had been made merely on the basis of lithostratigraphic observations and considerations, however, in the lack of biostratigraphic proofs it is only conditionally acceptable. A conspicuous petrological difference between the Pannonian and Bár basalts supports an idea of different age of Pannonian and Bár basalts and that of underlying formations.

#### PETROGRAPHIC CHARACTERIZATION OF THE BASALT

A fairly big portion of the explored basaltic rocks resembles macroscopically to the outcropped basalt. There is an exact description about the latter by I. VICZIÁN [1965]. Recognizing the special mineralogical composition of the rock (iddingsitic olivine, augite, plagioclase, analcite, etc.) he classified it as an analcite basalt. Origine of the analcite was assigned as a primary magmatic process related to the formation of plagioclases.

The fresh basaltic rock-material produced by deep drillings has a general grey colour with a dark shade at the compact parts and a lighter one at the miarolitic and churned sections. Vertical distribution and dimensions of the vesicles, miarolitic holes and churned parts of the rock-columns show a considerable variability. Rhythmic alteration of the vesicle-bearing and vesicle-free sections gives a "layered" character to the volcanites. The elongated vesicles are usually without any filling material, or they are encrusted by no more than one mm thick layer of zeolite, analcite and/or calcite crystals. The length of longitudinal axes of the holes are from a few mm up to 2—3 cm.

Perfectly compact vesicle-free parts are rather scarce in the basalt column and occur only in the deepest sections explored by Bár No. 6 deep-drilling. Parallel with the disappearance of vesicles from the basalt, grain size of the rock-forming minerals increases suddenly giving a dolerite-like look.

The Bár basalt microscopically shows a nearly general vitrophyric texture with the exception of the coarse-grained vesicle-free parts having a granophyric one. Euhedral porphyritic augite, leucite, plagioclase ( $An_{40}-An_{65}$ ), analcite and olivine crystals are embedded into a glassy or sometimes microcrystalline matrix (Fig. 2 and 3). All olivine therein have an iddingsite frame. Characteristic accessory minerals as tiny apatite and xenotime crystals, ilmenite and magnetite euhedrons moreover amphibole and biotite wrecks are also recorded.

Contrary to the outcropped basalt examined by I. VICZIÁN [1965] the subsurface one shows an appreciable leucite enrichment at the expense of the analcite. Leucite-free (analcite-bearing) rocks can be found only in the outcrop, but analcite-free (leucite-bearing) ones only at the inner part of the volcanic body exclusively. First of all the coarse grained basalt contains leucitehedral-shaped leucite crystals in rock forming quantity (Fig. 3). In the strongly porous and churned basalt samples

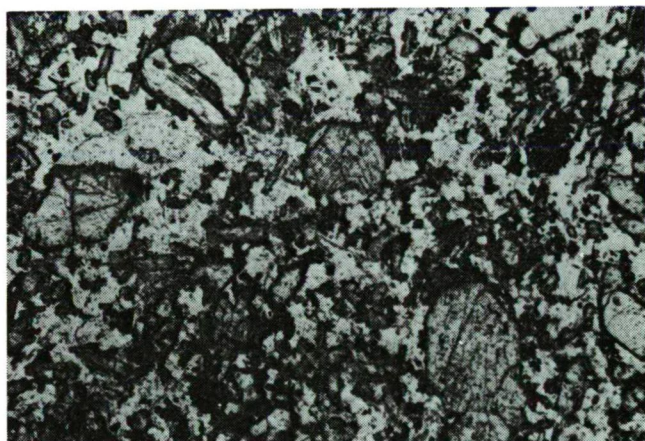


Fig. 2. Pyroxene and iddingsitic olivine crystals, interstitial plagioclase (white) and metallic particles (black). //N, 68x. Bár No. 6. 47,10 m.

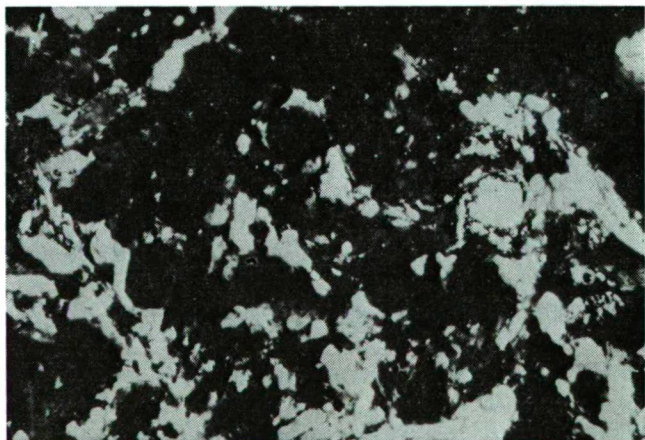


Fig. 3. Leucite euhedrons (black), interstitial plagioclase (white). +N, 125x.



(originated from either the inner or marginal parts) of the body the leucite are partly or perfectly substituted by analcite. It is proving that the analcites are secondary minerals which derived from leucite (and perhaps nepheline) and the frequency depends above all on the porosity and permeability of the basaltic rocks. The existence and distribution of leucite are proved by not only thin sections, but X-ray investigations, too.

# CHEMICAL COMPOSITION AND TRACE ELEMENT DISTRIBUTION OF THE BÁR BASALT

The basalt varieties of the studied rock-mass bear a great resemblance to each other in chemical composition (Table 1). Compared with that of average of "normal" basalts [F. TURNER and J. VERHOOGEN, 1960] there are, however, some considerable

TABLE 1

*Chemical composition and C. I. P. W. norms of South Transdanubian basalts*

Components Vol. %	Popovac Hill	Bár From outcrop		Bár-6 66,7 m	Bár-6 55,0 m	Bár-6 47,10 m	Bár-5 48,30 m
SiO <sub>2</sub>	54,24	48,05	48,70	46,63	49,99	50,03	49,76
TiO <sub>2</sub>	1,26	1,18	1,13	2,00	1,90	2,00	1,90
Al <sub>2</sub> O <sub>3</sub>	18,13	14,38	14,37	14,05	14,78	13,48	13,48
Fe <sub>2</sub> O <sub>3</sub>	2,69	5,17	6,47	1,25	3,65	3,55	3,77
FeO	4,24	4,02	3,14	6,52	4,66	2,87	2,72
MnO	Ny	0,14	0,15	0,10	0,10	0,06	0,08
MgO	4,95	8,24	6,92	7,86	6,71	7,31	7,11
CaO	6,17	8,79	7,35	7,65	5,84	5,42	5,29
Na <sub>2</sub> O	3,88	3,24	4,55	2,95	3,76	2,32	4,50
K <sub>2</sub> O	1,24	4,27	1,99	5,97	5,50	8,20	4,20
H <sub>2</sub> O <sup>+</sup>	2,48	1,17	3,55	1,34	0,64	0,79	3,42
H <sub>2</sub> O <sup>-</sup>	2,48	0,38	1,11	0,59	0,13	0,23	0,11
P <sub>2</sub> O <sub>5</sub>	0,24	0,75	0,80	1,40	1,34	1,40	1,42
SO <sub>3</sub>	0	0	0	0,12	0,13	0,16	0,08
CO <sub>2</sub>	Ny	0	0,11	0,78	0	0,09	0,26
Total:	99,52	99,78	100,34	98,44	99,25	98,00	98,00
Anal.:	MAURITZ, B.	SOHA, I.		BÍRÓ, J., SÜTÖ, Z.		BÍRÓ, J., SÜTÖ, Z.	
qz		22,5	23,0	24,3	23,9	28,2	23,4
or		2,0	—	—	—	—	2,0
ab		15,3	15,7	13,1	12,0	10,2	14,7
an		15,0	13,7	19,8	18,8	23,4	15,8
lc		5,3	7,8	3,7	6,7	2,5	7,7
ne		—	—	—	—	—	—
Ca <sub>2</sub> SiO <sub>4</sub>		14,0	15,2	13,2	12,8	10,7	9,6
CaSiO <sub>3</sub>		7,3	6,3	6,6	6,3	7,1	6,8
MgSiO <sub>3</sub>		4,3	5,2	3,3	3,2	2,9	3,5
FeSiO <sub>3</sub>		3,3	1,6	2,5	2,2	3,1	2,9
Mg <sub>2</sub> SiO <sub>4</sub>		3,2	3,1	2,4	2,3	2,0	2,5
Fe <sub>2</sub> SiO <sub>4</sub>		3,1	3,0	2,9	2,8	2,6	2,7
mt		3,6	2,5	3,5	3,4	3,2	3,4
il		2,0	2,3	4,0	3,9	4,1	4,6
ap		—	—	—	—	—	—
cc		—	—	—	—	—	—
Total:		100,9	99,4	99,3	98,3	100,0	99,6
M		40,8	39,2	38,4	36,9	36,6	36,0
Pyroxens		25,6	26,7	23,1	22,3	20,7	19,9
Olivines		6,5	4,7	4,9	4,5	6,0	5,4
Feldspathoids		20,3	21,5	23,5	25,5	25,9	23,5

differences between them. The most significant anomalies are: (1) a generally low CaO content; (2) a markedly high K<sub>2</sub>O and P<sub>2</sub>O<sub>5</sub> content; (3) a considerable excess of K<sub>2</sub>O in contrast to Na<sub>2</sub>O; and finally (4) a fairly high amount of total alkalis.

Semiquantitative spectrochemical analysis for 30 elements made by PGS quartz spectrography were carried out from three characteristic rock samples of the Bár basalt. Furthermore, quantitative measurements of some immobile elements as Ce, Ga, Nb, Sc, Zr, Y were also made (Table 2) which are suitable to determine of the origin and development of basaltic magma. Comparing these data with the average trace element content of basaltic rocks given by T. TUREKIAN, K. WEDEPOHL [1971] a conspicuous divergence can be found in the trace element distribution. Double amounts of Be, Ce and Y content are characteristic for the Bár basalt samples. According to K. WEDEPOHL [1971] extreme high values of Y (more than 0,1%) Zr, La, Be and Ce are typical of basalts derived from secondary differentiation of acidic magmas.

TABLE 2

*Trace element content of Bár basalt*

	Semi-quantitative			Quantitative		
	Bár-6 66,7 m	Bár-6 55,0 m	Bár-5 48,30 m	Bár-6 66,7 m	Bár-6 55,0 m	Bár-5 48,30 m
Ag	2,5	2,5	2,5			
As	—	—	—			
B	—	—	—			
Ba	2000	2000	2000			
Be	25	25	25			
Bi	—	—	—			
Ce	not examined			615	655	853
Cd	—	—	—			
Cr	100	100	100			
Co	10	10	10			
Cu	50	50	50			
Ga	100	125	100	138	199	158
Ge	—	—	—			
In	—	—	—			
La	100	100	250			
Mn	1000	1000	1000			
Mo	—	—	—			
Nb	40	40	25	84	—	77
Ni	100	100	100			
Pb	50	50	100			
Sb	—	—	—			
Sc	50	50	50	65	52	44
Sn	1	1	1			
Sr	2000	2000	2000			
Te	—	—	—			
V	1000	1000	1000			
W	—	—	—			
Zn	—	—	50			
Zr	600	700	1000	621	621	1080
Y	175	500	750	1378	1155	1575

Analysed by: KÁDAS, M.

An attempt to use the amount of immobile trace elements for classification of basalts by methods developed by J. PEARCE, J. CANN [1973] and R. SMITH [1976] and P. FLOYD, J. WINCHESTER [1978] was made. But due to their extreme high values this attempt was unsuccessful.

## PETROLOGY OF BÁR BASALT

By way of introduction it seems necessary to explain the interpretation of some petrological concepts related to basalts.

F. CHAYES [1966] has counted basalts with quartz in the norm as "subalkaline" (i. e. tholeiitic) and those with nepheline in the norms as "alkaline" (alkaline-olivine basalts).

A. MIYASHIRO [1975] had classified the volcanic rock-series of the Earth-crust into two main groups: (1) alkaline, and (2) nonalkaline ones. The latter may be subdivided into tholeiitic and calc-alkaline series. The most important characteristics of alkaline rocks are regarded as (1) peralkaline composition (i. e.  $\text{Na}_2\text{O} + \text{K}_2\text{O} > \text{Al}_2\text{O}_3$  in molecular ratio) leading to the formation of alkaline pyroxenes and/or amphiboles, and (2) silica undersaturation producing feldspathoids: e. g.  $(\text{Na}_2\text{O} + \text{K}_2\text{O}) > \text{SiO}_2$ . Well, the Bár basalt satisfies these criteria so it can really be qualified as an alkaline basalt.

It is known that in a large-scale alkaline volcanic association a normative nepheline content is very low in general. If the alkaline rocks originated from primary alkaline magma or by contamination of sub-alkaline magmas, the nepheline content is higher. But nepheline and hyperstene minerals are very sensitive to secondary changes mainly of oxidation so it is almost sure that under conditions of oxidation characteristic in the Bár basalt, they could not remain at all. In the light of these observations the real nepheline content of this rock should be changed probably into analcite perfectly.

For a distinction between alkaline and nonalkaline volcanic series and presentation of the place of the Bár basalt within them, a HARKER's-type variation diagram [1909] serves which is modified by G. A. MACDONALD, T. KATSURA [1964] and A. MIYASHIRO [1975]. Alkaline character of the Bár basalt seems to be evident (Fig. 4).

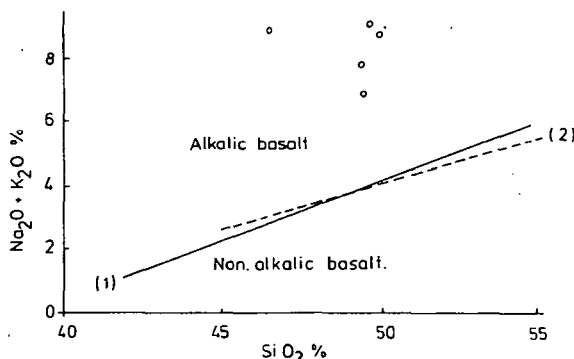


Fig. 4. Alkali-silica variation diagram. The curve (1) means the boundary between the alkalic and tholeiitic basalt in Hawaii [MACDONALD, G. A., KATSURA, 1964].

Place of the Bár basalt in the system of alkaline rocks made by A. STRECKEISEN [1980] is marked out by Fig. 5. Applying C. I. P. W. norms for an APF diagram, the projections of the rock samples get both on the field of No. 12 and No. 13, i. e. between phonolites and basanites in a close contact with the field of the latter. The high normative potassium feldspar content shows a trachybasaltic strain.

In the TRÖGER's-system [E. TRÖGER, 1935] the Bár basalt should be as leucite basanite having an extreme low CaO content. (Despite of the low portion of CaO

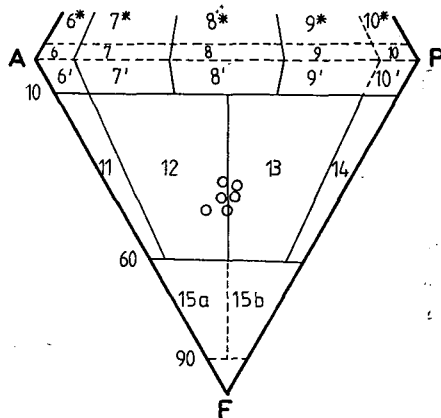


Fig. 5. Place of the Bár basalt samples in the STRECKEISEN's [1967] system.

a rather high olivine content helps to range this rock into the leucite basanite category.) in TURNER and VERHOOGEN's classification [1960] this basalt belongs to the leucite basanite type of a potassium-rich trachybasalt-leucite basalt association.

Due to the before-mentioned reasons there is no doubt about priority of leucite contrary to analcite is the term of the rock. But the importance of the analcite is also unquestionable among rock forming minerals in some parts of the basalt body. Therefore, our proposal for an exact name of the Bár basalt is *analcitic leucite basanite*.

#### PLACE OF THE BÁR BASALT VOLCANISM IN THE YOUNG BASALT VOLCANISM OF HUNGARY

Formerly a close genetical connection was supposed between Pannonian and Bár basalt volcanisms [I. VICZIÁN, 1965]. Having a great number of (232) analyses of Pannonian basalts [L. JUGOVICS, 1974]] there is a fairly good possibility to check this hypothesis. A variation diagram of total alkalines and  $\text{SiO}_2$  (Fig. 6) and another one of  $\text{K}_2\text{O}-\text{Na}_2\text{O}$  (Fig. 7) clearly show an appreciable geochemical divergence between Pannonian and Bár basalts. Further on there are some other remarkable differences among the bulk composition of both basalt groups (Table 3).

Considering all the geological, petrological and geochemical characteristics, it seems that the idea of close genetical connection between Pannonian and Bár volcanisms is ready for revision. Regarding the genetical connection between Popovac — Hill (Yugoslavia) andesitic-basalt and Bár basalt based on sole datum for the andesitic-basalt is proved to be unfounded [B. MAURITZ, 1920 and A. KASZAP, 1963].

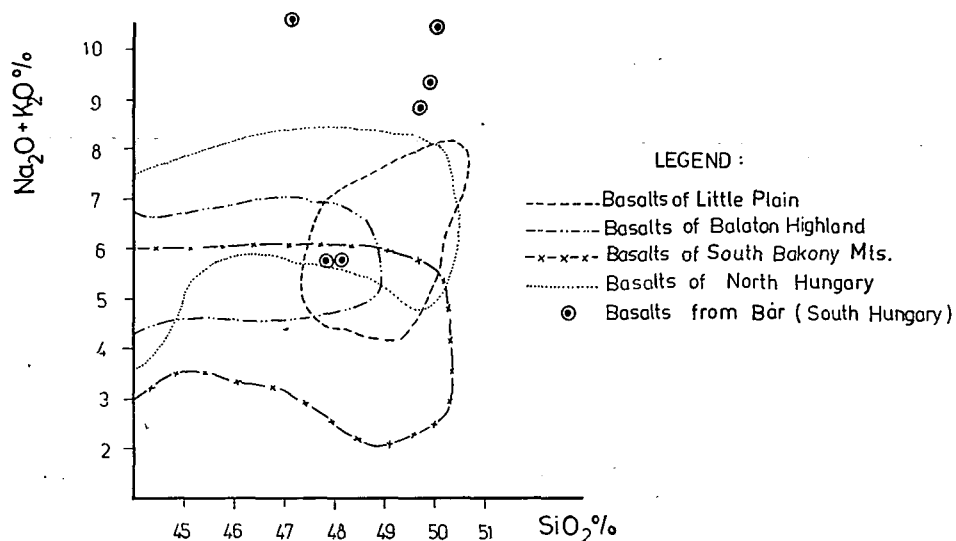


Fig. 6. (K<sub>2</sub>O+Na<sub>2</sub>O)—SiO<sub>2</sub> variation diagram of Cenozoic basalts of Hungary.

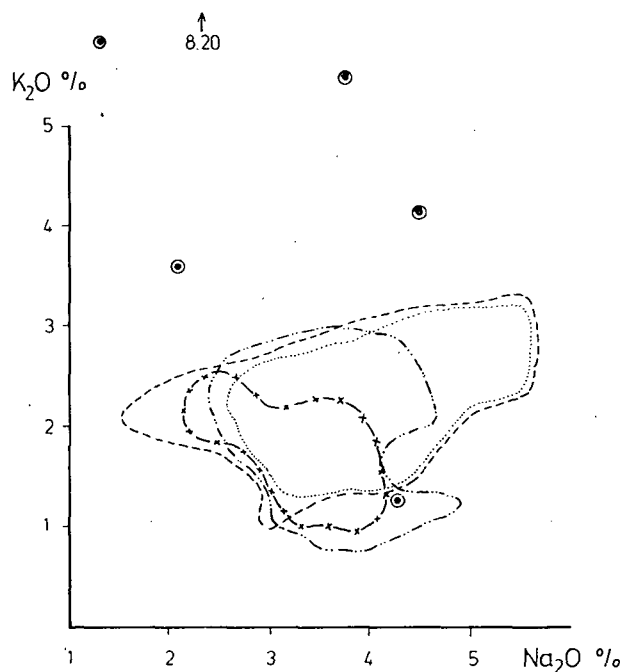


Fig. 7. K<sub>2</sub>O—Na<sub>2</sub>O variation diagram of Cenozoic basalts of Hungary. Legend: same as Fig. 6.

TABLE 3

*Remarkable chemical differences between young Hungarian basalts*

Average in vol. %	Bár basalt (6 samples)	Pannonian basalts (232 samples)
Al <sub>2</sub> O <sub>3</sub>	14,09	16,60
CaO	6,71	9,70
K <sub>2</sub> O	5,02	2,02
P <sub>2</sub> O <sub>5</sub>	1,20	0,62
Na <sub>2</sub> O/K <sub>2</sub> O	3,55/5,02	3,51/2,02

## REFERENCES

- CHAYES, F. [1966]: Alkaline and subalkaline basalts. *Amer. J. of Sci.*, **264**, 128—145.
- DEER, W. A., HOWIE, R. A., ZUSMANN, M. A. [1965]: *Rock Forming Minerals*. Longmans, London.
- FLOYD, P. A., WINCHESTER, J. A. [1978]: Identification and discrimination of altered and metamorphosed volcanic rocks using immobile elements. *Chem. Geol.*, **21**, 291—306.
- HARKER, A. [1909]: *The natural history of igneous rocks*. Macmillan, New York. (Reprinted 1965. Hafner, New York).
- HÖNIG, GY. [1971]: Jelentés a K-baranyai Bár község mellett 1971-ben végzett bazaltkutatrásról (Report about basalt prospecting carried out near Bár, E-Baranya, in 1971) Manuscript, Hung. Geol. Survey, Budapest.
- JUGOVICS, L. [1974]: A magyarországi bazaltok kémiai jellege. (Chemical character of basalts of Hungary) *Annual Rep. of Hung. Geol. Survey from 1974 Year*, 431—470.
- KASZAP, A. [1963]: A dél-baranyai mezozoos szigetrögök. (Mesozoic island-hills of South Baranya.) *Földt. Közl.*, **93**, 440—450.
- KUNO, H. [1966]: Lateral variation of basalt magma-types accross continental margins and island arcs. *Bull. Volcanology* **29**, 195—222.
- LÓCZY, L. JR. [1914]: A Báni hegység (Baranya) geológiai viszonyai. (Geology of Bán Mountains, Baranya County.) *Annual Rep. of Hung. Roy. Geol. Survey from 1913 Year*, 353—360.
- MACDONALD, G. A., KATSURA, T. [1964]: Chemical composition of Hawaiian lavas. *J. Petr.*, **5**, 82—133.
- MAURITZ, B. [1920]: A Báni hegység bazalt-szerű kőzetei. (Basalt-like rocks of Bán Mountains.) *Mat. Term. Tud. Ért.*, **37**, 62—65.
- MIYASHIRO, A. [1975]: Volcanic rock series and tectonic setting. *Annual Rev. Earth Planet. Sci. Letters* **3**, 251—269.
- MIYASHIRO, A. [1978]: Nature of alkalic rock series. *Contrib. Miner. Petr.*, **66**, 91—104.
- PEARCE, J., CANN, J. R. [1973]: Tectonic setting of basic volcanic rocks determined using trace element analyses. *Earth Planet. Sci. Letters* **12**, 290—300.
- SMITH, R. E. [1976]: Comments on the use of Ti, Zr, Y, Sr, K, P, and Nb in classification of basaltic magmas. *Earth Planet. Sci. Letters* **32**, 120—144.
- STRECKEISEN, A. [1967]: Classification and nomenclature of igneous rocks. *N. Jahrb. Miner. Abh.*, **107**, 144—240.
- SZEDERKÉNYI, T. [1962]: A II. sz. Kutatócsoport 1962 évi jelentése a Bátaszék környéki kutatásokról. (Annual Rep. of Expedition No. 2 about investigations of surroundings of Bátaszék in 1962 year.) *Műcsék Ore Mining Co., Pécs*, Manuscript.
- SZEDERKÉNYI, T. [1964]: A baranyai dunamenti mezozoos szigetrögök földtani viszonyai. (Geology of Mesozoic island-hills along Danube River, Baranya County.) *Földt. Közl.*, **94**, 448—452.
- SZEDERKÉNYI, T. [1970]: Javaslat a bár bazalt komplex földtani kutatására bányanyitás céljából. (Proposal on geological prospecting of Bár basalt for opencast exploitation.) Manuscript, Central Geol. Office, Budapest.
- TRÖGER, W. E. [1935]: *Spezielle Petrographie der Eruptivgesteine*. Verlag der Deutsch. Miner. Gesell. e. V., Berlin.
- TUREKIAN, K. K., WEDEPOHL, K. H. [1961]: Distribution of the elements in some major units of the Earth's crust. *Bull. Soc. Geol. Amer.*, **72**, 175—191.

- TURNER, F. J., VERHOOGEN, J. [1960]: Igneous and Metamorphic Petrology. McGraw-Hill, New York, Toronto, London, Sydney.
- WEDEPOHL, K. H. [1971]: Handbook of Geochemistry. Vol. 1. Springer — Verlag Berlin, Heidelberg, New York.

*Manuscript received, July 10, 1980.*

DR. TIBOR SZEDERKÉNYI  
Institute of Mineralogy,  
Geochemistry and Petrography  
Attila József University  
H-6722 Szeged, Egyetem u. 2—6.  
Hungary

## BEHAVIOUR OF MAJOR ELEMENTS IN THE GRANITIC ROCKS OF KADABORA PLUTON, EASTERN DESERT, EGYPT

MAHMOUD LOTFY KABESH, MOHAMED E. HILMY  
and ABDEL-KARIM AHMED SALEM

### ABSTRACT

The petrochemical features of the granitic rocks of Kadabora pluton, Eastern Desert, Egypt are presented. Results of twenty new chemical analyses are advanced and processed following several petrochemical parameters. The average chemical composition of Kadabora granitic rocks is in harmony with that of low-calcium granite of TUREKIAN and WEDEPOHL [1961]. The granitic rocks possess in general rather pronounced potassic characters with few sodic affinities. Chemical classification of the granitic rocks is attempted. Magmatic origin is suggested for the examined granitic rocks and is based on experimentally studied systems.

### INTRODUCTION

The granitic rocks of Kadabora are regarded by EL-RAMLY and AKAAD [1960], and SABET [1961] and EL-RAMLY [1972] as belonging to the younger group of granitoids. Recently the granitic pluton of Kadabora, together with several other granitic plutons have been considered by SABET *et al.* [1976] as belonging to the late Proterozoic-early Paleozoic intrusions. These authors further assigned such granitic plutons

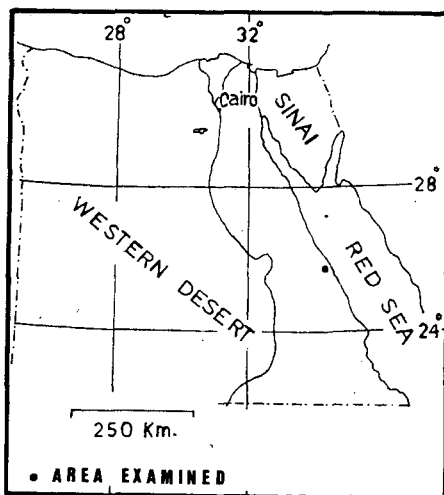


Fig. 1. Location map



to the "Cattarian Group" and to the phase of the coarse-grained biotite granite and the leucocratic granite.

The examined granitic rocks of Kadabora occur in the central Eastern Desert of Egypt (Fig. 1). They are two-feldspar granites in which the feldspars comprise plagioclase, orthoclase and microcline perthite. The chemistry of biotites separated from these granitic rocks proved the magmatic origin of the host granite [SALEM, 1975].

The present study forms part of a continuing program aiming at the petrochemical characterization and classification of the group of younger granitoids of Precambrian age in the Central Eastern Desert of Egypt. [KABESH *et al.*, 1975; KABESH *et al.*, 1976; and KABESH *et al.*, (in press)].

The purpose of the present work is to discuss the petrochemical characteristics of Kadabora granitic stock. A chemical classification of the granitic rocks is advanced based on normative feldspars.

#### GENERAL GEOLOGIC FEATURES OF KADABORA GRANITIC ROCKS:

The granitic rocks of Gabal Kadabora form a roughly circular mass with rather high relief covering a total area of about 154 sq. km. The granitic rocks show intrusive sharp contacts with medium to low-grade metasediments in the east as well as with dioritic rocks at the West and South, sometimes, showing discordant relations. Kadabora granitic rocks may be classified in the field on the basis of feldspar colour into grey, pink and red. They also comprise porphyritic and even-grained non-porphyritic types (Fig. 2). The boundary between these types is gradational and need not reflect mineralogical changes or important variation in the colour index. There-

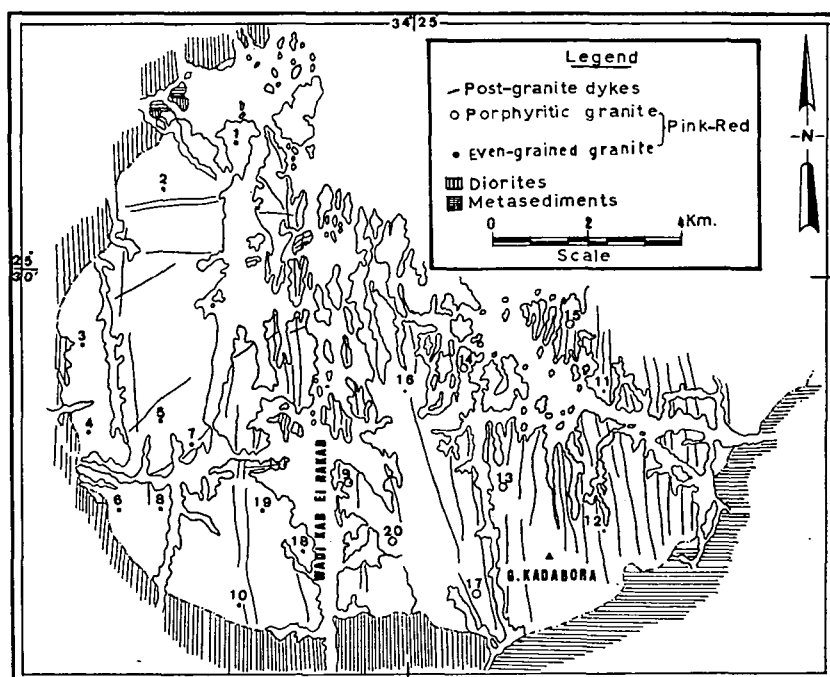


Fig. 2. Generalized geological map of Kadabora Stock showing granitic types and sample location

fore the granitic rocks of Kadabora my be regarded as homogeneous representing crystallization of the granitic magma in one phase of emplacement. Cuboidal and sheet jointing are well developed. Bouldery and exfoliation types of weathering are recognized. Several postgranitic dykes of acidic intermediate basic and alkaline composition are recorded. Milky quartz veins and lenses are found in several spots.

PETROGRAPHY

Petrographically three main types have been recognized namely biotite-granite, biotite-muscovite granite, and leucogranite. These granitic rocks show holocrystalline hypidiomorphic granular texture. They are generally medium-grained either non-porphyritic or porphyritic with megacrysts of microcline-perthite and occassionally quartz. The essential constituents are represented by quartz, microcline, orthoclase, microcline-perthite, albite, and little amount of oligoclase, biotite and muscovite. The accessory minerals are represented by euhedral zircon, apatite, sphene and iron oxides. Perthite intergrowths are of the patchy and the vein types. Microcline usually shows well by cross-hatching. Myrmekitic intergrowths are not uncommon.

Quartz sometimes forms megacrysts and usually forms intersitial aggregates. In rare cases quartz is intergrowth with alkali feldspars as micrographic texture.

Quartz is sometimes deformed and shows strong wavy extinction. Biotite forms irregular stout flakes, sometimes with torn ends and enclose zircon and iron oxides. Brown biotite is the common mafic while green biotite is rarely observed. Biotite is occasionally chloritized muscovite is common sometimes in association with biotite.

PETROCHEMICAL CHARACTERS

The chemical analysis of twenty samples representing the different types of the granitic rocks of Kadabora stock is given in Table 1 and the location of the analyzed sample is given in Fig. 2.

TABLE 1  
*Chemical analysis of the granitic rocks of Kadabora*

Sample number	SiO <sub>2</sub>	Al <sub>2</sub> O <sub>3</sub>	Fe <sub>2</sub> O <sub>3</sub>	FeO	MgO	MnO	CaO	Na <sub>2</sub> O	K <sub>2</sub> O	P <sub>2</sub> O <sub>5</sub>	TiO <sub>2</sub>	H <sub>2</sub> O <sup>+</sup>	H <sub>2</sub> O <sup>-</sup>	Total
1	73.85	13.89	1.07	0.86	0.11	0.03	0.39	4.26	4.50	—	0.01	0.84	0.08	99.89
2	74.99	13.63	0.59	0.68	0.20	0.03	0.46	4.73	4.00	—	—	0.45	0.08	99.84
3	74.24	14.53	0.81	0.31	0.01	0.03	0.36	4.32	4.00	—	0.01	0.50	0.09	99.21
4	75.14	13.35	0.96	0.68	0.01	0.02	0.56	3.10	5.29	—	0.02	0.45	0.01	99.59
5	73.27	14.59	0.30	0.31	0.02	0.01	0.46	4.36	5.81	—	0.02	0.42	0.26	99.83
6	72.76	14.48	0.85	0.37	0.03	0.03	0.39	4.24	5.36	—	0.02	0.65	0.07	99.25
7	73.55	13.89	0.79	0.37	0.03	0.02	0.32	4.21	5.06	—	0.03	0.68	0.23	99.18
8	73.99	13.90	0.57	0.81	0.20	0.02	0.40	4.69	5.06	—	—	0.40	0.25	100.29
9	74.80	13.04	0.40	1.68	0.02	0.02	0.88	3.15	5.11	0.04	0.05	0.51	0.17	99.87
10	73.18	13.88	0.40	1.24	0.03	0.03	0.37	4.35	5.22	—	0.05	0.75	0.15	99.65
11	73.93	14.04	0.30	0.44	0.14	0.03	0.33	3.94	5.74	—	0.03	0.45	0.08	99.45
12	74.62	14.44	0.22	0.50	0.20	0.02	0.40	3.73	4.14	0.14	0.02	0.75	0.08	99.26
13	71.88	14.96	1.00	1.18	0.22	0.02	0.99	3.88	4.82	0.14	0.06	0.41	—	99.56
14	73.28	14.79	0.67	0.56	0.03	0.02	0.34	4.15	5.59	0.14	0.09	0.32	—	99.98
15	73.79	15.37	0.08	0.44	0.01	0.02	0.36	3.88	4.85	—	0.05	0.85	0.14	99.84
16	73.85	13.40	0.61	1.87	0.02	0.02	0.70	3.50	4.65	—	0.03	0.85	0.27	99.77
17	72.77	13.40	0.81	1.62	0.02	0.02	0.70	4.04	4.82	—	0.03	0.85	0.21	99.29
18	73.88	13.33	0.26	0.47	0.21	0.01	0.33	3.75	5.57	—	0.02	0.85	0.15	98.83
19	73.55	14.50	0.50	1.18	0.14	0.01	0.91	2.39	5.47	—	0.06	0.65	0.14	99.50
20	73.43	14.46	0.69	0.50	0.03	0.01	0.54	3.40	5.52	—	0.05	0.55	0.11	99.29

Fig. 3 shows the variation of the weight percentages  $\text{Na}_2\text{O} + \text{K}_2\text{O}$ ,  $\text{FeO} + \text{Fe}_2\text{O}_3$  and  $\text{MgO}$  of Kadabora granitic rocks. It is evident that these granitic rocks are homogeneous in composition, rich in alkalis and poor in  $\text{FeO}$  and  $\text{MgO}$ .

Fig. 4 shows the variation of  $\text{SiO}_2$ ,  $\text{Al}_2\text{O}_3$ ,  $\text{Fe}_2\text{O}_3$ ,  $\text{MgO}$ ,  $\text{CaO}$ ,  $\text{Na}_2\text{O}$  and  $\text{K}_2\text{O}$  against differentiation index (D. I.) of THORNTON and TUTTLE [1960]. It is clear that

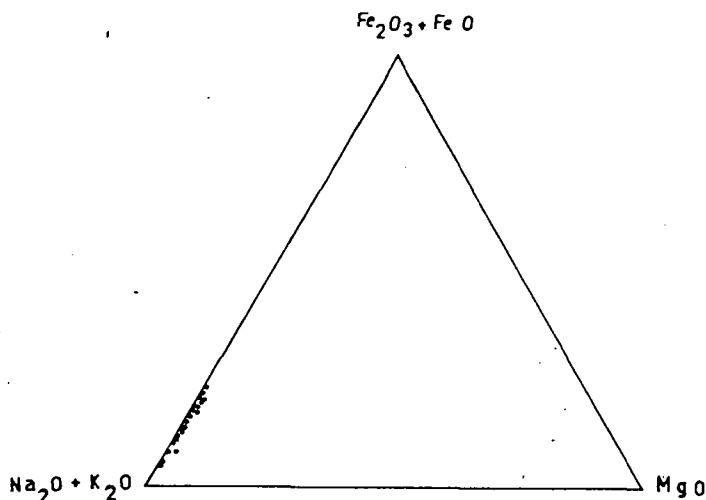


Fig. 3. Relationship between  $\text{MgO}$ ,  $(\text{FeO} + \text{Fe}_2\text{O}_3)$  and  $(\text{Na}_2\text{O} + \text{K}_2\text{O})$

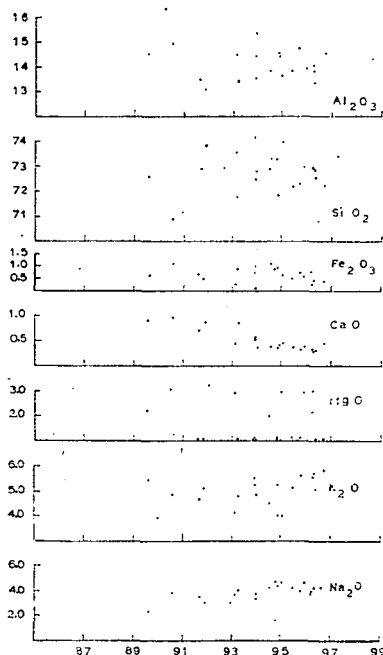


Fig. 4. Plots of percentages of major oxides versus THORNTON and TUTTLE's differentiation index

SiO<sub>2</sub>, Na<sub>2</sub>O and K<sub>2</sub>O increase with D. I., Al<sub>2</sub>O<sub>3</sub> and MgO show no definite trend. Fig. 5 shows the relative molecular ratio of K<sub>2</sub>O/Na<sub>2</sub>O of the granitic rocks. It is clear from the diagram that all the examined granitic rocks have K<sub>2</sub>O/Na<sub>2</sub>O ratio >0.6. According to RAGUIN [1965], these granitic rocks possess potassic characters. SEGERSTROM and YOUNG [1972] found a felsic mafic ratio to be very useful in classifying igneous rocks. This ratio is expressed by SiO<sub>2</sub>+K<sub>2</sub>O/Fe<sub>2</sub>O<sub>3</sub>+FeO+MgO+CaO. Using data by NOCKOLDS [1954] on average chemical composition of igneous rocks,

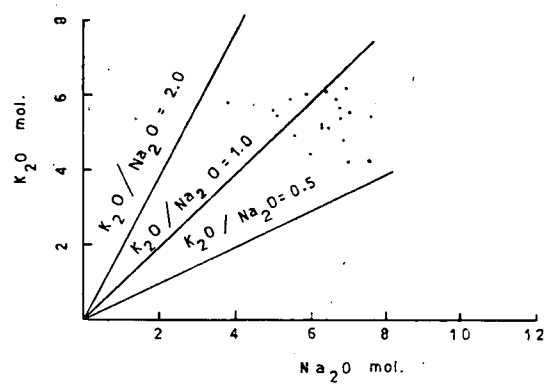


Fig. 5. Variations in alkalis of the granitic rocks

SEGERSTROM and YOUNG (op. cit.) advanced felsic mafic ratios for the various igneous rocks slightly modified by YOUNG, the distribution is as follows:

<i>Rock type</i>	<i>Felsic-mafic ratio</i>
Extreme alkali granite	>50
Alkali granite	25—50
Granite	15—25
Qz—monzonite	10—15
Granodiorite	7—10
Qz—diorite	5—7
Monzonite	3—5
Diorite	2.1—3
Gabbro	1.4—2.1
Ultramafics	<1.4

In the present work the felsic-mafic ratio of the analysed rocks ranges from 23.77 to 76.55 (Table 2). Thus they pertain to alkali granite and extreme alkali granite.

The calculated NIGGLI values of the examined granitic rocks are given in Table 3. The values of al are plotted against alk values of NIGGLI, (Fig. 6). It is clear that the granitic rocks of Kadabora fall within the relatively alkali rich according to BURRI—NIGGLI [1945]. Fig. 7 shows the plots of NIGGLI values of the analyzed granitic rocks. The diagram represents a section through the double tetrahedron al-fm-c-alk, as has been outlined by NIGGLI [1954].

From the diagram, it appears that all the examined granitic rocks of Kadabora pertain to the alkali-aluminosilicate magma type (type II in NIGGLI's calssification).

TABLE 2

*Felsic-mafic ratio for the examined granites*

Sample No.	Felsic-mafic ratio	Sample No.	Felsic-mafic ratio
1	33.99	11	69.10
2	43.38	12	62.49
3	55.41	13	23.77
4	37.80	14	51.89
5	76.55	15	92.72
6	50.22	16	25.62
7	55.58	17	25.91
8	42.29	16	65.51
9	42.87	19	29.82
10	40.56	20	46.79
Average			47.86

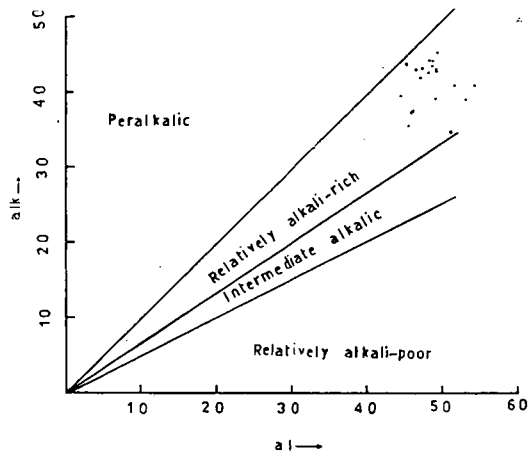
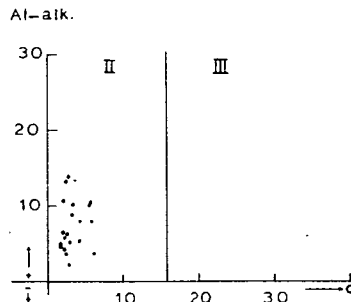
Fig. 6. Relationship of *al* and *alk* in the granitic rocks (after BURRI and NIGGLI, 1945)

Fig. 7. Plots of granitic rocks on NIGGLI's planar representation

TABLE 3

*Niggli values for the the examined granites*

Sample number	al	fm	c	alk	mg	k	qz	si
1	47.27	9.90	2.39	40.44	0.09	0.41	+164.86	426.62
2	47.24	7.88	2.90	41.98	0.22	0.36	+173.10	441.02
3	51.61	5.43	2.32	40.64	0.01	0.38	+184.96	447.52
4	48.66	8.18	3.72	39.44	0.01	0.53	+207.15	464.91
5	49.02	2.95	2.81	45.22	0.06	0.47	+136.82	417.70
6	48.90	5.58	2.37	43.15	0.04	0.45	+144.38	416.98
7	48.73	5.72	2.04	43.51	0.04	0.44	+163.92	437.96
8	45.97	7.99	2.39	43.64	0.21	0.41	+140.75	415.31
9	46.04	10.51	5.65	37.80	0.02	0.52	+196.90	448.10
10	46.67	7.99	2.26	43.07	0.03	0.44	+145.38	417.66
11	48.86	4.86	2.09	44.18	0.25	0.49	+159.90	436.62
12	52.89	5.57	2.65	38.89	0.33	0.42	+208.35	463.91
13	45.57	13.54	5.53	35.35	0.12	0.45	+130.24	371.64
14	49.23	5.84	2.07	42.85	0.04	0.47	+142.72	414.12
15	54.05	2.73	2.29	40.92	0.03	0.45	+176.81	440.49
16	46.28	12.12	4.37	37.23	0.01	0.46	+184.01	432.93
17	44.75	11.38	4.22	39.65	0.01	0.44	+153.90	412.50
18	48.19	5.53	2.17	44.10	0.35	0.49	+176.99	453.39
19	51.08	8.37	5.82	34.73	0.15	0.60	+200.77	439.69
20	50.60	5.83	3.41	40.33	0.04	0.52	+173.28	434.60

## CHEMICAL CLASSIFICATION

The chemical classification of the granitic rocks of Kadabora is advanced based on their normative feldspars. *Fig. 8* shows the normative classification suggested by HIETANEN [1963]. According to this scheme all the granitic rocks fall within the field of granite.

*Fig. 9* shows the normative classification of STRECKEISEN, [1976] for the quartz — feldspar rocks. It is clear that the majority of the granitic rocks of Kadabora fall within the field of alkali-feldspar granite with very few in the field of syeno-granite.

## PETROGENESIS

The normative quartz, orthoclase and albite proportions of the granitic rocks (Table 4) are plotted and the results compared with experimental data of TUTTLE and BOWEN [1958] (*Fig. 10*). It appears from the figure that the majority of the granitic rocks have their composition close to the minimum melting point at low to moderate water-vapour pressures in the  $\text{NaAlSi}_3\text{O}_8$ — $\text{SiO}_2$ — $\text{H}_2\text{O}$  system. From the close relationship between the minimum melting point for low water vapour pressures and the normative composition for the analyzed rocks in WASHINGTON's tables [1917] in which normative  $\text{Qz} + \text{Or} + \text{Ab}$  are 80%, TUTTLE and BOWEN [1958] concluded that there can be little doubt that magmatic liquids are involved in the genesis of these granitic rocks.

The plots of normative  $\text{Qz}$  —  $\text{Ab}$  and  $\text{Or}$  of the granitic rocks correlated with the synthetic systems  $\text{NaAlSi}_3\text{O}_8$ — $\text{KAlSi}_3\text{O}_8$ — $\text{SiO}_2$ — $\text{H}_2\text{O}$ , [LUTH *et al.*, 1964] are shown in *Fig. 11*. The granitic rocks fall in a region corresponding to the liquidus in the

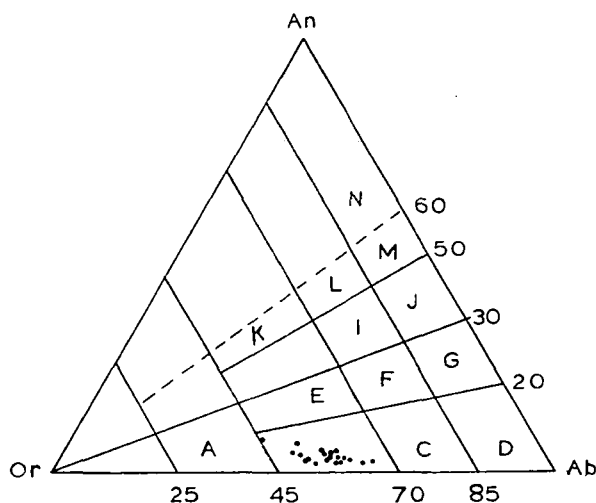


Fig. 8. Triangular diagram for An, Ab and Or normative ratio in the granitic rocks (after HIETANEN, 1963)

A Potassium granite; B Granite; C Granite-Trondhjemite; D Trondhjemite; E Quartz-monzonite; F Monzonite; G Tonalite; H Calci-granite; I Granodiorite; J Quartz diorite; K Calci-monzonite; L Granogabbro; M Gabbro; N Mafic gabbro

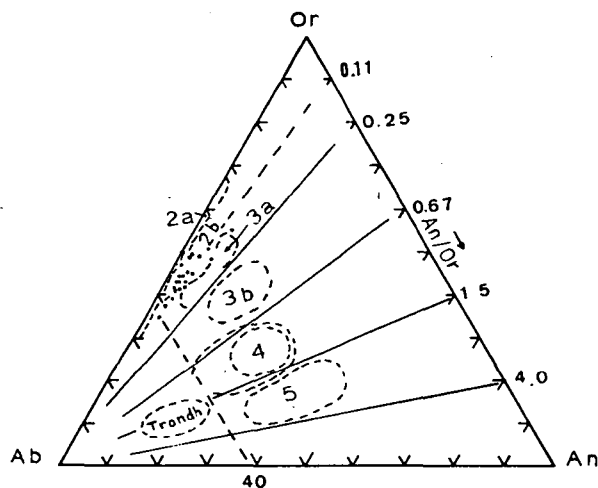


Fig. 9. Quartz-feldspar rocks (after STRECKEISEN, 1976)

2a Alkali granite, Alkali rhyolite; 2b Alkali-feldspar granite, Rhyolite; 3a (Syeno-) Granite, Rhyolite; 3b (Monzo-) Granite, Rhyodacite; 4 Granodiorite, Dacite; 5 Tonalite, Plagidacite, Trondhjemite

minimum system Ab — Or — and Qz — H<sub>2</sub>O at relatively low water — vapour pressures.

BOWES [1967] has also concluded that the closeness of the normative Qz, Or and Ab proportions of some of the paraautochthonous and intrusive Lewisian granitic

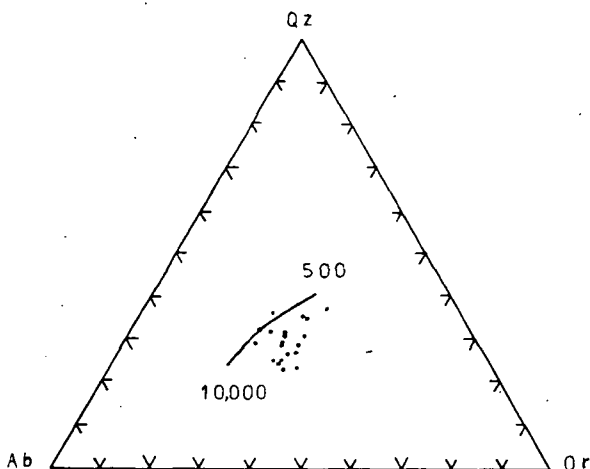


Fig. 10. Normative  $Qz$ ,  $Or$  and  $Ab$  proportions for the investigated granite mass. The solid line represent the variation in position of the minimum melting points in the granite system at water vapour pressures from 500 to 10,000 bars (after TUTTLE and BOWEN, 1958)

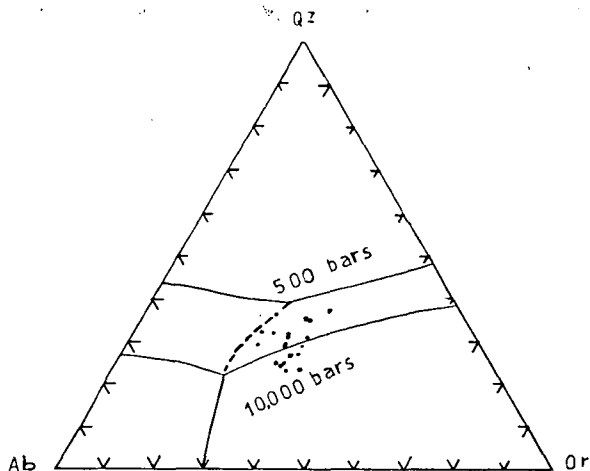


Fig. 11. Normative  $Ab$ ,  $Or$  and  $Qz$  of the granitic rocks, plotted in the system  $NaAlSi_3O_8-KAlSi_3O_8-SiO_2-H_2O$ . Field boundaries at 500 and 10,000 bars are shown. Dotted line represents the trace of the isobaric minimum or eutectic point at intermediate water pressures (after LUTH *et al.*, 1964)

rocks to the minimum melting point composition at low water-vapour pressure in the system  $NaAlSi_3O_8-KAlSi_3O_8-SiO_2-H_2O$  indicates genesis by selective melting followed by crystallization at low water vapour pressure. The normative  $Or+Ab$  and  $An$  proportion of the analyzed granitic rocks (Table 4) have been plotted in a ternary diagram (Fig. 12). The majority of the plots fall in the plagioclase field, mostly close to the isobaric univariant curve indicating that crystal equilibrium was the dominant mechanism involved in the genesis of these granites [JAMES and HAMILTON, 1972].



TABLE 4

## Norm values and D. I. for the investigated granites

Sample number	qz	or	ab	an	c	en	fs	mt	il	wo	ap	Total	D. I.
1	28.72	27.00	38.80	1.95	1.45	0.30	0.62	1.14	0.02	—	—	100.00	94.52
2	28.48	23.80	42.80	2.30	0.75	0.56	0.68	0.61	0.02	—	—	100.00	95.08
3	31.19	24.10	39.55	1.80	2.45	0.02	0.08	0.78	0.02	—	—	99.99	94.84
4	33.58	31.95	28.45	2.85	1.69	0.02	0.42	1.02	0.02	—	—	100.00	93.98
5	22.85	34.50	39.35	2.30	0.33	0.06	0.28	0.31	0.02	—	—	100.00	96.70
6	24.08	32.15	38.65	1.95	1.16	0.08	0.08	0.82	0.02	—	—	99.99	94.88
7	27.33	30.50	38.55	1.60	1.01	0.08	0.08	0.81	0.04	—	—	100.00	96.38
8	23.88	29.95	42.15	1.95	—	0.56	0.90	0.60	—	0.01	—	100.00	95.98
9	32.08	30.85	28.90	4.30	0.89	0.06	2.36	0.42	0.06	—	0.06	99.98	91.83
10	24.62	31.25	39.60	1.85	0.46	0.08	1.64	0.42	0.06	—	—	99.93	95.47
11	26.14	34.35	35.80	1.65	0.83	0.40	0.48	0.31	0.04	—	—	100.00	96.29
12	33.92	25.00	34.24	1.45	3.68	0.56	0.66	0.22	0.02	—	0.22	99.98	93.17
13	26.36	28.85	35.30	4.45	1.95	0.60	1.14	1.06	0.06	—	0.22	99.98	90.51
14	25.15	33.20	37.40	1.15	1.64	0.08	0.34	0.70	0.12	—	0.22	100.00	95.75
15	29.65	29.05	35.30	1.80	3.42	0.02	0.60	0.09	0.06	—	—	99.99	94.00
16	31.25	28.15	32.25	3.55	1.51	0.06	2.54	0.64	0.04	—	—	99.99	91.65
17	27.03	28.90	37.30	3.55	0.36	0.06	1.98	0.84	0.04	—	—	100.00	93.23
18	27.98	33.75	34.55	1.70	0.59	0.06	0.54	0.27	0.02	—	—	100.00	96.28
19	34.12	33.30	22.15	4.65	3.38	0.40	1.64	0.28	0.08	—	—	100.00	89.57
20	29.54	33.54	31.30	2.70	2.15	0.08	0.28	0.73	0.06	—	—	100.00	93.99

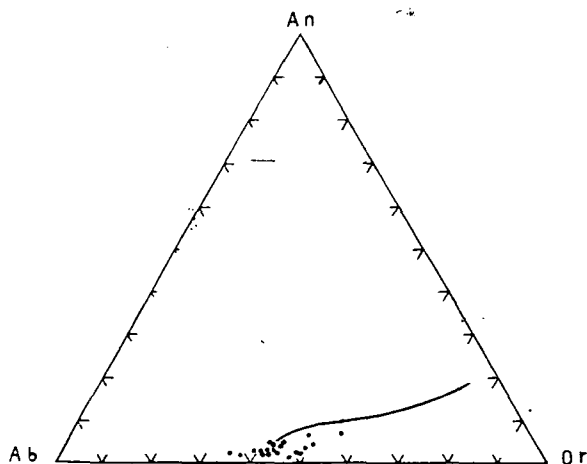


Fig. 12. Normative Ab, An, Or proportions for the investigated granite mass. The solid line represents the two feldspar boundary curve for the quartz saturated ternary feldspar system at 1000 bars water vapour pressure (after JAMES and HAMILTON, 1972)

The major normative difference among the granitic rocks of Kadabora lies in the normative An, which ranges between 1.15 and 4.65. Any consideration of experimentally studied systems must therefore take into account the difference in anorthite content. In this regard the normative Ab, An, and Qz proportions of the analyzed samples are plotted and results compared with the experimental data of VON PLATTEN [1965] for the system obsidian-anorthite-H<sub>2</sub>O having average Ab/An ratio of 17.14 (Fig. 13).

In this diagram there are three areas of crystallization (first for quartz, second for plagioclase and third for alkali feldspar) separated by three cotectic lines which meet in the eutectic point. It is evident that the examined granitic rocks lie in the plagioclase region. The diagram may reveal that the granitic rocks could have been produced by the fusion of a single pre-existing rock type.

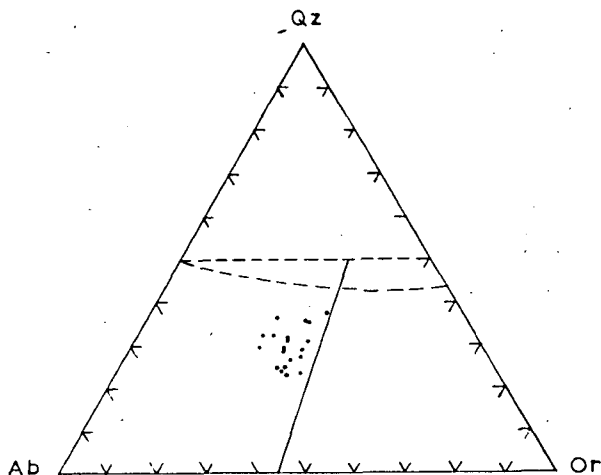


Fig. 13. Plots of normative Ab, Qz, Or of the granitic rocks in relation to cotectic lines and eutectic points valid for obsidian — anorthite — H<sub>2</sub>O having an Ab/An ratio 17.14.

### CONCLUSION

The granitic rocks of Gabal Kadabora, from the Precambrian basement of the central Eastern Desert Egypt are petrochemically evaluated. The average chemical composition of the investigated granites compares fairly well with that of low Ca-granite of TUREKIAN and WEDEPOHL [1961]. The granites of Kadabora show potassic characters with scarce sodic tendencies. Petrochemically the examined granitic rocks appear to represent a highly differentiated suite which comprise alkali granite, and syeno-granite. On the basis of experimentally studied systems it is argued that the granitic rocks of Kadabora are of magmatic origin.

### REFERENCES

- BOWES, D. R. [1967]: The petrochemistry of some Lewisian granitic rocks, *Miner. Mag.*, **36**, 342—363.
- BURRI, C. and NIGGLI, P. [1945]: Die jungen Eruptivgesteine des mediterranen Orogens I. Publ. Vulkaninstitut Immanuel Friedländer No. 3.
- EL-RAMLY, M. F. and AKAAD, M. K. [1960]: The basement complex in the Central Eastern Desert of Egypt, between latitudes 24° 30' and 25° 40' Geol. Surv. Cairo.
- EL-RAMLY, M. F. [1972]: A new geological map for the basement rocks in the Central Eastern and South-Western Deserts of Egypt. *Annals of the Geological Survey of Egypt*, Vol. II, 1—12.
- HIETANEN, A. [1963]: Idaho batholith near Pierce and Bunglow. Prof. Pap. U. S. Geol. Surv. **344 D**
- JAMES, R. S. and HAMILTON, D. L. [1972]: Phase relations in the system NaAlSi<sub>3</sub>O<sub>8</sub>—KAlSi<sub>3</sub>O<sub>8</sub>—CaAl<sub>2</sub>Si<sub>2</sub>O<sub>8</sub>—SiO<sub>2</sub> at 7 Kilobar water — vapour pressure. *Contr. Mineral. Petrol.*, **21**, 111—141.
- KABESH, M. L., REFAAT, A. M. and MONIR, M. A. [1975]: On the modal and chemical classification of the granitic rocks of Umm Naggat stock, Eastern Desert Egypt. *Chem. Erde*, **34**, 293—301.

- KABESH, M. L. HILMY, M. E., and RAGAB, A. G. [1976]: Some petrochemical characters of the granitic rocks of El-Atwai Stock, Eastern Desert Egypt. *Chem. Erde*, **35**, 185—191.
- KABESH, M. L., SALEM, A. K. A. and SALEM, M. A.: Petrochemistry and petrogenesis of El-Yatima Granitic Stock, Eastern Desert, Egypt. *Chem. Erde* (in press).
- LUTH, W. C., JAHNS, R. H., and TUTTLE, O. F. [1964]: The granitic system at pressures of 4 to 10 Kilobars. *J. Geophys. Research* **69**, 759—773.
- NOCKOLDS, S. R. [1954]: Average chemical composition of igneous rocks. *Bull. Geol. Soc. America* **65**, 1007—1032.
- NIGGLI, P. [1954]: Rocks and mineral deposits. W. H. Freeman.
- RAGUIN, E. [1965]: Geology of granite. Interscience Publ.
- SABET, A. H., V. V. BESSONENKO, B. A. BYKOV [1976]: The Intrusive Complexes of the Central Eastern Desert of Egypt. *Annals of the Geol. Surv. of Egypt* **V, VI**, pp. 53—73.
- SALEM, A. K. A. [1975]: Petrographical and Petrochemical Studies on the Granitic Rocks of Gabal Kadabora and Abu Iteila, Eastern Desert Egypt. Ph. D. Thesis, Ain Shams Univ., Egypt.
- SEGERSTOM, K., E. J. YOUNG, [1972]: General geology of the Hahns Peak and Farwell. Mountain Quadrangles, Routt County, Colorado. U. S. G. S., Bull., **1349**.
- STRECKEISEN, A. [1976]: Classification of the common igneous rocks by means of their chemical composition. A provisional attempt. *N. Jahrbuch. f. Mineralogie: Monatshefte*, pp. 1—15.
- THORNTON, C. P., O. F. TUTTLE [1960]: Chemistry of igneous rocks, Part I. Differentiation Index. *Amer. J. Sci.*, **258**, 644—684.
- TUTTLE, O. F., N. L. BOWEN [1958]: Origin of the granite in the light of experimental studies in the system  $\text{NaAlSi}_3\text{O}_8$ — $\text{KAlSi}_3\text{O}_8$ — $\text{SiO}_2$ — $\text{H}_2\text{O}$ . *Geol. Soc. Am. Mem.*, **74**.
- TUREKIAN, K. K., K. H. WEDEPOHL [1961]: Distribution of the elements in some major units of the Earth's crust. *Geol. Soc. Amer., Bull.* **72**, 175—192.
- PLATTEN, H. VON [1965]: Experimental anatexis and genesis of migmatites. Control of metamorphism. John Wiley, N. Y.
- WASHINGTON, H. S. [1917]: Chemical analyses of igneous rocks, U. S. Geol. Surv. Prof., Paper **99**.

*Manuscript received, July 6, 1979.*

PROF. DR. MAHMOUD LOTFY KABESH  
Earth Sciences Laboratory,  
National Research Centre,  
Dokki, Cairo, Egypt  
PROF. DR. MOHAMED E. HILMY,  
Faculty of Science,  
Ain Shams University,  
Cairo, Egypt  
DR. ABDEL-KARIM A. SALEM,  
Earth Sciences Laboratory,  
National Research Centre  
Dokki, Cairo, Egypt

## **PETROCHEMISTRY AND PETROGENESIS OF ABU DOB GRANITIC STOCK, EASTERN DESERT, EGYPT**

**MAHMOUD LOTFY KABESH, MOHAMED E. HILMY  
and ABDEL-KARIM AHMED SALEM**

### **ABSTRACT**

The granitic rocks of Abu Dob stock, Eastern Desert, Egypt are petrochemically characterized. Results of 12 new chemical analyses are presented and processed according to several chemical parameters. The average chemical composition of Abu Dob granitic rocks agrees broadly with low-calcium granite of TUREKIAN and WEDEPOHL, [1961]. The granitic rocks belong to the calc-alkaline series. Modal and chemical classifications of these granitic rocks are advanced. Magmatic origin is suggested for the investigated rocks based on experimentally studied systems.

### **INTRODUCTION**

EL-RAMLY and AKAAD [1960], SABET [1961] and EL-RAMLY [1972] regarded the granitic rocks of Abu Dob as belonging to the younger group of granitoids. SABET *et al.*, [1976] considered the granitic rocks of Abu Dob together with several granitic plutons in the Eastern Desert of Egypt as belonging to the late Proterozoic — Early Paleozoic intrusions. These authors also assigned such granitic plutons to the “Gattarian Group” and to the phase of the coarse — grained biotite granite and the leucocratic granite.

The investigated rocks of Abu Dob occur in the Central Eastern Desert of Egypt (*Fig. 1*). The present work constitutes part of a continuing program aiming at the petrochemical characterisation and petrogenesis of the younger granitoids of Precambrian age in the Central Eastern Desert of Egypt, [KABESH *et al.*, 1974; KABESH *et al.*, 1975; KABESH *et al.*, 1976; REFAAT *et al.*, 1977; RAGAB *et al.*, 1979; KABESH *et al.*, in press — a) and KABESH *et al.*, 1980 b]. In the present study the petrochemical features and petrogenesis of Abu Dob granitic stock are discussed. A chemical classification of the granitic rocks is advanced based on normative feldspars.

### **GEOLOGIC SETTING OF ABU DOB AREA**

Abu Dob area is dominantly formed of basement complex of Precambrian age. The rocks comprise schists, metavolcanics, diorites, granodiorites and granitic rocks. The previous basement rocks are cut by post-granitic dykes (*Fig. 2*). The granitic rocks of Gebel Abu Dob form a roughly circular mass showing intrusive sharp contacts with the metasediments, the meta-volcanics and the dioritic rocks. The granitic rocks form moderately elevated features and comprise three major distinct field types; granodiorites, coarse-grained pinkish white granites and coarse-grained pink-red granites. The relative age of these granitic rocks is determined in the field



on the basis of cross-cutting relations and presence of included xenoliths of the country rocks within the host granites. Boundaries between the granitic types may be sharp but generally they are gradational and need not reflect major changes in mineralogy. It is assumed therefore that the granites of Abu Dob may be considered as homogeneous representing crystallization of the granitic magma in one phase of emplacement. They appear in a general way to have reached their present position probably by forcible intrusion and shouldering apart of the country rocks. Moreover, the emplacement was likely accompanied by some kind of granite tectonics [SALEM, 1972].

## PETROGRAPHY

Petrographically, several types have been recognized namely biotite adamellite, biotite perthite-granite, muscovite perthite-granite, microcline-perthite granite and leuco-granite. Generally these granites exhibit holocrystalline hypidic micrographic granular texture. They are coarse-grained usually non-porphyritic and even-grained. Porphyritic types are not uncommon with megacrysts of quartz up to 5 mm across and microcline-perthite up to 3.5 mm across. The essential minerals are quartz, microcline-perthite, plagioclase (albite — oligoclase), biotite and muscovite. Few micrographic intergrowths are observed. Rare garnet crystals are seen in some of the pink — red granites.

The alkali feldspars particularly microcline — perthite are heavily charged with iron oxide inclusions along the cleavage planes which is responsible for the conspicuous red aspect imparted to these granites. Quartz is usually clear but is sometimes deformed by fracturing, showing strong undulose extinction and may enclose fine opaque trails. Biotite is the sole mafic and forms stout flakes with torn ends which may be chloritized. The brown variety is dominant while green biotite is rarely observed. Muscovite forms fine interstitial aggregates sometimes enclosed in quartz. Iron oxides, apatite, zircon, sphene and epidote are accessories.

## MODAL COMPOSITION

The quantitative mineral composition for 12 representative samples from Abu Dob granitic rocks are given in Table 1.

TABLE 1

*Modal analysis of Abu Dob granitic rocks*

	1	2	3	4	5	6	7	8	9	10	11	12
Quartz	27.20	34.20	34.40	34.10	37.90	36.20	38.50	36.10	33.00	34.90	26.80	30.60
Potash feldspars	46.30	41.50	32.40	46.50	32.60	43.40	44.70	46.50	37.20	39.10	19.30	20.50
Plagioclase	21.20	15.50	28.20	16.40	15.50	15.10	14.40	15.40	25.20	22.30	44.30	36.00
Biotite	3.70	—	—	—	1.00	—	—	—	—	—	7.80	11.80
Muscovite	—	6.60	—	—	—	4.10	—	—	2.70	—	—	—
Accessories	1.60	2.20	5.00	3.00	4.00	1.20	2.40	2.00	1.90	3.70	1.80	1.10
Total	100	100	100	100	100	100	100	100	100	100	100	100

Fig. 3 shows the classification suggested by the IUGS Subcommittee on the Systematics of Igneous Rocks, [1973]\* which was further reviewed by STRECKEISEN

\* IUGS Subcommittee on the Systematics of Igneous Rocks. Classification and nomenclature of plutonic rocks. Recommendations. *Geotimes* 18 (1973) 10, 26—30.

[1976], based on the modal quartz-alkali feldspar plagioclase relative proportions. According to this classification Abu Dob granitic rocks largely plot in the field of granites. However, one sample falls in the field of granodiorites.

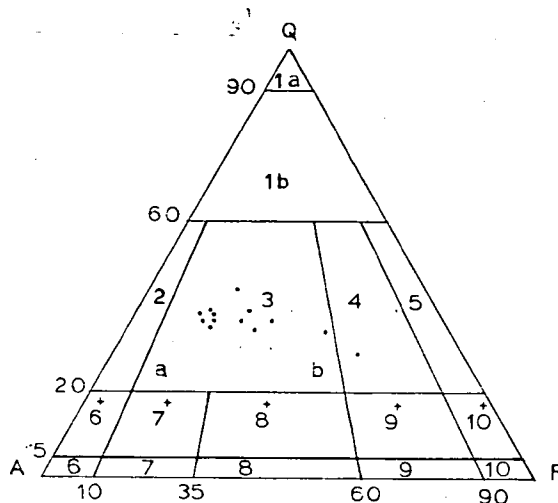


Fig. 3. Classification of Abu Dob granitic rocks on the basis of their quartz (Q), alkali feldspars (A) and plagioclase (P). (Diagram after the IUGS, 1973)

1a: Quartzolite (silexite); 1b: Quartz-rich granitoids; 2: Alkali-feldspar granite; 3: Granite; 4: Granodiorite; 5: Tonalite; 6: Alkali-feldspar syenite; (6<sup>+</sup>: Alkali-feldspar quartz syenite); 7: Syenite; (7<sup>+</sup>: Quartz syenite); 8: Monzonite; (8<sup>+</sup>: Quartz monzonite); 9: Monzodiorite; monzogabbro; (9<sup>+</sup>: Quartz monzodiorite, quartz monzogabbro); 10: Diorite, gabbro, anorthosite; (10<sup>+</sup>: Quartz diorite, quartz gabbro, quartz anorthosite)

### PETROCHEMICAL CHARACTERS

Petrochemical characters of the granitic rocks were deduced from the study of RITTMANN's suite index, normative minerals and NIGGLI values as calculated from chemical analysis.

The chemical analyses of 12 samples representing the different types of the granitic rocks of Abu Dob stock are given in Table 2, the location of the analysed samples is shown in Fig. 2.

### RITTMANN'S INDEX

RITTMANN's suite indices [1957] for Abu Dob granitic rocks are given in Table 2 and are plotted graphically in Fig. 4 against SiO<sub>2</sub>. It is evident from the diagram according to the quantitative subdivisions of RITTMANN that the granitic rocks range between Pacific and average Pacific (1.58—3.19) which correspond to a calc-alkaline character. Compared with the average RITTMANN's Index for some younger granitoid plutons in the Eastern Desert, Umm Naggat (1.82), El-Atawi (1.95), Gilad Said (2.02), and Kadabora (2.59), it is clear that all these granitic plutons belong to a calc-alkaline suite.

Fig. 5 shows the relation between the agpaite coefficient and SiO<sub>2</sub> percent. The agpaite coefficient from the ZAVARITSKI parameter [c. f. BAILY and MACDONALD,

1970] is plotted against  $\text{SiO}_2$  to show the nature of Abu Dob granitic rocks. According to the diagram all the investigated rocks are classified as miaskitic i. e. mol. ratio of  $\text{Na}_2\text{O} + \text{K}_2\text{O} / \text{Al}_2\text{O}_3$  is less than unity.

The calculated NIGGLI values of the granitic rocks are given in Table 3. The values of *al* are plotted against *alk* values of NIGGLI (Fig. 6). It is evident that nearly all the granitic rocks of Abu Dob fall within the relatively alkali-rich, with two samples (representing granodiorites) falling in the intermediate-alkali rocks according to BURRI [1964].

For purpose of comparison the average agpaitic coefficient and  $\text{SiO}_2$  of the granitic plutons of Umm Naggat; [REFAAT *et al.*, 1975], El-Atawi [KABESH *et al.*, 1976],

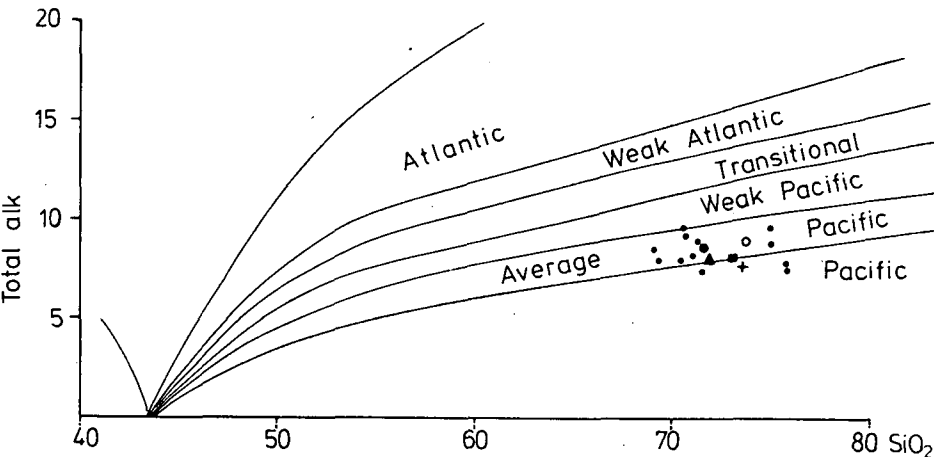


Fig. 4. Plots of RITTMANN's Index for Abu Dob granitic rocks and other localities  
Key to symbols:  
+ Um Naggat      ■ El-Atawi      ▲ Gilad Said  
○ Kadabora      ● Abu Dob (averages);      • Single measurements

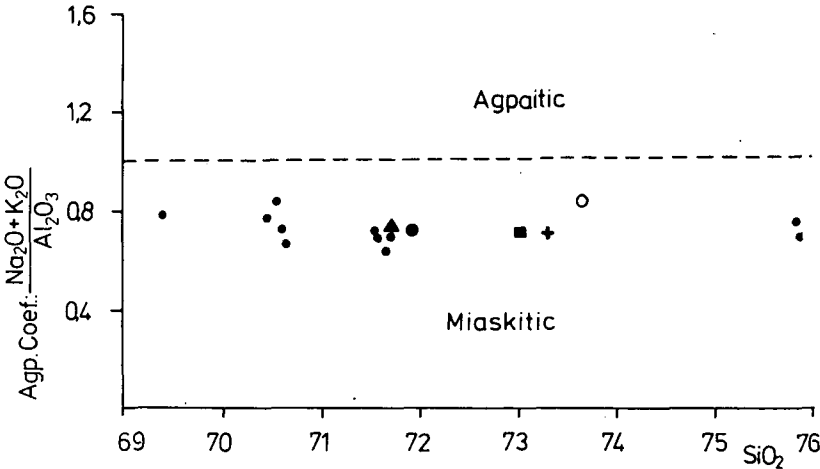


Fig. 5. Agpaitic Index versus  $\text{SiO}_2$  diagram (symbols see in Fig. 4)



TABLE 2a

## Chemical analyses of Abu Dob granitic rocks

	Pink-red granites								Pinkish white granites		Granodiorites		
	1	2	3	4	5	6	7	8	9	10	11	12	Average
SiO <sub>2</sub>	74.90	71.66	70.48	70.55	71.66	71.58	75.82	75.82	70.62	70.62	69.48	69.48	71.88
Al <sub>2</sub> O <sub>3</sub>	13.80	15.60	15.80	14.60	15.90	15.60	13.70	13.20	15.87	15.90	15.40	15.20	15.05
Fe <sub>2</sub> O <sub>3</sub>	0.44	0.43	0.85	0.40	0.35	0.55	0.43	0.53	0.97	0.60	0.50	0.80	0.57
FeO	0.36	0.72	0.95	1.92	1.46	1.40	0.72	0.72	1.91	0.83	1.68	0.90	1.13
MnO	—	—	—	—	0.26	—	—	—	0.26	—	0.30	0.30	0.09
MgO	0.40	0.50	0.30	0.60	0.40	0.50	0.20	0.22	0.20	0.88	1.10	1.30	0.55
CaO	0.61	0.53	0.66	0.90	0.61	0.70	0.44	0.35	0.61	0.37	1.05	1.05	0.69
Na <sub>2</sub> O	3.36	3.44	3.62	3.54	3.34	3.70	3.53	3.52	3.54	3.45	4.43	3.43	3.58
K <sub>2</sub> O	5.54	4.93	5.94	5.84	4.40	4.50	3.68	3.86	4.39	5.38	4.33	4.25	4.75
TiO <sub>2</sub>	0.03	0.03	0.03	0.03	0.04	0.09	0.07	0.05	0.06	0.04	0.03	0.09	0.04
P <sub>2</sub> O <sub>5</sub>	0.04	0.16	0.16	0.04	0.18	0.19	0.18	0.18	0.18	0.14	0.15	0.35	0.06
H <sub>2</sub> O	0.45	1.10	1.00	0.78	0.87	0.62	0.86	0.96	0.70	0.96	1.00	1.00	0.89
Total	99.93	99.10	99.79	99.20	99.47	99.43	99.63	99.41	99.31	99.17	99.45	99.15	99.40
Agp. coef.	0.84	0.70	0.76	0.83	0.65	0.70	0.71	0.75	0.67	0.72	0.78	0.78	0.74
RITTMANN'S Index	2.48	2.44	2.32	3.19	2.09	2.35	1.58	1.66	2.28	2.82	2.90	2.23	2.45

TABLE 2b

## Average of chemical analyses

	A	B	C	D
	Umm Naggat (21) <sup>+</sup>	El-Atawi (10) <sup>+</sup>	Gilad Said (20) <sup>+</sup>	Kadabora (20) <sup>+</sup>
SiO <sub>2</sub>	73.31	73.06	71.72	73.74
Al <sub>2</sub> O <sub>3</sub>	14.09	14.28	14.70	14.09
Fe <sub>2</sub> O <sub>3</sub>	0.71	0.85	1.28	0.59
FeO	1.13	0.75	0.88	0.80
MgO	0.64	1.27	1.15	0.08
CaO	1.19	1.20	1.13	0.51
Na <sub>2</sub> O	3.19	3.81	4.20	3.90
K <sub>2</sub> O	4.24	3.84	3.41	5.03
MnO	0.08	0.04	0.01	0.02
P <sub>2</sub> O <sub>5</sub>	0.11	0.05	0.14	0.02
TiO <sub>2</sub>	0.19	0.13	0.35	0.03
H <sub>2</sub> O <sup>+</sup>	0.43	0.43	0.57	0.61
H <sub>2</sub> O <sup>-</sup>	—	—	—	0.13
Total	99.31	99.71	99.54	99.55
Agp. coef.	0.70	0.73	0.72	0.84
RITTMANN'S Index	1.82	1.95	2.02	2.59

\* average of samples.

Gilad Said [RAGAB *et al.*, 1979] and Kadabora [KABESH *et al.*, 1980 b] are plotted. It is clear that Abu Dob granitic rocks are of the same miaskitic nature as all these plutons.

The calculated norm values of the investigated granitic rocks are given in Table 4.

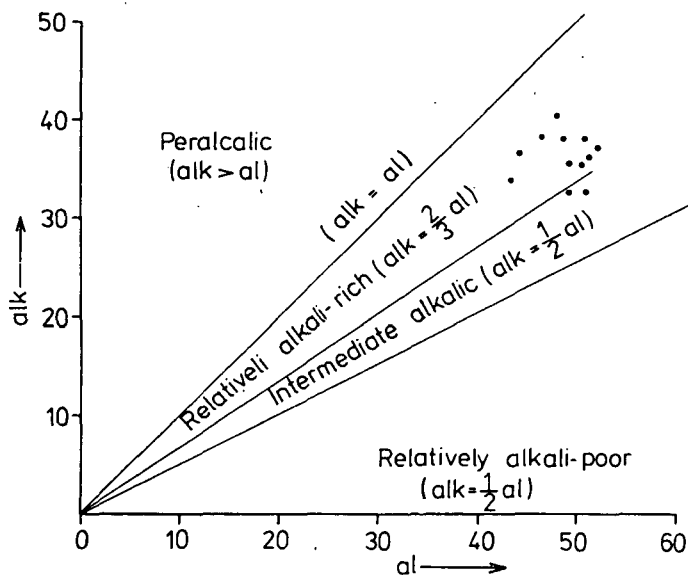


Fig. 6. *al* — *alk* diagram of Niggli

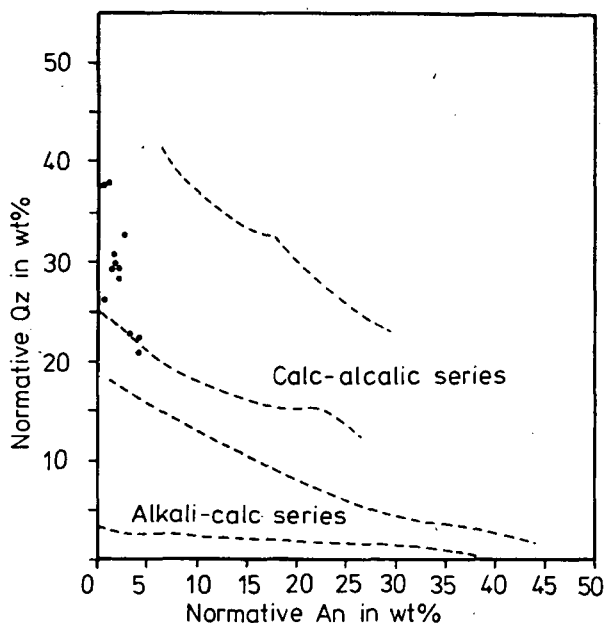


Fig. 7. Normative *Qz* — *An* relation for the investigated granites

Fig. 7 shows the normative quartz plotted against normative anorthite. From the diagram, it is evident that the examined granitic rocks fall within the calc-alkalic series.

TABLE 3

*NIGLI values for the examined granites*

	1	2	3	4	5	6	7	8	9	10	11	12
<i>qz</i>	+184.07	+155.43	+115.07	+114.73	+74.06	+151.94	+239.48	+240.73	+139.43	+129.07	+97.11	+100.93
<i>al</i>	48.39	51.33	48.50	44.06	51.01	50.62	51.96	50.65	49.01	49.32	43.36	43.41
<i>fm</i>	7.31	9.33	9.80	14.34	12.52	9.70	7.87	8.65	14.91	12.93	17.56	17.19
<i>c</i>	3.89	3.17	3.68	4.94	3.56	4.13	3.03	2.44	3.42	2.09	5.37	5.45
<i>alk</i>	40.41	36.17	38.02	36.65	32.91	35.55	37.13	38.25	32.66	35.66	33.71	33.95
<i>mg</i>	0.48	0.45	0.24	0.32	0.26	0.42	0.24	0.25	0.10	0.53	0.45	0.55
<i>K</i>	0.52	0.48	0.52	0.52	0.46	0.44	0.41	0.42	0.45	0.51	0.39	0.39
<i>si</i>	445.71	400.11	367.15	361.33	305.70	394.14	488.00	493.73	370.07	371.71	331.95	336.73

TABLE 4

*Norm values for the investigated granites*

	1	2	3	4	5	6	7	8	9	10	11	12
<i>qz</i>	30.23	29.34	23.35	22.17	30.97	29.17	38.02	38.05	29.08	26.28	20.82	22.14
<i>or</i>	33.10	29.85	35.60	35.15	26.55	27.15	22.25	23.45	26.55	32.40	25.90	25.45
<i>ab</i>	30.55	31.65	32.95	32.40	30.65	33.95	32.45	32.50	32.55	31.55	40.25	40.35
<i>an</i>	2.80	1.60	2.20	4.30	1.95	2.30	1.10	0.65	1.95	0.95	4.25	3.05
<i>c</i>	1.39	4.50	2.90	1.02	5.52	4.27	3.94	3.36	5.13	4.52	2.08	2.45
<i>en</i>	1.12	1.42	0.84	1.68	1.12	1.40	0.56	0.62	0.56	2.48	3.08	3.64
<i>fs</i>	0.22	0.88	0.86	2.72	2.42	0.64	0.74	0.35	2.72	0.82	2.74	1.22
<i>mt</i>	0.46	0.45	0.90	0.42	0.37	0.58	0.46	0.57	1.03	0.64	0.52	0.84
<i>il</i>	0.04	0.04	0.04	0.04	0.06	0.12	0.10	0.06	0.04	0.06	0.04	0.12
<i>ap</i>	0.08	0.35	0.35	0.08	0.37	0.40	0.37	0.37	0.37	0.29	0.32	0.73
Total	99.99	100	99.99	99.98	99.98	99.98	9.99	99.98	99.98	99.99	100	99.99

## CHEMICAL CLASSIFICATION

The chemical classification of Abu Dob granitic rocks is presented based on their normative feldspars.

Fig. 8 is the normative classification of HIETANEN, [1963]. It is clear that all the granitic rocks of Abu Dob fall within the field of granite.

Fig. 9 shows the normative classification suggested by STRECKEISEN [1976] for the quartz-feldspar rocks. It is evident that the granitic rocks of Abu Dob fall largely within the field of alkali granites.

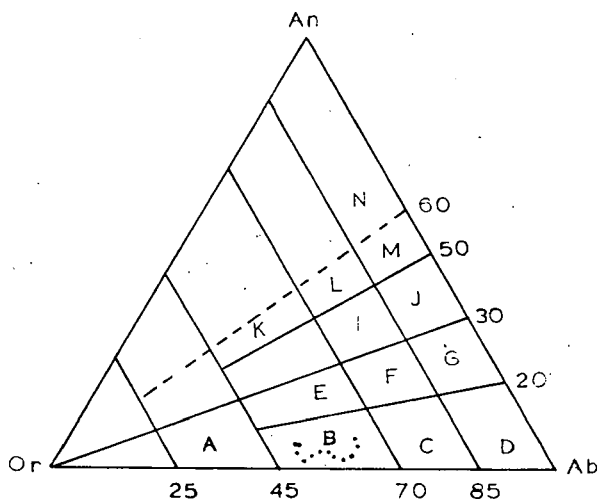


Fig. 8. Triangular diagram for An, Ab and Or normative ratio in the granitic rocks (after HIETANEN, 1963)

A Potassium granite; B Granite; C Granite-trondhjemite; D Trondhjemite; E Quartz monzonite; F Monzonite; G Tonalite; H Calci-granite; I Granodiorite; J Quartz diorite; K Calci-monzonite; L Granogabbro; M Gabbro, N Mafic gabbro

## PETROGENESIS

Consideration of the petrogenesis of Abu Dob granitic rocks is discussed on the basis of some experimentally studied systems using normative quartz-orthoclase and albite proportions of the examined granitic rocks (Table 4.)

Fig. 10 shows plots of the normative Qz — Or — Ab compared with experimental data of TUTTLE and BOWEN [1958]. It is clear from the figure that the majority of the granitic rocks have their composition close to the minimum melting point at low to moderate water vapour pressure in the  $\text{NaAlSi}_3\text{O}_8$ — $\text{SiO}_2$ — $\text{H}_2\text{O}$  system. From the close relationship between the minimum melting point for low water vapour pressure and the normative composition of the analysed rocks in WASHINGTON's tables [1917] in which normative Qz+Or+Ab are 80%, TUTTLE and BOWEN [1958] concluded that there can be little doubt that magmatic liquids are involved in the genesis of these granitic rocks.

The plots of Qz — Or and Ab of Abu Dob granitic rocks correlated with the synthetic system  $\text{NaAlSi}_3\text{O}_8$ — $\text{KAlSi}_3\text{O}_8$ — $\text{SiO}_2$ — $\text{H}_2\text{O}$  [LUTH *et al.*, 1964] are shown

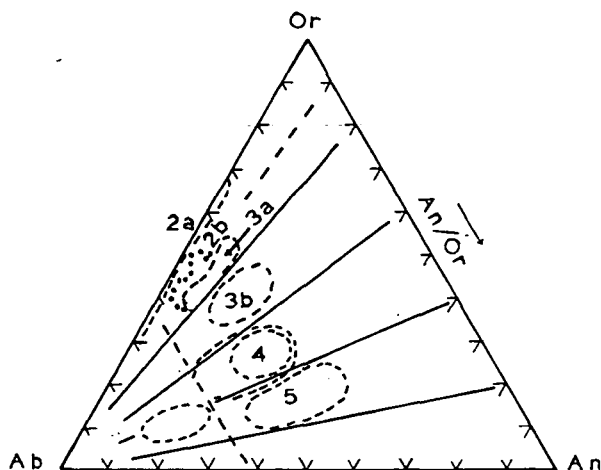


Fig. 9. Quartz — feldspar rocks (after STRECKEISEN, 1976)

2a Alkali granite, Alkali rhyolite; 2b Alkali-feldspar granite, Rhyolite; 3a (Syeno-) Granite, Rhyolite; 3b (Monzo-) Granite, Rhyodacite; 4 Granodiorite, Dacite; 5 Tonalite, Plagidacite, Trondhjemite

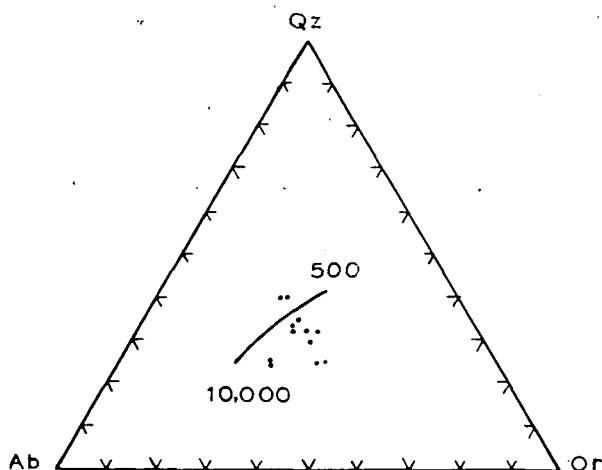


Fig. 10. Normative Qz, Or and Ab proportions for the investigated granite mass. The line represents the variation in position of the minimum melting points in the granite system at water vapour pressures from 500 to 10,000 bars (after TUTTLE and BOWEN, 1958)

in Fig. 11. The granitic rocks fall in a region corresponding to the liquidus in the minimum system Qz—Or— and Ab—H<sub>2</sub>O at relatively low water-vapour pressures.

BOWEN [1967] has concluded that the closeness of the normative Qz, Or and Ab proportions of some of the para-autochthonous and intrusive Lewisian granitic rocks to the minimum melting point composition at low water-vapour pressures in the system NaAlSi<sub>3</sub>O<sub>8</sub>—KAlSi<sub>3</sub>O<sub>8</sub>—SiO<sub>2</sub>—H<sub>2</sub>O indicates genesis by selective melting followed by crystallization at low water-vapour pressure. The normative Or — Ab —

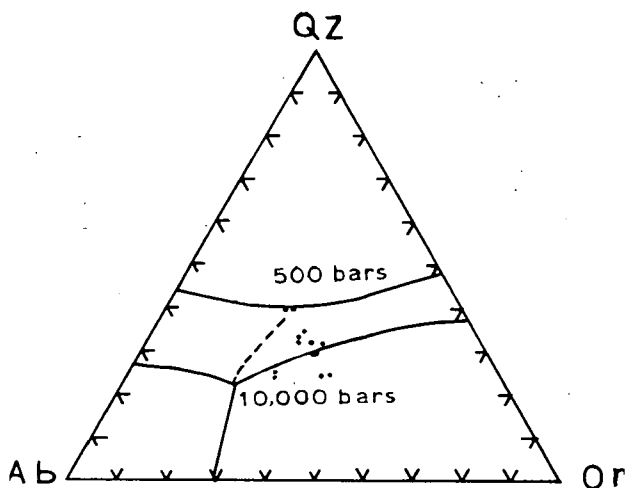


Fig. 11. Normative albite — orthoclase — quartz of the granitic rocks, plotted in the system  $\text{NaAlSi}_3\text{O}_8\text{—KAlSi}_3\text{O}_8\text{—SiO}_2\cdot\text{H}_2\text{O}$ . Field boundaries at 500 and 10,000 bars are shown. Dotted line represents the trace of the isobaric minimum or eutectic point at intermediate water vapour pressures (after LUTH *et al.*, 1964)

and An proportions of the analysed granitic rocks have been plotted in a ternary diagram (Fig. 12). It is evident that the majority of the plots are in the plagioclase field mostly close to the isobaric univariant curve indicating that crystal equilibrium was the dominant mechanism involved in the genesis of these granites [JAMES and HAMILTON, 1972].

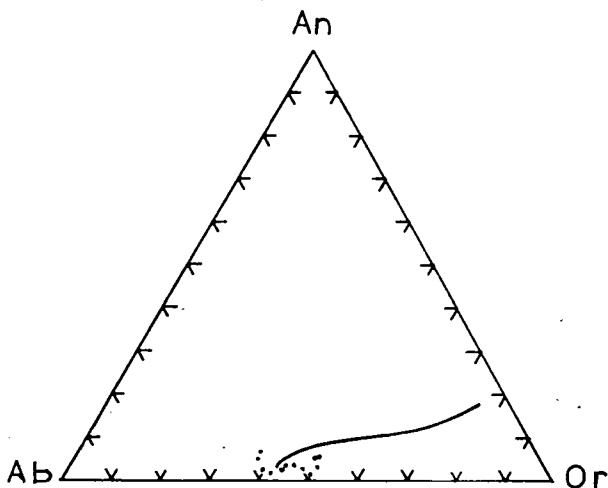


Fig. 12. Normative Or-Ab-An proportions for the investigated granite mass. The solid line represents the two feldspar boundary curve for the quartz saturated ternary feldspar system at 1000 bars water vapour pressure (after JAMES and HAMILTON, 1972)

## CONCLUSION

The granitic rocks of Gebel Abu Dob from the Precambrian of the Central Eastern Desert, Egypt are petrochemically characterized. The average chemical composition of the examined rocks agrees fairly well with that of low-calcium granite of TUREKIAN and WEDEPOHL [1961]. Petrochemically Abu Dob granitic rocks belong to the calc-alkalic series and appear to represent a differentiated suite which comprise alkali granite and granite. They are of miaskitic nature and compare fairly well with the younger granitoids of Umm Naggat, El-Atawi, Gilad Said and Kadabora. Based on experimentally studied systems the granitic rocks of Abu Dob are believed to be of magmatic origin.

## REFERENCES

- BOWES, D. R. [1967]: The petrochemistry of some Lewisian granitic rocks, *Miner. Mag.*, **36**, 342—363.
- BAILY, K. and MACDONALD, R. [1970]: Petrochemical variation among mildly peralkaline comendite obsidians from the oceans and continents. *Contr. Mineral. and Petrol.* v. **28**, 340—391.
- BURRI, C. [1964]: Petrochemical calculation, Basel Birkhauser Verlag, p. 304.
- BURRI, C. and NIGGLI, P. [1945]: Die jungen Eruptivgesteine des mediterranen Orogens I. *Publ. Vulkaninstitut Immanuel Friedlaender*, No. 3.
- EL-RAMLY, M. F. and AKAAD, M. K. [1960]: The basement complex in the Central Eastern Desert of Egypt, between Latitudes 24° 30' and 25° 40' N. *Geol. Surv.*, Cairo.
- EL-RAMLY, M. F. [1972]: A new geological map for the basement rocks in the Eastern and South — Western Desert of Egypt, *Annals of the Geological Survey of Egypt*, Vol. **II**, 1—12.
- HIETANEN, A. [1963]: Idaho batholith near Pierce and Bungalow. *Prof. Pap. U. S. Geol. Surv.*, **344-D**.
- JAMES, R. S. and HAMILTON, D. L. [1972]: Phase relations in the system  $\text{NaAlSi}_3\text{O}_8$ — $\text{KAlSi}_3\text{O}_8$ — $\text{CaAl}_2\text{Si}_2\text{O}_7$ — $\text{SiO}_2$  at 7 Kilobar water vapour. *Contr. Mineral. Petrol.*, **21**, 111—141.
- KABESH, M. L., REFAAT, A. M. and ALI, M. M. [1975]: On the modal and chemical classification of the granitic rocks of Umm Naggat stock, Eastern Desert Egypt. *Chem. Erde* **34**, 293—301.
- KABESH, M. L. and RAGAB, A. G. [1974]: The chemistry of biotite as a guide to the evolution trends of El-Atawi granitic rocks, Eastern Desert Egypt. *N. Jb. Miner.*, **7**, 307—316.
- KABESH, M. L. and RAGAB, A. G. [1976]: Some petrochemical characters of the granitic rocks of El-Atawi stock, Eastern Desert Egypt. *Chem. Erde* **35**, 185—191.
- KABESH, M. L., SALEM, A. K. A. and SALEM, M. A. [1980a]: Petrochemistry and petrogenesis of El-Yatima granitic stock, Eastern Desert, Egypt. *Chem. Erde* (in press).
- KABESH, M. L., HILMY, M. E. and SALEM, A. K. A. [1980b]: Behaviour of major elements in the granitic rocks of Kadabora pluton, Eastern Desert, Egypt. *Acta Miner. Petr.*, Szeged, **XXIV/2**, 245—256.
- LUTH, W. C., JAHNS, R. H. and TUTTLE, O. F. [1964]: The granite system at pressures of 4 to 10 Kilobars. *J. Geophys. Research* **69**, 759—773.
- RAGAB, A. G., KABESH, M. L., HILMY, M. E. and KHALIL, M. M. [1979]: Petrography, petrochemistry and petrogenesis of Gilad granitic stock, Eastern Desert Egypt. *N. Jb. Miner.*, **134**, 274—287.
- REFAAT, A. M., KABESH, M. L. and ZEINAB, M. A. [1977]: Behaviour of major elements in Ras Barud granitic rocks Eastern Desert Egypt. *J. Geol.* **21/1**.
- RITTMANN, A. [1957]: On the serial character of igneous rocks, Egypt. *J. Geol.*, **1**, 23—48.
- SABET, A. H. [1961]: Geology and mineral deposits of Gebel El-Sibai area Red Sea Hills, Egypt. Ph. D. Thesis, ITC., Delft, Holland.
- SABET, A. H., V. V. BESSONENKO, B. A. BYKOV [1976]: The intrusive complexes of the Central Eastern Desert of Egypt. *Annals of the Geol. Surv. of Egypt*, **VI**, 53—73.
- SALEM, A. K. A. [1972]: Geological and geochemical studies on Gebel Abu Dob area Eastern Desert, Egypt. M. Sc Thesis, Ain Shams Univ., Cairo.
- SALEM, A. K. A. [1976]: Petrographical and petrochemical studies on the granitic rocks of Gebel Kadabora and Abu Itella, Eastern Desert Egypt. Ph. D. Thesis, Ain Shams Univ., Egypt.
- STRECKEISEN, A. [1976]: Classification of the common igneous rocks by means of their chemical composition. A provisional attempt. *N. Jb. Miner., Monatshefte*, 1—15.
- STRECKEISEN, A. [1973]: To each plutonic rocks its proper name. *Earth Sci. Rev.*, **12**, 1—33. (I U G S Subcommittee on the Systematics of Igneous Rocks).

- TUTTLE, O. F. and BOWEN, N. L. [1958]: Origin of the granite in the light of experimental studies in the system  $\text{NaAlSi}_3\text{O}_8$ — $\text{KAlSi}_3\text{O}_8$ — $\text{SiO}_2$ — $\text{H}_2\text{O}$ . Mem. Geol. Soc. Am., **74**, 1—153.
- TUREKIAN, K. K. and WEDEPOHL, K. H. [1961]: Distribution of the elements in some major units of the Earth's crust. Geol. Soc. Amer., Bull. **72**, 175—192.
- WASHINGTON, H. S. [1917]: Chemical analyses of igneous rocks. U. S. Geol. Surv. Prof. Paper **99**.

*Manuscript received, December 1, 1979*

PROF. DR. M. L. KABESH  
Earth Sciences Laboratory,  
National Research Centre,  
Cairo, Egypt

PROF. DR. M. E. HILMY,  
Geology Department,  
Ain Shams University,  
Cairo, Egypt

DR. ABDEL-KARIM A. SALEM,  
Earth Sciences Laboratory,  
National Research Centre,  
Cairo, Egypt





## **GEOCHEMISTRY OF SOME GABBROS FROM MUHAMMAD QOL AREA, NORTHERN RED SEA HILLS, SUDAN REPUBLIC**

MAHMOUD L. KABESH, ADEL M. REFAAT and ZEINAB M. ABDALLAH

### **ABSTRACT**

The Muhammad Qol gabbros can be classified as 3 main rock units comprising olivine pyroxene gabbros, pyroxene gabbros and hornblende pyroxene gabbros. The modal and normative minerals together with the chemical data show that the three rock types were formed during a limited fractionation process in which a type of regular gradation in the chemical composition of the magma had taken place.

The early fractionation stage was characterized by a pronounced mafic liquidus phase from which gabbros bearing much olivine and pyroxene with little plagioclase were formed under high temperature. With progressive fractionation, the crystallized plagioclases became more abundant than the mafic minerals which comprise pyroxene and little olivine crystals. At late fractionation stage, the hydrous minerals began to crystallize under high water pressure and relatively low temperature producing hornblende pyroxene gabbros.

The strong alteration in some gabbroic rocks shows that they were affected greatly by late magmatic hydrothermal solutions. As a result, some major and trace elements in the mafic and felsic minerals had been redistributed during uraltization, chloritization and sericitization processes.

### **INTRODUCTION**

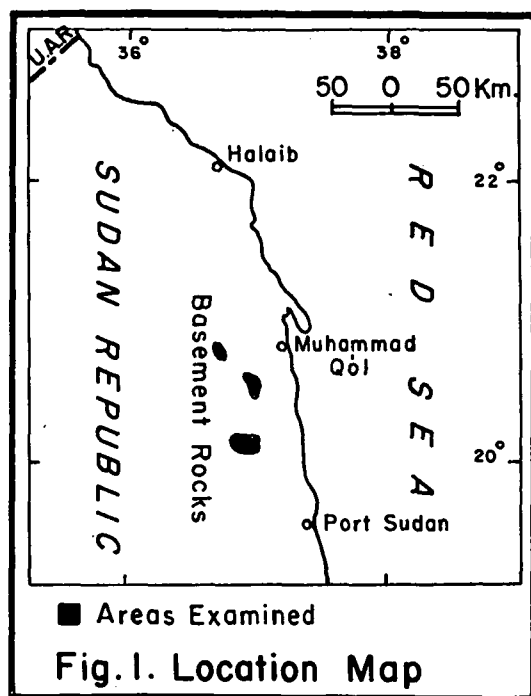
The present study deals with the petrochemistry and geochemistry of some gabbros from the basement complex of Muhammad Qol area, northern Red Sea Hills, Sudan Republic. Broadly, the Red Sea Hills Province is dominantly covered by basement rocks of Precambrian age. However, the Red Sea Hills of the Sudan had been the goal of several investigations. A number of syntheses have been attempted of the basement geology and associated mineralization. The most important are the works of RUXTON [1956], GABERT *et al.* [1960], KABESH [1962], KABESH and LOTFI [1962], LOTFI and KABESH [1964], NEARY *et al.* [1976] and AHMED [1977]. On the other hand, the general geology and economic mineral deposits of the Sudan Republic have been outlined by WHITEMAN [1971] and VAIL [1978].

The gabbroic rocks described and discussed in this work were collected by one of us [KABESH] from Muhammad Qol area in the north-east of the Sudan Republic (*Fig. 1*). The gabbros examined form several quantitatively insignificant masses in Muhammad Qol area. Invariably, the emplacement of the gabbro precedes that of the granitic rocks. This is confirmed by field evidence where gabbros are intruded and veined by granitic rocks [KABESH, 1962].

### **PETROGRAPHY**

The petrographic study of Muhammad Qol gabbros shows that they can be classified as 3 main rock units: olivine pyroxene gabbros, pyroxene gabbros and hornblende pyroxene gabbros.

1. The olivine pyroxene gabbros are composed of 23% olivine, 15% hypersthene, 11% augite, 7% iron ores and 44% plagioclase. These volume mineral percentages are the average of 3 varieties comprising olivine gabbro, olivine hypersthene gabbro and olivine augite gabbro.



2. The pyroxene gabbros contain 10% hypersthene, 6% diopside, 14% augite, 7% olivine, 5% iron ores and 58% plagioclase. These modal mineral percentages are the average of gabbroic varieties representing hypersthene diopside gabbro and augite gabbro.

3. The hornblende pyroxene gabbros comprise 17% hornblende, 8% augite, 6% chlorite, 5% iron ores and 64% plagioclase. These modal mineral percentages represent the average of 2 gabbroic varieties (hornblende augite gabbro and hornblende gabbro).

Both olivine pyroxene gabbros and pyroxene gabbros are nearly identical in their mineralogical constituents and textural features. Olivine mineral is considered the sole ferromagnesian mineral in rare gabbroic samples, while, the olivine and iron tend to occur as aggregates with hypersthene or augite in most gabbros. The olivine augite gabbro is characterized by subophitic intergrowth between normal zoned plagioclase and augite. The augite is light pink in colour and slightly pleochroic.

Some samples of gabbro contain pyroxene as dominant mafic minerals in which hypersthene and diopside or augite are associated with little amounts of olivine. Some gabbroic samples comprise strongly pleochroic hypersthene which sometimes have occasional diopside along their lamellae planes. Most of the pyroxene crystals are generally interstitial to the plagioclases.

In both olivine pyroxene gabbros and pyroxene gabbros, the plagioclases (labradorite) form euhedral crystals ranging in composition from  $An_{55}$  to  $An_{67}$ . The presence of high volume percentage of mafic minerals in the olivine pyroxene gabbros shows that they were crystallized early from a high basic magma compared to gabbros bearing pyroxenes as dominant mafic minerals.

On the other hand, the modal feldspar in the hornblende pyroxene gabbros indicates that this rock unit was crystallized from a declared plagioclase liquidus phase. The plagioclases form euhedral crystals ranging in composition from labradorite ( $An_{52-60}$ ) to andesine ( $An_{42-48}$ ). Hornblendes constitute subhedral crystals, pleochroic from pale yellowish green to dark or even dark brown. Some of the hornblendes enclose the early formed plagioclase crystals. Augite is present in minor amounts and has a typical sieve texture with the enclosing hornblende.

Some samples of the hornblende pyroxene gabbros in which the augite is of ferriferous type are strongly altered showing uraltization at the margins of the pyroxenes. Many augite crystals are altered to greenish hornblende preserving a distinct type of exsolution along their lamellae.

Uralitization, chloritization and sericitization are the common developed processes at late magmatic hydrothermal stage. As the hydrous mineral become more abundant, the hornblende largely replaces the pyroxene crystals. The pyroxene is rimmed by fine fibrous bluish green amphibole showing that a type of reaction relationship between both minerals had taken place due to the effect of hydrothermal solutions which attacked some gabbros at late magmatic stage.

#### GEOCHEMISTRY OF GABBROS

Eight new chemical analyses representing the different petrographic varieties of Muhammad Qol gabbroic rocks are discussed in this study. The major elements (Table 1) of these gabbros were determined by using volumetric and gravimetric methods of BENNETT and REED [1971]. The average analysis of 4 gabbroic samples from the north of Muhammad Qol area [NEARY *et al.* 1976] is given in Table 1 for comparison. The average analysis (analysis no. 9, Table 1) of NEARY *et al.* [1976] agrees to a certain extent with the analysis of augite gabbro (sample no 5, Table 1) in the present study. The normative minerals (Table 2) of the gabbros are calculated from their chemical analyses (Table 1).

Table 3 shows the trace elements (Rb, Sr, Ba, Co, Ni and Cr) for the examined gabbros. These trace elements were detected by spectrographic methods.

#### Major and trace elements

Fig. 2 shows a ternary relation between the  $FeO^*$ ,  $MgO$  and  $Na_2O + K_2O$  (Table 1). The diagram is subdivided into 3 fields in which field A comprises the gabbros of Mid-Oceanic Ridge [MIYASHIRO *et al.*, 1970], field B represents the serpentinites of Mid-Atlantic Ridge [MIYASHIRO *et al.*, 1969] and field C is the ultramafic and gabbroic rocks of Alpine Intrusive Complexes [THAYER, 1967].

It is evident that most samples (numbers 1 and 2) which are characterized by high mafic minerals particularly olivine and orthopyroxene fall within the field of ultramafic and gabbroic rocks. Whereas, the less mafic gabbros (samples numbers 3, 4, 5, 6, and 7) which comprise pyroxene and/or hornblende plot within the field of gabbro. The plotting of sample no. 8 out the 3 discriminated fields of gabbros

TABLE 1

Major elements analyses (%) and some elemental ratios of the Muhammad Qol gabbroic rocks

	1	2	3	4	5	6	7	8	9
SiO <sub>2</sub>	45.81	46.89	46.31	46.33	45.87	47.91	50.01	48.21	45.58
TiO <sub>2</sub>	1.23	1.82	1.02	2.98	1.63	1.59	0.61	0.71	1.01
Al <sub>2</sub> O <sub>3</sub>	13.01	14.63	13.59	14.83	15.93	15.59	16.69	17.21	18.28
Fe <sub>2</sub> O <sub>3</sub>	1.72	1.95	2.61	2.60	1.51	2.34	2.53	3.05	3.44
FeO	11.99	9.98	11.43	9.32	9.78	8.87	7.85	8.00	6.2
MnO	0.27	0.21	0.59	0.37	0.40	0.35	0.32	0.46	0.13
MgO	14.33	11.67	11.63	8.91	8.90	7.71	6.66	6.82	9.79
CaO	8.19	7.99	7.48	10.02	10.53	9.89	8.78	7.35	11.29
Na <sub>2</sub> O	1.34	1.62	2.06	1.61	2.12	2.63	2.91	3.42	1.98
K <sub>2</sub> O	0.20	0.25	1.11	0.35	0.36	0.30	0.45	0.91	0.18
P <sub>2</sub> O <sub>5</sub>	0.09	0.28	0.20	0.17	0.17	0.26	0.14	0.08	0.06
H <sub>2</sub> O	1.56	1.93	1.78	2.32	1.92	2.18	2.32	3.11	2.09
Total	99.81	99.22	99.81	99.29	99.12	99.59	99.27	99.33	100.08
FeO*%	46.16	46.41	48.19	51.75	49.44	50.76	50.24	49.06	
MgO%	48.89	46.18	40.70	39.54	39.53	35.67	33.06	31.15	
Na <sub>2</sub> O + K <sub>2</sub> O%	4.95	7.41	11.11	8.71	11.03	13.57	16.71	19.79	
Felsic index = (Na <sub>2</sub> O + + K <sub>2</sub> O) · 100 / Na <sub>2</sub> O + + K <sub>2</sub> O + CaO	15.82	18.96	29.76	16.73	19.06	22.85	27.67	37.07	
Mafic index = (Fe <sub>2</sub> O <sub>3</sub> + + FeO + MnO) · 100 / Fe <sub>2</sub> O <sub>3</sub> + + FeO + MnO + MgO	49.38	50.98	55.71	57.99	56.77	59.98	61.63	62.79	
100 MgO / (MgO + FeO)	54.30	53.90	50.43	48.87	47.64	46.50	45.89	46.01	
FeO* / MgO	0.94	1.00	1.18	1.30	1.25	1.42	1.52	1.57	

$$\text{FeO}^* = \text{FeO} + 0.899 \text{ Fe}_2\text{O}_3$$

and ultramafic rocks (Fig. 2) is attributed to the presence of high alkali elements (Na<sub>2</sub>O + K<sub>2</sub>O) in this rock variety as result of sericitization process.

The relation between mafic index and felsic index (Table 1) is shown in Fig. 3. The diagram is divided by DREVER and JOHNSTON [1966] into 2 fields comprising basic (upper field) and ultrabasic (lower field) rocks. All Muhammad Qol gabbros fall in the field of basic rocks but samples number 1, 2 and 4 are considered the nearest gabbroic rocks to the ultramafic field.

It is noted that the felsic index varies from 15.82 (olivine gabbro, Table 1) to 37.07 (altered gabbro) whereas, the mafic index ranges from 49.30 (olivine gabbro) to 62.79 (altered gabbro). The low value of mafic index in the olivine gabbro reflects its high content of MgO (14.33, Table 1) compared to MgO (6.82) in the altered gabbro. The great variations in the values of both felsic and mafic indices show that these gabbros were crystallized from a highly changeable magma in its chemical composition during a fractionation process.

Some major and trace elements are plotted against the MgO/(MgO + FeO) ratio in Fig. 4. MgO, FeO, Cr, Ni and Co increase gradually with increasing the MgO/(MgO + FeO) ratio whereas, Al<sub>2</sub>O<sub>3</sub>, Na<sub>2</sub>O, Ba and Rb deplete in the same direction. The contents of TiO<sub>2</sub> in the gabbroic varieties are scattered against the same ratio reflecting that the crystal structure of augite received Ti more rapidly

TABLE 2

## CIPW-norms of the Muhammad Qol gabbroic rocks

	1	2	3	4	5	6	7	8
or	1.16	1.47	6.56	2.05	2.12	1.77	2.65	5.38
ab	11.31	13.73	17.39	13.50	17.91	22.20	24.51	28.90
an	28.80	31.84	24.51	32.18	32.84	29.80	31.15	28.87
di	wo	4.57	2.50	4.71	6.86	7.64	7.34	4.81
	fs	1.49	0.76	1.72	2.08	2.90	2.73	1.92
	en	2.83	1.57	2.75	4.33	4.38	4.25	2.68
hy	fs	7.84	10.45	4.25	8.60	3.02	6.17	9.96
	en	14.63	21.62	6.77	17.94	4.55	9.58	13.96
	fa	7.58	2.22	9.47	—	6.81	2.72	—
ol	fo	12.83	4.16	13.65	—	9.30	3.80	7.30
mt		2.48	2.82	3.78	3.78	2.18	3.39	3.66
il		2.32	3.45	1.93	5.66	3.09	2.96	1.15
ap		0.21	0.66	0.47	0.39	0.39	0.61	0.32
or %	2.81	3.12	13.50	4.29	4.00	3.29	4.54	8.51
ab %	27.40	29.18	35.88	28.28	33.00	55.42	42.03	45.76
an %	69.79	76.70	50.62	67.43	62.13	41.29	53.43	45.73
ab + an	40.11	45.57	41.90	45.68	50.78	52.00	55.66	57.77
Di	12.47	15.20	23.95	15.55	20.03	23.97	27.16	34.28
CI	56.78	50.21	49.50	49.64	44.26	43.53	38.46	32.99
An	71.80	69.80	58.50	70.40	64.70	57.30	55.90	49.90
Di (Differentiation index) = $q + ab + or$ . Normative quartz ( $q$ ) in all samples = 0								
CI (Colour index) = $di + hy + ol + mt + il + ap$								
An (Anorthite content of plagioclase) = $an \times 100 / an + ab$								

TABLE 3

## Trace element concentrations (ppm) of the Muhammad Qol gabbroic rocks

	1	2	3	4	5	6	7	8
Rb	12	15	12	15	14	20	25	35
Sr	180	270	155	175	160	305	390	290
Ba	100	145	110	112	140	150	200	185
Co	95	75	90	63	55	50	45	40
Ni	355	295	380	250	150	180	110	85
Cr	795	580	455	285	185	250	205	130

rather than the other ferromagnesian minerals during the magmatic fractionation process. The behaviour of CaO (Fig. 4) shows a vibrated trend against the mafic ratio, *i. e.* the amounts and types of crystallized calcic minerals particularly plagioclases were controlled by 2 factors: the chemical changes in the pronounced mafic liquidus phase of the gabbroic melt at early stage in addition to the remarkable decreasing in the An contents of the plagioclases with progressive fractionation.

Generally, the MgO/(MgO + FeO) ratios vary from 45.89 in the hornblende gabbro to 54.30 in the olivine gabbro indicating that the chemical composition of the mafic constituents in these gabbros was graduated from a high mafic magma to less basic melt through a limited fractional crystallization process.

## Normative minerals

An, Ab and Or normative minerals (recalculated to 100% total, Table 2) are plotted in Fig. 5 [HIETANEN, 1963]. The examined rock types which are identified by petrographic criteria as gabbroic rocks fall in the fields of mafic gabbro (samples number 1, 2, 3, 4 and 5), gabbro (samples number 7 and 8) and quartz diorite (sample number 6).

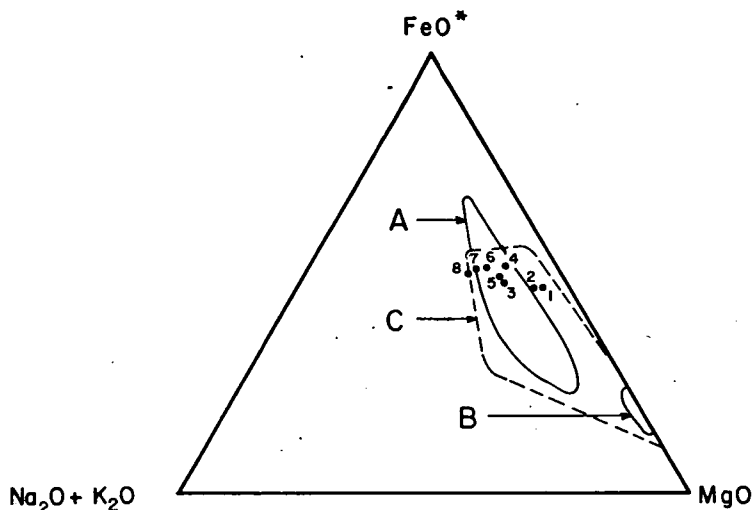


Fig. 2. FeO\*—Na<sub>2</sub>O+K<sub>2</sub>O—MgO diagram (THORPE, 1974).

A is the field of gabbro [MIYASHIRO *et al.* 1970],

B is the field of serpentinite [MIYASHIRO *et al.* 1969] and

C is the field of ultramafic and gabbroic rocks [THAYER, 1967.

$$\text{FeO}^* = \text{FeO} + 0.899 \text{ Fe}_2\text{O}_3$$

### Explanation:

Sample No.	Rock variety
1	Olivine gabbro
2	Olivine hypersthene gabbro
3	Olivine augite gabbro
4	Hypersthene diopside gabbro
5	Augite gabbro
6	Hornblende augite gabbro
7	Hornblende gabbro
8	Altered gabbro

It is interesting to mention that the gabbros which have high modal olivine and pyroxene are rich in their normative mafic minerals (C. I.=49.50 to 56.78, Table 2) whereas, gabbros bearing pyroxene as dominant mafics are characterized by normal amounts of mafic minerals (C. I.=44.26 to 49.64, Table 2). On the other hand, the low normative mafic minerals (C. I.=32.99 to 43.53, Table 2) are recognized in gabbros containing hornblende and little pyroxene. Both modal and normative plagioclases increase gradually with the decrease of mafic minerals during the progressive fractionation of a highly basic magma. The little crystallized plagioclases in the mafic gabbros have high normative An contents (58.50—71.80, Table 2) compared to those present in fair amounts in the hornblende pyroxene gabbros in which the

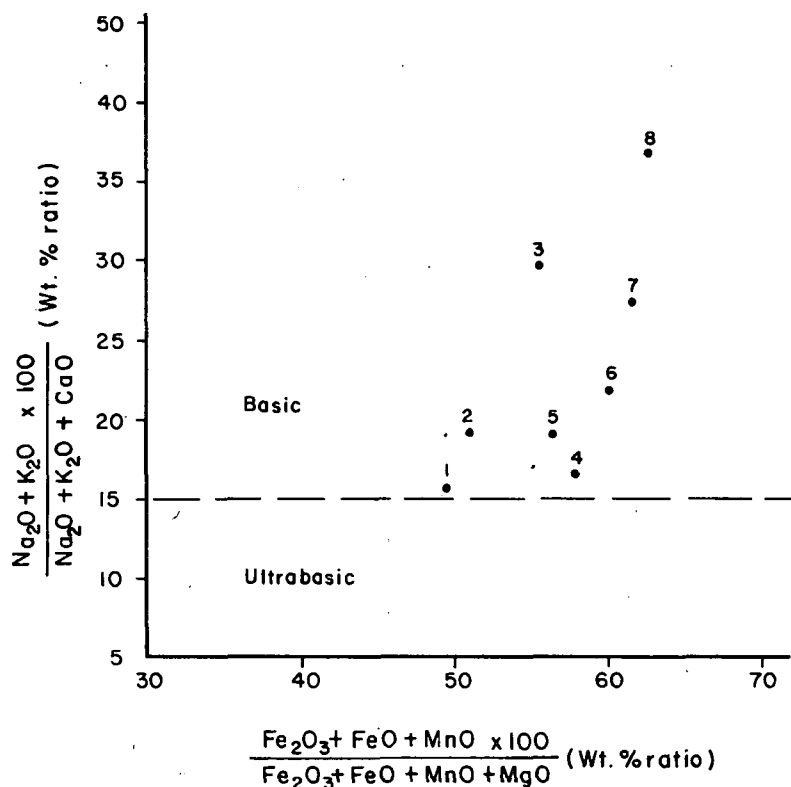


Fig. 3. The relationship between felsic and mafic index [DONALDSON, 1977]  
Dashed line represents the basic ultrabasic felsic index of DREVER and JOHNSTON [1966]. Index of numbers as in Fig. 2.

An contents range from 49.90 to 57.30 (Table 2). These An contents are calculated according to the following equation:

$$\text{An in plagioclases} = \frac{\text{Rock normative An} \times 100}{\text{Rock normative (An + Ab)}} \quad [\text{CARACAS and LEXINGTON, 1974}].$$

The differentiation index [THORNTON and TUTTLE, 1960] of the gabbroic varieties (Table 2) ranges from 12.74 in the olivine gabbro to 27.16 in the hornblende gabbro showing a certain changes in the chemical composition of the gabbroic melt with progressive fractionation.

### PETROGENESIS

The Muhammad Qol gabbroic rocks generally form an early crystallized pluton in which a highly basic magma was differentiated through a wide range producing a series of basic (gabbros), intermediate (diorites) and acidic (granitic rocks) intrusions respectively.

The gabbroic rocks which are characterized by high values of heavy elements ( $\text{Fe}^{2+}$ , Mg, Ni, Co and Cr) are considered the chief hosts for the early crystallized



olivine and pyroxene. Whereas, Al, Na, Ba, Rb and Sr are concentrated in the gabbros bearing hornblende and little pyroxene which had been crystallized at late stage. The modal and normative mafic minerals specially olivine and pyroxene decrease systematically from olivine gabbro to hornblende gabbro. Furthermore, a remarked

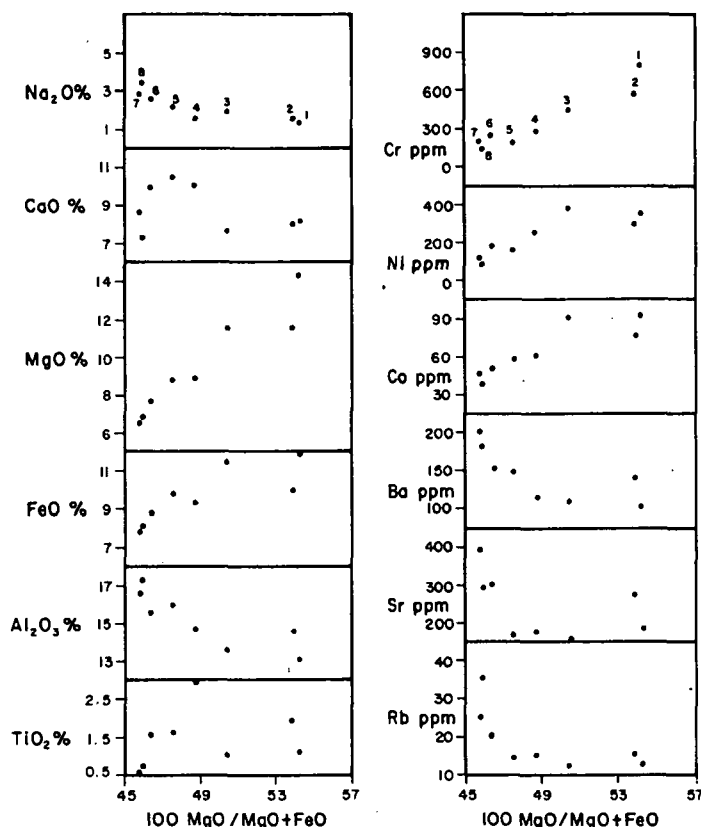


Fig. 4. Some major and trace element *versus* 100 MgO/MgO + FeO ratio. Index of numbers as in Fig. 2.

decrease in both measured and normative An contents (Table 2) of the plagioclases take place toward the hydrous end minerals. The  $\text{FeO}^*/\text{MgO}$  ratio (Table 1) increases from the olivine gabbro to the hornblende gabbro, i. e. both  $\text{Fe}^{2+}$  and Mg contents had been fractionated during the formation of the gabbroic sequence. All the above variations in the elements and their ratios together with the modal and normative minerals conform the existence of gradual chemical changes in the gabbroic magma during a short limited fractionation process [McSWEEN and NYSTROM, 1979]

The CaO shows an unusual behaviour through the fractionation of the gabbroic melt. At the beginning of crystallization, the mafic minerals (olivine and hypersthene) represented the main liquidus phase in the magma. Therefore, the crystallized plagioclases are not enough as it might be expected. As a result, low amounts of CaO (7.48—8.19%, Table 1) are recognized in the olivine pyroxene gabbros. With progressive

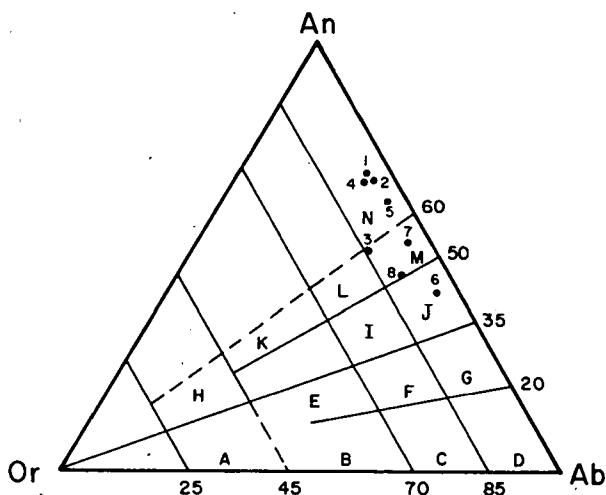


Fig. 5. Triangular diagram for An, Ab and Or normative ratio in the investigated gabbroic rocks [HIETANEN, 1963]. Index of numbers as in Fig. 2.

- |                       |                      |                           |
|-----------------------|----------------------|---------------------------|
| (A) Potassium granite | (B) Granite          | (C) Granit + trondhjemite |
| (D) Trondhjemite      | (E) Quartz monzonite | (F) Monzonite             |
| (G) Tonalite          | (H) Calci-granite    | (I) Granodiorite          |
| (J) Quartz diorite    | (K) Calci-monzonite  | (L) Granogabbro           |
| (M) Gabbro            | (N) Mafic gabbro     |                           |

fractionation, the crystallized olivine and hypersthene decreased with the increase of Ca-pyroxene and plagioclase, i. e. the main liquidus phase in the magma was represented by plagioclases in this stage in which the formed pyroxene gabbros are characterized by the highest values of CaO (10.02—10.53%, Table 1). At the end of fractionation, the hydrous minerals began to crystallize forming hornblende gabbros with little pyroxene. The composition of plagioclases in these gabbros vary from labradorite to andesine in state of labradorite only in the olivine pyroxene gabbros and pyroxene gabbros. This decrease in the An contents of plagioclases reflects the repeated depletion in the values of CaO (7.35—9.89%, Table 1) at the late fractionation stage.

The alteration processes which had taken place in some gabbros are not related to the granitic magma due to the absence of any hybridization effects in the examined gabbros in addition to the completely disappearance of any relics from the granitic materials within the gabbroic constituents. Petrographical and chemical evidences show that some gabbros were attacked by late magmatic hydrothermal solutions producing the altered gabbros through uralitization, chloritization and sericitization processes.

### CONCLUSION

The system of fractionation in the Muhammad Qol gabbroic sequence can be concluded according to the petrographical and chemical evidences. Firstly, fair amounts of olivine and pyroxene particularly hypersthene had been fractionated from a basic magma of significant mafic character. As a result, the formed mafic

EXPLANATION TO TABLE 1—3

Sample no.	Rock variety
1 2 3	Olivine pyroxene gabbros
	Olivine gabbro
	Olivine hypersthene gabbro
4 5	Olivine augite gabbro
	Pyroxene gabbros
	Hypersthene diopside gabbro
6 7 8	Augite gabbro
	Hornblende pyroxene gabbros
	Hornblende augite gabbro
9 10 11	Hornblende gabbro
	Altered gabbro
	Average analysis of 4 gabbroic samples from north of Muhammad Qol area (NEARY <i>et al.</i> 1976).

N. B. Sample numbers referring to various gabbroic rocks are the same throughout the present paper.

gabbros are characterized by low values of Ca contents due to the depletion of crystallized plagioclases in this stage.

The rate of crystallized pyroxene, specially Ca-pyroxene, increased with progressive fractionation in which pyroxene gabbros comprising largely of plagioclases and lesser of olivines are formed. In this stage, the pronounced plagioclase phase reflecting an enrichment in the Ca contents as compared to those in the early stage.

At the end of fractionation, the hydrous minerals began to crystallize under high water pressure and relatively low temperature producing hornblende gabbros which bear little augite and completely free from olivine. Although the plagioclases are greatly abundant in this late stage, the Ca contents fall again due to the remarkable decreasing in the An content of plagioclases from the olivine pyroxene gabbros to hornblende pyroxene gabbros passing through pyroxene gabbros.

In the altered gabbroic rocks, the uralitization, chloritization and sericitization processes are readily accepted as resulting from the action of late magmatic hydrothermal solutions rather than the effects of granitic magma on the gabbros.

#### REFERENCES

- AHMED, F. [1977]: Petrology and evolution of the Tehilla igneous complex, Sudan. *J. Geol.*, **85**, 331—343.
- BENNETT, H. and REED, R. A. [1971]: A handbook, chemical methods of silicate analysis. Academic Press, London.
- CARACAS, F. U. and LEXINGTON, W. H. B. [1974]: Investigations in the basement rocks of Gunnison County, Colorado: The igneous rocks. *N. Jb. Miner. Abh.*, **121**, 272—292.
- DONALDSON, C. H. [1977]: Petrology of anorthite-bearing gabbroic anorthite dykes in northwest Skye. *J. Petrol.*, **18**, 595—620.
- DREVER, H. I. and JOHNSTON, R. [1966]: A natural high-lime liquid more basic than basalt. *J. Petrol.*, **7**, 414—420.
- GABERT, G., RUXTON, B. P. and VENZLAFF, H. [1960]: Über Untersuchungen im kristallin der nördlichen Red Sea Hills in Sudan. *Geol. Jahrb.*, **77**, 241—270.
- HJERTANEN, A. [1963]: Idaho batholith near Pierce and Bungalow. *Prof. Pap. U. S. Geol. Surv.*, **344-D**.
- KABESH, M. L. [1962]: The geology of Muhammed Qol Sheet. *Mem. Geol. Surv. Sudan*, **3**, 61.

- KABESH, M. L. and LOTFI, M. [1962]: On the basement complex of the Red Sea Hills, Sudan, Bull. Inst. Desert d'Egypt, No. 12, 1—19.
- LOTFI, M. and KABESH, M. L. [1964]: On a new classification of the basement rocks of the Red Sea Hills, Sudan. Bull. Soc. Geogr. d'Egypt, 37, 93—99.
- McSWEEN, H. Y. JR. and NYSTROM, P. G. JR. [1979]: Mineralogy and petrology of the Dutchmans Creek gabbroic intrusion, South Carolina. Am. Mineral, 64, 531—545.
- MIYASHIRO, A., SHIDO, F. and EWING, M. [1969]: Composition and origin of serpentinites from the Mid-Atlantic Ridge near 24° and 30° north latitude. Contr. Mineral. Petrol., 23, 117.
- MIYASHIRO, A., SHIDO, F. and EWING, M.: Crystallization and differentiation in abyssal tholeiites and gabbros from Mid-Oceanic Ridges. Earth and Planet. Sci. Lett., 7, 361.
- NEARY, C. R., GASS, I. G. and CAVANAGH, B. J. [1976]: Granitic association of northeastern Sudan. Geol. Soc. Am. Bull., 87, 1501—1512.
- RUXTON, B. P. [1956]: Major rock groups of the northern Red Sea Hills, Sudan. Geol. Mag., 93, 314—330.
- THAYER, T. P. [1967]: Chemical and structural relations of ultramafic and feldspathic rocks in Alpine intrusive complexes. In: WYLLIE, P. J. (ed) Ultramafic and related rocks, 222—239. John Wiley and Sons, New York.
- THORNTON, C. P. and TUTTLE, O. F. [1960]: Chemistry of igneous rocks. Part 1, Differentiation index. Am. J. Sci., 258, 664—684.
- THORPE, R. S. [1974]: Aspects of magmatism and plate tectonics in the Precambrian of England and Wales. Geol. J., 9, 115—136.
- VAIL, J. R. [1978]: Outline of the geology and mineral deposits of the Democratic Republic of the Sudan and adjacent areas. Overseas Geol. and Miner. Resour. 49, London.
- WHITEMAN, A. J. [1971]: The geology of the Sudan Republic. London, Clarendon Press.

*Manuscript received, February 22, 1980*

PROF. DR. MAHMOUD L. KABESH  
National Research Centre,  
Dokki-Cairo, Egypt  
ASS. PROF. DR. ADEL M. REFAAT  
and DR. ZEINAB M. ABDALLAH  
Teachers' Institute of Education  
El-Odyia, Kuwait



## THE TECTONIC PATTERN OF GABAL MEATIQ AREA, (NORTH EASTERN DESERT OF EGYPT)

G. M. SALLOUM

### SUMMARY

The Gabal\* Meatiq area was studied geologically and petrographically in detail by several workers. The present study aims at the delineation of the tectonic pattern of this area. Two major tectonic cycles affected the area, these are: the *Early Proterozoic*, characterized by the deposition of pelitic, calcpelitic and arenaceous sediments accompanied by the eruption of some volcanics. These formations were metamorphosed, migmatized and granitized to the amphibolite facies. Such conditions prevailed in the Protoplatforms, relicts of which are now preserved as Median Masses.

The second tectonic cycle predominated during the *Late Proterozoic* during which an euogeosyncline developed. The tectonic evolution of this euogeosyncline included two stages. The Typical Geosyncline stage, which according to the rock types formed and the tectonic movements affecting them can be differentiated into three phases.

The second stage is the Orogenic Epigeosyncline, which again includes two tectonic phases. The orogenic epigeosynclinal stage continued during the lower Palaeozoic as evidenced by the presence of conglomeratic bands unconformably overlying the red-biotite granites of Um Had at Wadi\*\* Umm Hassa. These conglomerates are believed to be Lower Palaeozoic in age.

### TECTONIC PATTERN

Gabal Meatiq area was mapped geologically by NOWEIR [1968], DARDIR *et al.*, [1971] and SHAZLY [1971]. The present author, in an attempt to construct the tectonic pattern of this area was able to delineate two major tectonic cycles affecting it: The older cycle is of Early Proterozoic and was represented by the deposition of pelitic, calcpelitic and arenaceous sediments with the eruption of some volcanics. These rock formations were metamorphosed, migmatized and granitized to the amphibolite facies. The domal structure of Gabal Meatiq was formed at that stage. Such structural conditions are specific to the protoplatforms [PAVLOVSKY and MARKOV, 1963]. The second younger cycle predominated during the late Proterozoic times, it is characterised by the development of a geosynclinal system and the deformation of the older Early Proterozoic structures. The tectonic characteristics of this cycle indicate that, it pertains to the euogeosyncline type. The preserved relicts of the Early Proterozoic within the Late Proterozoic euogeosyncline are the *Median Masses* [EL RAMLY and SALLOUM, 1974]. The gneisses of Gabal Meatiq and Gabal Umm Had are considered as median masses. During the tectonic development of this euogeosyncline, two stages can be distinguished as follows:

The first stage is a *typical geosyncline* whereas the second is an *orogenic epigeosyncline*. Based on the rock types formed and the activity of the tectonic events, the typical geosynclinal stage can be differentiated into three tectonic phases. During

\* Gabal = Mountain.

\*\* Wadi = Valley

the *first tectonic phase*, a differential subsidence took place with the deposition of pelites, marls, silts, sands, grits and conglomerates. Coarse grained sediments predominate near the borders of the Median Masses (along the south western border of Gabal Meatiq Median Mass). Actually the Median Masses represent areas of source materials to the eugeosynclinal troughs from which they are separated by deep-seated faults. Admittedly, these faults were not so deep in the earth's crust and that is why the magmatic activity which accompanied these faults was of limited extent. During the *second phase*, tensile stresses predominated, resulting in the rejuvenation of the previously formed deep-seated faults and the development of new faults. Accordingly, the area was faulted into a number of blocks which were differentially depressed. The deep-seated faults, also extended to greater depths in earth's crust and probably reached the upper mantle, as indicated by the development of basic, intermediate and acidic volcanics. Basic and intermediate volcanics predominate in Wadi Kariem and Wadi Abu Diwan areas, whereas the acid varieties are best developed in Wadi Atalla and Wadi Asal areas. The section, in general, is composed of intercalations of quartzite, quartz sericite and chlorite schists with few layers of jasper and magnetite-hematite bands. In the area situated to the north of Gabal Meatiq, arenaceous sediments predominate with minor pelites and acidic volcanics. This area might be considered as a shelf and represents the comparatively shallow marine continuation of the Meatiq Median Mass. It was not subjected to intensive depression or faulting and it may occupy an intermediate position between the elevated Median Mass and the highly depressed geosynclinal troughs. At the borders of this intermediate phase, deep-seated faults extended to their maximum depth in the earth's crust as indicated by the intrusion of ultrabasic ophiolitic masses along them. During the *third tectonic phase*, the area was uplifted, thrust and deformed. The folds formed are of the linear type, asymmetric and usually complicated by faults. The trend of the fold axes is mainly NW, but sometimes they are submeridional, NE or sublatitudinal [EL-RAMLY and SALLOUM, 1974], this producing block faulting. The fold structures located close to the borders of the Median Masses are highly compressed and their limbs dip at angles of about  $80^{\circ}$ — $85^{\circ}$ , sometimes the folds are overturned. On the other hand, the fold structures in the geosynclinal troughs have submeridional, sublatitudinal or NE trends and are of the brachy type, their limbs dip at angles ranging between  $15^{\circ}$  and  $50^{\circ}$ . The process of folding was accompanied by the metamorphism of the country rocks up to the green schist facies [AKAAD and EL-RAMLY, 1960], then followed the intrusion of gabbros, diorites-granodiorites and granites.

The *Orogenic Epigeosynclinal stage*, includes two tectonic phases: The first phase began with the uplifting of the area under consideration, accompanied by the rejuvenation of the previously formed deep-seated faults and the formation of the *Intermountaine basins* of Wadi Hammamat, Wadi Karim and El Quei (see the map). The Hammamat basin is the largest in the area. There, the section is composed of shallow water sediments including sands, clays and grits. The presence of minor bands of chemical sediments in some parts of the section may indicate that the palaeogeographic conditions were favourable for their formation. The relief was more or less uniform. Such conditions were prevailing at the base of the section. Tectonic movements resulted in the deepening of the basins and the relief became remarkably contrasted. This resulted in the formation of coarse-grained sediments including a thick section of conglomerates. The field description of the Hammamat section, shows that, it is of the transgressive terrigenous type and that the basin was formed before the relief became contrasted. The area of Wadi Hammamat and the neighbouring areas were uplifted and subjected to partial erosion. In the Eastern part of the

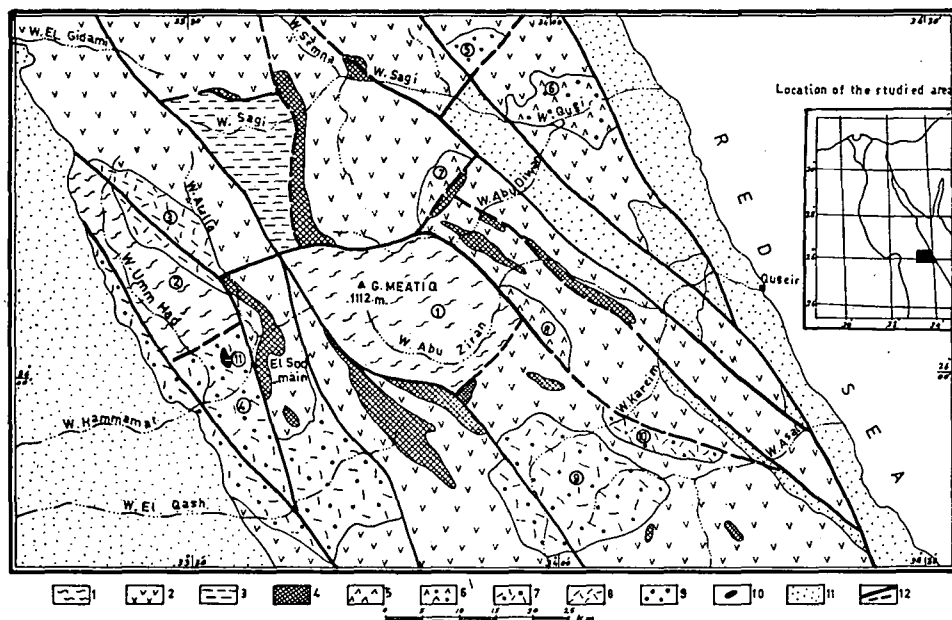


Fig. 1. Tectonic map of Gabal Meatiq area (by G. M. SALLOUM, 1980)

#### LEGENDS

- 1 — Median Masses.
- 2 — Geosynclinal troughs filled with terrigenous and volcanogenic rocks.
- 3 — Geosynclinal troughs filled with terrigenous and volcanogenic-siliceous rocks.
- 4 — Massives of serpentinized ultrabasic rocks.
- 5 — Intermountaine basins filled with Dokhan-type effusives.
- 6 — Intermountaine basins filled with molasse and Dokhan-type effusives.
- 7 — Intermountaine basins filled with molasse and Atalla-type effusives.
- 8 — Intermountaine basins filled with Atalla-type effusives.
- 9 — Intermountaine basins filled with molasses.
- 10 — Upper Paleozoic (?) sediments.
- 11 — Meso-Cenezoic sediments.
- 12 — Main zones of faulting and inferred zones (dotted lines).

Numbers in circles on the tectonic map refer to the name of tectonic zones.

#### Median Masses

- 1 — G. Meatiq
- 2 — G. Umm Had

#### Intermountaine Basins

- 3 — Atalla
- 4 — Hammamat
- 5 — Sagi
- 6 — Quei
- 7 — Abu Diwan
- 8 — Abu Ziran
- 9 — Karim I
- 10 — Karim II
- 11 — Umm Hassa

area thick volcanic piles were accumulated specially along the zones of deep-seated faults. These volcanic piles are of an intermediate composition at their lower parts, but they become acidic upwards with some thin intercalations of conglomerates, indicating breaks in the volcanic activity. The Wadi Atalla volcanics pertain to the acid types [SCHÜRMANN, 1953; AKAAD and EL-RAMLY, 1960]. They are most probably equivalent to the acidic volcanics in the Hammamat area, as they are controlled by the same zones of deep-seated faults.

In the Atalla Intermountaine basin, the outpouring of molten material took place before the formation of the basin itself, this assumption is based on the fact



that, the Atalla volcanics lie directly on the basement rocks with the absence of the molasse formations. It is believed, that the Abu Diwan and Abu Ziran Intermountaine basins which were filled with the Dokhan volcanics, were formed under similar tectonic conditions.

The section of Wadi Sagi Intermountaine basin, situated in the north-eastern part of the area (see Fig. 1), is composed of regressive terrigenous sediments. It began with very coarse grained sediments and ended with fine terrigenous sediments. Accordingly, it is possible to conclude that this basin began its development after the uplifting movement took place. In one way or the other, the sediments of this basin may be compared with those of the Hammamat basin.

Generally speaking, the Intermountaine basins were formed at different ages and were filled with a variety of rocks including molasse sediments, acidic, intermediate volcanics or combinations of such rocks. They are controlled by deep-seated faults, along which tectonic movements took place and magmatic materials were outpoured.

At the end of this phase, differential movements stopped and the intermountaine basins ceased to develop.

The second tectonic phase, began with the deformation of the previously formed sediments within the intermountaine basins. This deformation was accompanied by slow uplifting and the intrusion of granites essentially hornblende-biotite granites, followed by the intrusion of biotite and leucocratic granites. The fold structures formed within the intermountaine basins are always oriented parallel to the general trend of the basin itself. Thus, the folds have different trends as the basins are oriented in different directions. The angles of dip of the limbs of the folds range between  $20^{\circ}$  and  $40^{\circ}$ , but, the fold limbs of the structures situated close to the zones of faulting have angles of dip ranging between  $70^{\circ}$ — $86^{\circ}$ . Deep-seated faults played an important role during the tectonic development of the Late Proterozoic eugeosynclinal system.

The *Orogenic Epigeosyncline system*, continued during the Lower Palaeozoic time and its rocks now form part of the platformal structure of the Eastern Desert of Egypt.

In Wadi Umm Hassa, a small exposure of coarse-grained conglomerates unconformably overlies the red-biotite granites, which were intruded during the orogenic stage (probably Late Proterozoic). These conglomerates were formed under uneven rugged paleotopographic conditions. They are most probably, of Lower Palaeozoic age.

## REFERENCES

- AKAAD, M. K. and EL RAMLY, M. F. [1960]: Geological history and classification of the basement complex of the Central Eastern Desert. Geol. Surv. Egypt. Paper No. 9.
- AKAAD, M. K. and NOWEIR, A. M. [1969]: Lithostratigraphy of the Hammamat-Um Seleimat district, Eastern Desert. Egypt. Nature 223, No. 5203, pp. 284—285.
- DARDIR, A. A. *et al.* [1971]: Report on the geology of the basement rocks west of Gabal Duwi between latitudes  $26^{\circ} 07'$  and  $26^{\circ} 20' N$ , Eastern Desert. Geol. Surv., Egypt.
- EL RAMLY, M. F. and AKAAD, M. K. [1960]: The basement complex in the Central Eastern Desert of Egypt between Latitudes  $24^{\circ} 30'$  and  $24^{\circ} 40' N$ . Geol. Surv. Egypt, Paper No. 8.
- EL RAMLY, M. F. and SALLOUM, G. M. [1974]: The tectonic regioning of the basement rocks of the Eastern Desert of Egypt. Acta Mineralogica-Petrographica, Szeged XXI/2, pp. 173—181.
- EL SHAZLY, E. M. [1964]: On the classification of the Precambrian and other rocks of magmatic affiliation in Egypt. Intern. Geol. Congress, India.
- GHANEM, M. A. [1968]: The geology of Wadi Kareim area Ph. D. Thesis, Faculty of Science, Cairo University.

- NOWEIR, A. M. [1968]: Geology of the Hammamat-Umm Seleimat district. Eastern Desert. Ph. D. Thesis, Faculty of Science, Assuit University.
- PAVLOVSKY, E. V. and MARKOV, M. S. [1963]: Some general problems of geotectonics (on the irreversibility in the development of the Earth's crust). Acad. of Sciences USSR, Geol. Instit., Transactions Vol. 93.
- SCHURMANN, H. M. E. [1953]: The Precambrian of the Gulf of Suez Area. 19th Intern. Geol. Congr., Algeria, C. R. Sect. 1., Fac. 1, pp. 115—135.
- SCHURMANN, H. M. E. [1967]: The Precambrian along the Gulf Suez and the Northern part of the Red Sea. E. J. Brill., Leiden.
- SCHURMANN, M. M. E. [1964]: Rejuvenation of Precambrian rocks under epirogenetical conditions during old Palaeozoic times in Africa. Geol. Mijnb., 43, No. 5, p. 196—200.
- SHAZLY, A. G. [1971]: Geology of Abu Ziran area, Eastern Desert. Ph. D. Thesis, Faculty of Science, Assuit University.

*Manuscript received, June 5, 1980.*

DR. G. M. SALLOUM  
17, Ahmed Siddik Str., Flat 9  
Sidi Gaber — Alexandria  
Egypt



## THE OIL SHALE DEPOSIT OF VÁRPALOTA

G. SOLTÍ

### INTRODUCTION

After the discovery of the first Hungarian oil shale occurrence in the Balaton Highland near Pula village, in a maar-like tuff-ring, in 1973, we have paid much attention to Neogene sequences in confined or isolated basins. During mapping we have recorded alginite containing silty clay marls of Lower Pannonian age in shallow drill holes in the Kaposcs intramontane basin.

It was therefore necessary to carry out a thorough evaluation of the whole Transdanubian Mountain Range. The work was done by RAVASZ in 1977. In the course of these evaluations several samples were collected, one of which form an abandoned open pit at Bántapuszta near Várpalota by Cs. MUNTYÁN. According to thermal analysis this sample contained 47 weight % organic matter. This can be burnt and lit. While burning, it emanates a characteristic stearine odor. This finding has uprated the perspectivity of the Várpalota basin for finding oil-shales.

### THE GEOLOGY OF THE VÁRPALOTA BASIN

The Várpalota basin lies in the southern foreland of the Bakony between Csór and Öskü (*Fig. 1*). The basin shows a southward deepening. Its basement is composed of Silurian Carboniferous (?), Permian and Triassic rocks, getting gradually younger from the SE to the NW, being aligned in nearly SW-NE belts. The youngest member of the basement is the "Hauptdolomit", which also gives the northern border of the basin. The oldest members of the basement (Silurian and Carboniferous) can also be found in uplifted position in surface exposures (Szárhegy, Füle, Balatonfőkajár), and provide the souther boundary of the basin. The basin is filled by Tertiary sediments, of which the Eocene is subordinate, while the Miocene is nearly complete. From the five Miocene stages only the Badenian is discussed in detail, since only this stage has a closer relationship with oil shale formation. The discussion is based mainly on the references given by KÓKAY [1978]. In the Várpalota basin these Badenian sediments overlie the Carpathian Stage and can be subdivided into three stratigraphic units.

In the Lower Badenian (Moiavian) marine sediments were deposited, in which coarse-grained sandstones are frequent in the western part of the basin, while clays and fine grained sandstones are predominant in the eastern part. It is probably interesting that very few volcanic tuffs and bentonites have been found in the Lower Badenian sequence of Várpalota compared to the formations in the Herend-Márkó basin, which belongs to the same stage. The average thickness of the Lower Badenian sediments, including the sands exposed in the famous Szabó-quarry, varies between 20—40 m.

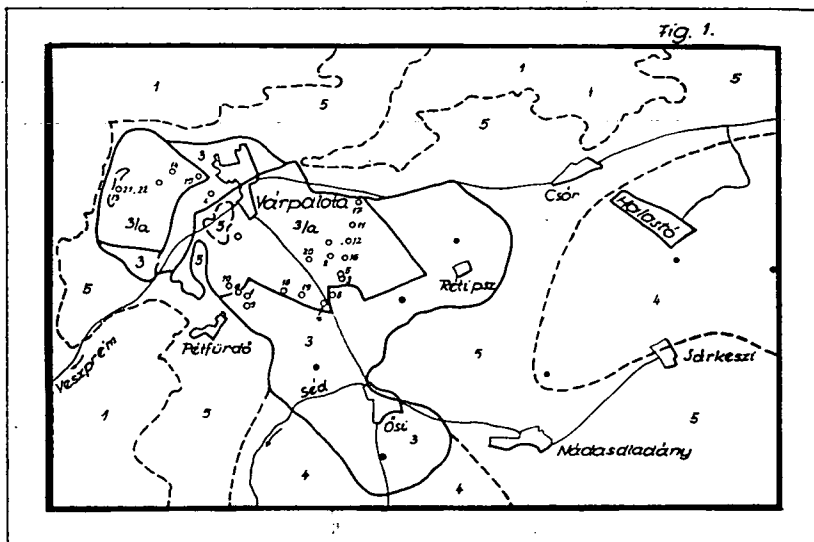


Fig. 1. Prognostic map of the oil-shale formation of the Várpálota basin  
Scale 1:100 000

LEGEND

1. Surface exposures of the formations underlying the diatomaceous clay marls.
2. Surface outcrops of the diatomaceous clay marls.
3. Sub-surface extension of the diatomaceous clay marl.
- 3/a. Diatomaceous clay-marl in the hanging-wall of striped-out coal-seams.
4. Possible extension of diatomaceous clay marls overlain by younger formations.
5. Areas where diatomaceous clay marl does not occur.
014. Location of samples
- Proposed drill holes.

Following an uplift at the end of the Early Badenian the Mid- to the Late Badenian sedimentation was introduced by a transgression, or more accurately, expansion of the sea [KÓKAY, 1978]. This new cycle started with development of swamps and lignite formation. As a result of the extensive development of swamps, lignite was formed over an area of 60 sq. km. On the top of the shallow swamp facies pink rhyolite tuffs fell into seawater, producing the so-called "middle strip". These tuffs provided an evidence of volcanic activity associated with moderate structural movements. This pink rhyolite tuff bed grows thicker northwestwards and attains 2—3 m in thickness, indicating an increasing rate of land-derived, terrigenous supplies.

The lignite seam is overlain by fossil-rich sediments containing *Neritina*, *Congeria*, *Teodoxus* and *Bulimus* in a thickness of few cm-s to several ten cm-s. This fossils often forms a lumachelle bed. With continued deepening of the lagoon the number of the Molluscs disappear. These layers represent the immediate foot-wall of the oil-shales of Várpálota.

In the Late Badenian the depth of the Várpálota Lagoon was at least 20 m. Laminated clay marl overlie the mollusc-rich hanging wall of the coal measure. The thickness of these strata is approximately 8—10 m. The rocks show greenish grey, green, occasionally brown colours and intense lamination characterized by alternation of very thin Ca-rich and clay laminae, which also contain some fossilized remnants of fish and produce a typical though slight, "oil-shale" odor when dried. This micro-bedding is probably due to seasonal changes [J. KÓKAY, 1966].

The lower diatomaceous clay marl series is overlain by rhyolite tuff throughout the basin in about one meter thickness. This tuff layer also shows a gradual thickening towards the peripheral parts. It is of loose sandstone character, being moderately sorted. Its bottom part is relatively coarse-grained and shows a gradual decrease in grain size upwards. Lapilli of 1 cm in diameter were occasionally found. In some parts it shows varying degrees of subsequent alteration to bentonite.

Absolute age determination of the rhyolite tuffs was made by using the K/Ar method [K. BALOGH *et al.*, 1979]. The most complete analyses were made on those samples which have been collected at Bántapuszta. The results obtained for different fractions did not exceed the limits of standard deviation. The average age, as determined by 3 measurements, is  $14.6 \pm 0.4$  m. y.

Above the tuff layer the deposition of the diatomaceous clay marls continued. The colours of the rock change to monotonous grey, and its laminated character gradually disappears. It shows thicker parting, the typical oil-shale odor is much weaker, the diatomite micro-layers are not abundant, and the unit weight of the rocks becomes similar to that of typical clay-marls.

The laboratory analyses for organic matter and the Fischer-tar-content (performed in the MÁFI and the MÁFKI) supported the conclusions of field observations, which had indicated the highest grade of oil shales immediately below the tuff layer in few m thickness. According to their lithological character, these rocks are called „paper-shale”. Like in the case of the oil-shales formed in crater-lakes, we have found evidence in Várpalota, too, that for the formation of oil-shales in confined landlocked basins and lagoons the existence of volcanic glass, which can easily devitrify, seems to be favourable.

Above the diatomite-clay marl series the sediments with molluscs (*Bulimus*, *Teodoxus*) reappear. This lithology indicates a regression, and accumulation. The disappearance of *Congerina* bears witness to a decreasing salinity.

The end-member of the sedimentary cycle is a coal-bed of high clay content and 1—2 m thickness [KÓKAY, 1978].

Significant differences from this typical sequence are known on the edges of the basin, the central part is filled with a monotonous diatomaceous clay-marl series, containing only one thin rhyolite tuff intercalation. Its maximum thickness, 142.9 m, was recorded in the DDH V-271, west from Várpalota. The average thickness in the basin is approximately 50 m.

The Badenian sediments are overlain by terrestrial pebbly variegated clay in the western part of the basin, in the eastern part Sarmatian oligohaline clay-marls and fine-grained clays are deposited, which are covered by a homogeneous Lower Pannonian clay-marl series. On the top of the stratigraphic column there are Pleistocene and Holocene sediments.

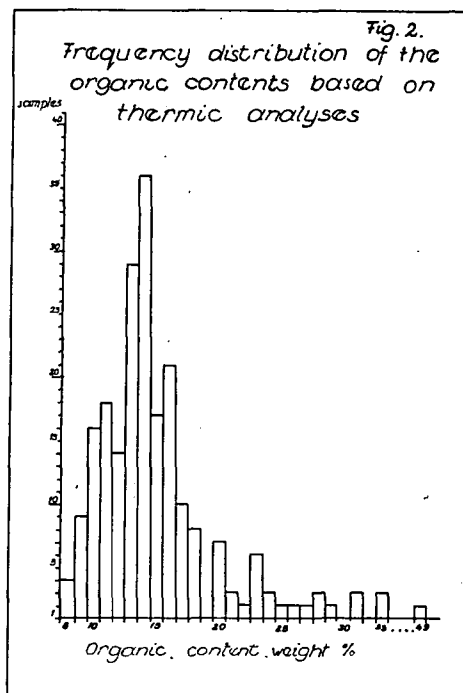
Apart from a few local disturbances the foot-wall surface of the diatomaceous clay-marl series (oil-shale) slopes steadily eastwards. The thickness of the overlying strata varies between 0—313.6 m, and shows and eastward increase. The variation in the thickness of the diatomaceous clay-marl does not seem to be related to the paleogeographical environment of the foot-wall formations or the thickness of the overlying strata. This is mainly due to the unconformity between the Badenian and the Sarmatian and the erosion that followed by development of diatomaceous clay-marls and preceded the deposition of the Sarmatian sands and gravels.

The best exposure of the diatomaceous shale (oil-shale) can be seen in a vertical section in the Bántapuszta open pit.

In addition to numerous drill hole intersections this formation is also known from underground workings, being the immediate hanging wall of the coal measure and usually hoisted to the surface and dumped as waste.

#### THE ORGANIC- AND CARBONATE CONTENT OF THE OIL-SHALES

Approximately 200 samples of oil-shales from 22 profiles in the Várpalota basin were investigated by thermal analysis. These measurements were performed by M. FÖLDVÁRY. The organic content of these samples was measured and found to vary between 8 and 49 weight %. The average organic matter content for the whole diatomaceous clay-marl series of the Várpalota basin is 15.33 weight %. A typical three-maxima distribution is seen on both organic content and carbonate content frequency diagrams of the diatomaceous clay-marl samples, according to the thermal results (Fig. 2).

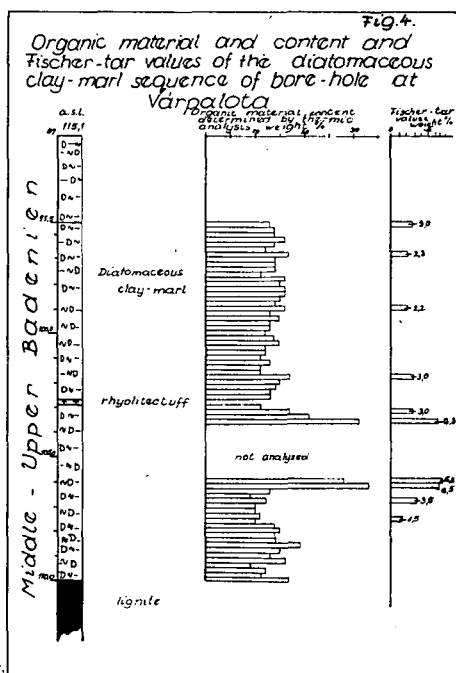
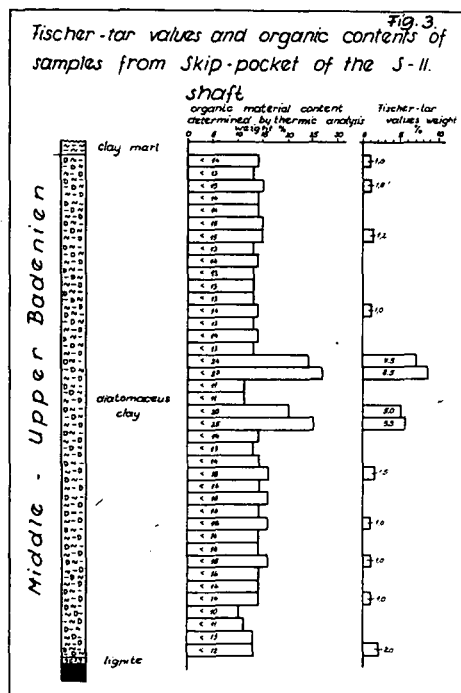


The three maxima, however, represent only poor concentration of these values since both the organic and the carbonate contents vary widely and even the "striking" peaks with 35 values form only 17.5 per cent of the total number of analyses. This implies at the same time an ample scale of variations from 8 to 48 weight % values in the case of organic matter and from 0 to 90% in that of carbonate. The calcite and organic matter of the diatomaceous clay-marls of Várpalota, as determined by thermal analyses, do not show any correlation with each other.

The Fischer-tar-analyses have shown convincingly that the diatomaceous clay-marl sequence in the Várpalota basin is an oil-containing rock which includes single

layers of excellent quality, but which, in sum total, can be rated as a low-grade oil shale (Figs 3, 4).

Among all the samples analyzed, the lowest tar content, 0.3 weight %, was recorded in a sample from DDH V—82, from a depth of 156.6—171.0 m. Remarkably enough, 17 weight % organic matter belongs to this tar content. With similar amount



of organic material, a sample from a drillhole V—75 108.0—113.43 m yielded 5.0 weight % shale oil. The maximum tar content was found in a sample from a test trench at Bántapuszta (Fig. 5). In this sample 49 weight % organic matter (which also represented a maximum) and 14.5 weight % tar were measured (160 l/ton shale oil). For those 71 samples, which contained at least 9 weight %, but mainly 15 weight % organic matter, the average Fischer-tar-content was 3.4 weight % (37 l/ton). These values fall in the range of low grade oil shales. As is shown in the distribution diagram of the Fischer-tar-content of the samples (Fig. 6) the modal mean value has fallen in the range of 1—2 weight % tar content. About one fourth of the total number of samples (17) fit into this interval.

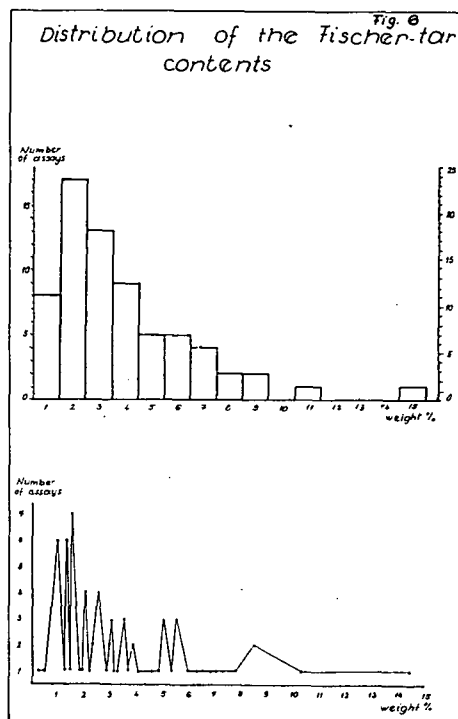
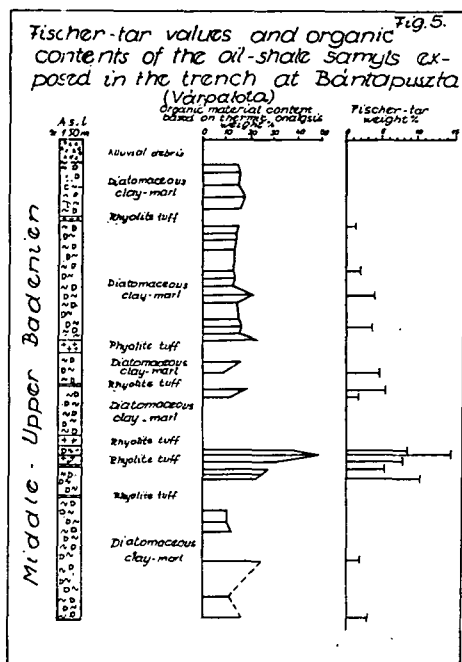
36 samples had a tar content of 2—7 weight %, over fifty per cent of the total number of samples.

The already known close correlation between the organic material content of the oil-shales determined by thermal analysis and their Fischer-tar-content is well seen in the correlation diagram of these samples too.

The 71 analyses are sufficient for a statistical evaluation. It should be mentioned that these data are only informative, since only those samples have been analyzed for oil content, which had shown at least 8 weight % or rather over 15 weight % orga-



nic matter. The correlation index for the organic content and Fischer oil-yield is  $r=0.848$ , marking a good correlation. The ratio of organic matter to tar is  $18.239:3.386=5.4:1$ , which means, that about 18.5 per cent of the organic matter can be converted into tar (shale-oil) by Fischer's distillation techniques. If we compare this



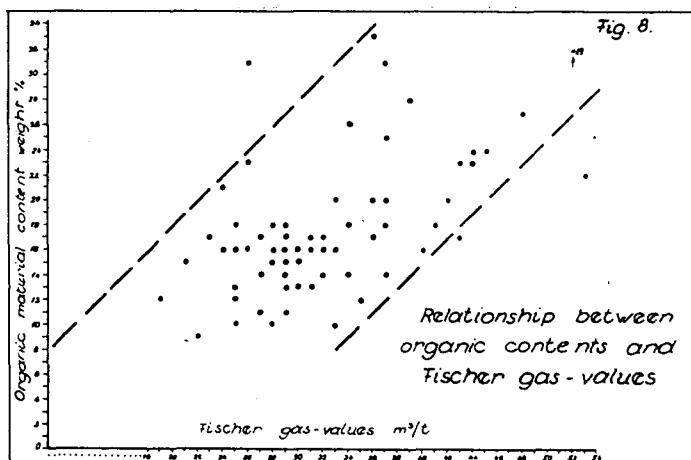
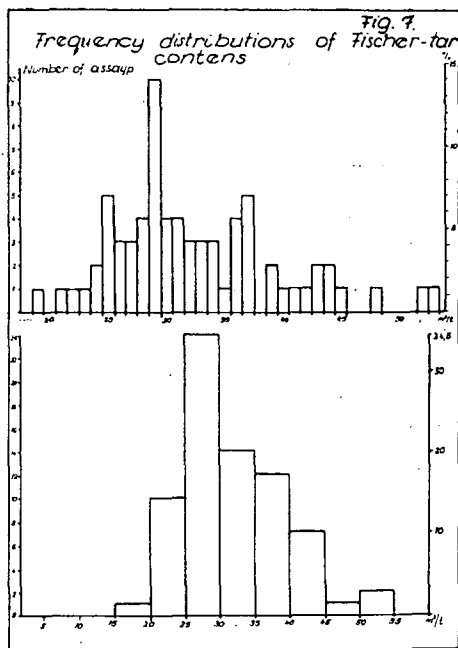
value to the 15.3 weight % average organic matter content of the analyzed 200 samples, we get 2.74% as an average Fischer-tar-content. The relationship between organic matter and tar in the 71 samples is expressed by

$$x = \frac{x}{3} - 1$$

while the total organic matter and the tar contents show a correlation, which can be described by

$$y = 0.1944 x$$

Apart from the recoverable oil content, the most important property of these oil-shales is their gas yield of low calorific value during Fischer distillation. The 71 samples produced 32 m<sup>3</sup>/ton average amount of gas. Although this gas content is not in a genetic relationship with the tar content, the results have shown that those samples, which have a higher tar content, yield a larger amount of gas. The maximum amount of gas (53 m<sup>3</sup>/ton) was recorded at 3.6 weight % tar content, but those samples having 14.5 weight % tar also produced 52 m<sup>3</sup>/ton gas. At the minimum — 19 m<sup>3</sup>/ton — gas yield, the tar content was 1.3 weight % in the sample (Figs 7, 8).



The analyses for coal quality of 4 samples from the Várpalota basin have given surprising results. The hanging-wall rock, which was hitherto considered a waste, has a calorific maximum value as 10 275 kJ/kg with 10.3% tar, 59% ash and 4.5% moisture. (Table 1.)

TABLE 1

Section No	Locality	Quality control (MEO)					Fischer-tar weight%			By derivatographic method				
		Calorific power kcal/kg    kJ/kg	Ash content A %	Moisture wt %	Vola- tile- con- tent	Tar	Underground moisture content	Moisture	Water as a decomposition product	Waste + koke	Gas and Losses	gas m <sup>3</sup> /t	Organic matter content	CaCO <sub>3</sub> content
13	Exploratory trench. lager 20	2454,1    10275	59,41	4,53	29,84    10,3	7,9	6,6	2,2	77,5	3,2	43	23	20-25	
15	Face 45 in Bántabánya mine	798,7    3344	38,16	21,76	16,70    5,0	21,9	6,6	0,9	36,5	1,0	44	23	72-73	
16	Sampling for Skyp S-II	1159,1    4853	67,50	5,51	24,62    8,5	11,8	5,4	1,6	82,0	2,5	48	27	9-10	
17	S-II mine 12/A face	369,7    1548	42,29	19,41	16,81    3,2	21,1	3,9	0,4	90,6	1,9	40	16	57-58	

# THE PALYNOLOGICAL INVESTIGATIONS OF THE OIL SHALE SAMPLES

Palynological analyses were made in 27 samples from the Várpalota basin by MRS. L. NAGY and E. BODOR. The results of these analyses have supported the relationship of these strata with the Hidas Formation, with *Sporomorphae* indicating Middle Miocene age.

The pollen content has not allowed any more accurate subdivision within the Badenian stage. In a sample from V—82 drillhole, 205.0—214.85 m section, *Cyrtilla-ceae*, *Savallipollenites* and *Ophioglossissporites* pollen grains, indicating the Lower Badenian, were observed.

In the DDH V—75, 65.2—98.7 m section the samples contained fewer tropical to subtropical elements, and an increasing number of arcto-Tertiary elements, an assemblage, which marks the upper horizons of the Badenian. Unlike the other freshwater *Sporomorphae* assemblages, these samples are of marine character, along with a large number of *Hidasia sp.* plankton specimens. This planktonic genus did not occur in other samples. Because of the relatively high abundance of *Coniferae*-pollenites in the samples, the climate of this area seems to have been moderately warm, subtropical during the Middle Badenian.

The character of vegetation shows an environment near to freshwater sources (*Myrica*, *Carya*, *Pterocarya*), swamp forests (*Taxodium*), and mainly wet deciduous forests (*Ulmaceae*) with a dense undergrowth near rivers and stream banks. The *Coniferae*, *Fagaceae* and *Ulmaceae* assemblage belongs to the vegetation of cooler mountain slopes. Local predominance of pine forests was indicated by a few samples (DDH V—128, 207.0—210.3 m).

TABLE 2

DDH	m	Amount of <i>Botryococcus</i>	Org. mat. content weight %	Fischer tar content
V-75	65.2— 98.7	rare 1—3	<16	1.3
V-82	205.0—214.85	none	<11	
V-90	173.0—209.9	none	<22	3.6
V-128	181.1—206.0	much 11—15	<17	1.4
V-128	207.0—210.3	dominant 16—00	<11	
V-122	73.2— 98.8	rare 1—3	<18	3.1
V-212	167.8—190.5	dominant 16—00	<15	2.3
V-212	206.0—207.0	none	trace	
V-317	95.5— 95.7	rare 1—3	<13	3.0
V-317	96.1— 96.3	few 4—5	<16	
V-317	96.7— 96.9	rare 1—3	<17	2.3
V-317	97.3— 97.5	none	<14	
V-317	97.9— 98.1	much 11—15	<15	
V-317	98.9— 99.1	much 11—15	<16	2.2
V-317	99.1—100.1	rare 1—3	<12	
V-317	101.9—102.1	few 4—5	<15	
V-317	102.9—103.1	much 11—15	<11	
V-317	103.5—103.7	rare 1—3	<31	6.3
V-317	106.9—107.1	dominant 16—00	<10	
V-317	107.9—108.1	rare 1—3	10—15	
V-317	108.9—109.1	dominant 16—00	9—13	
V-317	109.9—110.0	rare 1—3	<17	
I-13	157.0—160.0	none	<18	
S-II	shaft, reject-dump	dominant 16—00	<16	
S-II	shaft	much 11—15	<14	

## THE ALGAL CONTENT OF THE OIL SHALE SAMPLES

Whether an organic-rich rock qualifies for oil shale or not, depends to a large extent on the amount of the accumulated *Botryococcus* algae, which are actually hydrocarbon producers.

In the 27 analyzed samples from Várpalota, only five contained significant amounts of *Botryococcus braunii* algae, which account for the kerogene content of the oil-shales. There were 6 samples, in which no algae were found. In the remaining 16 prepares the number of the algae varied from 15 to 1.

The relationship of the abundance of *Botryococcus* versus organic matter and the Fischer-tar-content of the samples is shown in Table 2.

Suprisingly enough, the data shown by Table 1, indicate a negative correlation between the amount of *Botryococcus* and the organic matter content of the rocks determined by thermal analyses. At 17 weight% organic matter there were only 1—3 specimens of *Botryococcus braunii*. In those samples, in which *Botryococcus* was abundant, the amount of organic matter was less than 16 weight %.

M. HAJÓS has studied the *Diatomae* in the samples from drillholes in Várpalota. She found that the *Diatomae* content was very different from drillhole to drillhole, and even within the section of one drillhole. Limno-brackish and euryhaline genera are predominant in the assemblage. Typical representatives of the normal marine environment are absent.

## CONDITIONS OF DEPOSITION

The diatomaceous sediments of the basin are very rich in carbonized plant fossils, though contain only small amounts of *Diatomae* and other siliceous fossils. The site of sedimentation was a basin, relatively deep, with plankton-rich waters, in a regime of gradual accumulation, upfilling. The diatom assemblage is relatively simple, with only few genera, mainly planktonic types. This marks a lake-type sedimentation, forming a relatively smooth, muddy bottom.

The variability of the abundant halophytic *Coscinodiscus* species shows not only a decrease in salinity, but its constant fluctuations as well. Most of the other genera are also typical of limno-brackish, or freshwater environments. However, the typical freshwater elements are subordinate.

The molluscs, the rich pollen and spore remains, and mainly the planktonic diatoms undoubtedly indicate low salinity.

Using REMANE's classification, the salinity falls to the meso-haline range, with up to 5—7% concentration.

Finally, the *Diatomae* have again proved a Middle Miocene Badenian age of deposition.

## ECONOMIC SIGNIFICANCE OF THE OIL SHALES

For an estimation of the approximate hydrocarbon reserves contained in the diatomaceous shale series of the Várpalota basin the following data can be considered.

The extension of the formation is about 50 sq. km; its average thickness is 50 m; its unit weight is approximately 1 g/cm<sup>3</sup>. Calculating with these values we have obtained the results:

Possible shale oil reserves (2.7 weight %): 68 million metric tons;

Possible shale gas reserves (32 m<sup>3</sup>/ton): 80 billion m<sup>3</sup>.

Further subdivision of these reserves has not been possible in this exploration stage.

The 68 million tons of shale oil reserve are stored in low grade oil-shales. With present-day technologies and market situation its exploration is economically unfeasible. It should be mentioned, however, that in 1965 the lowest limit of the economic grade of oil shale was about 10 weight %. Recently in-situ production from oil-shales is known from as low as 8 weight % grade oil-shales. There are also reasonable possibilities for the use of this raw material as an additive to manufacturing cement and fibrous insulating materials, according to the specialists of the Hungarian Research Institute for Mineral Oil and Gas (A. FEHÉRVÁRI, J. BARLAI and G. KOC SIS).

The oil shale series of Várpalota has a favourable setting for the mine development. In the Bántapuszta area it has been already exposed in a face of several hundred m length with 1—4 m overburden. Here conventional strip mining of several ten million m<sup>3</sup> of oil-shale is possible, despite the increasing thickness of the overburden eastwards, since the analyses have shown gradually better grades in that direction.

Other deposits are not accessible to surface mining methods owing to higher overburden thicknesses.

Since underground coal mining is in operation in the area, underground technologies may also be considered for the extraction of the oil-shales using the same methods and equipment and labour as for coal. Along with the coal production up to 1—2 millions tons of oil-shale can also be hoisted. Since a large amount of this material is in any case hauled from the mine as waste, its processing as oil shale should be seriously considered. In judging the future perspectives of coal mining in Várpalota, the diatomaceous shale overlayers, which may yield hydrocarbon, should also be taken into account in the development plans, as the oil prices show a trend of steady increase in the world market.

#### REFERENCES

- ARATÓ, J., BELLA, L. [1976]: A pulai és gércei olajpala technológiai és kémiai vizsgálata. (Results of technological and chemical analyses of the oil shale of Pula and Gércé. In Hungarian, with English resume). Magyar Állami Földtani Intézet Évi Jelentése az 1974. évről, pp. 287—300.
- BENCE, G., JÁMBOR, Á., PARTÉNYI, Z. [1979]: A Várkesző és Malomsok környéki alginit (olajpala) és bentonitkutatások eredményeiről. (Exploration of alginite (Oil-shale) and bentonite deposits between Várkesző and Malomsok. In Hungarian with English resume). Magyar Állami Földtani Intézet Évi Jelentése az 1977. évről, pp. 257—267.
- FEHÉRVÁRI, A., BARLAI, J. [1979]: A dunántúli (Pula, Gércé, Várkesző) olajpálák (alginitek) komplex hasznosítási lehetőségei. Manuscript.
- HALMAI, J. [1977]: Olajpala-előfordulások lehetősége Észak-Magyarországon. Manuscript.
- GRASSELLY, GY., BERTALAN, M., SAJGÓ, CS. [1977]: Contributions to the knowledge of the Hungarian oil shale kerogen II. Results of preliminary DTA and IR-investigations on the kerogen of the oil shale occurrence at Pula. Acta Miner. Petr., Szeged XXIII/1, pp. 177—196.
- HETÉNYI, M., MAITZ, K., TÓTH, É. [1977]: Contributions to the knowledge of the Hungarian oil shale kerogen I. Preliminary report on the results of the pyrolysis and selective oxidation. Acta Miner. Petr. Szeged, XXIII/1, pp. 165—175.
- HETÉNYI, M., SIROKMÁN, K. [1978]: Structural information on kerogen from the Hungarian oil shale. — Acta Miner. Petr. Szeged XXII/2, pp. 211—222.
- HETÉNYI, M., VARSÁNYI, I. [1976]: Contributions to the isolation of the kerogen in Hungarian oil shales. — Acta Miner. Petr. Szeged XXII/2, pp. 231—239.
- JÁMBOR, Á. [1975]: Olajpala Magyarországon. Élet- és Tudomány 1975. XXX, pp. 1688—1693.
- JÁMBOR, Á., SOLTI, G. [1975]: Geological conditions of the Upper Pannonian oil shale deposit recovered in the Balaton Highland and at Kemeneshát. — Acta Miner. Petr. Szeged XXII/1, pp. 9—28.

- JÁMBOR, Á., SOLTÍ, G. [1976]: A Balatonfelvidéken és a Kemenesháton felkutatott felsőpannoniai olajpala-előfordulás földtani körülményei. (Geological conditions of the Upper Pannonian oil shale deposits recovered in the Balaton Highland and at Kemeneshát. In Hungarian with English resume). Magyar Állami Földtani Intézet Évi jelentése az 1974. évről, pp, 193—219.
- JÁMBOR, Á. [1977]: Jelentés a mányi medencerész neogén képződményei szervesanyagtartalmának, olajpala és kén előfordulás lehetőségeinek vizsgálatáról. — Manuscript.
- RADÓCZ, GY. (1980): Alginít indikáció a szarvaskői miocén barnakőszéntelepes rétegsorban. Magyar Állami Földtani Intézet Évi Jelentés 1979. évről (in press).
- RAVASZ, CS. [1976]: A pulai és gércei olajpala közettani vizsgálata. (Petrographic examinations of oil shale at Pula and Gérce. In Hungarian with English resume). Magyar Állami Földtani Intézet Évi Jelentése 1974. évről, pp, 221—229.
- RAVASZ, CS., SOLTÍ, G. [1980]: Sulphur-, gypsum- and alginite-bearing strata in the Zsámbék Basin. Acta Miner. Petr., Szeged, XXIV/2, 191—207.
- SOLTÍ, G. [1980]: A várpalotai olajpala. Magyar Állami Földtani Intézet Évi Jelentése 1979. évről (in press).
- VARSA NYI, J., LISZKAI, M. [1976]: Sediment volume of the Hungarian oil shales in organic solvents. — Acta Miner. Petr., Szeged XXII/2, pp, 221—245.
- VARSA NYI, I., BOROS, J., BERTALAN, M. [1978]: Correlation between the clay mineral and organic matter content in the sediments of the south Great Plain, Hungary. Acta Miner. Petr., Szeged XXIII/2, pp, 319—333.

*Manuscript received, June 4, 1980*

DR. GÁBOR SOLTÍ  
Hungarian Geological Survey  
Népstadion út 14.  
H-1442 Budapest, Hungary

## **THERMAL DEGRADATION OF THE ORGANIC MATTER OF OIL SHALE OF PULA (HUNGARY) AT 573—773 K**

**M. HETÉNYI**

### **INTRODUCTION**

The thermal degradation of oil shales is worthy of mention partly from the point of view of their industrial utilization, partly as the most important parameter of the evolution of the organic matter.

Shale oil and gas can be produced from the oil shale with best efficiency at the temperatures between 743 and 823 K. Thus the thermal treatment has been studied so far in this temperature range and the investigations aimed first of all the increase of the quantity of products *i. e.* of the shale oil and gas. In spite of the efficiency of the conversion of organic matter the considerable amount of mineral components highly lowers the efficiency of the process. It seemed to be obvious to eliminate the mining, transport and storing of these components. Consequently especially in case of large scale fields the *in situ* production is favoured both by researchers and by economic experts. In addition to numerous technological researches the processing *in situ* requires the investigation of the degradation process at lower temperatures, as well. Studies dealing with the thermal degradation of the Green River kerogen between 423 and 623 K were published by CUMMINS and ROBINSON [1972] CUMMINS, DOOLITTLE and ROBINSON [1974].

At the same time, the evolution of the organic matter and the formation of petroleum and natural gas have been one of the fundamental problems of organic geochemistry. The kerogen of strongly polycondensated structure being formed at low temperature and pressure under surficial conditions is in metastable state. The temperature and pressure increase produced by deposition and subsidence breaks the equilibrium between the kerogen and its environment. The progression of the evolution of kerogen is manifested by the effort to re-establish the equilibrium between the kerogen and its continuously changing environment. Most of the authors believe the temperature to be the most important factor among the environmental parameters. In first approximation the laboratory simulation of the thermal degradation seems to be improbable just because of the incommensurability of the geological and human ages. Nevertheless, numerous experiments and reaction kinetic calculations prove that by increasing the temperature the reaction rate can be increased to such an extent that the degradation process can be simulated even under laboratory conditions, as well. Observations concerning the possibility of time-temperature replacement are only qualitative, the numeric relationships are not cleared yet (TISSOT and WELTE, 1978).

According to the observations concerning the mechanism of decomposition, bitumen soluble in organic solvents develops from kerogen, together with CO<sub>2</sub>,



H<sub>2</sub>S, H<sub>2</sub>O and occasionally with hydrocarbons of shorter chains; then the bitumen is degraded to oil the phenomenon being accompanied by gas formation, and a more coalified organic matter remains [CANE, 1951; ABELSON 1967; VITOROVIĆ and JOVANOVIĆ, 1968].

Having compared the experiences of laboratory simulation of the kerogen evolution with the maturity of the organic matter of sediments TISSOT and WELTE [1978] found that when treating the kerogen of type II at normal pressure and in neutral gas atmosphere, the temperature ranges of the phases of evolution can be determined even in laboratory. By means of degradation below 623 K the diagenesis, between 623 and 773 K the catagenesis and above 773 K the metagenesis can be simulated.

This paper gives a summary of the observations concerning the thermal degradation of the oil shale of Pula (Hungary) with special regard to the distribution of products of temperature, as well as to the change of character of the non-converted organic matter during the artificial genesis. Since the oil shale of Pula is a near-surface alginite rich in organic matter, it may be suitable for these experiments. The sample deriving from small depth (0—45 m) did not endure considerable changes of temperature and pressure, thus it contains organic matter of immature state being at the beginning of its genesis, as it has been proved by the preliminary investigations [HETÉNYI and SIROKMÁN, 1978]. The kerogen isolated from the oil shale has been degraded already at 473 and 573 K [HETÉNYI, 1979]. In the experiments in question the oil shale was degraded at different temperatures between 573 and 773 K and at different durations. We aimed the laboratory simulation of the process of catagenesis and to determine the transition between the dia- and catagenesis in case of the studied organic matter, of course under laboratory conditions. Further, at several characteristic temperatures based on the experiences of the measurements above the kerogen isolated from the oil shale was also degraded in order to determine the coal rank and H/C atomic ratio of the non-converted organic matter.

## EXPERIMENTAL

The sample in question is a Pliocene (Upper Pannonian) oil shale of Pula (Hungary) which was formed in a miohaline crater lake of 283—285 K, and the precursor of which is the *Botryococcus braunii* KÜTZ. [JÁMBOR and SOLTÍ, 1976]. During the measurements air-dried sample of 0.05—0.15 mm diameter was used, its ash content is 49.9%, C<sub>inorg</sub>=2.6%, C<sub>org</sub>=27.4%. Before isolating the kerogen the bitumen was extracted in Soxhlet extractor by means of chloroform (Bit-A=3.3%). Based on the differences in specific gravity, the kerogen was enriched physically. Parameters of the kerogen are: ash content=9.0%, C<sub>inorg</sub>=0.6%, C<sub>org</sub>=70.2%.

Thermal degradation was carried out in a glass-made heating tube and the samples were measured in boats made from the same glass. The heating tube was surrounded by a programmed furnace. Heating and cooling to room temperature were carried out in continuous nitrogen flow. The products were collected in two traps. The first was air-cooled in which the oil was practically precipitated. The second collector was cooled by salted ice where first of all the water and a small quantity of oil precipitated. Gases were not measured. The oil shale and the kerogen were extracted in the mixture of benzene:acetone:methanol of 75:15:15 ratio after degradation.

The determination of hydrogen and carbon contents was carried out by means of CHN-1 analyser.

The degree of degradation was determined according to the ASTM-standard [CUMMINS *et al.*, 1974]; taking the carbon content (C<sub>R</sub>) of the sample after heating

at 773 K in inert atmosphere during 30 minutes and referring this value to the carbon content ( $C_T$ ) before the thermal treatment.

The products of thermal degradation of the oil shale, i. e. the quantities of gas + water, oil, bitumen, non-converted matter and the quantity of the non-converted organic carbon are summarized in Table 1.

TABLE 1

*Different matters originated from oil shale by thermal degradation*

Heating temperature (K)	period (h)	Gas + water (%)	Shale oil (%)	Bitumen (%)	Unconverted oil shale (%)	$C_{org}$ (%)
573	48	8,1	0,9	1,4	89,6	21,9
	96	11,2	0,9	0,5	87,4	17,6
	336	12,8	1,2	0,5	85,5	16,6
598	5	7,9	1,1	2,9	88,1	18,7
	10	7,9	1,1	2,4	88,6	17,0
	24	8,3	1,7	2,4	87,5	15,7
	48	10,3	2,7	2,4	84,6	13,1
623	1	8,1	0,9	3,6	87,4	14,4
	5	9,6	1,4	3,0	86,0	13,2
	10	13,3	2,7	2,8	83,2	13,6
	24	12,0	4,0	3,4	82,6	—
648	1	8,1	1,9	3,3	86,7	16,6
	5	9,9	5,1	5,3	79,7	12,4
	10	11,3	6,7	4,3	77,7	10,6
673	1	12,1	5,9	7,4	74,6	8,3
	5	14,8	10,2	6,4	68,6	8,0
	10	13,6	11,4	2,0	73,0	9,6
723	1	19,4	4,6	1,9	74,1	8,2
	2	22,1	5,9	0,9	71,1	5,8
	5	16,8	12,2	0,7	70,3	5,1
773	1	16,9	12,1	1,6	69,4	4,8
	2	18,2	14,8	0,4	66,6	3,0
	5	19,0	14,0	0,3	66,7	2,8

The formation of the most important product of the process, i. e. of the shale oil could be observed already at the applied lowermost temperature (573 K) and during a relatively short time. During 48 hours 0.9% shale oil was formed. When having increased the duration of thermal treatment, the production has hardly changed, it reached only 1.2% even during 336 hours.

Parallel with the increasing temperature the quantity of the shale oil is rapidly increasing. In Fig. 1 the increase of the quantity of shale oil can be seen as a function of the degradation temperature during thermal treatment of 5 hours. From the temperature of 623 K the production steeply increases, while between 673 and 773 K it is also intense but less rapid than before. Consequently, it seems so that the main oil producing phase of the studied Hungarian oil shale of type I falls between 623 and 773 K under laboratory conditions, i. e. this temperature interval is suitable to the laboratory simulation of the catagenesis.

As it is well-known, the quantity of the oil is increased both by the increase of temperature and of duration of degradation: the change is exponential in the former and linear in the latter case. Under the applied experimental conditions certain overlaps could be observed between each temperature-time pairs. Nearly the same quantity

of oil was formed at 673 K during 10 hours, at 723 K during 2 hours and 773 K during one hour (Table 1). These results refer also to the fact that the results of degradation carried out under laboratory conditions at higher temperatures and shorter duration are commensurable at least concerning the quantitative relations with the evolution under natural conditions at lower temperatures but longer durations.

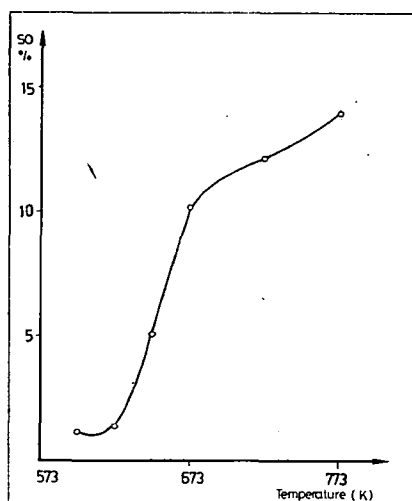


Fig. 1. Yield of the shale oil as a function of temperature of degradation.

In addition to the shale oil being the most important from the industrial point of view, gas and water as well as bitumen were formed at all the studied temperatures and during each degradation time. The temporal change of these products, as well as of the non-converted organic matter, and of the organic carbon content of the latter can be seen in Figs 2—5.

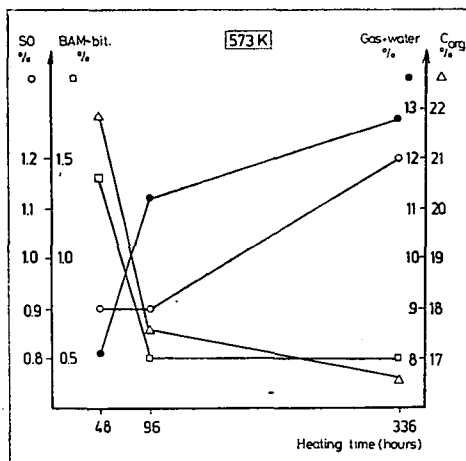


Fig. 2. Materials degraded from oil shale and organic carbon content of the unconverted oil shale in function of the heating period at 573 K.

At 573 K and during 48 hours the bitumen content of 4.6% of the original sample decreased to 1.4%, simultaneously the gas and water release was started and 0.9% shale oil formed. The organic carbon content decreased from 30.0% to 21.9%. When having increased the duration of degradation, between 48 and 96 hours the subsequent bitumen decrease was not accompanied by the increase of the quantity of shale oil, but the quantities of the released gas and water were considerably increased. Between 96 and 336 hours the quantity of bitumen seemed to remain unchanged, but at the same time the oil predominated out of the reaction products, the joint quantity of gas and water was increased only to smaller extent. When characterizing the whole of the conversion by the change of the  $C_{org}$  content the reaction is more intense at the beginning, then the efficiency of transformation seems to decrease. Presumably, the degradation of the bitumen being present in the original sample and of relatively large amount, has started already in the first minutes of thermal treatment, the release of gases could be observed by sense, as well. The transformation of kerogen has presumably also started, but this needs much more time than the decomposition of the bitumen, thus equilibrium between the formation and transformation of bitumen followed only between 96 and 338 hours.

When increasing the temperature the rate of reaction is increased and the oil production becomes more intense. At 598 K (Fig. 3) the character of the process

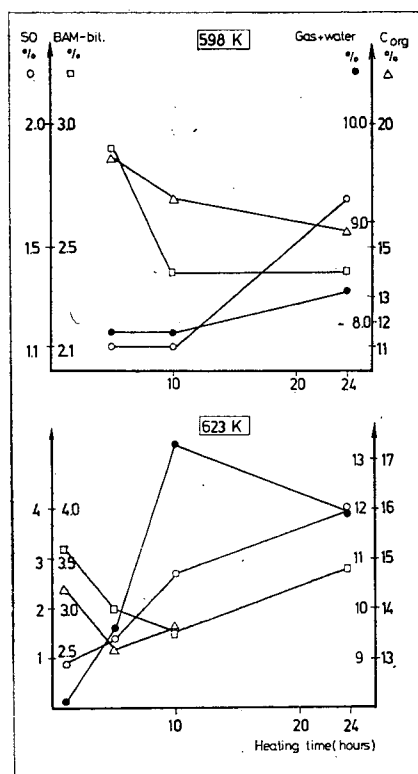


Fig. 3. Materials degraded from oil shale and organic carbon content of the unconverted oil shale in function of the heating period at 598 K and 623 K.

is similar to that observed at 573 K but all changes take place within a much shorter duration. The increase of oil production becomes stronger and the formation of water and gas is less significant.

At higher temperature already from 623 K (Fig. 3) the equilibrium followed previously in the formation and decomposition of bitumen seems to be disturbed. After the initial decrease (between 1 and 10 hours) the bitumen content increases again between 10 and 24 hours. The quantity of shale oil increases as a function of time already from the start of the reaction as against the constant value observed at 96 and 10 hours, respectively. The gas and water content increases first as a function of time, then shows a decreasing tendency. This is valid not only at 623 K but also at higher temperatures, i. e. at 673 K and 723 K.

At 648 K (Fig. 4) the bitumen content shows a relatively high value during the whole process of degradation. It decreases down to 3.3% at the end of the first hour while in the 5th hour it exceeds the 4.6% of the original sample, but between 5 and 10 hours it is slightly decreasing again. Simultaneously, the quantities of oil, gas + water increase continuously, presumably due to the more intense degradation of bitumen between 5 and 10 hours.

At 673 K (Fig. 4) considerable quantities of bitumen and oil developed during 1 and 5 hours. Between 5 and 10 hours the transformation of bitumen into oil is

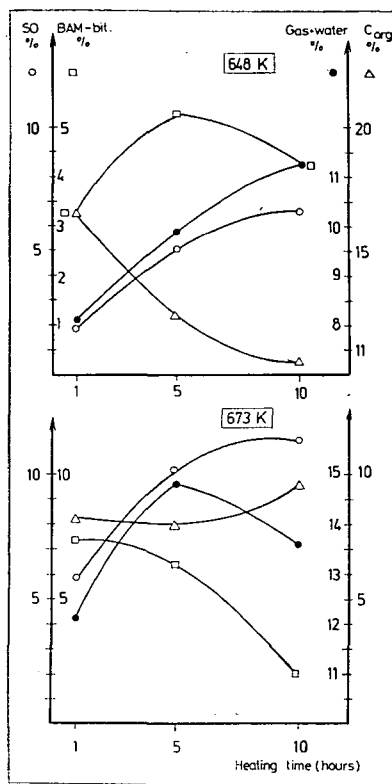


Fig. 4. Materials degraded from oil shale and organic carbon content of the unconverted oil shale in function of the heating period at 648 K and 673 K.

stronger, the bitumen content considerably decreased. Under the studied experimental conditions, at this temperature considerably greater quantity of bitumen could be extracted as compared with the results of other degradation processes carried out at other temperatures but during the same duration.

At 723 and 773 K (Fig. 5) the character of the changes is nearly the same. The tendency seems to predominate that some equilibrium should develop in the quantitative ratios of all products studied. Of course, at higher temperature this may follow during shorter durations.

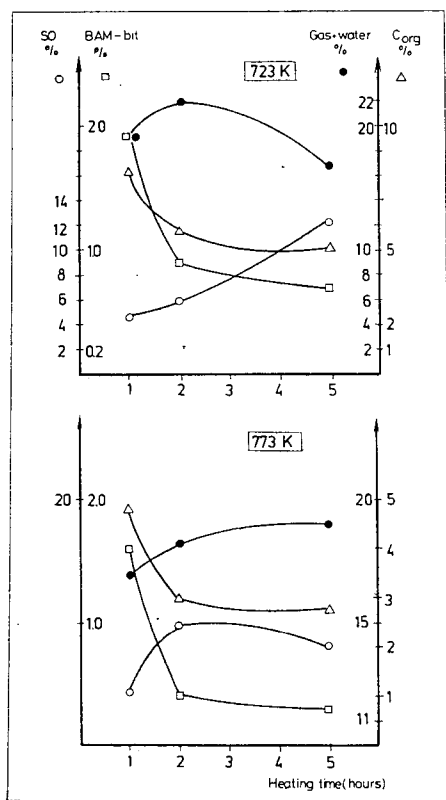
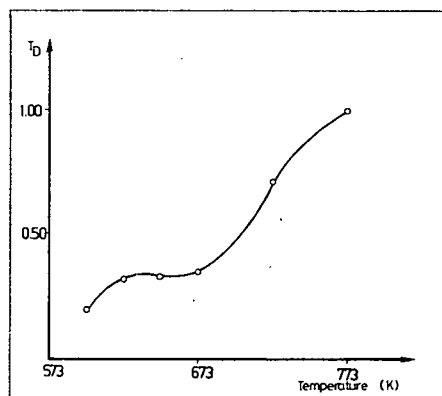


Fig. 5. Materials degraded from oil shale and organic carbon content of the unconverted oil shale in function of the heating period at 723 K and 773 K.

As it has been demonstrated above, during the natural and artificial degradation gas, water and oil develop depending on the conditions of the process (e. g. temperature, time). Their ratio is not constant. In the meantime, by means of gradual elimination of the smaller, shorter carbon-chain units the organic matter is also transformed and a more condensed and more complex matrix remains. Since at the beginning of the process the units more abundant in hydrogen are released, the unconverted kerogen becomes ever more coalified. To characterize the unconverted organic matter the degree of degradation ( $T_D = C_R/C_T$ ) is given. In Table 2 the quotients are listed which derive from the samples of 5 hours thermal treatment and extracted in BAM,

Degradation coefficient ( $T_D$ ) of unconverted oil shale

Heating period (h)	temperature (K)	Degradation coefficient $T_D = C_R/C_T$
5	598	0,20
5	623	0,32
5	648	0,33
5	673	0,35
5	723	0,71
5	773	1,00

Fig. 6. Degradation coefficient ( $T_D$ ) as a function of temperature.

further these are shown as a function of temperature in Fig. 6. The determination  $T_D$  was carried out according to the ASTM-standard at 773 K. Though the type and measure of diagenesis of the organic matter of sediments were characterized by the  $C_R/C_T$  ratio at 1172 K by GRANSCH and EISMA [1966], the temperature value of 773 K proved to be more favourable both numerically and in the subsequent investigations in case of oil shales [GIRAUD, 1970; CUMMINS *et al.*, 1974]. According to the authors above the  $C_R/C_T = 0.09-0.27$  is characteristic of alginites, the values of 0.60—1.00 of humic coals, peat and lignite. Further, in case of  $C_R/C_T > 0.6$ , the organic matter is so highly coalified that it becomes unable to oil production. When making the determination of  $T_D$  at lower temperature the limits above will be probably displaced to higher values. The organic matter of the Hungarian oil shale is alginitic. Knowing its feature conclusions can be drawn from the  $T_D$  value to its degree of diagenesis. The  $T_D \approx 0.10$  value of the original sample is increased during 5 hours only up to 0.25 at 598 K and up to 0.35 at 623, 648 and 673 K. The value given for the alginites hardly exceeds the limit value already in the range of catagenesis. Consequently, the samples degraded for such short durations show only slight transformation already at relatively high temperatures. Above 673 K the conversion considerably increased and at 723 K the sample is hardly able to further oil generation, i. e.  $T_D$  is around the limit value. In case of thermal treatment at 773 K, because the determination of  $T_D$  is carried out at this temperature the  $T_D = 1$  could be expected in all cases. After 5 hours treatment this value was obtained. The  $C_R/C_T$  ratio of the

unconverted oil shale degraded at 773 K during 1 and 2 hours was also determined and this proved to be 0.64 and 1.00. These results, i. e. the quantitative relations of the value reflecting the character of the remaining matter and of the products (see the data of Table 1 and Fig. 5) show that at 773 K practically equilibrium follows after 2 hours. The duration of 2 hours is sufficient to reach the most favourable conversion and when increasing the duration the transformation of the organic matter is not continued at this temperature.

In Fig. 6 showing the change of the unconverted organic matter as a function of the temperature, a break can be seen at 763 K in addition to the approximate temperature of 623 K assumed to be the boundary between the dia- and catagenesis. Similar relationship can be observed also in Fig. 1 showing the relationship between the shale oil quantity and temperature. As to our opinion some change follows in the reaction mechanism at this temperature. The quantity of the extractable bitumen is greatest also at this temperature. Since the evaluation of bitumen quantity is complicated by the fact that not only the bitumen formed during the laboratory degradation but also the bitumen developed during the natural evolution are present in the sample, it proved to be expedient to degrade thermally the kerogen itself also at several characteristic temperatures. For this very reason, the kerogen concentrate was heat-treated at 598, 673 and 773 K during 5 hours. The temperature of 598 K falls to the range of diagenesis as proved by the experiments carried out previously with the oil shale while the values of 673 and 773 K represented the stage of catagenesis. The quantitative distribution of the products are involve in Table 3.

TABLE 3

*Different matters originated from kerogen by thermal degradation*

Heating temperature (K)	period (h)	Gas + water (%)	Shale oil (%)	Bitumen (%)	Unconverted kerogen (%)
598	5	11,1	0,9	1,5	86,5
673	5	39,8	13,2	17,6	29,4
773	5	41,9	38,1	0,3	19,7

In the range of diagenesis (598 K) only a relatively small portion of kerogen, i. e. about 13% was converted. Major part of the products is gas and water, small quantity of shale oil was formed and 1.5% bitumen was extracted. Since the starting matter did not contain bitumen, the total quantity was formed from kerogen as a result of thermal treatment under laboratory conditions. The shale oil of 0.9% is also the product of the artificial evolution of kerogen. It could be assumed that during the degradation of oil shale the subsequent degradation of the original bitumen produced an oil formation. The low temperature degradation of the bitumen-free kerogen, however, proved that the laboratory temperature of diagenesis provided also sufficient energy to start the bitumen and oil formation. According to the experiences of the preliminary measurements bitumen can be observed also at lower temperatures, i. e. at 473 and 573 K, and the generation of oil at 573 K, respectively. These results of the artificial evolution as well as the fact that the studied oil shale being in the initial stage of diagenesis contains large quantities of original bitumen refer to the start of evolution of the organic matter in the stage of diagenesis, and to the start of oil generation at the end of this stage. From the economic point of view this oil quantity is negligible, the phenomenon, however, throws light upon the fact that



though the main phase of oil generation is assigned to the catagenesis, the generation itself cannot be bound only to this stage.

Catagenesis was simulated at 673 and 773 K by means of thermal degradation, with the same durations. The efficiency of conversion has considerably increased, about 70% of the kerogen concentrate was converted at 673 K and about 80% at 773 K. The quantity of the products, first of all that of the shale oil, was multiplied. When comparing the quantities of the products at 673 and 773 K the gas+water quantities are nearly the same, that of the shale oil continuously increases. The quantity of the extracted bitumen, however, changes inversely as a function of temperatures: at 673 K 17.6%, at 773 K very small quantity of bitumen (0.3%) was obtained.

The question is arisen whether only the quantity or probably the quality of bitumen change at 673 K. The bitumen formed during the thermal degradation of kerogen was characterized by its hydrogen and carbon content as well as by its H/C atomic ratio (Table 4). As a comparison: the H/C ratio of the bitumen extracted from the original oil shale is 1.76. The H/C ratio of the BAM-bitumen formed from the kerogen concentrate at 473 K during one day is 1.75. For the bitumens obtained after degradation of seven days the H/C values are as follows: at 573 K 1.69 and at 573 K 1.67. The same, i. e. 1.67 value was obtained for the BAM-bitumen degraded at 598 K during 5 hours. At 673 K the H/C atomic ratio considerably decreases (1.50) while at 772 K the value is some higher again (1.60). Consequently, in case of degradation at 673 K not only more bitumen was formed but its quality also differed from the average. Parallel with increasing temperature presumably ever greater structural units are cut off from the kerogen and become the constituents of the bitumen fraction. At the beginning of the process, at low temperature only the  $H_2O$ ,  $H_2S$ ,  $CO_2$ , i. e. the most instable groups are eliminated, this is followed by the release of the hydrocarbons of shorter chains. Parallel with increasing temperature the release of ever greater units becomes possible and the character of bitumen follows this change; its H/C atomic ratio is slightly decreased. At 773 K the rate of reaction of bitumen  $\rightarrow$  oil has so considerably increased that the intermediary product can hardly be isolated. The bitumen of very small quantity was more degraded than that of 673 K and its H/C atomic ratio is higher, as well.

TABLE 4

*Hydrogen and carbon content of the bitumen extracted from degraded kerogen*

Heating temperature (K)	Carbon content (%)	Hydrogen content (%)	H/C atomic ratio
598	75,3	10,5	1,67
673	75,1	9,4	1,50
773	67,7	9,0	1,60

In the quality of the unconverted organic matter this type of change could not be observed. The hydrogen and carbon contents as well as the H/C atomic ratios of the unconverted kerogen are shown in Table 5, and a supplement is given consisting of the same parameters of the kerogen concentrate and of the kerogen treated at 473 and 573 K. In the latter cases the duration of thermal treatment was 24 hours [HETÉNYI, 1979]. As it can be seen in Fig. 7 the H/C atomic ratio is nearly constant in the  $T \leq 598$  K temperature range representing the stage of diagenesis, small decrease with the increasing temperature can be observed. The sudden change observed in the

stage of catagenesis relates to the rapid conversion, "coalification" of the organic matter.

The qualification of the organic matter of sediments is impossible only on the basis of the H/C ratio. On the basis of this series of experiments the conclusion should be drawn that the value of this quotient depends not only on the character of the

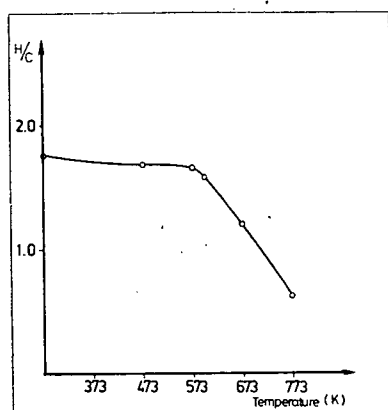


Fig. 7. H/C atomic ratio of the unconverted kerogen as a function of temperature of degradation.

Hydrogen and carbon content of the raw and degraded kerogens

TABLE 5

Heating temperature (K)	period (h)	Carbon content (%)	Hydrogen content (%)	H/C atomic ratio
raw kerogen	—	70,2	10,3	1,76
473	24	71,3	10,0	1,68
573	24	70,7	9,7	1,65
598	5	70,4	9,3	1,58
673	5	59,2	5,9	1,20
773	5	39,7	2,1	0,62

starting organic matter (terrestrial or marine origin, algal or humic constituents, etc.) but also on its evolution. According to the traditional classification the original kerogen and the kerogen treated at  $T \leq 598$  K are "alginite", since their H/C ratios fall between 1.4 and 1.8 [GRANSCH and EISMA, 1966]. On the basis of only this quotient the samples degraded at higher temperatures should be assigned to the group of humic coals, peat and lignite, the H/C atomic ratio of which varies between 1.4 and 0.4. In this case the alginite has considerably transformed during the artificial treatment, so that during the gradual coalification it reached the "peat"-state.

## CONCLUSIONS

The thermal degradation of the organic matter of the oil shale of Pula (Hungary) was simulated under laboratory conditions in the temperature range of 573 to 773 K in neutral gas atmosphere.

The raw material is a Pliocene (Upper Pannonian) near-surface oil shale containing organic matter in the first stage of its evolution. Its H/C atomic ratio is 1.76, the degree of degradation is 0.07. The precursor is the alga *Botryococcus braunii*. As it was proved by the preliminary investigations it is a kerogen formed from strongly polymerized algal fatty acids which is of type I according to the classification of VAN KREVELĖN.

On the basis of the laboratory experiments it can be stated that during the laboratory evolution of the oil shale both the quantity and some qualitative characteristics of the products, and the features of the unconverted organic matter refer to the end of the first phase of genesis to be at 623 K. This temperature may correspond to the simulated boundary between dia- and catagenesis.

With increasing temperature first the smaller peripheral units are cut off from the kerogen during the diagenesis:  $\text{CO}_2$ ,  $\text{H}_2\text{O}$ ,  $\text{H}_2\text{S}$  and hydrocarbons of shorter chains are released in form of gas. The temperature of 473 K provides sufficient energy to the degradation of greater units which can be extracted by means of organic solvents and which are the constituents of the so-called bitumen fraction. When increasing the reaction time gas and water are formed again during the subsequent degradation of these units and the bitumen content slightly decreases. Under such conditions remarkable oil generation was observed first at 573 K. The quantity of oil is at 573 K 1% on the average which hardly changes as a function of the degradation time: between 24 and 336 hours it increases from 0.9 to 1.2%. At 598 K this quantity amounts to 1.1 to 2.7% during 5 to 48 hours.

The formation of shale oil is produced by the kerogen of the oil shale and it is the intermediary product of the kerogen oil transformation. In the raw oil shale relatively large quantity of original bitumen is found the transformation of which into oil should have been also taken into account. Presumably, the subsequent transformation of this oil being of much simpler structure and consisting of shorter chains than the kerogen, takes place much more rapidly even at such low temperature than the oil generation from the gel-network (kerogen) of complicated three-dimensional structure. As a function of time an equilibrium follows in the bitumen quantity and both temperatures (573 and 598 K). As it has been proved by the increase of the oil quantity, this equilibrium is dynamic, i. e. the bitumen is continuously formed and transformed.

The H/C atomic ratio of the BAM-bitumen formed in the stage of diagenesis is somewhat lower than that of the original bitumen and when increasing the simulation temperature or the duration, the value of this ratio slightly decreases. This decrease relates to the fact that parallel with both the increasing temperature and duration the bitumen which can be isolated as an intermediary product becomes somewhat more degraded already in this range.

The increase of coalification of the unconverted organic matter is more expressed though as compared to the change in the stage of catagenesis, this can be neglected. The degree of degradation is a low value ( $T_D=0.20$ ) also after 5 hours degradation at 598 K. Taking into account that the degradation degree of the raw material is 0.07, it is fairly demonstrated that the artificial evolution proceeds relatively intensely also during short time.

Based on the H/C atomic ratio and on the  $T_D$  quotient the organic matter of the sample treated thermally at 598 K can be qualified as an "alginitic" sample of diagenetic stage. Taking into consideration the change of products of degradation as well as of the "coalification" of kerogen as a function of temperature (Figs 1—6)

it can be stated that the temperature of 623 K or the higher temperatures show the degradation under catagenic conditions. The transition between the two stages is unbroken and cannot be bound to one temperature value. Under the experimental conditions applied the temperature around 623 K seems to be the probable boundary. This observation is in harmony with the boundary value determined by TISSOT and WELTE [1978] for the kerogen of type II. The authors above studied the degradation during continuously temperature increase. In the experiments discussed above the raw sample was heated to the required temperature only during several minutes and the samples were kept at the temperature in question for different durations. It is remarkable that the two series of experiments differing not only in the raw material but also in their conditions, provided the same results.

Catagenesis was simulated by degradation carried out in the temperature range  $623 \leq T \leq 673$  K. As it is well-known, catagenesis is the main phase of oil generation, accordingly at the temperature  $T > 623$  K sudden increase could be observed in the oil generation. Nevertheless, when investigating the dependence on the temperature the samples treated during the same time (i. e. 5 hours) were compared with each other, while at the given temperature values degradations of three different durations were investigated. Oil generation is increased by the increase of both the temperature and duration, the former showing more rapid, the latter less intense change. At 773 K and after degradation of 2 hours the quantity of shale oil does not increase anymore. At this temperature practically the equilibrium follows concerning all the products and the whole conversion.

The quantity of the bitumen, i. e. of the intermediary product is more varied in this stage than in the stage of diagenesis. The quantity will be nearly constant at the extreme temperature values of catagenesis when increasing the duration. At 773 and 723 K 1% bitumen can be extracted after 2 hours. At the beginning of this stage (623 K) the value varies between 3.0 and 3.5%, i. e. the quantity of bitumen is practically independent of the time. The temperature of 673 K seems to be favourable from the point of view of bitumen formation: during 5 hours 17.6% bitumen was formed from the kerogen concentrate. Presumably, at this temperature and during this duration the further fractionation of bitumen takes place only to relatively small extent. The change of only one experimental parameter, i. e. the increase of duration, however, also promotes the transformation of the intermediary product as it has been proved by the experiments when the oil shale was degraded (Table 1).

In this stage of genesis the conversion of kerogen shows rapid increase. 70—80% of the kerogen concentrate was converted at 673 and 773 K, respectively. The remaining organic matter is more "coalified", its H/C atomic ratios are 1.20 and 0.62, i. e. reaches the characteristic values of the humic coals, peat and lignite.

When having simulated the thermal degradation of kerogen under laboratory conditions we tried to compensate the considerable decrease of duration by applying much higher temperatures. It seems so that the laboratory boundary between the dia- and catagenesis is at around 623 K independently of the duration of degradation and of other experimental conditions (e. g. gradual or sudden increase of temperature) and of the type of the starting material. The quantity of the produced oil increases parallel both with the temperature and with the duration. The experimental parameters affect first of all the formation and further fractionation of the intermediary product, i. e. of the bitumen, as well as the quality of the bitumen extractable in each phase. Except the H/C atomic ratio the qualitative characteristics have been neglected here.

## ACKNOWLEDGEMENT

The author expresses her thanks to DR. Á. JÁMBOR for providing the samples investigated and to DR. H. HÁMOR, Director of the Hungarian Geological Institute for encouraging and assisting this research work.

## REFERENCES

- ABELSON, P. H. [1967]: Conversion of biochemicals to kerogen and n-paraffins. In: P. M. ABELSON: Research in Geochemistry, v, 2, p. 63—86.
- CANE, R. F. [1948]: The chemistry of the pyrolysis of torbanite. Journal et Proceedings, p. 62—68.
- CANE, R. F. [1951]: The mechanism of the pyrolysis of torbanite. In: Oil shale and cannel coal, 2, Institute of Petroleum, London.
- CANE, R. F. [1976]: The origin and formation of oil shales. In: Oil shale, edited by T. F. YEN and G. V. CHILINGARIAN. Elsevier Scientific Publishing.
- CUMMINS, J. J., F. G. DOOLITTLE and W. E. ROBINSON [1974]: Thermal degradation of Green River kerogen at 150° to 350 °C. Composition of products. U.S. Bur. Mines Rep. Invest., 7924, p. 18.
- CUMMINS, J. J. and W. E. ROBINSON [1972]: Thermal degradation of Green River kerogen at 150° to 350 °C. Rate of product formation. U.S. Bur. Mines Rep. Invest., 7620, p. 15.
- GIRAUD, A. [1970]: Application of pyrolysis and gas chromatography to geochemical characterization of kerogen in sedimentary rock. AAPG Bulletin 54, No. 3, p. 439—455.
- GRANSCH, S. A. and E. EISMA [1966]: Characterization of the insoluble organic matter of sediments by pyrolysis. In: Advances in Organic Geochemistry, edited by G. D. HOBSON and G. C. SPEERS, p. 407—427, Pergamon Press.
- HETÉNYI, M. and K. SIROKMÁN [1978]: Structural informations on the kerogen of the Hungarian oil shale. Acta Miner. Petr., Szeged, XXIII/2, p. 211—222.
- HETÉNYI, M. [1979]: Thermal degradation of the oil shale kerogen of Pula (Hungary) at 473 and 573 K. Acta Miner. Petr., Szeged, XXIV/1, 99—111.
- JÁMBOR, Á. and G. SOLTÍ [1976]: Geological conditions of the Upper Pannonian oil shale deposit recovered in the Balaton Highland and at Kemeneshát (Transdanubia, Hungary). In Hungarian Annual Report of the Hungarian Geological Institute of 1974, p. 193—220.
- ROBINSON, W. E. [1979]: The origin, deposition and alteration of the organic material in Green River shale. Organic Geochemistry, Vol. 1, pp. 205—218.
- TISSOT, B. P. and D. H. WELTE [1978]: From kerogen to petroleum. In: D. H. WELTE: Petroleum formation and occurrence. Springer-Verlag, p. 148—184.

*Manuscript received, July 20, 1980*

MISS DR. M. HETÉNYI  
Institute of Mineralogy  
Geochemistry and Petrography  
Attila József University  
H-6701 Szeged, Pf. 428  
Hungary

## DIAGENETIC AND LITHIFICATION PROCESSES OF RECENT HYPERHALINE DOLOMITES ON THE DANUBE-TISZA INTERFLUVE

B. MOLNÁR, M. SZÓNOKY and S. KOVÁCS

### SUMMARY

In the hypersaline lacustrine dolomite and dolomite mud profiles of the Danube-Tisza-Interfluve four members can be distinguished on the basis of formation, composition, diagenesis and lithification. In the three lower members, i. e. in the dolomitic limestone and dolomite the starting phase of anadiagenesis, in the upper dolomite mud the syndiagenesis take place. The latter lithification is one of the most important factor of syndiagenesis. The formation, evolution, filling processes of pores, the chemical composition of the filling material as well as their crystal forms depend on these processes and change according to their affects.

### INTRODUCTION

The dolomite formation of sodaic lakes lying among the dunes of the blown-sand area of the Danube-Tisza-Interhuve has been dealt with in particular [MOLNÁR, B., M. MURVAI, I., 1975, 1976; MOLNÁR, B., M. MURVAI, I., HEGYI—PAKÓ, J., 1976; MOLNÁR, B., 1979]. It has been stated that the early diagenetic dolomite formation is produced by the evaporation caused by drought, by the CO<sub>2</sub>-depriving effect of plants and by the admixture of freshwater of considerable quantity deriving from the autumn precipitation.

In the Danube-Tisza-Interfluve two rock-types of dolomite occur. In the northern parts and in the existing sodaic lakes dolomite muds soft and plastic in wet state, and loose crumble in dry state are known. Mainly in the southeastern part of the Danube-Tisza-Interfluve and in the warmer sodaic lakes being now covered partly by the wind-blown sand, hard dolomite is found at the bottom of the carbonate profiles and in the upper parts loose dolomite mud similar to that mentioned above, can be found. Accordingly, in case of dolomites of the Danube-Tisza-Interfluve the diagenetic and lithification processes take place in sight of us and this provides a fair opportunity to study this very significant sedimentological changes of carbonate formation.

The pores of carbonate rocks are considerably modified during lithification. To elucidate this process, it is highly significant from the point of view of the hydrocarbon and water reserving carbonate rocks. Further, the chemistry of carbonate rocks is strongly connected to the chemistry of the water from which the rocks were deposited. The carbonate formation of closed lake basins may provide information on the changes of chemistry and water table of the former lake, on the measure of evaporation and on the climatic changes.

In Hungary numerous terrestrial lacustrine carbonate intercalations are known, e. g. in the Permian formations of the Mecsek Mountains, in the Lower Eocene strata

of the Transdanubian Central Mountains or in the Pannonian and Pleistocene formations of the Tolna Hills [ÁDÁM, L., MAROSI, S., SZILÁRD, J., 1959; FORGÓ, L., MOLDVAY, L., STEFANOVITS, P., WEIN, GY., 1966; SZENTES, F., 1968; ÁDÁM, L., 1978]. These are to be processed and may provide useful paleogeographic relationships, too.

In the following the diagenetic and lithification processes of the carbonates of the Danube-Tisza-Interfluvium will be demonstrated.

## CONCEPT OF DIAGENESIS AND LITHIFICATION

In the Hungarian literature the *diagenesis* is called in general *lithification*. Accordingly, the hardening to rock-state, i. e. the lithification is only a part-process of diagenesis.

A. In the international literature a lot of definitions of *diagenesis* are known. It is especially hard to find common view when concerning the limits of diagenesis. Most of the concepts, however, agree that the processes between the states of deposition and metamorphism are understood as rock diagenesis.

In general, diagenesis includes all the physical, physico-chemical, chemical and biological changes which follow in the sediments at low temperatures and pressures, i. e. mostly near the surface. In case of a given sediment, however, diagenetic processes can be determined already in the sedimentation cycle and in the weathering cycle, respectively.

Recently, several authors dealt with the diagenesis of carbonates and carbonate rocks [BRICKER, O. P., 1971; BATHURST, R. G. C., 1970, 1971; CHILINGAR, G. V., BISELL, H. J., WOLF, K. H., 1967; FAIRBRIDGE, R. W., 1967; FOLK, R. L., 1965, 1974; FRIEDMAN, G. M., 1964, 1975; MILLIMAN, J. D., 1974; and PRUDY, E. G., 1968].

According to FAIRBRIDGE, R. W. [1967] the diagenesis consists of three phases: 1. syndiagenetic; 2. anadiagenetic; and 3. epidiagenetic phases.

The geochemical processes of the *syndiagenetic* phase is primarily controlled by the pore water of large quantity and lying between the mineral grains with changing bonding force.

The *anadiagenesis* is started by the burial deeper than in the previous case. The main process is the lithification. The liquid content of the sediment is strongly migrating in this phase and its total amount considerably decreases.

The *epidiagenesis* is the phase being subsequent to the uplift of the sediment (or rock). The main affecting factor is the downward migrating water being influenced by atmospheric effects.

According to CHILINGAR, G. V., BISELL, H. J., WOLF, K. H. [1967] the most important processes of the diagenesis of carbonatic sedimentary rocks are as follows: 1. Physical processes: compaction, drying, shrinking; 2. Physico-chemical processes: solution, leaching, discoloration, oxidation, reduction, re-precipitation, recrystallization, cementation, authigenic mineral formation, etc.; 3. Biochemical and organic processes: cave formation, formation of organic and inorganic compounds.

FÜCHTBAUER, H. [1974], MILLIMAN, J. D. [1974] and FOLK, R. L. [1974] classified the diagenetic processes as follows:

I. Destructive diagenesis, which as a result of biological or mechanical erosion and chemical solution produces the sedimentation of carbonates.

II. Constructive diagenesis, which produces the reformation and transformation of carbonates.

A species of the latter type is the *iso-chemical diagenesis* which does not change the chemical composition of the sediment. The early and late diagenetic cement formation are assigned to this type. Neomorphism denotes the recrystallization, e. g. from the greater crystals of biogenic shell fragments smaller crystals are developed or when during dissolution calcite is formed from aragonite. Finally, the selective processes, e. g. the encrusting solution processes are assigned to this group which produce stilolite and secondary porosity.

Another type of constructive diagenesis is the *allochemical diagenesis* when the sediment is transformed also chemically. Examples are the early or late diagenetic dolomitization, dedolomitization, the dissolution and transformation to calcite of the Mg-bearing calcite, clay mineral formation, zeolitization and the formation of authigenic minerals.

B. *Lithification*, i. e. the rock formation is considered in general to be one of the most important process of diagenesis. According to CHILINGAR, G. V., BISELL, H. J. WOLF, K. H. [1967] lithification is the assemblage of processes which transforms the newly deposited sediments into solid rocks. This transformation may take place in any phase of diagenesis. In the processes of lithification compaction, cementation, recrystallization, dolomitization and pressure solution are the most important factors.

The essential difference between the diagenetic and lithification processes is that the appearance of diagenesis is a function of the facies, and the structure of the sediment, respectively, i. e. this is specific; while lithification may occur in all sediments. Lithification can be considered to be one of the evolution phases of the rock which may follow at any time during diagenesis and due to nearly all diagenetic processes.

In the course of lithification of carbonate rocks the carbonate mud is transformed to hard carbonate rock during which the pore content decreases from original water-abundant 50—70% down to 2—3%. If in case of this process the role of compaction is subordinate, enormous carbonate quantities should be available to cementation. According to BATHURST, R. G. C. [1970] in case of fine grained carbonates the lithification should be traced back to the joint effect of cementation and neomorphism and it is fundamentally determined by the following processes.

1. Dissolution of the very fine-grained components and the predominance of greater components;
2. Transformation of aragonite into calcite;
3. Recrystallization of the high-Mg-calcite while the divalent magnesium remains in the pore water;
4. At the grain contact pressure solution occurs;
5. During cementation syntaxial growth occurs at the grain's surface.

The fact that what process plays the predominant role out of the processes enumerated above during lithification, depends always on the mineralogical features of the carbonate components, on their form and grain size, on the clay mineral and organic matter content as well as on the depth of deposition.



## COMPOSITION AND TEXTURAL EVOLUTION OF THE CARBONATES OF THE DANUBE-TISZA-INTERFLUVE

Four characteristic carbonate profiles were chosen from the southeastern part of the Danube-Tisza-Interfluve (*Fig. 1*). Out of them the Csólyospálos-South is a nature conservation area just because it is a sedimentologically rare and interesting geological formation as proved by the previous investigations [MUCSI, M., 1963; MOLNÁR, B., 1979].

Three of the studied carbonate profiles overlie strongly ochre-spotted fine-grained blown-sand while the the Csólyospálos-North profile was deposited on black organic matter containing fine-grained blown-sand. The hydrochloric-acid-soluble part of the blown-sand amounts from 10 to 20%, in general.

Within the carbonate profiles the following strata members can be distinguished:

a) The carbonate profiles start everywhere with sandy carbonate of looser structure containing red ferriferous precipitations of 10 to 30 cm, which possesses a hydrochloric-acid soluble part of 30 to 60%, the value increasing upwards (*Fig. 1*).

b) The next member is a light-grey hard carbonate rock of 15–30 cm thickness showing macroscopically homogeneous fabric; its hydrochloric-acid-soluble part is always above 50%, in some cases this amounts to 80%. Because of its peculiarities this member was used as foundations matter in the neighbourhood and in a few cases it is used recently, too.

c) The light-grey carbonate rock is over- and underlain by a darker-grey carbonate rock which is very hard and contains carbonate matter above 80%, it shows well-developed bedding planes (its folk term is "pechmeg").

d) The closing member of the carbonate profiles is a 40–60 cm thick loose light-grey carbonate mud being crumble in dry state; its hydrochloric-acid-soluble part varies between 30 and 80% showing an upward decreasing tendency. The upper part of the profiles became soil in a thickness of 10–25 cm.

15 characteristic samples were taken from each members and detailed different sedimentological analysis were carried out on them (*Fig. 1*, I. 1–15, Table 1).

X-ray diffractometric records were made on all the 15 typical samples. The characteristic X-ray records are seen in *Fig. 2*. Only the sections of the curves are demonstrated which reflect first of all the composition of the carbonates. When evaluating the curves by profile sections it can be seen that in the loose sandy carbonate containing ferriferous precipitations, i. e. in the member *a*, calcite predominates but considerable dolomite quantity can also be identified as proved by the sample No. 1 of Kömpöc. In harmony with the macroscopic appearance, it contains also quartz and feldspar (*Fig. 2*, sample No. 1).

In the light-grey hard carbonate, i. e. in the member *b* the same minerals predominate, only the quantity of feldspars is somewhat less (*Fig. 2*, samples No. 4–6).

The composition of the darker-grey hard carbonate ("pechmeg"), i. e. of the member *c* is different as proved by the two X-ray records (*Fig. 2*, samples No. 8 and 9). In the sample deriving from the Kömpöc-South outcrop dolomite shows smaller while calcite greater quantities. In the sample of the Kömpöc-North outcrop (sample No. 9) dolomite is also significant in addition to calcite.

As it was shown, above the "pechmeg" considerable change could be recognized macroscopically. The harder formation is replaced in member *d* by carbonate mud of looser structure. According to the X-ray records, in its compositions changes follow, too. As against the calcite and dolomite identified is the samples above in these samples dolomite predominates (*Fig. 2*, samples No. 11–15).

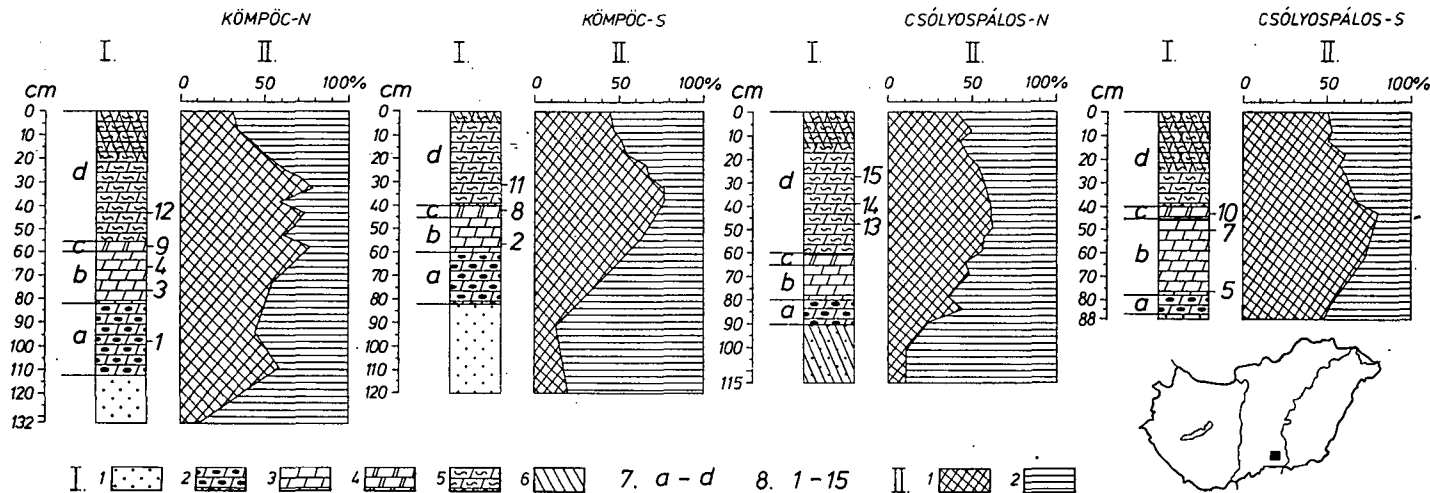


Fig. 1. Formations of the investigated carbonate profiles of the Danube-Tisza-Interfluve. —

I. 1 — fine-grained sand; 2 — sandy, limy dolomite and dolomitic limestone of looser structure containing ferriferous precipitations; 3 — light-grey hard dolomite; 4 — dark-grey hard dolomite ("pechmeg"); 5 — light-grey dolomite mud; 6 — humic strata; 7a-d — indication of the carbonatic members within the profile; 8. 1-15 — site and number of samples of the profile. Numbers are the same as in Table 1.

II. 1 — hydrochloric-acid-soluble; 2 — insoluble in hydrochloric acid.

TABLE 1

Position and number of samples within the profiles chosen for investigation

Position of sample within the profile	No. of sample	Location of sample
Light-grey dolomite mud  member <i>d</i>	15	Csölyospálos-N, upper 5 cm of the 25—50 cm
	14	Csölyospálos-N, middle 5 cm of the 25—50 cm
	13	Csölyospálos-N, lower 5 cm of the 25—50 cm
	12	Kömpöc-N 40—45 cm
	11	Kömpöc-S 30—35 cm
Dark-grey hard dolomite ("pechmeg") member <i>c</i>	10	Csölyospálos-S, 60—65 cm
	9	Kömpöc-N, 60—65 cm, fine-stratified
	8	Kömpöc-S, 40—45 cm
Light-grey hard dolomite  member <i>b</i>	7	Csölyospálos-S, top of the bank (c)
	6	Csölyospálos-S, bottom of the bank (b)
	5	Csölyospálos-S, bottom of the bank (a)
	4	Kömpöc-N, 60—82 cm (a)
	3	Kömpöc-N, 60—82 cm (b)
	2	Kömpöc-S, 45—60 cm, from the upper part
Sandy, looser dolomite and dolomitic limestone of looser structure containing ferri-ferrous precipitations member <i>a</i>	1	Kömpöc-N, 82—102 cm

Parallel with the X-ray diffractometric records derivative (DTA) records were also made from the same samples. The results obtained from the sandy carbonate (*a*-member) containing ferri-ferrous precipitation) and from the light-grey hard carbonate (*b*-member) are quite similar. The values concerning the  $\text{CaCO}_3$  varies between 71 and 77%, those of  $\text{MgCa}(\text{CO}_3)_2$  between 19.4 and 22.3%, i. e. within rather narrow range. Out of the double endothermal peak of dolomite the first one is rather poorly-developed, the second one, however, is characteristic (Fig. 3., samples No. 1—6).

The  $\text{CaCO}_3$ -value of the dark-grey hard carbonate (*c*-member) decreases down to 65.1 to 66.6%, the dolomite value increases up to 26.5 to 32.1% (Fig. 3, samples No. 8—9). The samples No. 9 of the Kömpöc-N outcrop, the X-ray diffractometric record of which showed also intense dolomite peak, is characteristic and shows well-developed double endothermal dolomite peak (Fig. 3, sample No. 9).

The curves of carbonate muds show more intense double endothermal peaks (Fig. 4, samples No. 11—15). In harmony with the X-ray records, the values of  $\text{CaCO}_3$  and  $\text{CaMg}(\text{CO}_3)_2$  vary between 36.1 to 65.6 and 34.8 to 59.0%, respectively, i. e. within rather wide range and the value of the latter considerably increases. It is worthy of note that the first endothermal peak of dolomite is found at lower temperature, i. e. between 715 and 735 °C than usual. As to literature data, two reasons may be responsible for this phenomenon, i. e. either the weaker degree of crystallization of the presence of water-soluble salts may produce it [BERG, L. G., 1943; FÖLDVÁRI—VOGL, M., 1958; FÜCHTBAUER, H., GOLDSCHMIDT, H., 1965; MÜLLER G., 1969; MÜLLER, G., IRION, G., FÖRSTER, U., 1972; MÜLLER, G., WAGNER, F., 1978; FÖLDVÁRI, M., 1974].

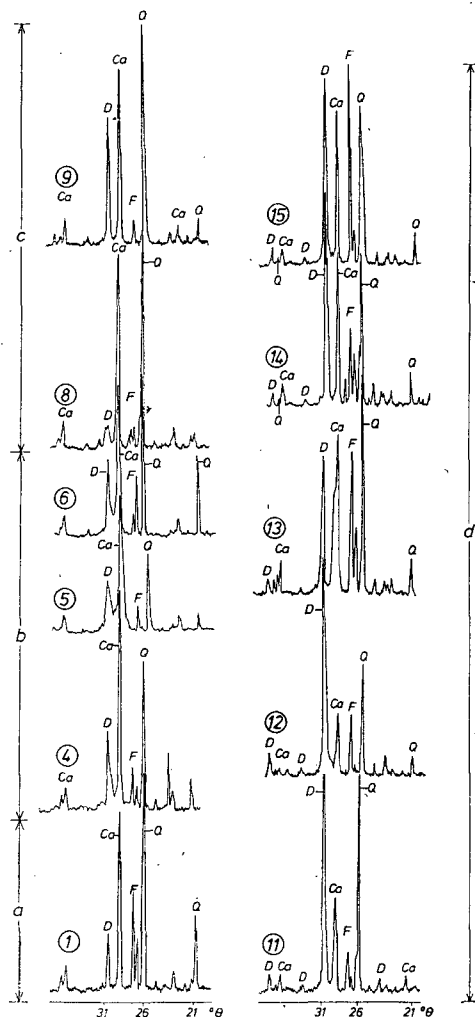


Fig. 2. X-ray diffractometric records of different members (a—d) of the studied profiles. Recording conditions:  $\text{CuK}\alpha$ , Ni-filter, 32 kV, 24 mA, 2 $\theta$ /min. Numbers are the same as in Table 1; D=dolomite, Ca=calcite; F=feldspar, Q=quartz.

Since according to the investigations of the carbonates of the Danube-Tisza-Interfluvium, protodolomite (or high Mg-calcite), i. e. dolomite of less ordered structure or of weaker crystallization degree, even in case of more elongated X-ray diffractometric records, only the second reason could be taken into account. Carbonates were precipitated from strongly alkalic sodaic lakes where out of the water-soluble salts the  $\text{NaHCO}_3$  and  $\text{Na}_2\text{CO}_3$  are always present [MOLNÁR, B., M. MURVAI, I., HEGYI—PAKÓ, J., 1976; MOLNÁR, B., 1979]. The temperature decrease of the first endothermal peak could be caused by these salts. FÜCHTBAUER, H. (Professor of the Geological Department of the Bochum University) analyzed also this material. Based on his X-ray records he stated that the values of dolomite mud are as follows:  $\text{Ca}_{0.55}\text{Mg}_{0.45}$ ,

consequently, as to their composition these are calcium dolomites. Their order-line is  $35.2^\circ$  ( $2\theta$ ), i. e. these are medium-ordered and real dolomites. According to FÜCHTBAUER the calcium surplus is the evidence of the in-situ formation. These results agree with our ones and prove them.

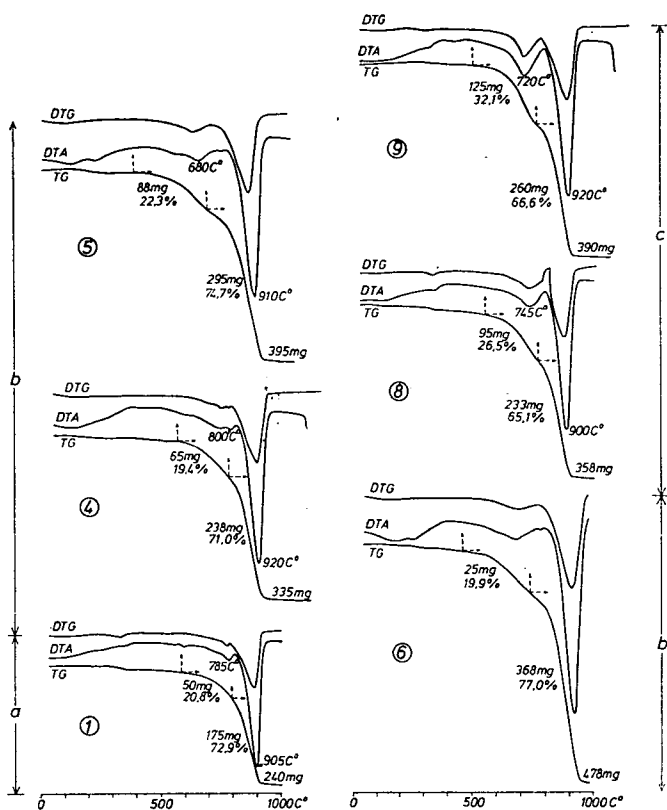


Fig. 3. Derivatographic records of the members a—c of the studied profiles. — DTG=derived thermogravimetric change; DTA=differential thermal analysis; TG=thermogravimetric change. Sensibility: DTG 1/10, DTA 1/10, TG 500 mg, duration: 100 min.; heating speed  $10^\circ/\text{min}$ . Number of samples is the same as in Table 1.

Perpendicularly of the "stratification" thin section and scanning electron microscopic pictures were made from the typical samples. In order to distinguish between calcite and dolomite the thin sections were coloured by Na-alisarine-sulfonate. Evaluating the results by strata members the following could be stated:

According to the evaluation of FOLK's texture elements the thin section of the member a contains micrite of 64.1% [FOLK, R. L., 1959] (Fig. 5., sample No. 1). According to colouring the major part of micrite is limy material. Dolomite spots occur only in size below 1 mm. The quantity of the detrital eolian quartz and feldspar grains is considerable, i. e. 23% (Plate I/1). In the sample there are in several percent lime grains and unfilled pores.

The matrix fills the interparticle space. The proportion of detrital grains is so high that according to the DUNHAM's classification the rock is assigned to wackestone

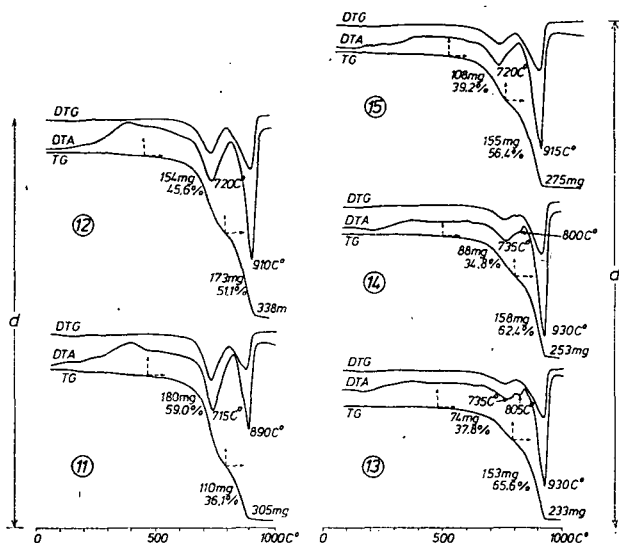


Fig. 4. Derivatograms of the member *d* of the investigated profiles. Recording conditions: see in Fig. 3. Numbers of samples are the same as in Table 1.

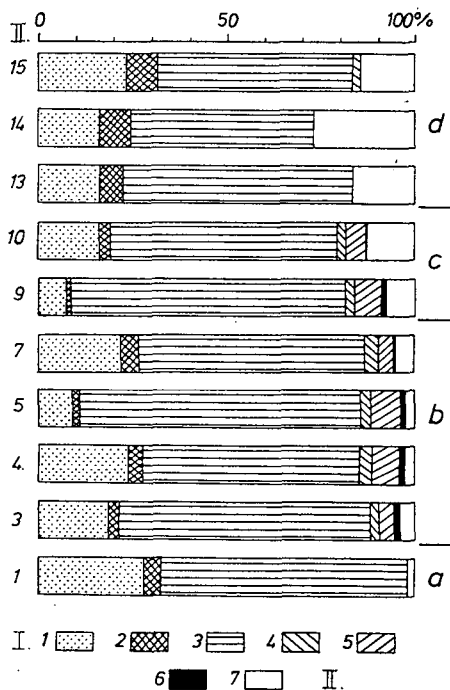


Fig. 5. Fabric constituents of thin sections determined by means of the FOLK-method.

I. 1 — quartz and other detrital grains; 2 — carbonatic detrital grains; 3 — micrite; 4 — microsparite; 5 — sparite; 6 — bioclastics; 7 — unfilled pores.

II. 1—10 — No. of thin section (the same as in Table 1); a—d: indication of the individual members.

category and shows the so-called mud-supported deposition structure ([DUNHAM, R. J., 1962].

In most cases the proportion of the detrital grains is higher than that of the evaluated samples. The distribution of the matrix and grains is unequal and very changing. E. g. the ferriferous precipitations contain less grains than their environment (Plate I/2). Thus, in case of these samples the measurements could not be carried out since within the sample areally very different results could be obtained. The more granular parts reach already the grain supported fabric structure of DUNHAM.

According to the scanning electron microscopic records the micrite consists of anhedral crystals (Table I/5). Most of the pores is of plant of interparticle origin [CHOQUETTE, PH. W., PRAY, L. C., 1970] (Plate I/1). The latter ones were generated in the manner that the carbonate precipitating from the solution did not fill a part of the interparticle space. The process of filling the pores has started. The filling material is always microsparite or sparite which based on the scanning electron microscopic pictures is a fibrous calcite elongated in the c-axis (Plate I/3—4).

If the member *a* contains fossils, this consists of mainly morphologically unbroken shells being filled by ferriferous micrite.

The member *b* shows fabric development being much more uniform than that of the member *a* (Plate I/6). The detrital grains show more uniform distribution. Out of the fabric elements the micrite varies between 57.6 and 74.4% (Fig. 5., samples No. 3—7). Based on colouring the matrix consists of calc- or dolomicrite but dolomitic calcimicrite also occurs. The quantity of detrital quartz and feldspar varies between 9.0 and 28.5%. This member contains also grains of detrital  $\text{CaCO}_3$ , pore-filling microsparite, sparite as well as bioclastics, all these amounting to several percent, and the pores are unfilled to some major extent than in case of member *a* (Plate I/6, Plate II/1—2). Dolomite euhedral also occur. According to the DUNHAM's classification the member *b* is assigned to the mud supported wackestones. On the basis of scanning electron microscopic records the micrite consists of anhedral crystals (Plate II/6).

The pores are very different considering both their shape and their origin. Numerous varieties occur. e. g. plant-generated pores consisting of different tubes or branching tubes being arranged irregularly and independent of the stratification, horizontal shrinkage pores nearly perpendicular of the stratification (Plate II/3), particle, interparticle as well as solution pores (Plate II/5). The picture of Plate II/2 shows the pore within the mollusc shell.

The filling of the pores is also different similarly to their shape and origin. All the varieties showing no filling up to total filling can be found (Plate II/2, and II/5, Plate III/1—2). Filling starts in general with microsparite and is continued by druse calcite of sparite size. The material of filling is concentrically precipitated at the walls of the pores (Plate II/4).

The pores within the mollusc shells were generated as follows: only a part of the original carbonate mud flowed into the shell, the other part remained empty. The mud within the shell could also shrink during micrite formation, thus the lower part of the shell is filled by dolomicrite in general, while in the upper the later diagenetic micro-calcisparite of calcisparite are found.

The shrinkage pores are of horizontal position and parallel with the pore's walls ferriferous precipitation can be observed. Similar pores and phenomena were described by FISCHER [1964] in the Alpine Triassic. The ferriferous precipitation has been regarded as a product of precipitation caused by the hydrometeorological differences between the summer and winter seasons. In our case the same can be

assumed with high probability. The solution pores were generated by the subsequent solutions.

Fossils occurring in member *b* consisting mainly also of gastropods, are unbroken or occur as fragments. The gastropod shells are found often in non-horizontal, i. e. in oblique or vertical position (Plate II/2). Rarely Charales oospores also occur.

The fabric of the member *c* is rather varied (Plate III/3—6; Plate IV/14). It consists of micrite of 60.0 to 73.0% (Fig. 5., samples 9 and 10). Based on colouring, in sample No. 9 the matrix is dolomicrite, in sample No. 10 calcimicrite and dolomitic calcimicrite. In sample No. 9 the detrital quartz and feldspar amounts not more than 7%, this is the least value obtained so far. In sample No. 10 their amount is only 16%. The quantity of detrital carbonate grains is several percent. As compared to those observed till now, the great percentage of pores is a considerable change, which is fairly demonstrated by the fabric pictures under microscope. The pore-filling microsparite, sparite and bioclastics show nearly the same quantity as earlier. The member *c* is assigned also to the mud supported wackestones.

Proved by the scanning electron microscopic pictures, the micrite consists of subhedral crystals (Plate IV/2).

Within the whole carbonate profile the pores are most varied here, in all aspects. Their macroscopic appearance has been dealt with MOLNÁR, B., [1979]. According to the microscopic analyses the following species of pores occur. The pores discussed earlier, i. e. the plant-originated (produced mainly by rhizoids), the shrinkage, gas and intra-shell pores are accompanied by a new variety. This is the so-called protected or shelter pore which is generated as follows: the carbonate mud cannot flow into the downward lying convex shell fragment, thus a shelter pore is generated (Plate III/4) [CHOQUETTE, PH. W., PRAY, L. C., 1970]. The gas pores within the member are quite beautiful. Based on numerous observations these show isomeric forms in the wet carbonate mud. In the course of drying, i. e. during lithification these are deformed and get the irregular shape (Plate III/6, Plate IV/1). In this member the interparticle pores are subordinate.

The filling of pores is also rather varied. All the kinds including the unfilled up to the totally filled pores can be found (Plates III/3, 4, 6; Plate IV/1, 3, 4). In the shrinkage pores lying parallel to each other it can be observed in the so-called sheet cracks that the incompletely consolidated carbonate mud flowed into the pore from the top. The material of filling is similar to that observed till now. In the unfilled part mostly druse calcite occurs (Plate IV/3, 4; Plate V/1). Along the walls of the shrinkage pores the ferriferous precipitations are also frequent.

Major part of fossils is represented by unbroken gastropod shells, but fragments also occur. The unbroken shells are of horizontal deposition. The frequent Charales oo-spores, however, are of different imbedding positions (Plate IV/1).

In the carbonate mud (member *d*) micrite varied between 48.8 and 60.1% (Fig. 5., samples No. 13—15). Under colouring it proved to be always dolomicrite. The detrital quartz and feldspar occurred between 16.0 and 23.5% with upward increasing values. As against the so far predominating grain size of 0.1 to 0.2 mm, the detrital grains of the carbonate mud are finer, i. e. mostly between 0.02 and 0.06 mm (Plate V/2, 3, 4). The percentages of the finer-grained detrital carbonates also increased and varied between 6.5 and 8.5%. As against the mainly eolian detrital carbonatic extraclasts, these grains are probably interclasts which in the course of total drying of lakes the wind took up from the incompletely consolidated bottom and redeposited again. According to the SEM photos the dolomicrite-matrix consists predominantly of euhedral crystals (Plate V/5).



The pore-filling microsparite and sparite are absent in this member. These occur only in minimal quantity in the soil zone as a result of soil formation. The quantity of the unfilled pores is highly increased. Especially high values are obtained (17.0—27.0%) below the soil horizon, and higher values can be found also in the soil part than in the deeper parts of the profile (*Fig. 5*, samples No. 13—15).

In the carbonate mud the shrinkage, plant and especially the gas pores predominate (Plate V/2, 3, 4, 6). It can be observed in the thin sections the pore formation and the formation of their shape, respectively, is in progress now, too.

Out of the fossils the Charales rhizoid is significant in addition to the gastropod shells mentioned earlier. This is probably due to the fact that the decomposition process did not eliminate them in the rock.

#### DIAGENETIC AND LITHIFICATION PROCESSES OF THE CARBONATES OF THE DANUBE-TISZA-INTERFLUVE

Before analyzing the diagenetic and lithification processes, let us study the demonstration of fabric elements in the FOLK's triangle diagram. According to FOLK when demonstrating the microcrystalline, allochemical and sparic calcite proportion of carbonate rocks, three basic carbonate types can be distinguished according to the individual ranges [FOLK, R. L., 1959]. To demonstrate the carbonate studied according to the original imagination, it was troublesome that the allochemical and terrigenous detrital grains could not be distinguished unambiguously. Further, the pore-filling microsparite and sparite are produced by diagenetic processes, as it will be discussed later.

Thus, the demonstration was modified, i. e. in the first point (I) the micrite, in the second (II) comprehensively the detrital quartz, feldspar, the intra- and extra-clastic grains as well as the bioclastics, while in the third point (III) the proportions of the pore-filling microcalcisparite and calcisparite, as well as that of the unfilled pores are demonstrated (*Fig. 6*).

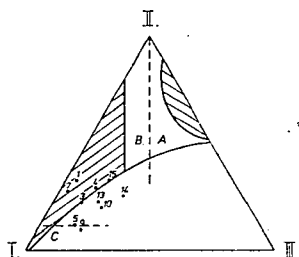


*Fig. 6.* Demonstration of the FOLK's fabric elements of carbonates of the Danube-Tisza-Interfluve in triangle diagram.

I. micrite; II. detrital grains, quartz, feldspar, other carbonatic grains and bioclastics; III. sparite and microsparite, pore-filling sparite and microsparite; unfilled pores; 1—15, No. of thin sections, numbers are the same as in Table 1.

Based on this figure, the carbonates of the Danube-Tisza-Interfluve are assigned to the group of microcrystalline allochemical and microcrystalline orthochemical carbonates. This means that in the course of deposition the energy of motion of the sedimentation medium was low while the precipitation was rapid [FOLK, R. L., LAND, L. S., 1975].

As it has been referred to in the introduction, due to the higher total salt content of the lakes and to the  $Mg^{++}/Ca^{++}$  ratio of 7 to 12 the carbonates of the Danube-Tisza-Interfluvium precipitate as high Mg-calcite and are transformed into dolomite in the early diagenesis [MOLNÁR, B., 1979].

The particular diagenetic and lithification processes of the different strata members can be evaluated as follows:

The loose sandy-lime dolomite containing ferriferous precipitations and the dolomitic limestone derive from the water infiltrating through the cover of higher carbonate content. This is proved also by the increased significance of the ferriferous precipitation here. The downward filtrating carbonatic solution filled the sand of the bottom, first of all the space among the sand particles. This caused the phenomenon that the quantity of the detrital matter is highest in this part, and the distribution of the detrital and carbonic matter is unequal. The dolomite occurring in higher horizons was transformed to certain extent during dissolution and downward filtration. The downward moving water might have high Mg-content after these processes, the concentrated salt quantity, however, was absent, thus in the sediments lime plays also an important role in addition to dolomite, consequently, in case of certain patches it can be called also dolomitic limestone.

The pore filling is always of  $CaCO_3$  content also here as well as in higher levels of the profile. When analyzing the average sample under laboratory conditions this is responsible for the fact that both the X-ray-diffractometric and the derivative curves indicate not pure dolomite. In the sample the primary dolomicrite and the secondary pore-filling microcalcisparite and calcisparite cannot be mechanically separated before the analyses. The separation could be performed only in thin sections by means of colouring with Na-alizarine sulfonate.

Based on the above facts it is obvious that in this member why the interparticle predominate over the gas pores.

The light-grey hard dolomite (member *b*) is an independent geological formation. The detrital grains got the dolomite as extraclasts in addition to the dolomicrite precipitating from the lake's water. The diagenetic pore-filling microcalcisparite and calcisparite play more important role than in the previous member. Thus, the X-ray diffractometric and derivative records do not show considerable difference as compared to the previous member though  $CaCO_3$  plays here much less important role. This is proved also by the fact that in the matrix fairly well-developed dolomite euhedral occur.

The attention should be called to two kinds of pores, i. e. the occurrence of shrinkage pores which from here downwards becomes common, and the exsolution pore which is generated by the dissolving effect of the subsequent solutions. Its formation is probably caused by the downward filtrating water which generated also the member *a*. The pores within the gastropod shells showing geopetal structure are also worthy of note.

The ferriferous precipitations occurring parallel with the walls of the shrinkage pores reflect the differences of hydrometeorology, occasionally of vegetation characterizing the different seasons. The matter of the ferriferous spots of the member *a* may derive from the dissolution of them.

In the course of deposition of the member *c*, i. e. for the "pechmeg" a sudden change followed as compared to the conditions before. This is also indicated by the bedding plane developed between the members *b* and *c*. In the "pechmeg" there is the greatest quantity of micrite matrix and the smallest proportion of the detrital grains. This fact as well as the cementation are responsible for the phenomenon that

this is the hardest member though the pores and especially the macroscopic pores show very high proportions. In the upper bedding plane of the "pechmeg" a lot of drying cracks can be observed [MOLNÁR, B., 1979]. The fossil shrinkage collapses are also frequent. Similar phenomenon can be observed in the recently drying lake bottom in the loose carbonate mud [MOLNÁR, B., KOPECZKY, A., 1979]. There is a great number of shrinkage and gas pores of microscopic size.

Consequently, the "pechmeg" accumulated very rapidly. Meanwhile the lakes were often dried. In the lake's life probably this period is most extreme concerning the climatic conditions. This is proved by the liquid carbonate mud intruding into the shrinkage pores or into those formed after drying.

A new and significant change followed in the course of deposition of the loose carbonate mud (member *d*) overlying the "pechmeg". As it was demonstrated, the proportion of pores is greatest in this member, and these pores are unfilled. Thus, the X-ray diffractometric and derivatographic records show the characteristic dolomite composition of the matrix and calcite seems to be subordinate.

While in members *a* and *b* the matrix was fairly well cemented and the rock was hardened during pore filling, here the rock remained loose just because of the lack of rock saturation accompanying the pore-filling cementation. Thus, in the members *a* and *b* the lithification is in a progressed state. In these members the diagenesis, in the carbonate mud the lithification can be observed. In the carbonate mud only shrinking and drying took place, as well as compaction proceeded.

This gradual lithification is demonstrated also by the fact that the Charales did not decompose here and is rather frequent, while in the deeper members it is rather rare. The change of the shape of gas pores shows the same process. These are more or less isometric when the lakes are drying and the carbonate mud is wet; later parallel with drying and carbonate mud compaction, their shape becomes irregular. Disturbing the bottom mud of sodaic lakes of the Danube-Tisza-Interfluvium huge quantity of gas is released in form of bubbles. Shrinkage pores are developed also in this loose state.

The pores of the carbonates of the Danube-Tisza-Interfluvium are assigned to the fabric selective pores (except the shrinkage pore) being generated in the so-called eogenetic zone (classification according to CHOQUETTE—PRAY). Shrinkage pores may be fabric selective or not.

It is characteristic of the pores of the eogenetic zone that these are generated by processes starting from the surface or near-surface. According to their size the pores can be assigned to the micro- ( $<0.065$  mm), meso- (0.065—4.0 mm) and rarely to the mega-pores (4.0—32.0 mm) [CHOQUETTE, PH. W., PRAY, L. C., 1967].

According to the classification of diagenesis of FAIRBRIDGE [1967], the *dolomite muds* of the Danube-Tisza-Interfluvium show *syndiagenetic processes*. According to BATHURST [1970], too, in this phase great quantities of water is released being bound with changing force between the particles, and this produces the shrinking and compaction of the sediment and the change of shape of the pores, first of all of gas pores.

*Dolomites* are in the starting phase of *anadiagenesis*. The main factor is the completion of their lithification. The liquid content of the sediment is considerably migrating, thus the former carbonate mud is saturated, then hardened and pore-filling is also started. As it has been stated, the latter consists of microcalcisparite or calcisparite as against the dolomicrite of the matrix and this is caused by the slower crystallization resulted in by the different i. e. lower  $Mg^{++}/Ca^{++}$  ratio of the pore waters [FOLK, R. L., LAND, L. S., 1975]. The smaller Mg/Ca ratio of the pore water and lower Mg-content may be produced by the consumption of  $Mg^{++}$  during the

early diagenetic dolomite formation. Magnesium is present in the pore water though in smaller quantities than before. This is proved by the fibrous and druse calcite crystals growing at the pore walls perpendicularly of it and being *elongated in their c-axis* [MOLNÁR, B., 1979].

In this state drying and shrinkage take place out of the diagenetic physical and cementation out of the physico-chemical processes of CHILINGAR *et al.* [1967].

Out of the diagenetic processes of FÜCHTBAUER, MILLIMAN and FOLK the constructive allochemical diagenesis predominates. This causes the early diagenetic transformation of the primary high Mg-calcite into dolomite [MÜLLER, G., IRION, G., FÖRSTER, U., 1972; FÜCHTBAUER, H., 1974; MILLIMAN, J. D., 1974; FOLK, R. L. 1974; MOLNÁR, B., 1979].

The lithification and diagenetic processes of carbonates of the Danube-Tisza-Interfluvium are in many aspects similar to those of the similar formations of Shark Bay (Western Australia) or of Coorong Lagoon, Southern-Australia [LOGAN, B. W. CEBULSKI, D. E., 1970; LOGAN, B. W., 1974; LOGAN, B. W. *et al.*, 1974; ALDERMAN, A. R., SKINNER, H. C. W., 1957; SKINNER, H. C. W., 1960; 1963; SKINNER, H. C. W., SKINNER, B. J., RUBIN, M., 1963] VON DER BORCH, C., 1965; Further, similarities can be concluded concerning the carbonate formations of the Persian Gulf and Bahama Islands [PRUDY, E. G., 1963 (SHINN, E. A., GINSBURG, R. N., 1964; PURSER, B. H., (ed., 1973)].

Our investigations have been based on the concept that the present is a key to the geological past. The further aim is the practical use of the results, after the stable isotope determinations of  $C^{12}/^{13}$  and similar investigation of carbonate formations of other areas.

#### REFERENCES

- ALDERMAN, A. R., SKINNER, H. C. W. [1957]: Dolomite Sedimentation in the Southeast of South Australia. *Am. Journ. Sci.*, **255**, pp. 561—567.
- ÁDÁM, L. [1978]: Géographie du paysage de la région de collines de Tolna. *Földr. Ért.*, **27**, 3—4, pp. 313—355.
- ÁDÁM, L., MAROSI, S., SZILÁRD, J. [1959]: *Physische Geographie des Mezőföld.* — Akadémiai Kiadó, Budapest, p. 361.
- BATHURST, R. G. C. [1970]: Problems of Lithification in Carbonate Rocks. *Proc. Geol. As. Leeds*, **81**, 3, pp. 429—440.
- BATHURST, R. G. C. [1971]: Carbonate Sediments and Their Diagenesis. *Dev. Sediments* 12, Elsevier, Amsterdam, p. 620.
- BERG, L. G. [1943]: Influence of Salt on Dissociation of Dolomite. *Dokl. Akad. Nauk., SSSR*, **38**, pp. 24—27.
- BRICNER, O. P. (ed.) [1971]: Carbonate Cements. *John Hopkins Univ. Stud. Geol.*, **19**, Baltimore, London, p. 376.
- BORCH, C. VON DER [1965]: The Distribution and Preliminary Geochemistry of Modern Carbonate Sediments of the Coorong Area, South Australia. *Geochim. Cosmochim. Acta* **29**, pp. 781—799.
- CHILINGAR, G. V., BISELL, H. J., WOLF, K. H. [1967]: Diagenesis of Carbonate Rocks. *In: LARSEN, G., CHILINGAR, G. V. [1967]: Diagenesis in Sediments.* pp. 179—332. Amsterdam.
- CHOQUETTE, PH. W., PRAY, L. C. [1970]: Geologic Nomenclature and Classification of Porosity in Sedimentary Carbonates. *Am. Ass. Petr. Geol. Bull.*, **54**, pp. 207—250.
- DUNHAM, R. J. [1962]: Classification of Carbonate Rocks according to Depositional Texture. *In: HAM, W. E. (ed.): Classification of Carbonate Rocks.* *Am. Ass. Petr. Geol., Mem.* **1**, pp. 108—121.
- FAIRBRIDGE, W. R. [1967]: Phases of Diagenesis and Authigenesis. *In: LARSEN, G., CHILINGAR, G. V. [1967]: Diagenesis in Sediments.* Amsterdam pp. 19—90.
- FORGÓ, L., MOLDAVAY, L., STEFANOVITS, P., WEIN, GY. [1966]: Magyarászó Magyarország 200 000-es földtani térképsorozatához L-34 XIII. Pécs. (Legend to the Geological Map Series of Hungary of 1:200 000 Scale). MÁFI Budapest, p. 196.

- FISCHER, A. G. [1964]: The Lofer Cyclothems of the Alpine Triassic. Symposium on Cyclic Sedimentation. Kansas Geol. Surv. Bull., 169, 1. pp. 107—149.
- FOLK, R. L. [1959]: Practical Petrographic Classification of Limestones. Am. Ass. Petr. Geol. Bull., 43, 1, pp. 1—38.
- FOLK, R. L. [1959]: Petrology of Sedimentary Rocks. Hemphill's Austin. p. 154.
- FOLK, R. L. [1965]: Some Aspects of Recrystallization in Ancient Limestones. In: Dolomitization and Limestone Diagenesis, A Symposium (Ed. PRAY, L. C. and MURRAY, R. C.). Spec. Publ. Soc. Econ. Paleont. Miner., 13, pp. 14—48.
- FOLK, R. L. [1974]: The Natural History of Recrystalline Calcium Carbonate: Effect of Magnesium Content and Salinity. Journ. Sed. Petr., 44, 1, pp. 40—53.
- FOLK, R. L., LAND, L. S. [1975]: Mg/Ca Ratio and Salinity: Two Controls over Crystallization of Dolomite. — Am. Ass. Petr. Geol. Bull., 59, 1, pp. 60—68.
- FÖLDVÁRI, M. [1974]: Thermal and IR analysis of carbonates — Formation, analysis and economic significance of carbonate rocks. Lectures at Veszprém (8—12th April, 1974) organized by the Youth Committee of the Hungarian Geological Society; pp. 259—275.
- FÖLDVÁRI-VOGL, M. [1958]: The role of differential thermal analysis in mineralogy and geological raw material prospect. Műszaki Könyvkiadó, Budapest, p. 90.
- FRIEDMAN, G. M. [1964]: Early Diagenesis and Lithification in Carbonate Sediments. Journ. Sed. Petr., 34, 4, pp. 777—813.
- FRIEDMAN, G. M. [1975]: The Making and Unmaking of Limestones or the Down and Ups of Porosity. Journ. Sed. Petr., 45, pp. 379—398.
- FÜCHTBAUER, H. [1974]: Sediments and Sedimentary Rocks I. In: ENGELHARDT, W. V., FÜCHTBAUER, H., MÜLLER, G.: Sedimentary Petrology, part II. — p. 464. Schweizerbart Verlag, Stuttgart.
- FÜCHTBAUER, H., GOLDSCHMIDT, H. [1965]: Beziehungen zwischen Calciumgehalt und Bildungsbedingungen der Dolomite. Geol. Rundschau 55, pp. 29—40.
- LOGAN, B. W. [1974]: Inventory of Diagenesis in Holocene—Recent Carbonate Sediments, Shark Bay, Western Australia. Am. Ass. Petr. Geol. Mem., 22, pp. 195—249.
- LOGAN, B. W. *et al.* [1974]: Evolution and Diagenesis of Quaternary Carbonate Sequences, Shark Bay, Western Australia. Am. Ass. Petr. Geol., p. 358.
- LOGAN, B. W., CEBULSKI, D. E. [1970]: Sedimentary Environments of Shark Bay, Western Australia. In: Carbonate Sedimentation and Environments, Shark Bay Western Australia. Am. Ass. Petr. Geol. Mem., 13, pp. 1—37.
- MILLIMAN, J. D. [1974]: Marine Carbonates Recent Sedimentary Carbonates, Part 1. p. 375. Springer Verlag, Berlin, Heidelberg, New York.
- MISIK, M. [1972]: Lithologische und fazielle Analyse der mittleren Trias der Kerngebirge der Westkarpaten. Acta Geol. Geograph., Univ. Comenianae, Geol., 22, pp. 5—154.
- MOLNÁR, B. [1979]: Hypersaline lacustrine dolomite formation in the Danube-Tisza-Interfluve. Földt. Közl., (in print).
- MOLNÁR, B., M. MURVAI, I. [1975]: Geohistorical Evolution and Dolomite Sedimentation of the Natron Lakes of Fülöpháza, Kiskunság National Park, Hungary. Acta Miner.-Petr., Szeged, 22, 1, pp. 73—86.
- MOLNÁR, B., M. MURVAI, I. [1976]: Building und geologische Geschichte der Sodaseen Fülöpháza im Kiskunság Nationalpark. Hidrol. Közl., 56, 2, pp. 67—77.
- MOLNÁR, B., KOPECZKY, A. [1979]: Sedimentological investigation of Recent lacustrine hypersaline dolomite profiles in the Great Plain. Acta Geol. Acad. Sci. Hung., (in print).
- MOLNÁR, B., M. MURVAI, I., HEGYI-PAKÓ, J. [1976]: Recent Lacustrine Dolomite Formation in the Great Hungarian Plain. Acta Geol. Acad. Sci. Hung., 20, 3—4. pp. 179—198.
- MUCSI, M. [1963]: Examen de la stratigraphie fine des formations carbonatées d'eau douce du Kiskunság (Hongrie centrale). Földt. Közl., 93, 3, pp. 373—386.
- MÜLLER, G. [1969]: Sedimentbildung in Plattensee (Ungarn). Naturwissenschaften 56, 12, pp. 606—615.
- MÜLLER, G. [1970]: High-magnesian calcite and protodolomite in Lake Balaton (Hungary) sediments. Nature 226, pp. 749—750.
- MÜLLER, G., IRION, G., FÖRSTER, U. [1972]: Formation and Diagenesis of Inorganic Ca-Mg Carbonates in the Lacustrine Environment. Naturwissenschaften 59, 4, pp. 158—164.
- MÜLLER, G., WAGNER, F. [1978]: Holocene Carbonate Evolution in Lake Balaton (Hungary): a Response to Climate and Impact of Man. In: Modern and Ancient Lake Sediments. Blackwell Sci. Publ., Oxford, London, Edinburgh, Melbourne, pp. 57—81.
- PRUDY, E. G. [1963]: Recent Calcium Carbonate Facies of the Great Bahama Bank. Journ. Geol., 71, pp. 334—355; 472—497.
- PRUDY, E. G. [1968]: Carbonate Diagenesis: an Environmental Survey. Geol. Romana 7, pp. 183—228.

- PURSER, B. H. (ed.) [1973]: The Persian Gulf: Holocene Carbonate Sedimentation and Diagenesis in a Shallow Epicontinental Sea. Springer Verlag, New York, p. 471.
- SHINN, E. A., GINSBURG, R. N. [1964]: Formation of Recent Dolomite in Florida and the Bahamas (abs.) — *Am. Ass. Petr. Geol. Bull.*, **48**, p. 547.
- SKINNER, H. C. W. [1960]: Formation of Modern Dolomite Sediments in South Australia's Lagoons. — *Bull. Geol. Soc. Am.*, **71**, p. 1976.
- SKINNER, H. C. W. [1963]: Precipitation of Calcium Dolomites and Magnesian Calcites in the Southeast of South Australia. *Am. Journ. Sci.*, **261**, pp. 449—457.
- SKINNER, H. C. W., SKINNER, B. J., RUBIN, M. [1963]: Age and Accumulation of Dolomite bearing Carbonate Sediments in South Australia. *Sci.*, **139**, pp. 335—336.
- SZENTES, F. [1968]: Magyarász Magyarország 200 000-es földtani térképsorozatához L—34. I. Tatabánya. (Legend to the Geological Map Series of Hungary of 1:200 000 Scale). MÁFI, Budapest, p. 158.

*Manuscript received, July 28, 1979.*

DR. BÉLA MOLNÁR  
DR. MIKLÓS SZÓKOKY  
József Attila University  
Department of Geology  
and Paleontology  
DR. SÁNDOR KOVÁCS  
H—6701 Szeged, Pf. 428  
Hungarian State Geological  
Institute  
H-1143 Budapest  
Népszabadság út 14.  
Hungary

## EXPLANATION OF PLATES

### PLATE I

Microscopic and SEM photos of the sandy dolomite and dolomitic limestone (member *a*, photos 1—5), and of the light-grey hard dolomite (member *b*, photo 6.) of looser structure, containing hypersaline lacustrine ferriferous precipitations (Danube-Tisza-Interfluve).

(Photos were made from thin sections and preparates perpendicular of "stratification").

1. Kömpöc-N, 82—102 cm. Biogenic pores in dolomicrite matrix between quartz grains, partly filled by calcisparite. 1 N, M=50 x.
2. Same location: iron spot in which the proportion of detrital grains is less than in the environment 1 N, M=10 x.
3. Same location: SEM-photo of a broken surface. Left: pore-filling fibrous calcite; Middle: matrix Right: part of a quartz grain. M=1000 x.
4. Same location: SEM picture of sparite and fibrous calcite pore filling between detrital grains, on etched surface. M=540 x.
5. Same location: SEM picture of calcimicrite matrix consisting of anhedral crystals, in broken surface. M=6000 x.
6. Csölyospálos-S. Fabric of the bottom of light-grey hard dolomite bank. Cross-section of partly filled biogenic pores in dolomicrite matrix and gastropod shell fragments. 1 N, M=10 x.

### PLATE II.

Microscopic and SEM photos of the hypersaline lacustrine light-grey hard dolomite (member *b*) of the Danube-Tisza-Interfluve.

1. Kömpöc-N. 60—82 cm. Partly filled biogenic pores and detrital quartz grains in dolomicrite matrix. 1 N, M=100 x.
2. Same location: unfilled and smaller completely filled biogenic pores as well as gastropod shell cross-section showing geopetal structure. 1 N, M=20 x.
3. Kömpöc-N 45—60 cm. Partly biogenic partly shrinkage (in the middle horizontally lying) pores. Parallel with the walls of shrinkage pores ferriferous accumulation occurs. 1 N, M=20 x.
4. Csölyospálos-S. Upper part of the dolomite bank (sample *c*). Interparticle pore between detrital grains originally unfilled by micrite, at the walls subsequent fibrous calcite filling has started. Smaller pores are completely filled by microsparite and sparite. 1 N, M=100 x.

5. Csólyospálos-S. Lower part of the dolomite bank (sample *a*). Exsolution (?) pore in dolomicrite matrix filled subsequently by microsparite. 1 N, M=100 x.
6. Csólyospálos-S. Lower part of the dolomite bank. (sample *b*). SEM-photo of the fabric of matrix consisting of anhedral crystals in broken surface. M=1000 x.

#### PLATE III.

Microscopic and SEM photos on the hypersaline lacustrine light-grey dolomite (member *b*, photos 1—2) and on the dark-grey dolomite, i. e. on the so-called "pechmeg" (member *c*, photos 3—6) of the Danube-Tisza-Interfluve.

1. Csólyospálos-S. SEM picture of pores of different size on ground surface. M=200 x.
2. Same location: SEM picture of the pore lying in the middle of Photo 1, under greater magnification (720 x).
3. Kömpöc-N. 55—60 cm. Completely filled (top) and unfilled (bottom) shrinkage pores. 1 N, M=20 x.
4. Same location: So-called shelter pores partly filled by fibrous calcite (bottom), and partly filled shrinkage pores (top). 1 N, M=100 x.
5. Same location: Cross section of Charales oo-spore recrystallized. 1 N, M=100 x.
6. Csólyospálos-S. Gas pores, at the walls with the starting fibrous filling calcite generation. 1 N, M=100 x.

#### PLATE IV.

Microscopic and SEM photos on the hypersaline lacustrine dark-grey hard dolomite, i. e. "pechmeg" (member *c*) of the Danube-Tisza-Interfluve.

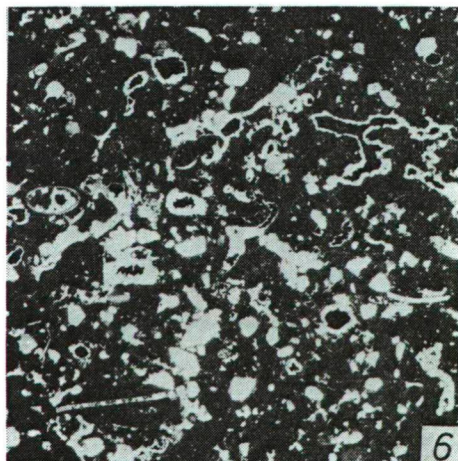
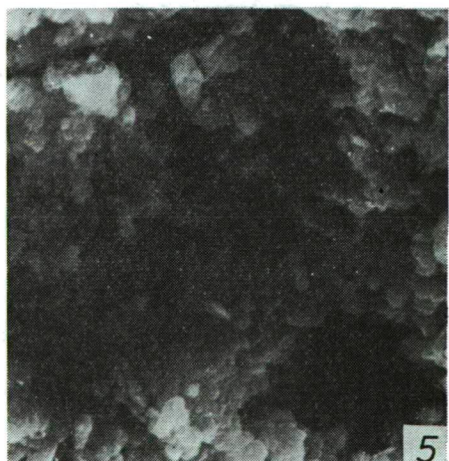
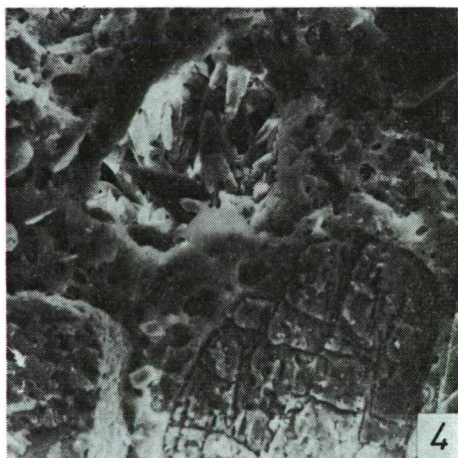
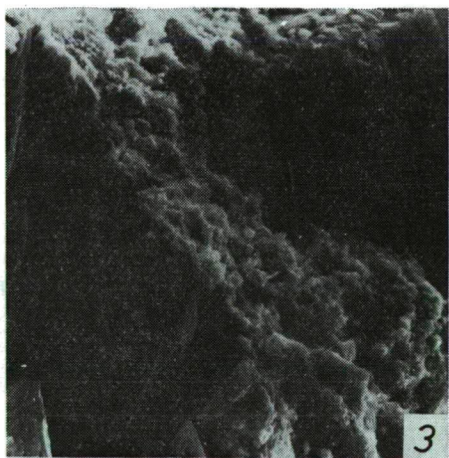
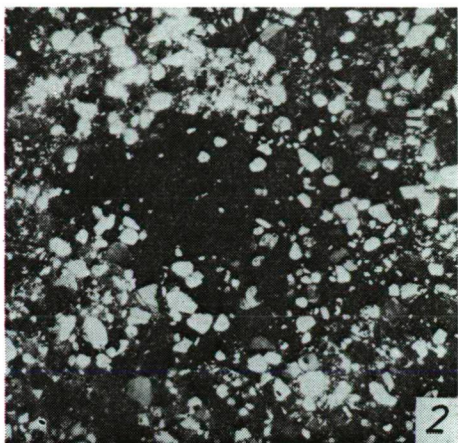
1. Kömpöc-N. Fabric of the fine-stratified hard dolomite. In the dolomicrite matrix perpendicularly of stratification horizontal shrinkage (SK), rounded biogenic (RP) and irregular gas (GA) pores with different filling. Horizontally imbedded gastropod shells (G) and Charales oo-spore cross sections (O). 1 N, M=9 x.
2. Same location: SEM picture of dolomicrite matrix consisting of subhedral crystals in etched surface. M=6000 x.
3. Same location: SEM picture of druse calcite filling in broken surface. M=360 x.
4. Same Location: SEM picture of shrinkage pore filled by druse calcite in etched surface. Around the pore filling quartz grains are shown. M=100 x.

#### PLATE V.

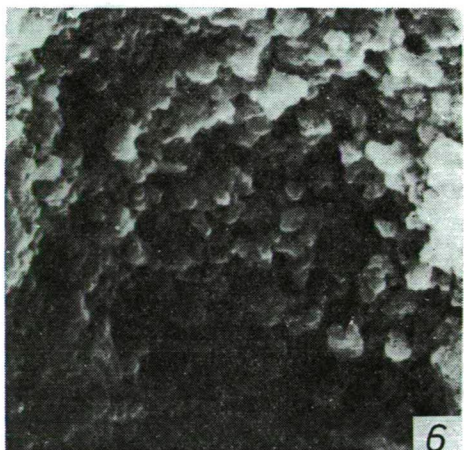
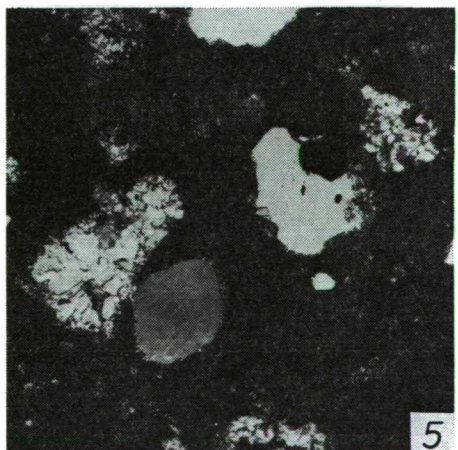
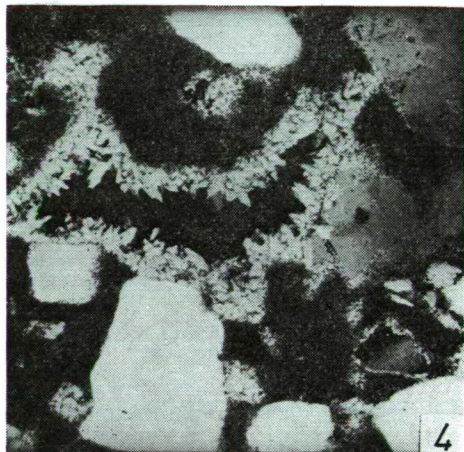
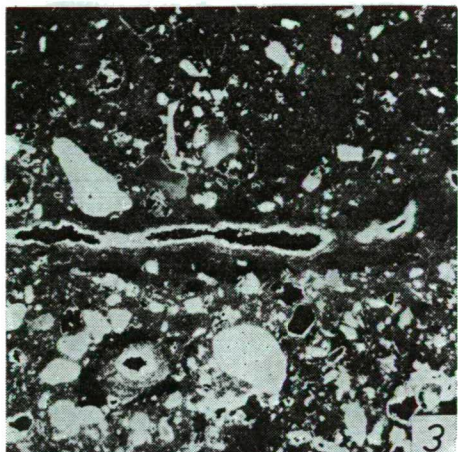
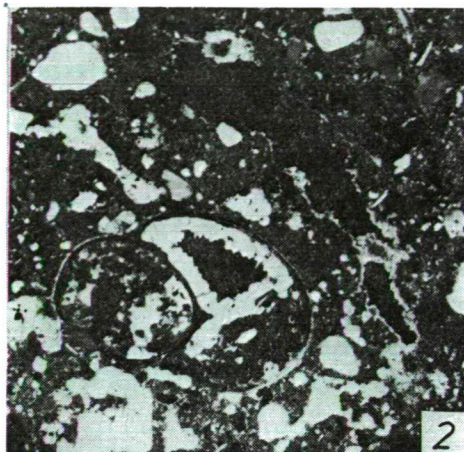
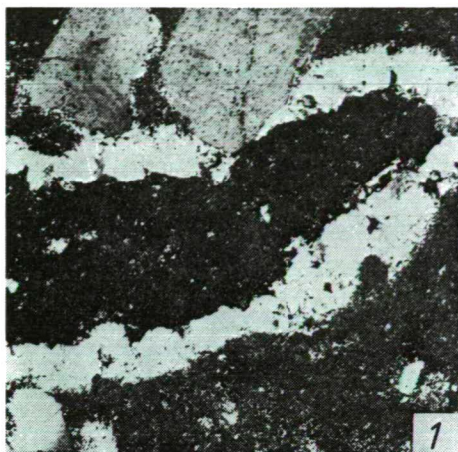
Microscopic and SEM pictures on the hypersaline lacustrine dark-grey hard dolomite, i. e. "pechmeg" (member *c*, photo 1) and on the light-grey dolomite mud (member *d*, photos 2—6) of the Danube-Tisza-Interfluve.

1. Kömpöc-N. SEM picture of completely filled (in the middle) and partly filled (top-right) pores in etched surface. Filling matter is druse calcite. M=100 x.
2. Csólyospálos-N. 25—50 cm, lowermost 5 cm. Irregular-shaped, gas-generated pores showing neither the beginning of filling. 1 N, M=20 x.
3. Csólyospálos-N. 25—50 cm, middle 5 cm. Great, unfilled biogenic pore. 1 N, M=20 x.
4. Csólyospálos-N. 25—50 cm, uppermost 5 cm. Great, irregular-shaped gas-generated pores; at the pore walls with very thin micrite coating as first indication of filling. 1 N, M=20 x.
5. Csólyospálos-S. SEM picture of pore wall generated by roots and rhizoids respectively, in broken surface. The matrix consists of euhedral dolomite crystals. M=6000 x.
6. Same location: SEM picture of absolutely unfilled biogenic pores in broken surface. M=48 x.

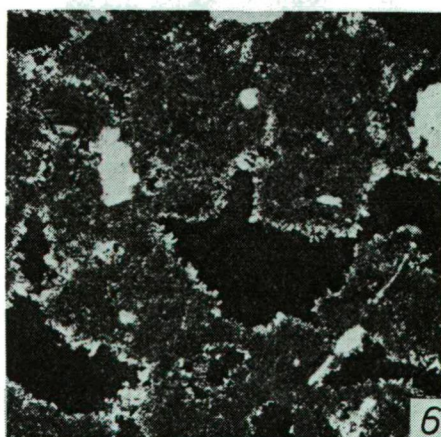
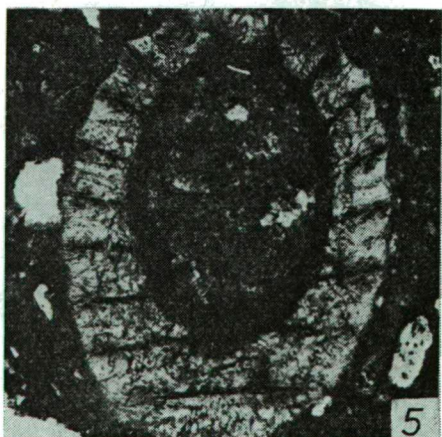
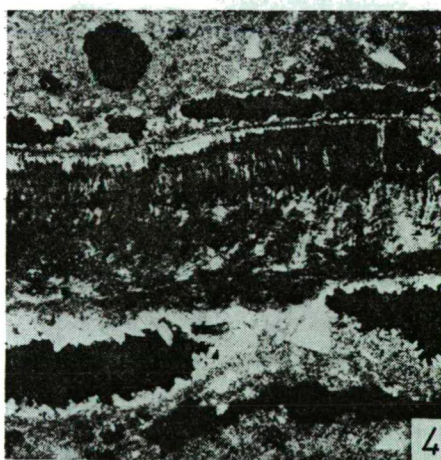
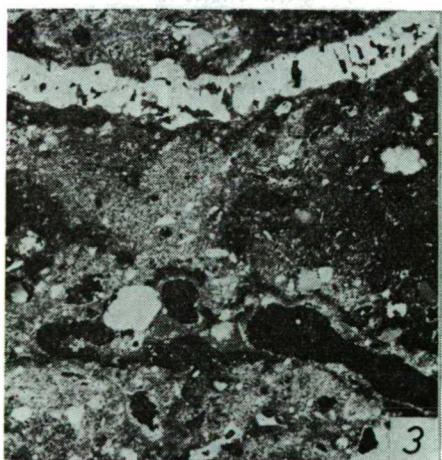
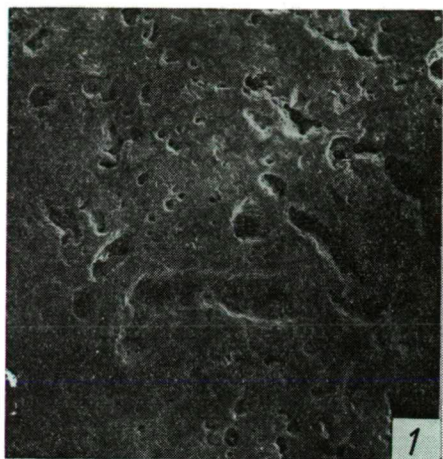




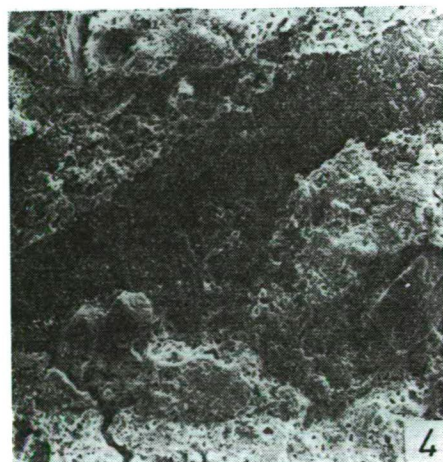
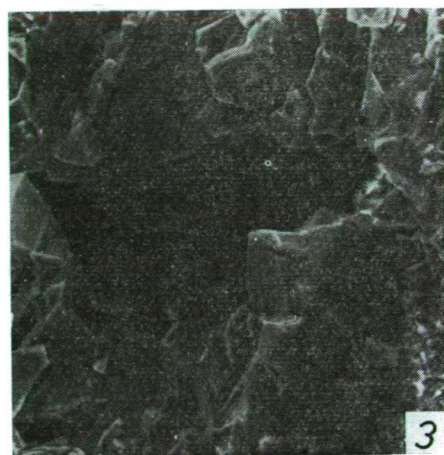
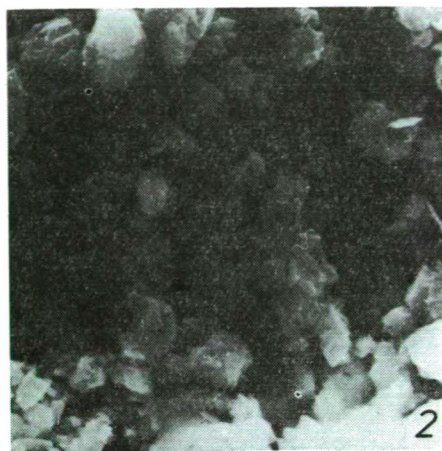
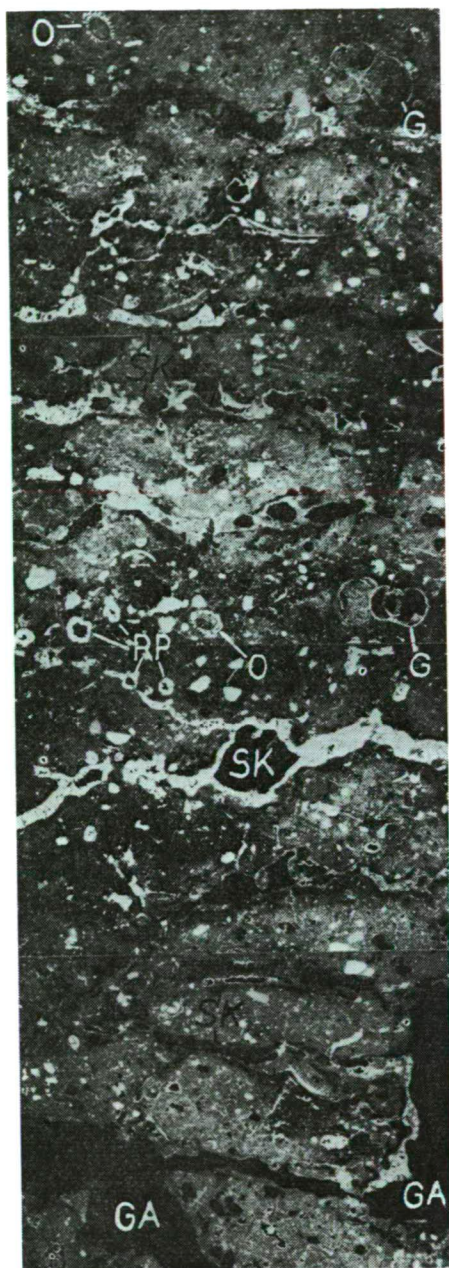




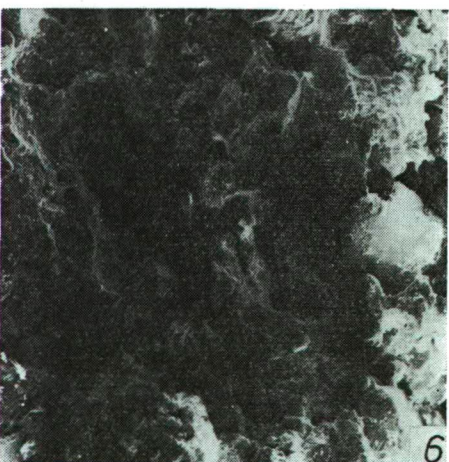
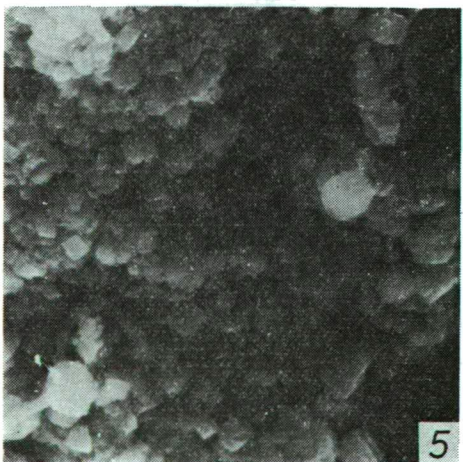
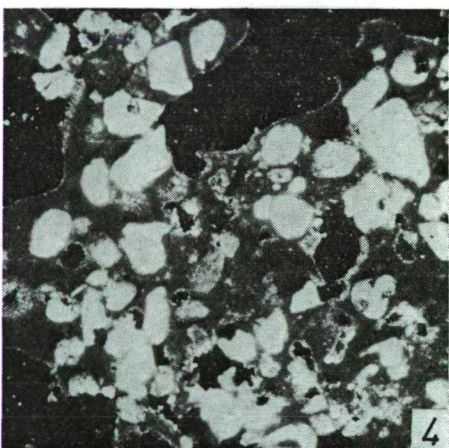
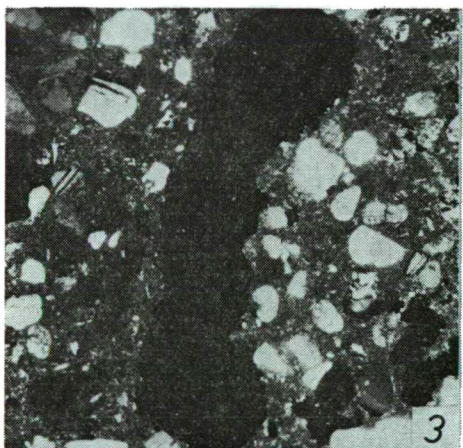
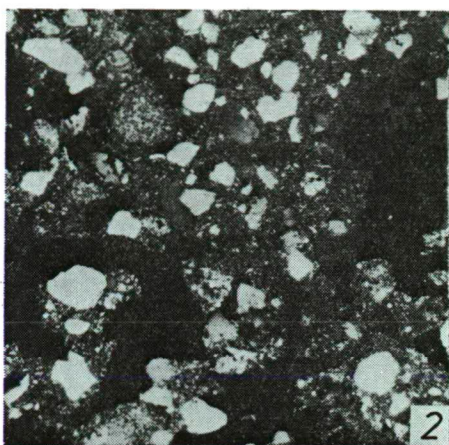
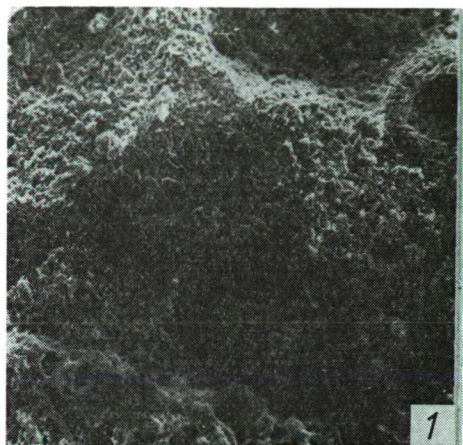














## CHANGES OF SOURCE AREAS AS REFLECTED BY THE DEPRESSION OF THE KÖRÖS RIVERS\*

B. MOLNÁR

### INTRODUCTION

Since the new phase of geological mapping in the Great Hungarian Plain, i. e. since 1964, boreholes of about 1200—1500 m depth were drilled by the Hungarian State Geological Institute, nearly parallel with the Tisza-bed in N-S direction, as well as in E-W direction also parallel with Körös River, East of the Tisza. These boreholes discovered the major of Pliocene formations in the Great Plain, and the complete section of the Quaternary formations.

The boreholes aimed to provide the more particular knowledge of the geological and hydrogeological features of the subsidence-filling sediments, already after the sedimentological, paleontological as well as paleomagnetic investigations carried out in the last years.

In the eastern part of the W-E profile a new borehole was drilled in 1976—77 down to the depth of 1137 m, i. e. the borehole Dv..No. 1 at Dévaványa-Kéthalom.

This village is situated some km North of Dévaványa. The point of borehole lies North of the Recent Hármaskörös. The Rivers Fehér Körös, Fekete Körös, Sebes Körös and Berettyó join each other east of the point, thus the borehole was situated in the axis of the alluvial fan of the Körös discovering its sedimentary sequence (*Fig. 1*).

The sedimentological, paleontological and paleomagnetic investigations of the borehole profile of Dévaványa showed that the Late Pliocene and Quaternary formations were penetrated [FRANYÓ, F., 1977; RÓNAI, A., 1978, 1979; RÓNAI, A., SZEMETHY, A., 1979]. In Hungary the Pliocene formations are divided into two major units, i. e. the Upper and Lower Pannonian. Each of them are usually subdivided into three members [JÁMBOR, Á., KÖRPÁS—HÓDI, M., 1971; BARTHA, F., 1975]. Accordingly, the Dévaványa profile discovered the upper part of the Upper Pannonian sequence.

On the basis of paleontological and paleomagnetic investigations, in the profile, the Pliocene-Pleistocene boundary denoting approximately 2.4 million years, lies in a depth of 420 m. Starting from the rate of deposition within the Pleistocene, the GAUSS—GILBERT-boundary (i. e. 3.4 million years) lies in 620 m, while the 5 million years in about 920 m, as to the preliminary estimations [RÓNAI, A., SZEMETHY, A., 1979]. This, however, contradicts to the new concept, i. e. the lower boundary of the Pliocene can be marked at 5 million years.

Within the Pleistocene the Olduvai begins in 320 m (1.8 million years), while the BRUNHE—MATUYAMA-boundary lies in 120 m (0.7 million years) [RÓNAI, A., SZEMETHY, A., 1979; RÓNAI, A., COOKE, H. B. S., HALL, J. M., 1979]. In the profile

freshwater lacustrine formations are found between 490 and 1137 m, while between 490 m and the surface fluvial sediments can be observed [FRANYÓ, F., 1977].

Out of the many-sided investigations governed and sponsored by the Hungarian State Geological Institute, in this paper, the results of micromineralogical analyses will be dealt with. These analyses aimed to mark the boundaries between major changes within the sequence, i. e. to dissect the sequence also in this manner. Further, the characteristics of the source areas had to be determined, as well as having micro-mineralogically characterized the whole profile to search for connections with the known formations of the surrounding areas.

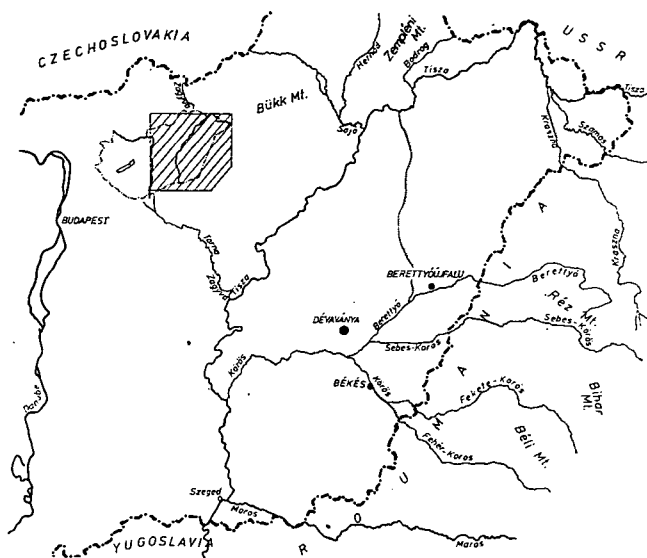


Fig. 1. Location of the borehole.

It is well-known from the previous investigations carried out in the Great Plain that the change in the grain size distribution highly affects the composition of heavy minerals. Even in case of the same source area considerable differences are found in the mineral composition of the coarser and finer-grained sediments [MOLNÁR, B., 1969]. E. g. in coarser-grained sediments the quantity of magnetite-ilmenite and garnet, in the finer-grained ones that of chlorite and micas are considerably increased.

Thus, in favour of realistic conclusions, the analysis of grain-size distribution of the chosen samples was also carried out (Figs 2—3, II). The strata which contained the required fraction of 0.1—0.2 mm only in small percentage were not investigated from the heavy-mineral point of view. In each sample 300 grains were investigated and this was the basis to the percentual determination of the different mineral grains. Under certain critical review the results proved to be comparable and provided the possibility for the realistic evaluation.

After the grain-size distribution analyses the sand samples of the Dévaványa profile were divided into fractions, then the minerals of the fraction of 0.1—0.2 mm were separated into groups of minerals of lighter and heavier than 2.8 by means of the traditional bromoform method.

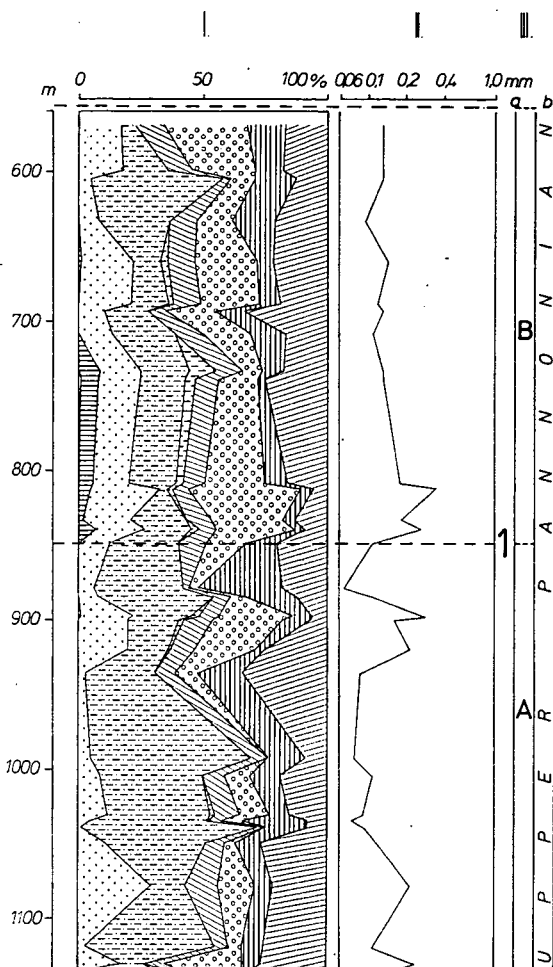


Fig. 2. Heavy mineral and grain-size distribution results of the section between 430 and 1135 m in the Dévaványa profile (Legend: see in Fig. 3).

The most important investigations results concerning the Dévaványa profile were demonstrated in a comprehensive profile (Figs. 2—3). When grouping the results according to the geological age the following statements can be mentioned.

#### RESULTS CONCERNING THE UPPER PANNONIAN FORMATIONS

The Upper Pannonian was discovered by the borehole between 420 and 1137.5 m, i. e. in a length of 713.5 m. According to FRANYÓ [1977] and to our grain-size distribution analyses, in this sequence of Dévaványa the sandy strata are frequent, this it is rather suitable to heavy mineral analyses. 42 samples were analyzed from this section of the profile. The predominating grain-size of the analyzed sand strata is between 0,065 and 0.36 mm, i. e. within a rather wide range.



On the basis of the heavy mineral composition three greater sections can be distinguished in the sequence (Fig. 2).

### Section 1

1/A. In the section between 847.57 and 1135.31 m i. e. of 287.0 m thickness the micromineralogical analysis of 17 sand strata was carried out. The grain size varies between 0.065 and 0.28 mm. The heavy mineral composition is characterized by simplicity, only a few mineral species occur. Regarding the quantities, the most important mineral is the chlorite showing 9 to 44 percent. Garnet and magnetite-ilmenite are also important but their quantities strongly fluctuate (Fig. 2.).

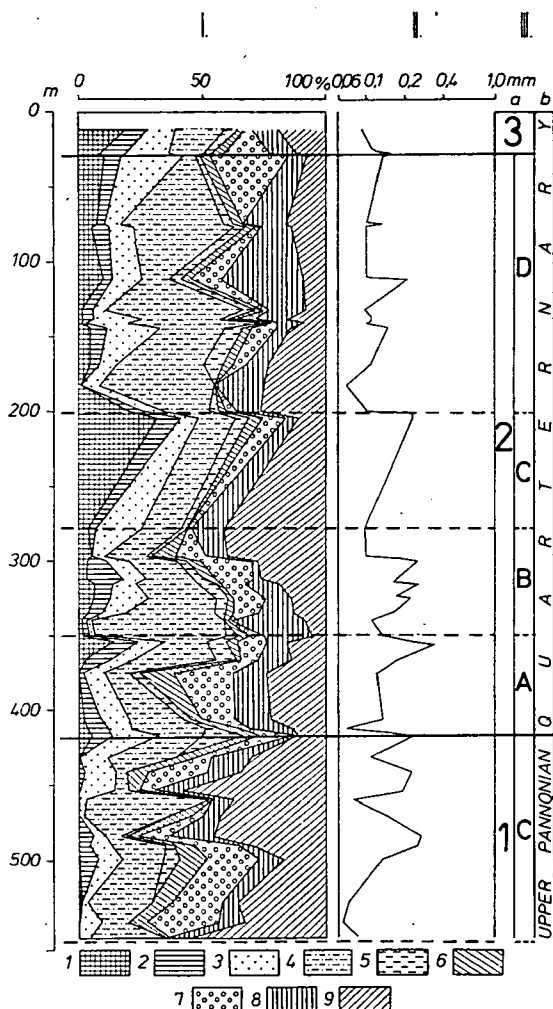


Fig. 3. Heavy mineral and grain-size distribution results of the section between 0 and 551 m in the Dévaványa profile.

Legend: 1=hypersthene and augite; 2=basaltic amphibole; 3=magnetite-ilmenite; 4=biotite and chlorite; 5=hornblende; 6=tourmaline; epidote, clinozoisite, rutile and actinolite-tremolite; 7=garnet; 8=other minerals, total; 9=weathered minerals.

It is worthy of mention that rutile is represented by relatively high, i. e. 0.4 to 6.4% values and the otherwise rarely occurring glaucophane; the latter occurred in the two deepest strata.

The pictures 1 and 2 of Plate I show the occurrence of the minerals in the sequence introduced above. In the pictures small number of mineral species is found. In photo No. 1. chlorite, garnet and weathered mineral predominate. In Photo No. 2 the carbonatic rock detritus can be seen deriving from 878—879 m. Within the whole profile this sample showed the highest carbonate mineral content, i. e. 23.4%.

1/B. 14 strata were analyzed from the 270 m long section between 568.34 and 839.00 m from the micromineralogical point of view. The predominating grain size of the samples varies between 0.095 and 0.36 mm. Omitting, however, the smallest value, this figure lies between 0.11 and 0.36 mm. Consequently, samples consist of the fine- and medium-grained sand being most suitable for heavy mineral analyses [MOLNÁR, B., 1970b].

When looking at *Fig. 2* the difference from the under- and overlying strata can be fairly well seen. The sequence is here more varied and more mineral species occur. In addition to the metamorphic minerals the igneous minerals become also important due to the higher frequency of the basaltic amphibole of igneous origin. As compared to the section 1/A magnetite is of greater importance and its quantities amount from 5 to 21.4%. Chlorite, however, is somewhat decreased but its quantity shows greater fluctuations between 2.8 and 52.5%. Rutile is also slightly decreased but belongs to the minerals the significance of which is increased. The assemblage consisting of tourmaline, epidote, clinozoisite, rutile and actinolite-tremolite shows somewhat higher percentages (*Fig. 2, 1/5*). The weathered minerals show more equilibrated values.

In photos No. 3 and 4 of Plate I the changes mentioned above can be fairly well observed. Several new minerals occur, e. g. the basaltic amphibole, the hornblende, the actinolite-tremolite, or the tourmaline. Of course, in the photo the minerals known from the previous sections also occur, e. g. garnet, chlorite and the weathered mineral.

1/C. Eleven strata were analyzed from the section of 121 m between 430.33 and 551.77 m. As it has been mentioned in the introduction, the lower lacustrine facies of the sequence below 490 m contains first of all fine sand, while upward, to the fluvial facies, mainly coarser, fine- and medium-grained sand. The lowest and highest values of the predominating grain-size are 0.065 and 0.26 mm, respectively (*Fig. 3, II*).

As compared to the underlying sequence the following changes can be observed in the heavy mineral composition. The percentage of magnetite-ilmenite decreases. In some strata apatite becomes unusually abundant, e. g. in the depth between 470.57 and 470.90 m it amounts to 5.8%. Biotite and chlorite play more and less significant role, respectively, the value of both of them changes rapidly. Titanite which occurred in the former samples not always but rather frequently, is practically absent here.

Garnet is abundant in the lower parts and topwards decreases gradually except one layer (440—441 m). Siderite occurs in this section first between 497 and 498 m.

The amount of weathered, incrustated minerals which cannot be determined by means of optical methods, suddenly increases. The differences in weathering caused by climatic effects may be responsible for this phenomenon. This sequence was deposited at the boundary of the warmer Pliocene and cooler Quaternary at which moment the climate change had decisive impact on many geological processes. The total absence of carbonate minerals is worthy of note which can be related also to the increased intensity of weathering of the changed character of weathering itself.

It can be seen, however, that during facies change, i. e. between the lacustrine and fluvial formations no change in mineral composition followed.

Photos 1 and 2 of Plate II shows fairly well most of the differences mentioned above. More weathered minerals occur. In photo No. 1 well-developed biotites can be seen.

## INVESTIGATION RESULTS OF THE QUATERNARY FORMATIONS

In the Quaternary formations the change in heavy mineral composition is more rapid than observed before. Thus, one sedimentary cycle is of smaller thickness. In the Great Plain the fluvial sedimentation becomes common after the Pliocene; in the environs of Dévaványa the sediment formation of four rivers may alternate in space and time on the alluvial fan of the River Körös. Thus, this rapid change seems to be possible.

Within the Quaternary formations two fairly well distinguishable sections can be identified on the basis of the changes in heavy mineral composition. Out of the two greater phases, the *lower* represents the Pleistocene and can be divided into four smaller sub-units. As to our opinion, the *upper* section can be identified with the Holocene formation. Each sedimentary sections can be characterized as follows.

### Section 2

2/A. Eight samples were analyzed from 64 m thick sequence between 352.67 and 416.80 m (*Fig. 3*). In *Fig. 3* the heavy mineral compositions are demonstrated comprehensively or in average due to dense sampling and in favour of better demonstration.

The predominating grain-size of the studied strata varies between 0.07 and 0.32 mm. In this depth interval, however, only fine- and medium-grained sands occur except the only fine-grained sand layer.

As compared to the underlying Pliocene sequence considerable change follows in the heavy mineral composition. Between 416.70 and 430.33 m a sharp boundary can be delineated which could be drawn so far, neither. Upward from this depth mineral composition is much more varied and much more species of minerals occur. The proportion of igneous minerals is increased. Hypersthene, augite, basaltic amphibole as well as the hornblende become much more important. This change does not suddenly follow. First, the igneous and metamorphic characters alternate, then the metamorphic character disappears. The minerals occurring in these sediments are also significant ingredients of the alluvium of the rivers flowing to the Great Plain from the east [MOLNÁR, B., 1964a, b]. The sediments were, thus, deposited by these rivers or by their ancestors.

Taking into account the occurrence and changes of the mineral species the following can be stated. Hypersthene was practically absent so far. Nevertheless, between 354 and 356 m its quantity exceeds 10%, though its amount shows fluctuations, e. g. between 374 and 375 m it is absent. The same can be said in case of augite. The basaltic amphibole, however, shows nearly the same quantities, i. e. between 5 and 10%, except one case. Chlorite is much as compared to the recent alluvia of the rivers getting the Great Plain from the east. Rutile was found in all strata. The hornblende shows more uniform values than in the preceding section of 1/C. The quantity of garnet is somewhat greater, while that of the weathered mineral is somewhat less. Siderite occurs with relatively high percentages between 365 and 366 m.

The changes shown above are demonstrated in the photos No. 3 and 4 of Plate II. Minerals unusual till now occur, e. g. hypersthene, or augite, and the basaltic amphibole is also more frequent.

2/B. Twelve samples were analyzed in the 72 m thick section between 278.15 and 350.98 m. The grain-size distribution of the sand samples is uniform. Nearly all the strata are fine-grained or similar grain-size sands.

It is characteristic of the heavy mineral composition of the sequence that somewhat less mineral species are found than in the section 2/C. First of all, the metamorphic minerals are lacking. E. g. the quantities of tourmaline, epidote, clinozoisite and kyanite decrease. Hypersthene is found though in smaller amounts than in the preceding section. The quantity of chlorite increases again. The upward increasing quantity of the weathering mineral is worthy of mention.

Minerals deriving from this section can be seen in Plate III. The corroded augites and hypersthene are frequent. In photo No. 3 spherical siderites can be seen.

2/C. Three strata were analyzed from the 5 m thick fine- and medium-grained sand between 200.35 and 205.70 m. Between the end of section 2/A and the beginning of section 2/C, i. e. between 205.70 and 278.15 m only strata finer than sands are deposited in a thickness of 75 m, so in this part no heavy mineral investigations could be carried out.

Being in possession of the regularities of cyclic built-up of the fluvial sedimentary sequences of the Great Plain, it can be stated that subsequently to this fine-grained section a new fluvial accumulation cycle is started at section 2/C which can be traced back to tectonic reasons [MIHÁLTZ, I., 1955; MOLNÁR, B., 1967, 1968, 1970a, b, 1973, 1975].

This change is also reflected by the change of the heavy mineral composition. Hypersthene and augite show considerable percentages though with rather fluctuating values (Fig. 3). Grain-size becomes coarser upwards and this is not accompanied by the expected accumulation of garnet, thus this phenomenon reflects difference in the source area. The quantity of chlorite is higher only in the uppermost fine-grained sand sample. When comparing this composition with that of the recent rivers reaching the Great Plain from the east, it can be stated that this sediment was deposited by the rivers Fekete and Fehér Körös [MOLNÁR, B., 1964a, b].

2/D. The results obtained from twelve samples in the 110 m thick section between 74.56 and 185.12 m showed that this section is the repetition of the sequence of 2/B between 278.15 and 350.98 m, in many respects. The difference is caused first of all by the greater amounts of biotite and smaller quantities of weathered minerals. The three significant igneous minerals, i. e. hypersthene, augite and basaltic amphibole shows here also similar fluctuating values. The metamorphic minerals are even less important, this is reflected e. g. by the smaller percentages of tourmaline.

The photos in Plate IV. illustrate the facts listed above. In photo No. 1 characteristic biotites are seen. Photo No. 2 shows the heavy minerals of the stratum between 112.0 and 112.6 m. In the picture several hypersthene, augite and mainly basaltic amphibole can be seen. Photo No. 3 proves the increased quantity of chlorite. In photo No. 4 the mineral assemblage is more varied again.

### Section 3

The heavy mineral analysis of 5 strata was carried out in the 17 m thick section between 12.10 and 29.41 m. Except the uppermost layer, all the strata show the predominating grain-size within the fine-grained sand, in rather uniform distribution, i. e. between 0.11 and 0.15 mm, without considerable fluctuations. The uppermost layer proved to be fine-grained sand.

The heavy mineral composition is characterized by uniform distribution. Hypersthene, augite and the basaltic amphibole play important role. Magnetite-ilmenite shows nearly the same quantity in all samples. As compared to section 2/C it is significant change that biotite and chlorite shows smaller while garnet greater quantities. When comparing this sequence with the alluvia of recent rivers it can be stated that it was deposited by the river Hármas-Körös. The heavy mineral composition is the same as in the alluvium of the Hármas-Körös [MOLNÁR, B., 1964a, b].

Photos in Plate V. show this variegated mineral assemblage showing small quantities of chlorite. Within the whole section the mechanical weathering and rounding of minerals can be observed only in one layer, between 25.45 and 26.16 m (Plate V, 2). In other sections chemical weathering effects, mainly corrosion are characteristic of the minerals.

The sediments of section 3 were deposited during the Holocene. The Pleistocene-Holocene boundary lies somewhere between 29.41 and 74.56 m, but rather closer to the shallow depths. The beginning of the recent Hármas-Körös sedimentation means a new accumulation cycle and this is accompanied by Holocene cutting and subsequent filling everywhere in the southern part of the Great Plain, e. g. in case of the river Tisza [MIHÁLTZ, I., 1967].

### CONCLUSIONS

On the basis of the micromineralogical analyses of the Dévaványa profile the following can be stated:

1. The heavy mineral composition of the upper part of Upper Pannonian and of the Quaternary formations differs from each other. The quantity of metamorphic minerals decreases downwards. In the Quaternary sequence hypersthene, augite and basaltic amphibole play more important role than in the underlying strata.

2. The change in the heavy mineral composition, i. e. the change of source area is less frequent in the Upper part of Upper Pannonian, and more frequent in the Quaternary. The thickness of the sedimentary section of the same composition amounts to 120—270 m in the Upper Pannonian and only to 5—110 m in the Quaternary.

3. On the basis of the heavy minerals composition the repetition of sequences can be observed in the Quaternary strata, this is provided by the fluvial facies deposited beside and above each other in space and time.

4. The most important change in the heavy mineral composition can be identified in 416.0 m. Above this boundary, i. e. in the Quaternary formations the sediments of the recent rivers or their ancestors can be found. This is proved first of all by the presence of three characteristic igneous minerals, i. e. hypersthene, augite and basaltic amphibole.

5. The alluvium of the recent Hármas-Körös can be identified upwards from 29.41 m.

6. The boundary determined in a depth of 416.0 m at Dévaványa corresponds fairly well to the thickness map contoured earlier for the sediments of the River Tisza and its tributaries. Starting from the Tisza-line the lower boundary of the sediments deposited by the recent Tisza and its tributaries becomes ever greater depths. In Berettyóújfalu-Békés profile lying east of Dévaványa this boundary is found in a depth of about 500 m.

7. The northern tributaries of the Tisza, the alluvia of which contains first of all hypersthene and augite and less basaltic amphibole, never reached the line of the Hármas Körös [Molnár, B., 1965, 1966a, b, 1968, 1970a, b].

## REFERENCES

- BARTHA F. [1975]: A magyarországi pannon képződmények horizontális és vertikális összefüggései és problematikája. (Horizontale und vertikale Verbindungen der Pannonablagerungen von Ungarn und ihre Problematik.) *Földt. Közl.*, **105**, 4, pp. 399—418.
- FRANYÓ, F. [1977]: Report on the works. on the geological and hydrogeological results of the prospecting bores of Dévaványa (1116, 670, 3, 222 and 31 m). MÁFI Ad., p. 65.
- MIHÁLTZ, I. [1955]: Erosionszyklen — Anhäufungszyklen. *Acta Miner. Petr.*, Szeged **8**, pp. 51—62.
- MIHÁLTZ I. [1967]: A Dél-Alföld felszínközeli rétegeinek földtana. (Geologie der oberflächennahen Schichten des südlichen Teiles der Grossen Ungarischen Tiefebene.) *Földt. Közl.*, **97**, 3, pp. 294—307.
- MOLNÁR B. [1959]: A statisztikus nehézasvány-vizsgálat hibalehetőségei. (Fehlermöglichkeiten der statistischen Schwermineral-Analyse.) *Földt. Közl.*, **89**, 3, pp. 294—297.
- MOLNÁR B. [1964a]: Magyarországi folyók homoküledékeinek nehézasvány-összetétel vizsgálata. (Untersuchung der Schwermineralien-zusammensetzung der Sandablagerungen der Flüsse Ungarns.) *Hidr. Közl.*, **44**, 8, pp. 347—355.
- MOLNÁR, B. [1964b]: On the relationship between the lithology of the abrasion area and the transported sediments. *Acta Miner.-Petr.*, Szeged, **16**, 2, pp. 69—88.
- MOLNÁR B. [1965]: Ősvízrajzi vizsgálatok a Dél-Tiszántúlon. (Urhydrographische Untersuchungen im südlichen Tiszántúl.) *Hidr. Közl.*, **45**, 9, pp. 397—404.
- MOLNÁR B. [1966a]: Pliocén és pleisztocén lehordási területváltozások az Alföldön. (Veränderungen der abtragungsgebiete auf der Grossen Ungarischen Tiefebene. während des Pliozäns und Pleistozäns.) — *Földt. Közl.*, **96**, 4, pp. 403—413.
- MOLNÁR B. [1966b]: Lehordási területek és irányok változásai a Dél-Tiszántúlon a pliocénben és a pleisztocénben. (Änderungen der Abtragungsgebiete und — Richtungen im Süd — Tiszántúl im Pliozän und Pleistozän.) *Hidr. Közl.*, **46**, 3, pp. 121—127.
- MOLNÁR B. [1967]: A Dél-Alföld pleisztocén feltöltődésének ritmusai és vízföldtani jelentőségük. (Rhythmen der Pleistozän-Auffüllung des südlichen Teils der Grossen Ungarischen Tiefebene und ihre hydrogeologische Bedeutung.) *Hidr. Közl.*, **47**, 12, pp. 537—552.
- MOLNÁR, B. [1968]: Sedimentationszyklen in den pleistozänen Ablagerungen des südlichen Ungarischen Beckens. *Geol. Rundschau* **57**, pp. 532—557.
- MOLNÁR B. [1969]: A szemcsenagyság és nehézasvány-összetétel összefüggései. (Zusammenhänge zwischen Korngrösse und Schwermineralienzusammensetzung.) *Földtani Kutatás* **12**, 2, pp. 8—17.
- MOLNÁR, B. [1970a]: Pliocene and Pleistocene Lithofacies of the Great Hungarian Plain. *Acta Geol. Acad. Sc. Hung.*, **14**, pp. 445—457.
- MOLNÁR, B. [1970b]: Relationship between Grain Size and Heavy Minerals Content. *Acta Miner.-Petr.*, Szeged, **19**, 2, pp. 159—171.
- MOLNÁR B. [1973]: Az Alföld harmadidőszak-végi és negyedkori feltöltődési ciklusai. (Latest Tertiary and Quaternary Sedimentary accumulation cycles of the Great Hungarian Plain.) *Földt. Közl.*, **103**, 3—4, pp. 294—310.
- MOLNÁR, B. [1975]: Über die Gesetzmässigkeiten der terrestrischen klastischen Sedimentation in der Ungarischen Tiefebene. *Zeitschr. Geol. Wiss.*, **9**, 10, pp. 1349—1367.
- RÓNAI, A. [1978]: Das Quartär des Grossen Ungarischen Tieflandes. In: *Exkursionsführer von Transdanubien anlässlich der DEUQUA-Tagung*. Budapest. 3—5, pp. 65—72.
- RÓNAI, A. [1979]: Stratigraphical Problems in Deep Boreholes in the Great Hungarian Plain. In: *Conference and Field-Workshop on the Stratigraphy of Loess and Alluvial Deposits*, Budapest—Szeged. Abstract of papers, pp. 42—45.
- RÓNAI, A., COOKE, H. B. S., HALL, J. M. [1979]: Sedimentary, Climatic and Paleomagnetic Record from the Dévaványa Borehole, Hungary. In: *Conference and Field-Workshop on the Stratigraphy of Loess and Alluvial Deposits*. Budapest—Szeged. Abstract of papers. pp. 45—47.
- RÓNAI, A., SZEMETHY, A. [1979]: Paleomagnetic Investigation of the 1110 M Sediment Core from the Dévaványa Scientific Exploration Borehole. In: *Guidebook for Conference and Field-Workshop on the Stratigraphy of Loess and Alluvial Deposits*, pp. 63—82. Budapest—Szeged.

*Manuscript received, July 20, 1980.*

DR. BÉLA MOLNÁR  
Attila József University  
Department of Geology  
and Paleontology  
H-6701 Szeged, Pf. 428.  
Hungary

## EXPLANATION OF PLATES

### PLATE I

Heavy minerals of sand samples of the Upper Pannonian of the Dévaványa profile (Section 1; A: Photos 1—2; B: Photos 3—4).

Photos were made by transmitted light microscope, with parallel nicols, minerals were imbedded in nitrobenzene of 1.552 refraction. In all pictures the heavy minerals of the fraction 0.1—0.2 mm are seen. — Abbreviations: *H*=hypersthene; *Au*=augite; *Di*=diopside; *BH*=Basaltic amphibole; *M*=magnetite-ilmenite; *B*=biotite; *Ch*=chlorite; *T*=tourmaline; *E*=epidote; *Cz*=clinozoisite; *Ho*=hornblende; *Ac—Tr*=actinolite-tremolite; *G*=garnet; *K*=kyanite; *C*=calcite-dolomite, or carbonatic detritus; *S*=siderite; *Wm*=weathered minerals.

1. 1132.67—1135.31 m
2. 878.91— 879.43 m
3. 838.27— 839.00 m
4. 732.64— 733.56 m

### PLATE II

Heavy minerals of the Upper Pannonian and Pleistocene samples of the Dévaványa profile (Section 1C: Photos 1—2; Section 2A: Photos 3—4).

1. 459.02—459.80 m
2. 440.60—441.18 m
3. 415.87—416.42 m
4. 352.67—358.85 m

### PLATE III

Heavy minerals of Pleistocene sand samples of the Dévaványa profile (Section 2B: Photos 1—4)

1. 325.45—325.90 m
2. 315.84—316.50 m
3. 324.25—315.34 m
4. 298.30—298.92 m

### PLATE IV

Heavy minerals of Pleistocene sand samples of the Dévaványa profile (Section 2D: Photos 1—4)

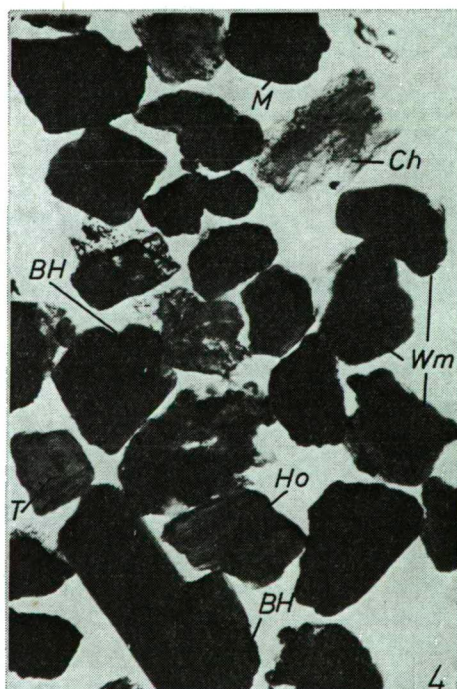
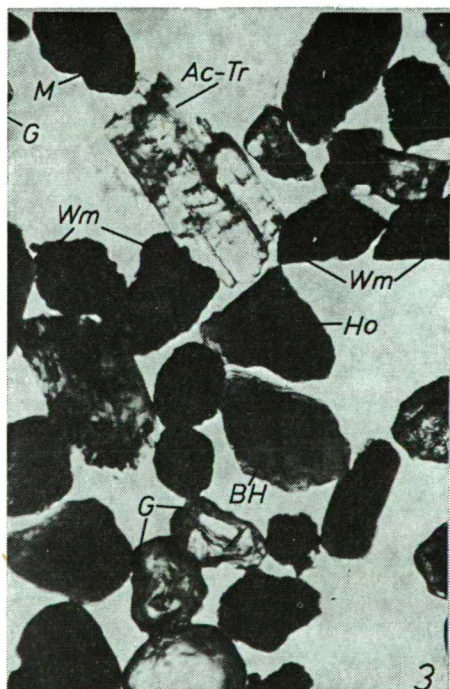
1. 168.55—169.66 m
2. 112.00—112.16 m
3. 111.76—111.85 m
4. 76.64— 77.00 m

### PLATE V

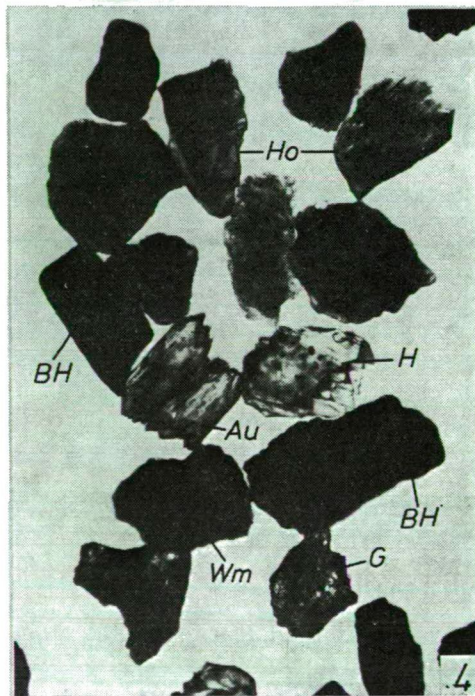
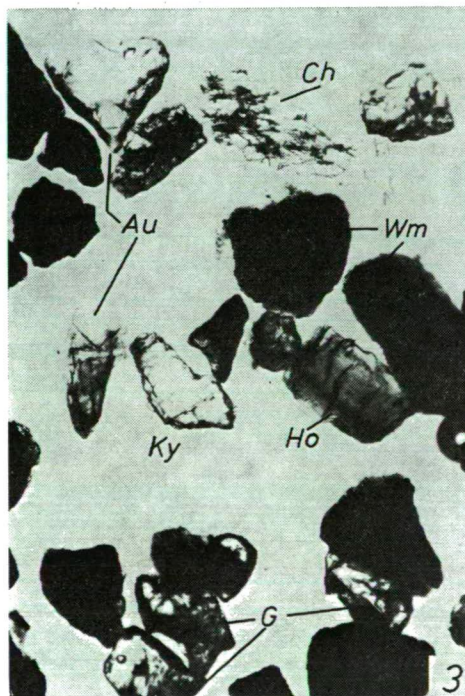
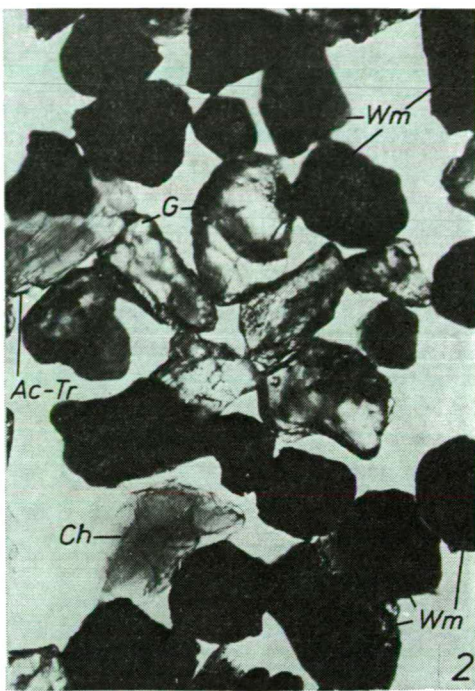
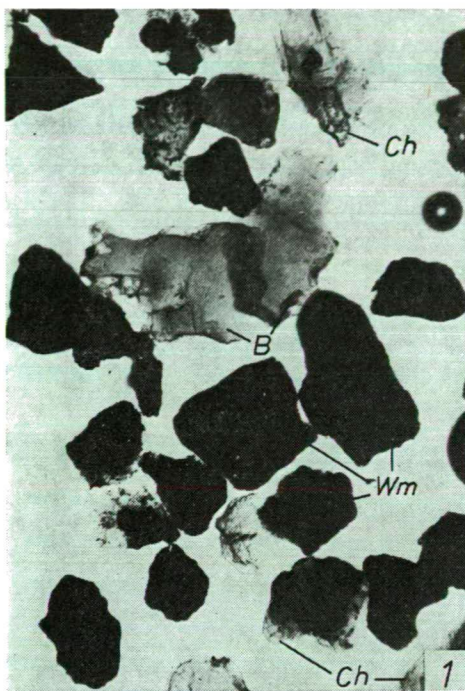
Heavy minerals of Holocene sand samples of the Dévaványa profile (Section 3: Photos 1—4)

1. 29.15—29.24 m
2. 25.45—26.16 m
3. 12.10—12.41/a m
4. 12.10—12.41/b m

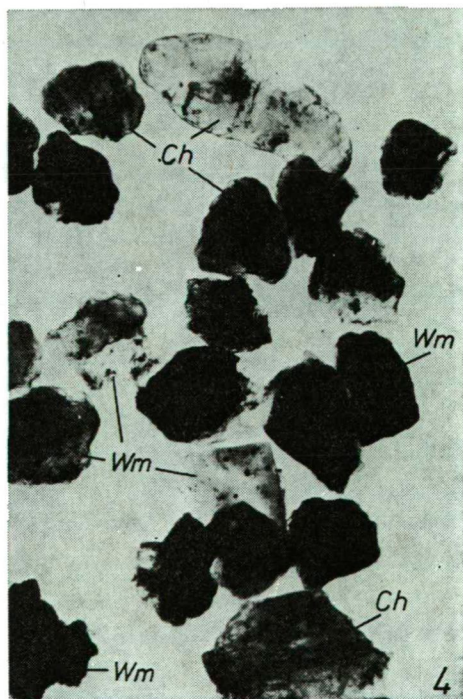
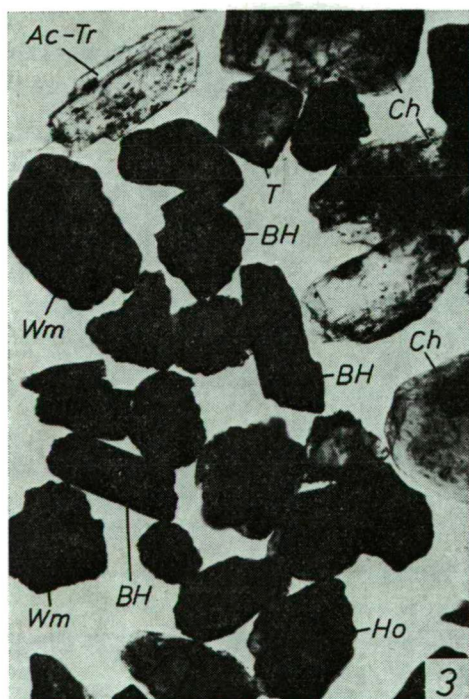
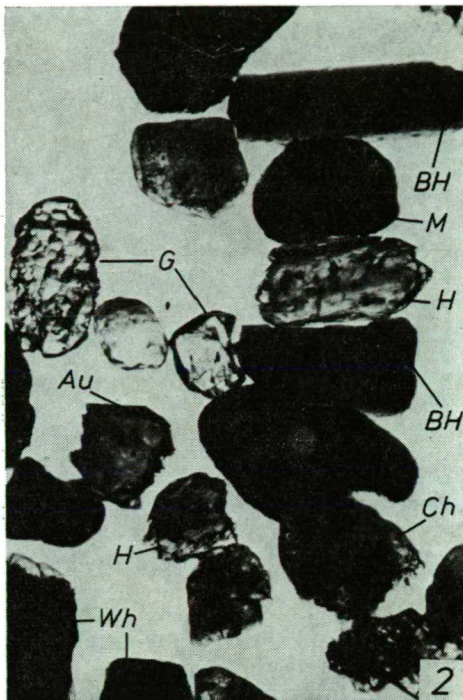
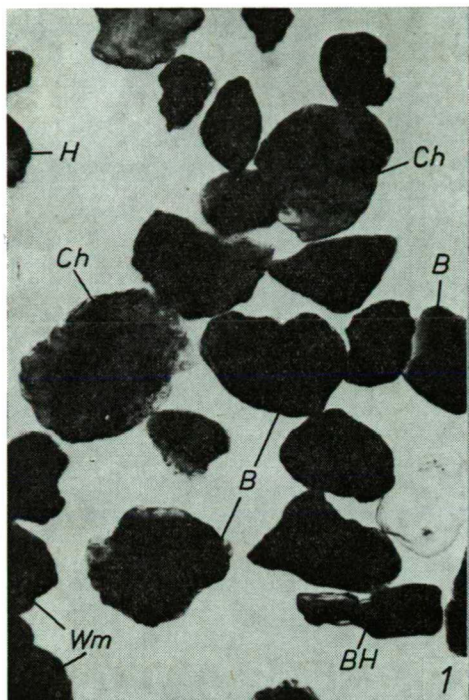




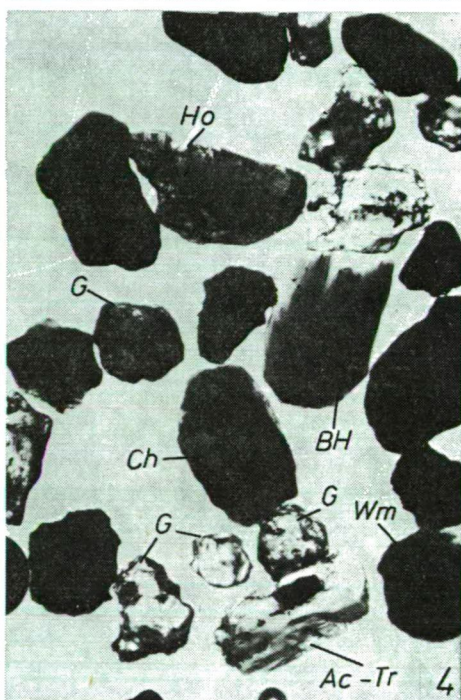
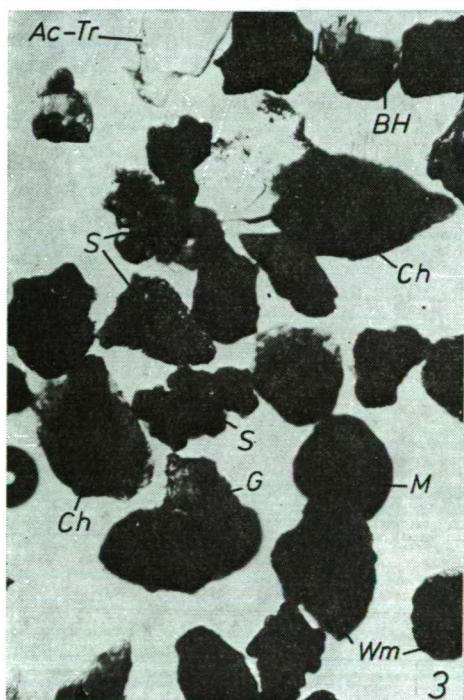
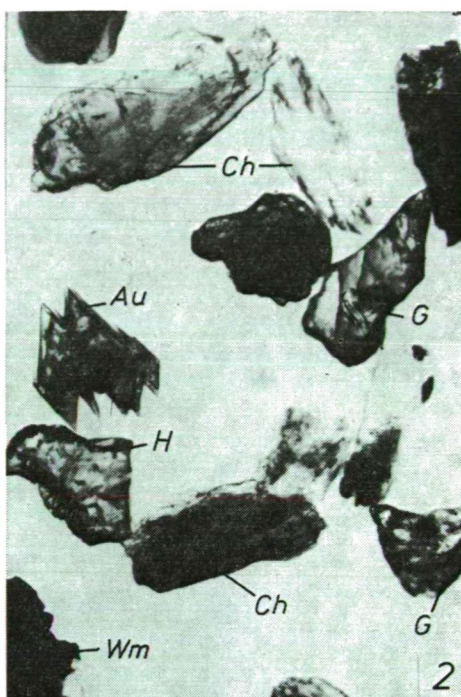
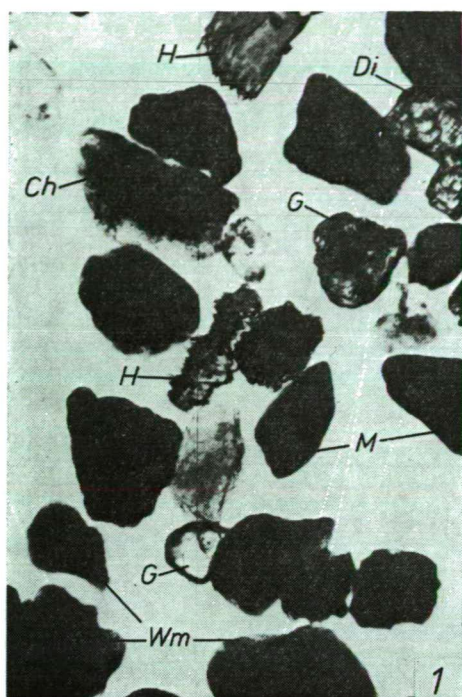




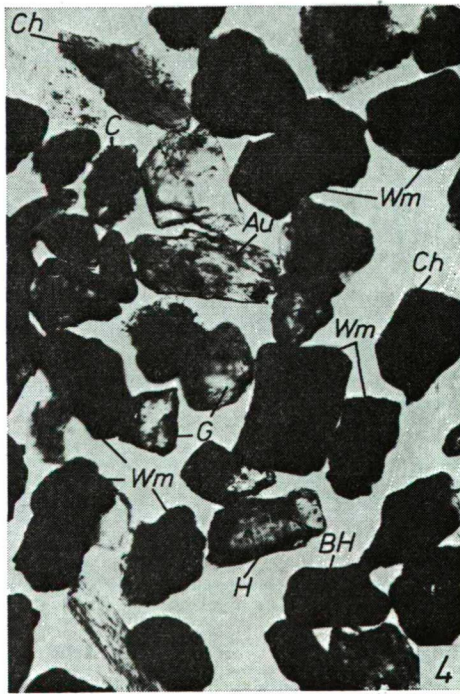
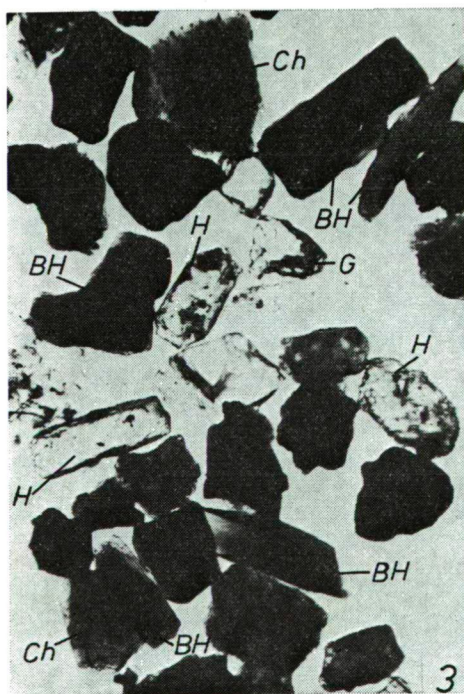
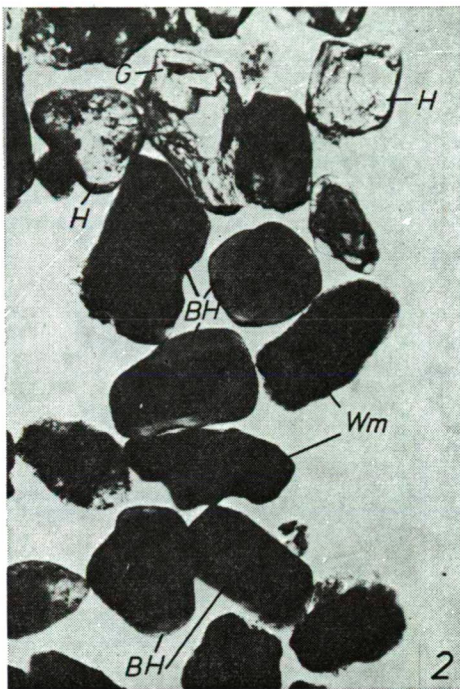
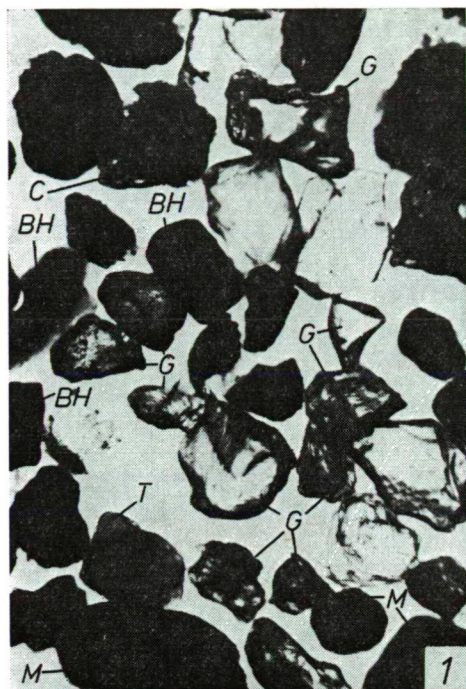














## PALYNOLOGICAL INVESTIGATIONS ON SEDIMENTS OF THE LOWER DANIAN (FISH CLAY, DENMARK) II

M. KEDVES

### ABSTRACT

This paper, which is the second and the final report of the palynological investigations on lower Danian Fish Clay layers, summarize the *Pteridophyte* spores and the *Gymnospermous* pollen grains. Fifty form-species were demonstrated, of these 47 are spores, and only three *Gymnospermous* pollen grains. The new taxa are as follows: *Leiotriletes hojrupensis*, *Triremisporites minor*, *Disthamulatisporites daniensis*, *Biretisporites croxtonae*, *Granulatisporites concavus*, *Verreticulisporis bangii*, *Verrucosporites stockmarrii*, *Phaeocerosporites croxtonae*, *Phaeocerosporites stockmarrii*, *Phaeocerosporites bangii*, *Croxtonaesporites hojrupensis*, *Croxtonaesporites daniensis*, *Polypodiaceoisporites hojrupensis*, *Polypodiaceoisporites stockmarrii*, *Polypodiaceoisporites bangii*, *Polypodiaceoisporites croxtonae*, *Verrucingulatisporites hojrupensis*, *Segmentizonosporites daniense*, *Inundatisporites krutzschii*. The botanical affinities of the spores can be well establish. The contribution of the tropical elements in the spore-pollen assemblage is important; these taxa are: *Cyatheaceae*, *Schizaeaceae*, *Gleicheniaceae*, *Pteridaceae*.

It is noteworthy that the *Lycopodiaceae* spores, and in particular of the livermoss spores (*Anthocerotaceae*), are present and which are interpreted to indicate a marshy ecological condition of the sedimentary basin border.

### INTRODUCTION

In a previous publication (KEDVES, 1979), the problems of the subjects the material and methods were published so that these topics will not be dealt with. The emphasis of this paper is the taxonomy of the spores and gymnospermous pollen grains and their interpretation.

### RESULTS

Fg.n.: LEIOTRILETES (NAUMOVA 1937) R. POT. et KRP. 1954.

1. *Leiotriletes hojrupensis* n. fsp. (Plate I, fig. 1, 2)

#### Diagnosis

Equatorial contour triangular with straight or slightly concave sides. Surface smooth. Wall thickening is general  $0.7\ \mu$ , two layered with the two layers being equal. The laesurae are long, but not extend to the apices of the spore,  $r=4/5$ . Near the laesures there is a torus like thickening.

Maximum size:  $36\ \mu$  ( $25-38\ \mu$ ).

Holotype: Plate I, 1, 2, slide D<sub>2</sub>—1—3, co-ordinates 6.4/110.2.

Locus typicus: Højrup.

Stratum typicum: Fish Clay.

Derivatio nominis: From Højrup of the locality type.

Differential diagnosis: The longer laesurae of this species make it distinct from *L. tenuis* (LESCHIK 1955) BHARDWAJ and SINGH 1964, and from the *L. balowensis* DÖRING 1965. The thinner wall of this new taxon separate well from *L. regularis* (PF. 1953) W. KR. 1959, and from *L. neddenioides* W. KR. 1962.

Botanical affinity: Cf. *Schizaeaceae*.

Occurrence: Højrup, Højstrup, Stevns Klint.

Fg:n.: CYATHIDITES COUPER 1953.

1. *Cyathidites minor* COUPER 1953 (Plate I, fig. 3, 4)

Botanical affinity: After COUPER (1953) the genus *Cyathea*; based on SLADKOV's (1961) publication, the genus *Coniogramma* may be a possible affinity.

Occurrence: Højstrup.

Fg:n.: TRIREMISPORITES DELCOURT and SPRUMONT 1957.

1. *Triremisporites delcourtii* DÖRING 1965 (Plate I, fig. 5, 6)

Botanical affinity: *Gleicheniaceae*.

Occurrence: Højrup, Højstrup.

2. *Triremisporites minor* n. fsp. (Plate I, fig. 7, 8)

Diagnosis

Equatorial contour is triangular with concave sides. Surface smooth. The laesurae extend to the apices of the spore. On the apices the wall is very thin, in general 0.5  $\mu$ . On the sides, between the apices the thickening is maximally 2—3  $\mu$ .

Maximum size: 20—24  $\mu$ .

Holotype: Plate I, 7, 8, slide D<sub>2</sub>—1—5, co-ordinates 9.6/108.3.

Locus typicus: Hørup.

Stratum typicum: Fish Clay.

Derivatio nominis: From the small size.

Differential diagnosis: The *G. laetus* (BOLCH, 1953) is more concave than this new form-species.

Botanical affinity: *Gleicheniaceae*.

Occurrence: Højstrup.

Remark. — A synthesis of the distribution of *Gleicheniaceae* in the geological past was published by BOLKHOVITINA (1966).

Fg:n.: CONCAVISPORITES PF. 1953.

1. *Concavisporites laeviconcavus* W. KR. 1959 (Plate I, fig. 9, 10)

Botanical affinity: *Gleicheniaceae*.

Occurrence: Højstrup.

Fg:n.: OBTUSISPORIS (W. KR. 1959) POCKOCK 1970

1. *Obtusisporis obtusangulus* (R. POT. 1934) W. KR. 1959 (Plate I, fig. 11—14)

Botanical affinity: *Gleicheniaceae*.

Occurrence: Højstrup.

2. *Obtusisporis minimus* W. KR. 1962 (Plate I, fig. 15—18)

Botanical affinity: *Gleicheniaceae*.

Occurrence: Højstrup, Højstrup.

Remark. — KRUTZSCH (1962) described this form-species from upper Tertiary layers of eastern Germany; these specimens are probably rebedded. Later, KRUTZSCH and VANHOORNE (1977) found forms similar to the *Gleicheniidites apilobatus* BRENNER 1963 (pl. 2a, b) in the Paleocene layers.

Fgen.: DISTHAMULATISPORITES n. fgen.

Fgen. typus: *Disthamulatisporites daniensis* n. fsp. (Plate I, fig. 19—22)

Diagnosis

Trilete spores, contour concave. The laesurae of the tetrad scar are long, reach to or almost to the contour of the spore. Proximal surface is smooth, the distale ornamentation is hamulate. Sometimes a small obtusi formation may also occur. Genus type: Plate I, 19, 20, slide D<sub>2</sub>—1—x—1, 16.5/113.9.

Locus typicus: Højrup.

Stratum typicum: Fish Clay.

Derivatio nominis: From the characteristic distal ornamentation.

Differential diagnosis: The hamulate sculpture of the distal side make this taxon distinct from *Obtusisporis* (W. KR. 1959) Pocock 1970.

1. *Disthamulatisporites daniensis* n. fsp. (Plate I, fig. 19—22)

Diagnosis

Equatorial contour concave with rounded apices. Proximal surface smooth or scabrate. The laesurae are long, and sometimes extend to the equatorial contour,  $r=4/5-5/5$ . The thickness of the ectexospore is below  $1\mu$ , and two layered; the two layers are on equal thickness. The hamulate sculpture of the distal surface is well shown, the elements of the ornamentation are  $0.5\mu$  large.

Maximum size: 20—28  $\mu$ .

Botanical affinity: *Gleicheniaceae*.

Occurrence: Højrup, Højstrup.

Remark. — For further information, see the form-generic description.

Fgen.: UNDULATISPORITES Pf. 1953.

1. *Undulatisporites undulapolus* BRENNER 1963 (Plate I, fig. 23—26)

Botanical affinity: *Gleicheniaceae*.

Occurrence: Højrup.

2. *Undulatisporites elsikii* FREDERIKSEN 1973 (Plate I, fig. 27, 28, plate II, fig. 1, 2)

Remark. — FREDERIKSEN (1973) described this species from Eocene layers; from the work of ELSIK (1968) this species is well known from the Paleocene of Texas. There is a probable connection of this species with the form-genus *Biretisporites* DELCOURT and SPRUMONT 1955.

Botanical affinity: *Gleicheniaceae*.

Occurrence: Højrup, Stevns Klint.

Fgen.: BIRETISPORITES DELCOURT and SPRUMONT 1955.

1. *Biretisporites croxtonae* n. fsp. (Plate II, fig. 3, 4)

Diagnosis

Equatorial contour is circular to triangular with convex sides and rounded apices. The thickness of the wall is  $1\mu$  about. The surface is finely granular some times covered with coni. The laesurae extend almost to the equator, but  $r=4/4$ . On the laesurae, there well defined lamellar thickenings.

Maximum size: 45—60  $\mu$ .

Holotype: Plate II, 3, 4, slide Stevns Klint—4; 11.4/115.2.

Locus typicus: Stevns Klint.

Stratum typicum: Fish Clay.

Derivatio nominis: In honour of Dr. I. C. CROXTON.

Differential diagnosis: The form of the equatorial contour distinct from *B. potonie*



DELC. and SPRUM. 1955, *B. spectabilis* DETTMANN 1963 and from *B. convexus* SAH and KAR 1969; greater in size than *B. bellus* SAH and KAR 1969, thinner walled and a different equatorial contour than *B. crassilabratulus* ARCHANGELSKY 1972.

Fgen.: GRANULATISPORITES (IBR. 1933) R. POT. and KRP. 1954.

1. *Granulatisporites concavus* n. fsp. (Plate II, fig. 5, 6)

Diagnosis

Equatorial contour triangular with concave sides and largely rounded apices. The laesurae of the tetrad square does not reach the equator,  $r=2/3-3/4$ . The exospore is thin, on the average  $0.7\ \mu$ . Surface finely granular, granules  $1.5-2.5\ \mu$ , in diameter. Maximum size:  $33-40\ \mu$ .

Holotype: Plate II, 5, 6, slide Højstrup—1, co-ordinates 16.4/104.5.

Locus typicus: Højstrup.

Stratum typicum: Fish Clay.

Derivatio nominis: From the equatorial contour of the spore.

Differential diagnosis: The ornamentation of *G. palaeogenicus* KDS. 1966a is uniform and more dense than this new form-species.

Occurrence: For the time being, it is only known from the type locality.

Fgen.: ISCHYOSPORITES BALME 1957.

1. *Ischyosporites asolidus* (W. KR. 1959) W. KR. 1967 (Plate II, fig. 7, 8)

Occurrence: Højstrup.

Botanical affinity: *Schizaeaceae*, *Lygodium*.

Fgen.: TRILITES COOKSON 1947 ex COUPER 1953, W. KR. 1967.

1. *Trilites triangulus* KDS. 1966 (Plate II, fig. 9, 10)

Occurrence: Højstrup.

Botanical affinity: *Schizaeaceae*, *Lygodium*.

2. *Trilites paravallatus* W. KR. 1959 (Plate II, fig. 11, 12)

Occurrence: Højstrup.

Botanical affinity: *Schizaeaceae*, *Lygodium*.

Fgen.: VERRETICULISPORIS W. KR. 1959.

1. *Verreticulisporis bangii* n. fsp. (Plate II, fig. 13, 14)

Diagnosis

Equatorial contour is triangular with convex sides. The laesurae extend or almost reach the apices of the spore,  $r=4/5-5/5$ . The exospore is  $1-1.2\ \mu$  thick, two layered, the external layer is a little thicker than the inner layer. The verrucae are flat with a diameter of  $1-2\ \mu$  and form a negative reticulum.

Maximum size:  $30-40\ \mu$ .

Holotype: Plate II, 13, 14, slide D<sub>3</sub>—49, co-ordinates 16.5/120.9.

Locus typicus: Højstrup.

Stratum typicum: Fish Clay.

Derivatio nominis: In honour of Dr. I. BANG.

Differential diagnosis: The thinner exospore and the longer laesurae make this species distinct from *V. eoverrucosus* W. KR. 1959.

Occurrence: At present this taxon is only known from the type locality.

Botanical affinity: *Pteropsida*.

Fgen.: VERRUCOSISPORITES IBRAHIM 1933.

1. *Verrucosisporites stockmarrii* n. fsp. (Plate II, fig. 15, plate III, fig. 1).

Diagnosis

Equatorial contour is triangular with convex sides and rounded apices. Exospore is 1—1.5  $\mu$  thick, two layered, with each layer having approximately the same thickness. The laesurae are relatively short,  $r=1/2-3/4$ . The ornamentation is irregular, mostly rugulate, but sometimes verrucate; the size of the sculptural elements is 1.5—2.5  $\mu$ .

Maximum size: 38—44  $\mu$ .

Holotype: Plate II, 15, plate III, 1, slide Højstrup—49, co-ordinates 8.6/111.9.

Locus typicus: Højstrup.

Stratum typicum: Fish Clay.

Derivatio nominis: In honour of Dr. J. STOCKMARR.

Differential diagnosis: The smaller size and the larger ornamental elements distinguish this species from *V. quintus* (TH. and PF. 1953) W. KR. 1959.

Occurrence: At present this taxon is only known from the type locality.

Botanical affinity: *Osmundaceae* or *Schizaeaceae*.

Fgen.: FOVEOTRILETES VAN DER HAMMEN 1954 ex R. POT. 1956.

1. *Foveotriletes* fsp. (Palate III, fig. 2, 3)

Occurrence: Stevns Klint.

Botanical affinity: *Pteridophyte*.

Fgen.: RETITRILETES (VAN DER HAMMEN 1956 ex PIERCE) emend. DÖ., W-KR., MAI, and SCH. 1963.

1. *Retitriletes incomptus* (MANUM 1962) W. KR. 1963 (Plate III, fig. 4, 5)

Occurrence: Højstrup.

Botanical affinity: *Lycopodiaceae*.

Fgen.: SAXOSPORIS W. KR. 1963.

1. *Saxosporis* fsp. ex groupe *gracilis* W. KR. and PACLTOVÁ 1963 (Plate III, fig. 6, 7)

Occurrence: Højstrup.

Botanical affinity: *Anthocerotaceae*, *Phaeoceros*.

2. *Saxosporis disconformis* (STOVER 1973) n. comb. (Plate III, fig. 8, 9)

Syn.: 1973, STOVER, in STOVER and PARTRIDGE, *Baculatisporites disconformis* STOVER n. sp., p. 245, 246, pl. 13, 8.

Occurrence: Højstrup, Stevns Klint.

Botanical affinity: *Anthocerotaceae*.

Fgen.: ECHINATISPORIS W. KR. 1959.

1. *Echinatisporis* fsp. (Plate III, fig. 10, 11)

Occurrence: Højstrup.

Botanical affinity: *Selaginellaceae*, *Selaginella*.

Fgen.: PHAEOCEROSPORITES E. NAGY 1968, here emended

Emended diagnosis

Trilete spores, contour circular or extremely convex, triangular. The laesurae extend to the equatorial contour; around the laesurae there are characteristic exospore thickenings. The wall of the spore is relatively thick. The proximal surface is smooth or scabrate. The ornamentation of the distal surface is variable, circular, polar annulus or half-moon-shaped thickenings or sometimes granules, verrucae or irregular thickenings.

Remark. — KRUTZSCH (1963) modified the description of *Foraminisporis* W. KR. 1959 by additional notes the original diagnosis remains however intact; he didnt

emended it so that *Foraminisporis zonaloides* W. KR. 1963 must be reclassified so that *Foraminisporis* W. KR. 1959 will not be a heterogenous form-genus. The conception of KRUTZSCH (1963) was accepted without criticism by PACLTOVÁ and SIMONCSICS (1970).

*Phaeocerosporites zonaloides* (W. KR. 1963) n. comb. Syn.: 1963, KRUTZSCH.  
— *Foraminisporis zonaloides* n. fsp., p. 40, pl. 1, 1—6.

1. *Phaeocerosporites croxtonae* n. fsp. (Plate III, fig. 12, 13)

Diagnosis

Equatorial contour is circular. Proximal surface scabrate or punctate. The laesurae of the tetrad scar extend to the equator bifurcating near the equator. The thickening on each side of the laesurae is 1.5—2  $\mu$ . Exospore is 2—2.3  $\mu$  thick, two layered, the external layer is thicker than the inner. The external part of the spore wall is channelled, similar to the tubulate structure. Around the distal pole there are three half-moon or asymmetrical annuli that form thickenings. Moreover, there are granules or verrucae with a base diameter of 1—3  $\mu$ .

Maximum size: 32—40  $\mu$ .

Holotype: Plate III, 12, 13, slide Højstrup—50, co-ordinates 14.3/103.8.

Locus typicus: Højstrup.

Stratum typicum: Fish Clay.

Derivatio nominis: In honour of Dr. I. C. CROXTON.

Differential diagnosis: The very characteristic three thickening around the distal pole distinguish well this taxon from the other species of this form-genus.

Occurrence: From the time being, it is only known from the type locality.

Botanical affinity: *Anthocerotaceae*.

2. *Phaeocerosporites stockmarrii* n. fsp. (Plate IV, fig. 1, 2)

Diagnosis

Equatorial contour circular or elliptical. Proximal surface is finely granular. The laesurae of the tetrad scar extend to the equator and divide before reaching the equatorial contour. Near the laesures there are large, 3  $\mu$  uncharacteristic thickenings. The exospore is 2  $\mu$  thick, two layered, the external wall is thicker than the internal one. The external wall is transversed by channels; structure tubulate. The most characteristic feature of the distal ornamentation is a polar, asymmetrical annulus, or U form thickening. Adjacent to them are granules with 1—2.5  $\mu$  diameter.

Maximum size: 30—45  $\mu$ .

Holotype: Plate IV, 1, 2 slide Højstrup—6, co-ordinates 7.4/107.0.

Locus typicus: Højstrup.

Stratum typicum: Fish Clay.

Derivatio nominis: In honour of Dr. J. STOCKMARR.

Differential diagnosis: The distal annulus or U form thickening distinguishes this species from *Ph. baranyaensis* E. NAGY 1968.

Occurrence: Højstrup, Stevns Klint.

Botanical affinity: *Anthocerotaceae*.

3. *Phaeocerosporites bangii* n. fsp. (Plate IV, fig. 3, 4)

Diagnosis

Equatorial contour is circular or triangular with convexe sides. Proximal surface is finely granular. The laesurae of the tetrad scar extend to the equator and divide near the equator. Around the laesurae, the thickening is 1.5  $\mu$  wide. The wall is 2  $\mu$  thick, in general two layered; the external wall is thicker than the internal, the external wall is channelled. The distal surface is granular, the size of the sculptural

elements range from 0.5 to 2.5  $\mu$ . The important distal characteristic feature is the irregular thickenings around the distal pole.

Maximum size: 28—34  $\mu$ .

Holotype: Plate IV, 3, 4, slide Stevns Klint—20, co-ordinates 5.1/102.8.

Locus typicus: Høstrup.

Stratum typicum: Fish Clay.

Derivatio nominis: In honour of Dr. I. BANG.

Differential diagnosis: The form of the distal pole thickenings is irregular. This characteristic feature distinguishes this taxon from *Ph. croxtonae* n. fsp. On the distal pole of the latter form-species, three half-moon thickenings are formed around the distal pole.

Occurrence: From the time being, this species is only known from the type locality.

Botanical affinity: *Anthocerotaceae*.

Fgen.: CROXTONAESPORITES n. fgen.

Fgn. type: *Croxtonaesporites hojrupensis* n. fsp. (Plate IV, fig. 5, 6)

Diagnosis

Zonotrilete spores, cingulum is not undulating and on the sides and at the apices. it has the same thickness. There are tori around the laesurae; the proximal and the distal surfaces of the central body are smooth.

Locus typicus: Højrur.

Stratum typicum: Fish Clay.

Derivatio nominis: In honour of Dr. I. C. CROXTON.

Differential diagnosis: The torus on the apices of *Toringulatisporites* SIMONCSICS 1964 described from the neogene deposits penetrate into the cingulum so that there is essentially a segmented cingulum, which has a diagnostic character. This features is not observable on the spores from the Fish Clay.

1. *Croxtonaesporites hojrupensis* n. fsp. (Plate IV, fig. 5, 6)

Diagnosis

Equatorial contour is triangular with straight or slightly convex sides. Cingulum is 4—5  $\mu$  wide. The laesurae do not reach the inner contour of the cingulum. The torus is 2—3  $\mu$  wide and narrows toward its distal end. Both surfaces are smooth. Maximum size: 40—50  $\mu$ .

Holotype: Plate IV, 5, 6, slide D<sub>3</sub>—20, co-ordinates 14.3/120.9.

Locus typicus: Højrur.

Stratum typicum: Fish Clay.

Derivatio nominis: From the locality type.

Occurrence: For the time being, this species is only known from the type locality.

2. *Croxtonaesporites daniensis* n. fsp. (Plate IV, fig. 7, 8)

Diagnosis

Equatorial contour triangular, generally straight or only very slightly convex or concave sides. The laesurae of the tetrad scar reach or almost reach, the inner edge of the cingulum. The inner side of the torus is undulating. The torus is 2—2.5  $\mu$  wide. Around the torus it is a other torus-like triangular-like thickening which is 2  $\mu$  wide. The cingulum is 3  $\mu$  wide.

Maximum size: 37—45  $\mu$ .

Holotype: Plate IV, 7, 8, slide D<sub>2</sub>—1—7, co-ordinates 12.6/122.5.

Locus typicus: Højrur.

Stratum typicum: Fish Clay.

Derivatio nominis: From Denmark.

Differential diagnosis: The so called double torus distinguished this taxon from the former form-species.

Occurrence: For the time being, this species is only known from the type locality.

Fgen.: CONTIGNISPORITES DETTMANN 1963.

1. *Contignisporites* fsp. (Plate IV, fig. 9, 10)

Occurrence: Højrup.

Botanical affinity: Ancestral type *Schizaeaceae* spore.

Remark. — This form-genus is well known from the Jurassic. It is possible that during lower Danian time the fern that produced these spores was still extant. But on the other hand, it is not impossible that these spores are reworked from older sediments.

Fgen.: POLYPODIACEOISPORITES R. POT. 1956 non 1951.

1. *Polypodiaceoisporites triangulus* KDS, and J. R. 1965 (Plate IV, fig. 11, 12)

Occurrence: Stevns Klint.

Botanical affinity: *Pteridaceae*.

2. Cf. *Polypodiaceoisporites* fsp. (Plate IV, fig. 13, 14)

Occurrence: Højrup.

3. *Polypodiaceoisporites brejanii* CERNJAVSKA 1970 (Plate V, fig. 1, 2)

Occurrence: Højrup.

Botanical affinity: *Pteridaceae*.

4. *Polypodiaceoisporites vancampoae* KDS. 1967 (Plate V, 3, 4)

Occurrence: Højrup, Stevns Klint.

Botanical affinity: *Pteridaceae*.

5. *Polypodiaceoisporites hojrupensis* n. fsp. (Plate V, 5, 6)

Diagnosis

Equatorial contour is triangular, with straight or slightly convex sides. The surface of the cingulum is smooth and 3  $\mu$  wide. The proximal surface of the central body is ornamented with small verrucae (1—2  $\mu$ ) or with rugulae with a diameter of 1.5  $\mu$ . The laesurae of the tetrad scar reach, or almost reach, the inner edge of the cingulum. The ornamentation of the distal surface of the central body is essentially rugulate, sometimes foveate or reticulate. The muri are 2—3  $\mu$  wide.

Maximum size: 40—50  $\mu$ .

Holotype: Plate V, 5, 6, slide D<sub>3</sub>—41, co-ordinates 20.1/116.3.

Locus typicus: Højrup.

Stratum typicum: Fish Clay.

Derivatio nominis: From Højrup the locality type.

Differential diagnosis: The distal ornamentation of the central body is a very distinctive and characteristic feature.

Occurrence: For the time being, this taxon is only known from the type locality.

Botanical affinity: *Pteridaceae*.

6. *Polypodiaceoisporites maximus* E. NAGY and L. RÁKOSI 1966 (Plate V, 7, 8)

Occurrence: Højrup, Stevns Klint.

Botanical affinity: *Pteridaceae*.

7. *Polypodiaceoisporites snopkova* KDS. 1973 (Plate V, 9, 10)

Occurrence: Højrup, Højstrup.

Botanical affinity: *Pteridaceae*.

8. *Polypodiaceoisporites hungaricus* KDS. 1961 (Plate V, 11, 12)

Occurrence: Højrup.

Botanical affinity: *Pteridaceae*.

9. *Polypodiaceoisporites stockmarrii* n. fsp. (Plate V, fig. 13, 14)

Diagnosis

Equatorial contour is triangular, generally with straight or only slightly convex or concave sides. The contour of the cingulum is slightly undulating, 4—5  $\mu$  wide on the sides and 3  $\mu$  on the apices. The laesurae of the tetrad scar are slightly undulating and extend to the inner margin of the cingulum. The proximal surface of the central body is verrucate or rugulate, the diameter of the ornamental elements ranges from 2—6  $\mu$ .

Maximum size: 20—30  $\mu$ .

Holotype: Plate V, 13, 14, slide Stevns Klint—14, co-ordinates 8.7/121.2.

Locus typicus: Stevns Klint.

Stratum typicum: Fish Clay.

Derivatio nominis: In honour of Dr. J. STOCKMARR.

Differential diagnosis: The new form-species separate well from *P. hungaricus* KDS. 1961 by its equatorial contour.

Occurrence: From the time being it is only known from the type locality.

Botanical affinity: *Pteridaceae*.

10. *Polypodiaceoisporites gracicingulis* W. KR. 1959 (Plate VI, fig. 1, 2)

Occurrence: Højrup.

Botanical affinity: *Pteridaceae*.

11. *Polypodiaceoisporites granulatus* KDS. 1966b (Plate VI, fig. 3, 4)

Occurrence: Højrup.

Botanical affinity: *Pteridaceae*.

12. *Polypodiaceoisporites bangii* n. fsp. (Plate VI, fig. 5, 6)

Diagnosis

Equatorial contour is triangular with rounded apices and slightly convex or concave sides. The surface of the cingulum is smooth, 3  $\mu$  wide. The laesurae of the tetrad scar do not reach the inner margin of the cingulum,  $r=3/4$  in average. Near, the laesurae, the verrucae are aligned. The basal diameter of the verrucae is 1—2  $\mu$  the diameter of the rugulae is 2  $\mu$ . On the distal side of the central body, there is a triangular thickened form; near this thickening there are rugulae. The elements of this ornamentation are 1.5  $\mu$  wide.

Maximum size: 40—50  $\mu$ .

Holotype: Plate VI, 5, 6, slide Højstrup—2, co-ordinates 2.8/106.7.

Locus typicus: Højstrup.

Stratum typicum: Fish Clay.

Derivatio nominis: In honour of Dr. I. BANG.

Differential diagnosis: The characteristic thickening of the distal side of the central body makes this species distinct from the other taxa of the *Polypodiaceoisporites*, with similar great size.

Occurrence: From the time being, it is only known from the locality type.

Botanical affinity: *Pteridaceae*.

13. *Polypodiaceoisporites croxtonae* n. fsp. (Plate VI, 7, 8)

Diagnosis

Equatorial contour is triangular, with concave sides. The cingulum is 2.5—3  $\mu$  wide. The proximal surface of the central body is ornamented with granules of 1  $\mu$  diameter. The laesurae of the tetrad scar extend to the inner margin of the cingulum. Around the laesurae there is a characteristic thickening. The distal surface of the

central body is finely granular, the size of the ornamental elements is  $0.5\ \mu$ ; sometimes the ornamentation is finely reticulate or rugulate.

Maximum size:  $16-23\ \mu$ .

Holotype: Plate VI, 7, 8, slide  $D_3-72$ , co-ordinates  $13.5/111.2$ .

Locus typicus: Højrup.

Stratum typicum: Fish Clay.

Derivatio nominis: In honour of Dr. I. C. CROXTON.

Differential diagnosis: The smaller size, and the sculpture of the central body distinguish this species from *P. obuncus* W. KR. 1959, and *P. microconcaus* W. KR. 1967.

Occurrence: For the time being, this taxon is only known from the type locality.

Botanical affinity: *Pteridaceae*.

14. *Polypodiaceoisporites laevigatus* KDS. and J. R. 1965 (Plate VI, fig. 13, 14)

Occurrence: Højstrup.

Botanical affinity: *Pteridaceae*.

15. *Polypodiaceoisporites haemussensis* CERNJAVSKA 1966 (Plate VI, fig. 15, 16)

Occurrence: Dania.

Botanical affinity: *Pteridaceae*.

Fgen.: VERRUCINGULATISPORITES KDS. 1961.

1. *Verrucingulatisporites hojrupensis* n. fsp. (Plate VI, fig. 9, 10)

Diagnosis

Equatorial contour is triangular, with concave sides, the apices are rounded. The width of the cingulum is variable and is between  $5$  and  $10\ \mu$ . The verrucae on the cingulum are between  $3-5\ \mu$  high. The proximal side of the central body is ornamented with flat verrucae, there are very characteristic at the end of the laesurae. The laesurae does not reach the inner margin of the cingulum,  $r=1/2-3/4$ . The distal surface of the central body is verrucate-rugulate, the size of the ornamental elements is around  $3\ \mu$ .

Maximum diameter:  $32-40\ \mu$ .

Holotype: Plate VI, 9, 10, slide  $D_3-61$ , co-ordinates  $8.9/108.3$ .

Locus typicus: Højrup.

Stratum typicum: Fish Clay.

Derivatio nominis: From the locality type.

Differential diagnosis: The most characteristic and distinctive feature of this species is the ornamentation of the cingulum.

Occurrence: For the time being this taxon is only known from the type locality.

Botanical affinity: *Pteridaceae*.

Fgen.: SEGMENTIZONOSPORITES KDS. 1966b.

1. *Segmentizonosporites daniense* n. fsp. (Plate VI, fig. 11, 12)

Diagnosis

Equatorial contour is triangular with slightly convex sides. The zona is  $6\ \mu$  wide on the sides and  $3\ \mu$  wide at the apices. The laesurae of the tetrad scar are long, but do not extend to the inner margin of the cingulum;  $r=3/4$ . The proximal side of the central body is covered with granules, but these granules anastomose often so that the surface appears finely rugulate. The distal part of the central body is less characteristic, the ornamental elements are tiny granules —  $0.5\ \mu$  in size, and finely rugulate. On the border of the cingulum and the central body there are granules with a diameter of  $1-2\ \mu$ .

Maximum size:  $30-36\ \mu$ .

Holotype: Plate VI, 11, 12, slide  $D_2-1-6$ , co-ordinates  $23.1/121.6$ .

Locus typicus: Højrup.

Stratum typicum: Fish Clay.

Derivatio nominis: From Dania.

Differential diagnosis: The small ornamental elements of the central body distinguish this taxon well from the other species of this form-genus.

Occurrence: For the time being, this species is only known from the type locality.

Botanical affinity: Based on the publication of KREMP (1967), *Pteridaceae*: *Taenitis blechnoides*, pl. I, 36, 37.

Fgen.: HAMULATISPORIS W. KR. 1959.

1. *Hamulatisporis heskemensis* (PFLANZL 1955) n. comb. (Plate VII, fig. 3, 4)

Syn.: 1955. PFLANZL, in MÜRRIGER and PFLANZL, *Cingulatisporites heskemensis* n. sp., p. 85, pl. 5, 1—3.

1959. — KRUTZSCH, *Camarozonosporites heskemensis* (PFLANZL 1955) n. comb., p. 187.

Occurrence: Højstrup.

Fgen.: INUNDATISPORIS W. KR. 1963 stat. nov. Syn.: *Camarozonosporites* (*Inundatisporis* W. KR. 1963)

1. *Inundatisporis krutzschii* n. fsp. (Plate VII, fig. 1, 2)

Diagnosis

Equatorial contour triangular, convex, sometimes nearly circular. The laesurae of the tetrad scar reach the equator, but before the equator they divide. The sculpture, on both sides is hamulate, the sculptural elements are 0.5—1  $\mu$  wide.

Maximum size: 45—50  $\mu$ .

Holotype: Plate VII, 1, 2, slide Dania—29, co-ordinates 17.2/115.1.

Locus typicus: Dania.

Stratum typicum: Fish Clay.

Derivatio nominis: In honour of Dr. W. KRUTZSCH.

Differential diagnosis: The large size of this species and the fine sculpture distinguish it from the other members of this form-genus.

Occurrence: For the time being, this taxon is only known from the type locality.

Botanical affinity: *Lycopodiaceae*.

Fgen.: ALISPORITES DAUGHERTY 1941.

1. *Alisporites* cf. *bilateralis* ROUSE 1959 (Plate VII, 5, 6)

Occurrence: Højrup.

Botanical affinity: *Abietales*.

Fgen.: PITYOSPORITES SEWARD 1914.

1. *Pityosporites labdacus* (R. POT. 1931) TH. and PF. 1953 subfsp. *labdacus* (Plate VII, 7, 8)

Occurrence: Højrup, Dania.

Botanical affinity: *Abietaceae*, *Pinus*.

Fgen.: PARVISACCITES COUPER 1958.

1. *Parvisaccites* fsp. (Plate VII, fig. 9, 10)

Occurrence: Højrup.

Botanical affinity: *Coniferopsida*.



## DISCUSSION

In the earlier published work of this investigation, 57 *Angiospermatophyte* pollen form-species, now 3 *Gymnospermatophyte* pollen, and 47 spore form-species were described. From the vegetational evolutionary and stratigraphical point of view, the abundance of the zonotritele spores is noteworthy. The origin is of these spores is to be found in the Lower Cretaceous. But they are known in greater quantity from the Cenomanian. The acme (golden age) of these forms probably occurring at the Cretaceous-Tertiary transition. This is worth mentioning, because the well known tropical fern families (e. g. *Gleicheniaceae*, *Schizaeaceae*) are present in the largest quantity in the lower Cretaceous BOLKHOVITINA (1966, 1967, 1968). The livermoss spores represent a marsh vegetation.

The very small quantity of the *Gymnospermous* pollen grains is interesting. It seems that during the lower Danian there was not autochthonous *Classopollis* or *Classoidites*. The extinction of these probable *Cheirolepidaceae* taxa are distinct from those of the Maestrichtian. In addition, a number of species of gymnospermous pollen with bladders occur in high quantity first in the Thanetian of the Paleocene. If we accept that the *Normapolles* producing plants were shrubs in a marsh vegetation, we may assume a series of extinction in the Lignosa — tree taxa. This view is supported by the *Pteridophyta*/*Angiospermatophyta* ratio.

## ACKNOWLEDGMENTS

The writer is deeply indebted to Prof. Dr. E. A. STANLEY (The Graduate School Indiana University of Pennsylvania, U. S. A.) for critically reading the manuscript for linguistic errors.

## REFERENCES

- ARCHANGELSKY, S. [1972]: Esporas de la formacion Rio Turbio (Eoceno) Provincia de Santa Cruz. — Revista del Museo de la Plata 6, 65—100.
- BALME, B. E. [1957]: Spores and pollen grains from the Mesozoic of Western Australia. — Com. Sci. Ind. Res. Org. (Australia), Coal Res. Sect., Ref. T. C. 25, 1—50.
- BHARDWAJ, D. C. and SINGH, H. P. [1964]: An Upper Triassic miospore assemblage from the coals of Lunz Austria. — The Palaeobotanist 12, 28—44.
- BOLCHOVITINA, N. A. [1966]: Distribution of the ferns of the family Gleicheniaceae in the past. — The Palaeobotanist 15, 11—15.
- BOLCHOVITINA, N. A. [1967]: The fossil spores of the family Gleicheniaceae (Morphology and Taxonomy). — Rev. Palaeobotan. Palynol., 3, 59. 64.
- BOLCHOVITINA, N. A. [1968]: The spores of the family Gleicheniaceae ferns and their importance for the stratigraphy (Russian). — Acad. Sci. of the USSR Geol. Inst., 176, 1—115.
- BRENNER, G. J. [1963]: The spores and pollen of the Potomac Group of Maryland. — Dept. of Geol., Mines and Water Res., 27, 1—215.
- ЧЕРНЯВСКА, С. [1966]: Горноеоценски спори от Кафявите Вълци в източно България. — Труд. Върху Геол. на България 8, 143—180.
- CERNJAVSKA, S. [1970]: New spore and pollen species from coal-bearing Paleogene sediments in Bulgaria. — Rev. of the Bulgarian Geol. Soc., 31, 33—40.
- COUPER, R. A. [1953]: Upper Mesozoic and Cainozoic Spores and Pollen Grains from New Zealand. — New Zealand Geol. Surv. Paleont. Bull., 22, 1—77.

- COUPER, R. A. [1958]: British Mesozoic microspores and pollen grains. A systematic and stratigraphic study. — *Palaeontographica B*, **103**, 77—179.
- DAUGHERTY, L. R. [1941]: The Upper Triassic flora of Arizona. — *Carnegie Inst. Wash., Pub.* **526**, 1—108.
- DELCOURT, A. et SPRUMONT, G. [1955]: Les spores et grains de pollen du Wealdien du Hainaut. — *Mém. de la Soc. Belge de Géol. de Paléont. et d'Hydrol. N. S.* **5**, 5—73.
- DELCOURT, A. et SPRUMONT, G. [1957]: Quelques microfossiles du Wealden de Féron-Glageon, France. — *Bull. Soc. Belge Geol., Paleont., Hydrol.* **66**, 57—67.
- DETTMANN, M. E. [1963]: Upper Mesozoic microfloras from south-eastern Australia. — *Royal Soc. of Victoria* **77**, 1—148.
- DÖRING, H. [1965]: Die sporenpaläontologische Gliederung des Wealden in Westmecklenburg (Struktur Werle). — *Geologie* **14 BH 47**, 1—118.
- ELSIK, W. C. [1968]: Palynology of a Paleocene Rockdale Lignite, Milam County, Texas. I. Morphology and Taxonomy. — *Pollen et Spores* **10**, 263—314.
- FREDERIKSEN, N. O. [1973]: New mid-Tertiary spores and pollen grains from the Mississippi and Alabama. — *Tulane Studies in Geology and Paleontology* **10**, 65—86.
- KEDVES, M. [1961]: Études palynologiques dans le bassin de Dorog — II —. — *Pollen et Spores* **3**, 101—153.
- KEDVES, M. [1966a]: Contribution sporo-polliniques à la connaissance paléobotanique des couches fossilifères de la manière de Tatabánya. — *Acta Bot. Acad. Sci. Hung.* **12**, 55—88.
- KEDVES, M. [1966b]: Palynológiai adatok a solymári eocén kori barnakőszenes rétegekből — M.A.F. I. évi jelentése az 1964 évről 339—347.
- KEDVES, M. [1967]: Études palynologiques des couches du Tertiaire inférieure de la Région Parisienne I. Spores. — *Pollen et Spores* **9**, 521—552.
- KEDVES, M. [1973]: Paleogene fossil sporomorphs of the Bakony Mountains. Part I. — *Studia Biologica Hungarica* **12**, 1—134.
- KEDVES, M. [1979]: Palynological investigations on sediments of the Lower Danian (Fish Clay, Denmark) I. — *Acta Miner.-Petr.*, XXIV/1, 167—181.
- KEDVES, M. and RÁKOSI, J. [1965]: Zonotritele microspores from the Eocene bauxite layers of Gánt in Hungary. — *Acta Biol. Szeged* **11**, 233—244.
- KREMP, G. O. W. [1967]: Tetrad marking pteridophytic spores and their evolutionary significance. *Rev. Palaeobotan. Palynol.* **3**, 311—323.
- KRUTZSCH, W. [1959]: Mikropaläontologische (sporenpaläontologische) Untersuchungen in der Braunkohle des Geiseltales. — *Geologie* **8 BH 21/22**, 1—425.
- KRUTZSCH, W. [1962]: Atlas der mittel- und jungtertiären dispersen Sporen- und Pollen- sowie der Mikroplanktonformen des nördlichen Mitteleuropas. Lief. I. — VEB Deutscher Verlag der Wissenschaften, Berlin.
- KRUTZSCH, W. [1963]: Atlas der mittel- und jungtertiären dispersen Sporen- und Pollen- sowie der Mikroplanktonformen des nördlichen Mitteleuropas. Lief. II. — VEB Deutscher Verlag der Wissenschaften, Berlin.
- KRUTZSCH, W. [1967]: Atlas der mittel- und jungtertiären dispersen Sporen- und Pollen sowie der Mikroplanktonformen des nördlichen Mitteleuropas. Lief. IV, V. — VEB Gustav Fischer Verlag, Jena.
- KRUTZSCH, W. und VANHOORNE, R. [1977]: Die Pollenflora von Epinois und Loksbergen in Belgium. — *Palaeontographica B*, **163**, 1—110.
- MÜRRIGER, F. und PFLANZL, G. [1955]: Pollenanalytische Datierung einiger hessischer Braunkohlen. — *Notizbl. Hess. L.-Amt. Bodenforsch.*, **83**, 71—89.
- NAGY, E. [1968]: Moss spores in Hungarian Neogene strata. — *Acta Bot. Acad. Sci. Hung.* **14**, 113—132.
- NAGY, E. és RÁKOSI, L. [1966]: A Bánd 2. és Bánd 3. sz. fúrások összehasonlító palynológiai vizsgálata. — *M. Áll. Földtani Int. évi jel. az 1964 évről*, 265—283.
- PACLTOVÁ, B. and SIMONCSICS, P. [1970]: New Types of Spores (Genera and Species) from the Bohemian Miocene. — *Paläont. Abh. B*, **3**, 599—617.
- POCOCK, S. A. J. [1970]: Palynology of the Jurassic sediments of Western Canada. — *Palaeontographica B*, **130**, 73—136.
- POTONIÉ, R. [1956]: Synopsis der Gattungen der Sporae dispersae. — *Beih. Geol. Jb.* **23**, 1—103.
- POTONIÉ, R. and KREMP, G. O. W. [1954]: Die Gattungen der palaeozoischen Sporae dispersae und ihre Stratigraphie. — *Geol. Jb.* **69**, 111—194.
- ROUSE, G. E. [1959]: Plant microfossils from the Kootenay Coal-measures strata of British Columbia. — *Micropaleontology* **5**, 303—324.
- SIMONCSICS, P. [1964]: Einige neue Sporen aus dem Salgótarjánér Kohlengbiet in Ungarn. — *Fortschr. Rheinld. u. Westf.* **12**, 97—104.

STOVER, L. E. and PARTRIDGE, A. D. [1973]: Tertiary and Late Cretaceous Spores and Pollen from the Gippsland Basin, Southeastern Australia. — Proc. R. Soc. Vict. 85, 237—286.

СПАДКОВ, А.Н. [1961]: Споры настоящих папоротников подсемейства Pterideae Diels. СССР. — Вестник Московского Университета 6, 45—52.

Manuscript received, February 10, 1980.

DR. MIKLÓS KEDVES  
Attila József University,  
Dept. of Botany  
H-6722 Szeged, Egyetem u. 2—6.  
Hungary

## EXPLANATION OF PLATES

### PLATE I

- 1, 2. — *Leiotriletes hojrupensis* n. fsp., *Schizaeaceae*, cf. *Lygodium*, D<sub>2</sub>—1—3; 6.4/110.2.
  - 3, 4. — *Cyathidites minor* COUPER 1953, *Cyatheaceae*, D<sub>2</sub>—2—1; 20.5/123.4.
  - 5, 6. — *Triremisporites delcourti* DÖRING 1965, *Gleicheniaceae*, Højstrup—39; 20.2/109.6.
  - 7, 8. — *Triremisporites minor* n. fsp., *Gleicheniaceae*, D<sub>2</sub>—1—5; 9.6/108.3.
  - 9, 10. — *Concavisporites laeviconcavus* W. KR. 1959, *Gleicheniaceae*, D<sub>2</sub>—1—7; 20.2/120.1.
  - 11, 12. — *Obtusisporis obtusangulus* (R. POT. 1934) W. KR. 1959, *Gleicheniaceae*, D<sub>2</sub>—1—7; 9.8/122.2.
  - 13, 14. — *Obtusisporis obtusangulus* (R. POT. 1934) W. KR. 1959, *Gleicheniaceae*, D<sub>2</sub>—1—x—4; 5.8/102.7.
  - 15, 16. — *Obtusisporis minimus* W. KR. 1962, *Gleicheniaceae*, D<sub>2</sub>—82; 4.5/107.5.
  - 17, 18. — *Obtusisporis minimus* W. KR. 1962, *Gleicheniaceae*, D<sub>2</sub>—78; 17.2/109.6.
  - 19, 20. — *Disthamulatisporites daniensis* n. fgen. et fsp., *Gleicheniaceae*, D<sub>2</sub>—1—x—1; 16.5/113.9.
  - 21, 22. — *Disthamulatisporites daniensis* n. fgen. et fsp., *Gleicheniaceae*, D<sub>2</sub>—78; 10.2/110.6.
  - 23, 24. — *Undulatisporites undulapolus* BRENNER 1963, *Gleicheniaceae*, D<sub>2</sub>—1—x—4; 21.7/116.1.
  - 25, 26. — *Undulatisporites undulapolus* BRENNER 1963, *Gleicheniaceae*, D<sub>2</sub>—34; 22.3/121.4.
  - 27, 28. — *Undulatisporites elsikii* FREDERIKSEN 1973, *Gleicheniaceae*, D<sub>2</sub>—2; 8.3/106.4.
- ×1000

### PLATE II

- 1, 2. — *Undulatisporites elsikii* FREDERIKSEN 1973, Stevns Klint—23; 10.4/117.6.
- 3, 4. — *Biretisporites croxtonae* n. fsp., Stevns Klint—4; 11.4/115.2.
- 5, 6. — *Granulatisporites concavus* n. fsp., Højstrup—1; 16.4/104.5.
- 7, 8. — *Ischyrsporites asolidus* (W. KR. 1959) W. KR. 1967, *Schizaeaceae*, *Lygodium*, D<sub>2</sub>—19; 5.5/104.6.
- 9, 10. — *Trilites triangulus* KDS. 1966, *Schizaeaceae*, *Lygodium*, Højstrup—4; 19.6/115.7.
- 11, 12. — *Trilites paravallatus* W. KR. 1959, *Schizaeaceae*, *Lygodium*, D<sub>2</sub>—1—x—8; 19.7/104.1.
- 13, 14. — *Verruculisporites bangii* n. fsp., D<sub>2</sub>—1—x—8; 19.7/104.1.
15. — *Verruculisporites stockmarrii* n. fsp., *Osmundaceae* or *Schizaeaceae*, Højstrup—49; 8.6/111.9.

×1000

### PLATE III

1. — *Verrucosisporites stockmarrii* n. fsp., *Osmundaceae* or *Schizaeaceae*, Højstrup—49; 8.6/111.9.
- 2, 3. — *Foveotrilites* fsp., Stevns Klint—26; 18.6/115.3.
- 4, 5. — *Retitrilites incomptus* (MANUM 1962) W. KR. 1963, *Lycopodiaceae*, D<sub>2</sub>—2—5; 6.3/125.1.
- 6, 7. — *Saxosporis* fsp. ex group *gracilis* W. KR. and PACLTOVÁ 1963, *Anthocerotaceae*, *Phaeoceros*, D<sub>2</sub>—64; 17.7/115.1.
- 8, 9. — *Saxosporis disconformis* (STOVER 1973) n. comb., *Anthocerotaceae*, Stevns Klint—7; 18.6/107.3.
- 10, 11. — *Echinatisporis* fsp., *Selaginellaceae*, *Selaginella*, Højstrup—24; 16.5/103.4.
- 12, 13. — *Phaeocerosporites croxtonae* n. fsp., *Anthocerotaceae*, Højstrup—50; 14.3/103.8.

×1000

#### PLATE IV

- 1, 2. — *Phaeocerosporites stockmarrii* n. fsp., *Anthocerotaceae*, Højstrup—6; 7.4/107.0.
  - 3, 4. — *Phaeocerosporites bangii* n. fsp., *Anthocerotaceae*, Stevns Klint—20; 5.1/102.8.
  - 5, 6. — *Croxtonaesporites hojrupensis* n. fsp.,  $D_3$ —20; 14.3/120.9.
  - 7, 8. — *Croxtonaesporites daniensis* n. fsp.,  $D_3$ —1—7; 12.6/122.5.
  - 9, 10. — *Contignisporites* fsp.,  $D_3$ —40; 8.2/120.5.
  - 11, 12. — *Polypodiaceoisporites triangulus* KDS. and J. R. 1965, *Pteridaceae*, Stevns Klint—13; 3.4/118.3.
  - 13, 14. — Cf. *Polypodiaceoisporites* fsp.,  $D_3$ —77; 17.8/124.3.
- ×1000

#### PLATE V

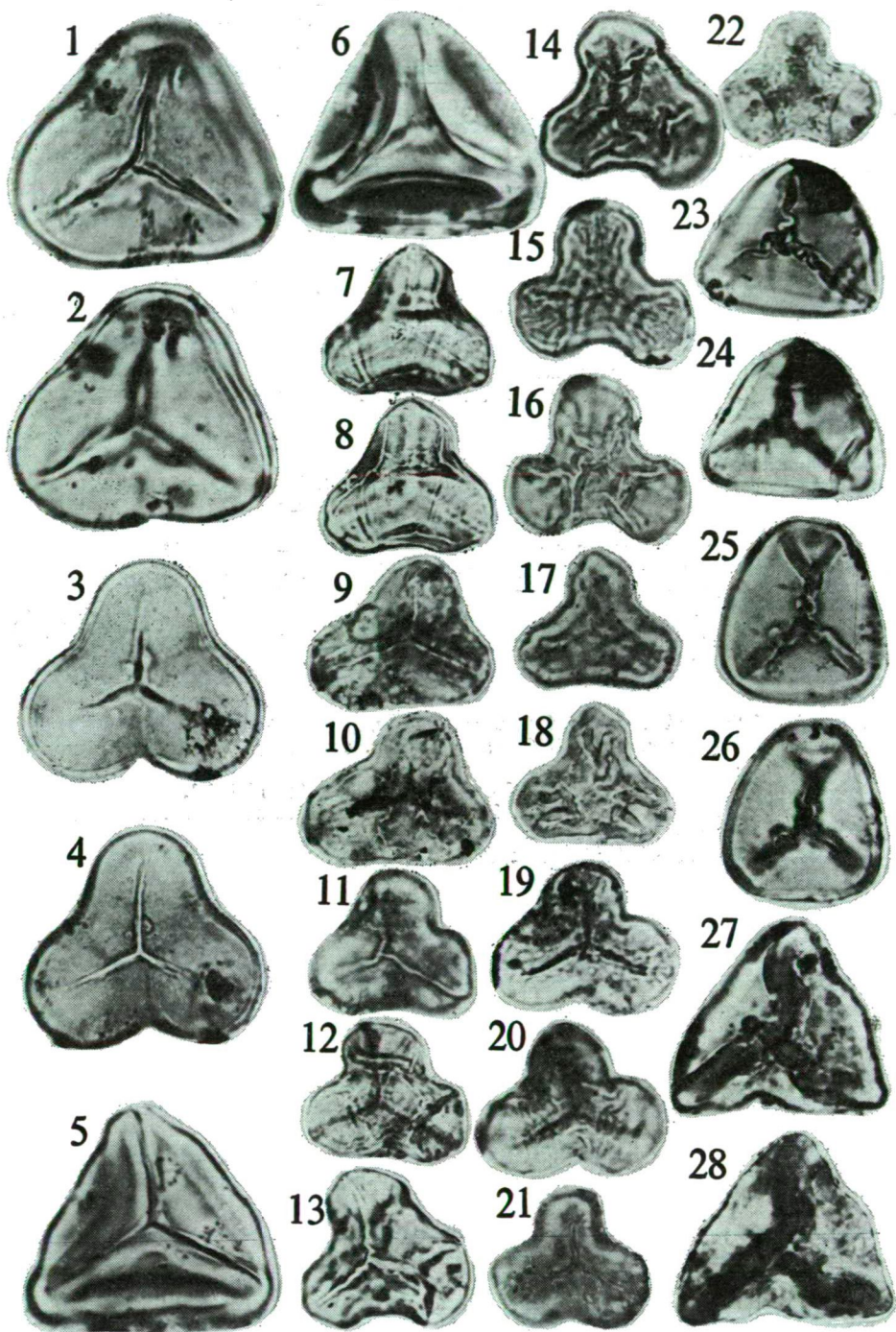
- 1, 2. — *Polypodiaceoisporites brejani* CERNJAVSKA 1970, *Pteridaceae*,  $D_3$ —79; 4.2/103.8.
  - 3, 4. — *Polypodiaceoisporites vancampoe* KDS. 1967, *Pteridaceae*, Stevns Klint—9; 21.7/111.2.
  - 5, 6. — *Polypodiaceoisporites hojrupensis* n. fsp., *Pteridaceae*,  $D_3$ —41; 20.1/116.3.
  - 7, 8. — *Polypodiaceoisporites maximus* E. NAGY and L. RÁKOSI 1966, *Pteridaceae*,  $D_3$ —71; 23.3/116.4.
  - 9, 10. — *Polypodiaceoisporites snopkova* KDS. 1973, *Pteridaceae*,  $D_3$ —2—x—4; 13.6/122.5.
  - 11, 12. — *Polypodiaceoisporites hungaricus* KDS. 1961, *Pteridaceae*,  $D_3$ —1—x—10; 4.7/105.0.
  - 13, 14. — *Polypodiaceoisporites stockmarrii* n. fsp., *Pteridaceae*, Stevns Klint—14; 8.7/121.2.
- ×1000

#### PLATE VI

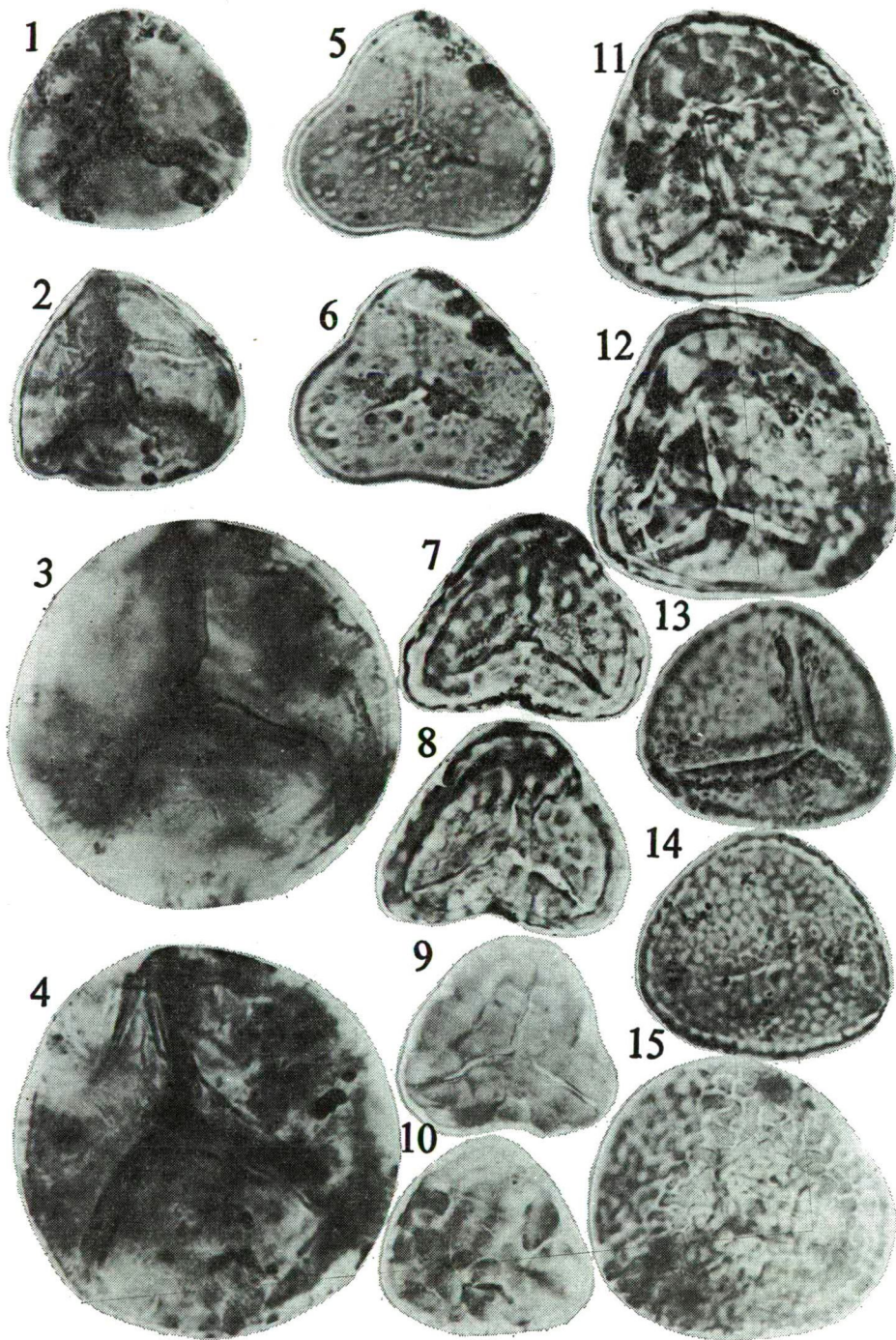
- 1, 2. — *Polypodiaceoisporites gracilingulis* W. KR. 1959, *Pteridaceae*,  $D_3$ —32; 13.7/103.2.
  - 3, 4. — *Polypodiaceoisporites granulatus* KDS. 1966, *Pteridaceae*,  $D_3$ —1—x—6; 2.7/111.5.
  - 5, 6. — *Polypodiaceoisporites bangii* n. fsp., *Pteridaceae*, Højstrup—2; 2.8/106.7.
  - 7, 8. — *Polypodiaceoisporites croxtonae* n. fsp., *Pteridaceae*,  $D_3$ —72; 13.5/111.2.
  - 9, 10. — *Verrucingulatisporites hojrupensis* n. fsp., *Pteridaceae*,  $D_3$ —61, 8.9/108.3.
  - 11, 12. — *Segmentizonosporites daniense* n. fsp., *Pteridaceae*,  $D_3$ —1—6; 23.1/121.6.
  - 13, 14. — *Polypodiaceoisporites laevigatus* KDS. and J. R. 1965, *Pteridaceae*, Højstrup—49; 4.2/104.7.
  - 15, 16. — *Polypodiaceoisporites haemussensis* CERNJAVSKA 1966, *Pteridaceae*, Dania—35; 14.4/112.3.
- ×1000

#### PLATE VII

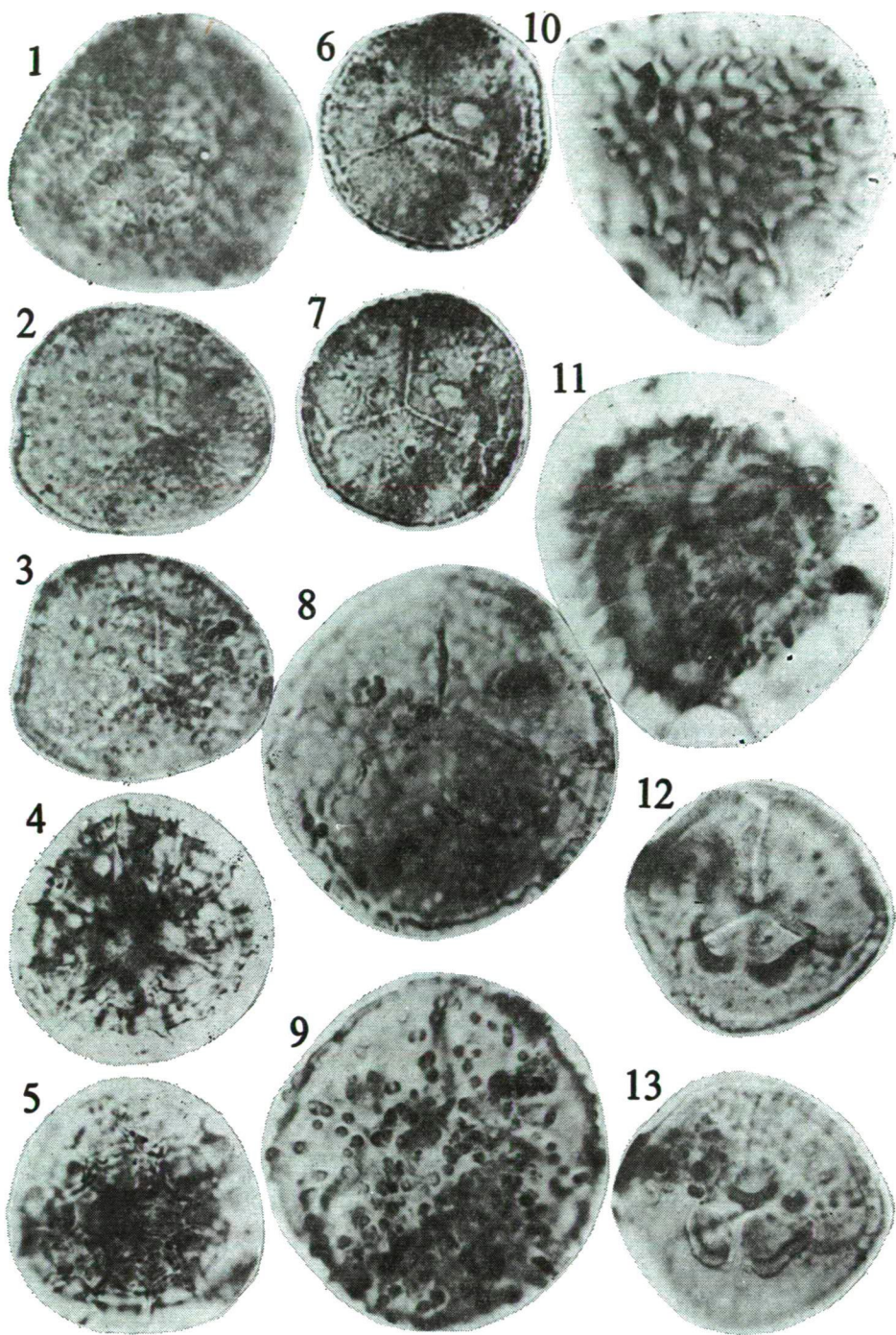
- 1, 2. — *Inundatisporis krutzschii* n. fsp., *Lycopodiaceae*, Dania—29; 17.2/115.1.
  - 3, 4. — *Hamulatisporis heskemensis* (PLANZL 1955) n. comb., *Lycopodiaceae*, Højstrup—29; 7.0/108.3.
  - 5, 6. — *Alisporites* cf. *bilateralis* ROUSE 1959, *Abietales*,  $D_3$ —41; 23.2/111.1.
  - 7, 8. — *Pityosporites labdacus* (R. POT. 1931) TH. and PF. 1953 subfsp. *labdacus*, *Abietaceae*, *Pinus*. Dania—24; 4.7/113.7.
  - 9, 10. — *Parvisaccites* fsp., *Coniferopsida*,  $D_3$ —6; 23.6/111.2.
- ×1000



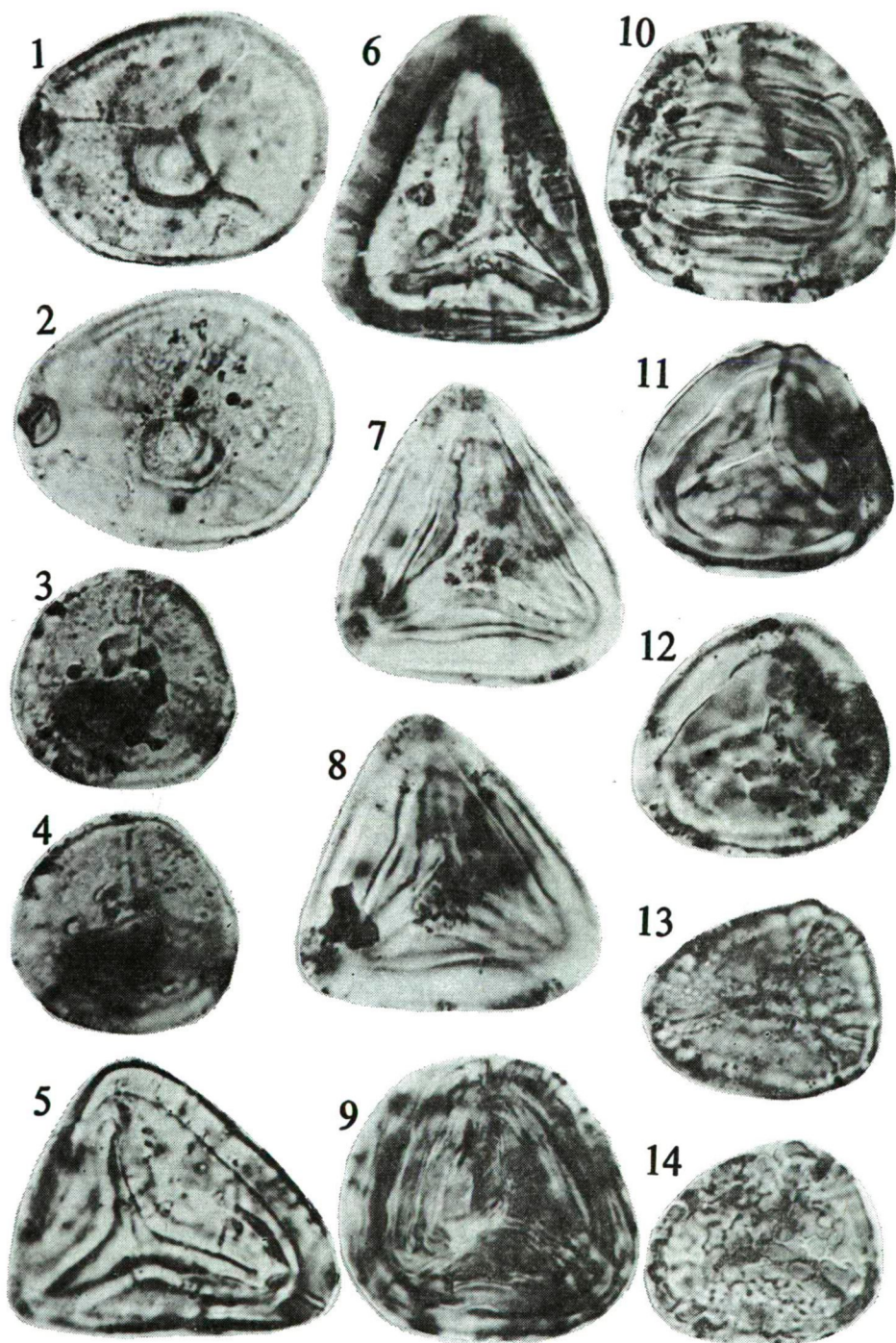




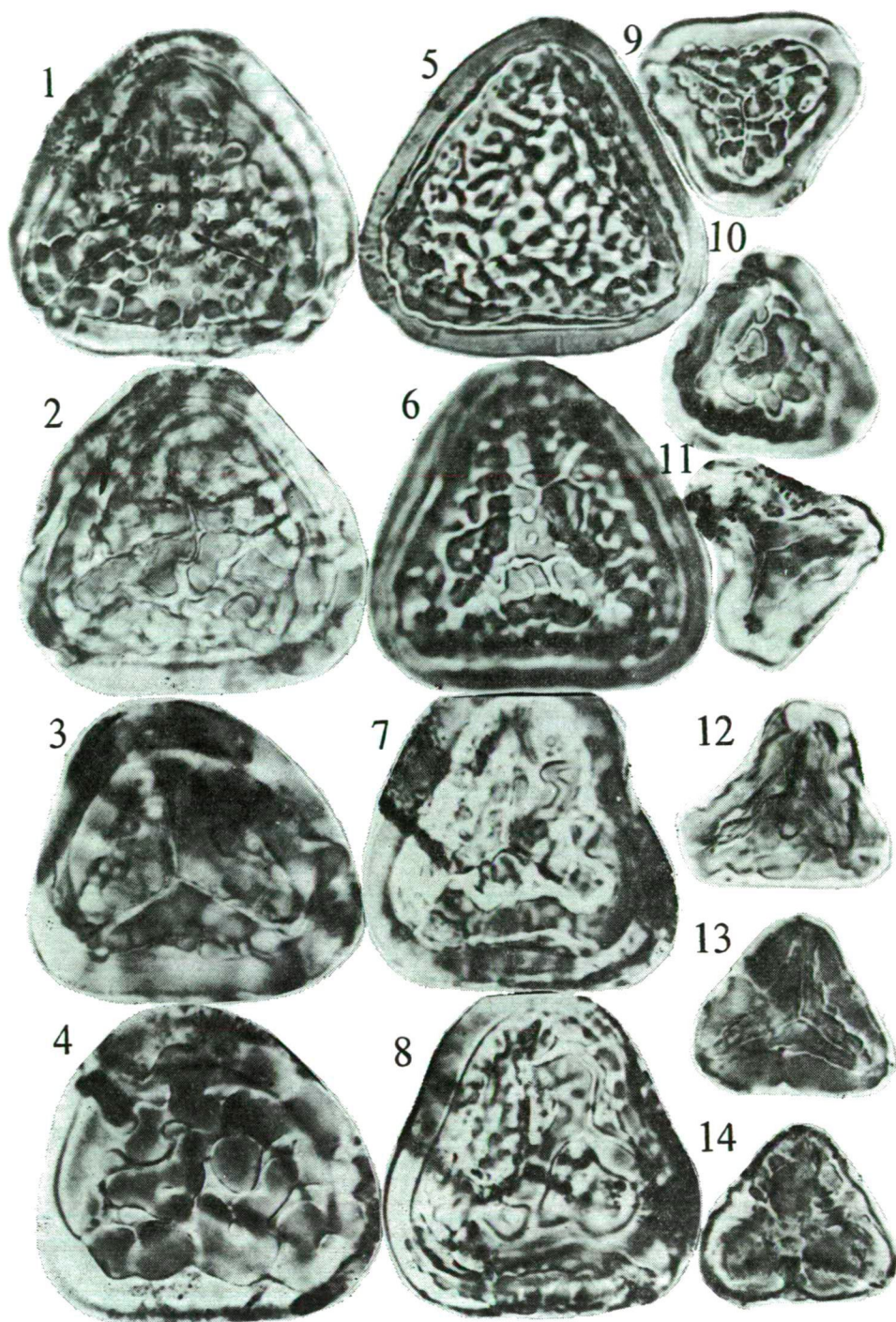




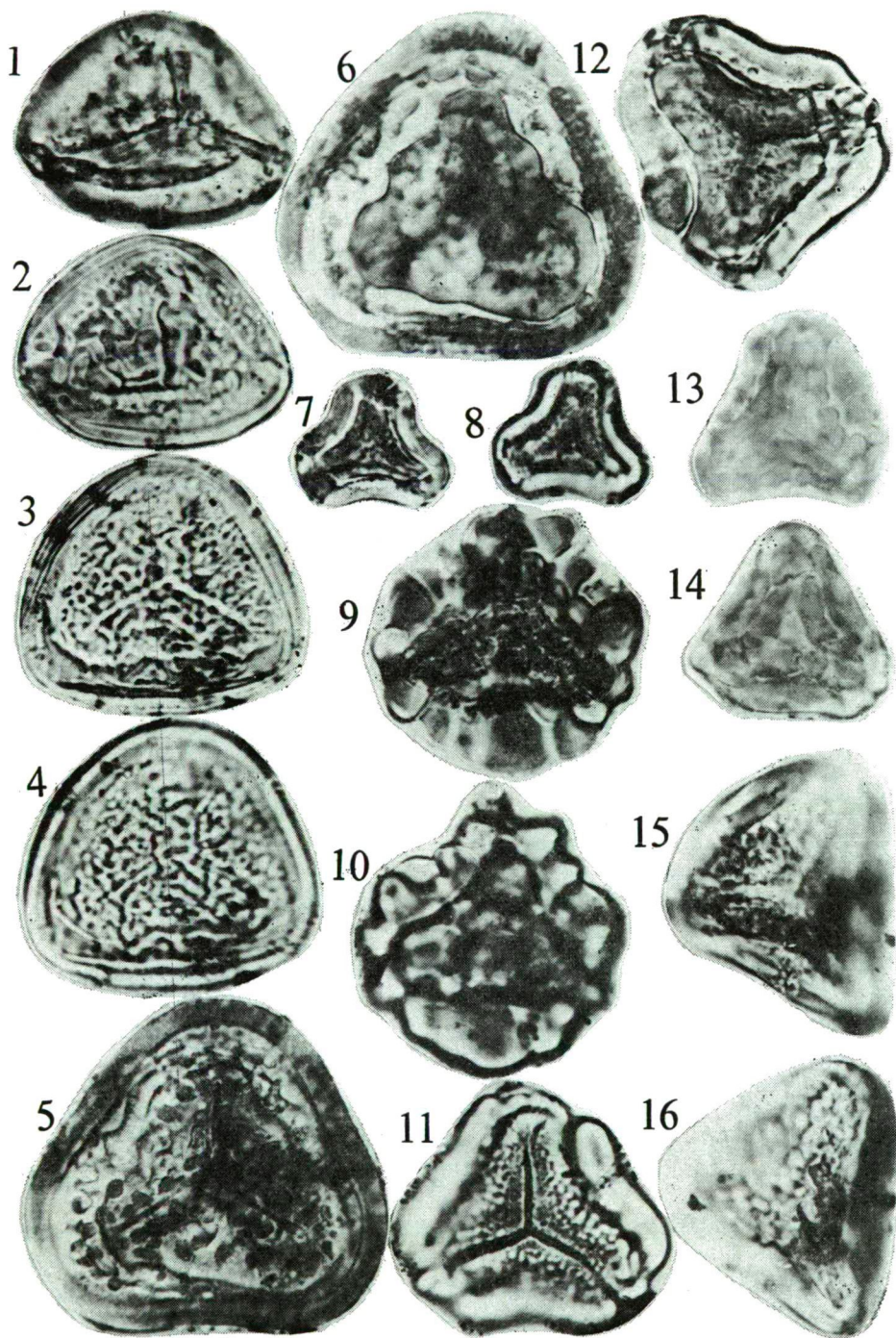


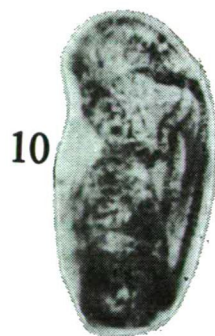
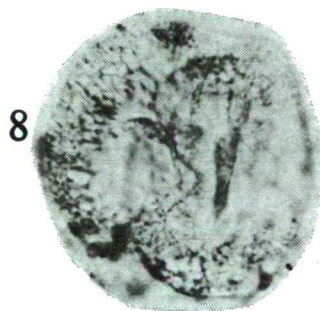
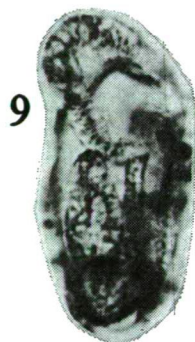
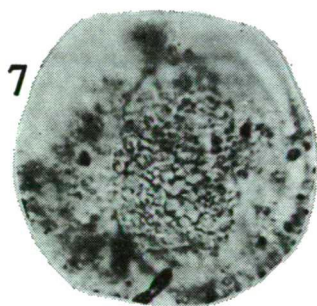
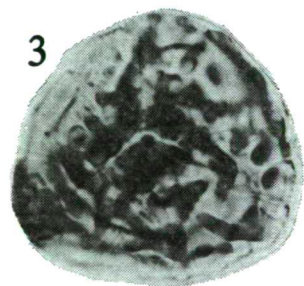
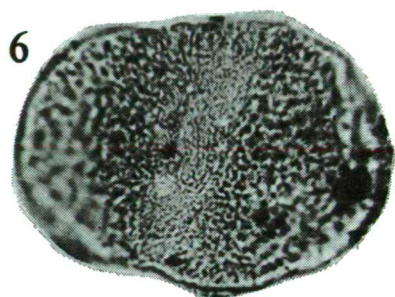
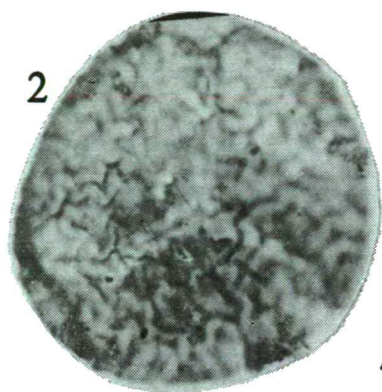
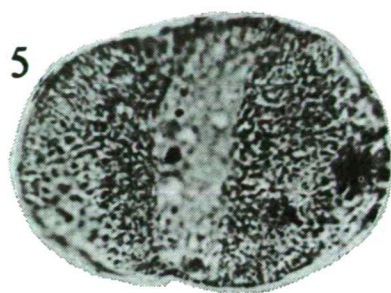
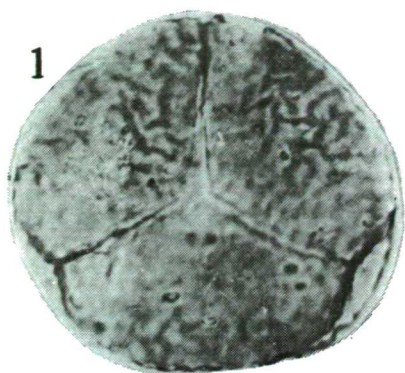














## CONTENTS

RAVASZ, Cs. and G. SOLTÍ: Sulphur-, gypsum- and alginite-bearing strata in the Zsámbék Basin .....	191
MOHSIN, SYED IQBAL and GHULAM SARWAR: Preliminary studies of fluorite mineralization in Kalat region, Baluchistan Province, Pakistan .....	209
AL-FADHLI, I. and KHALIL A. MALICK: Phosphorites in Sinjar Formation of Sulaimaniah area, Iraq .....	219
SZEDERKÉNYI, T.: Petrological and geochemical character of the Bár basalt, Baranya County, South Hungary .....	235
KABESH, M. L., M. E. HILMY and ABDEL-KARIM A. SALEM: Behaviour of major elements in the granitic rocks of Kadabora pluton, Eastern Desert, Egypt .....	245
KABESH, M. L., M. E. HILMY and ABDEL-KARIM A. SALEM: Petrochemistry and petrogenesis of Abu Dob granitic stock, Eastern Desert, Egypt .....	257
KABESH, M. L., ADEL M. REFAAT and ZEINAB M. ABDALLAH: Geochemistry of some gabbros from Muhammad Qol area. Northern Red Sea Hills, Sudan Republic .....	271
SALLOUM, G. M.: The tectonic pattern of Gabal Meatiq area, North Eastern Desert, Egypt .....	283
SOLTÍ, G.: The oil shale deposit of Várpalota .....	289
HETÉNYI, M.: Thermal degradation of the organic matter of oil shales of Pula (Hungary) at 573—773 K .....	301
MOLNÁR, B., M. SZÓKOKY and S. KOVÁCS: Diagenetic and lithification processes of Recent hypersaline dolomites on the Duna-Tisza interfluvium .....	315
MOLNÁR, B.: Reflection of erosional changes on the area of the Körös rivers' depression .....	339
KEDVES, M.: Palynological investigations on sediments of the Lower Danian (Fish Clay, Denmark) II .....	355

Felelős kiadó: Grasselly Gyula  
Készült: Monószedéssel, íves magasnyomással, 16,7 A5 ív terjedelemben,  
az MSZ 5601—59 és 5602—55 szabvány szerint  
Példányszám: 625  
81-4301 — Szegedi Nyomda — Felelős vezető: Dobó József igazgató